CONFERENCE SERIES

Contributions

3rd International Conference on
Proton Transfer Reaction
Mass Spectrometry and Its Applications

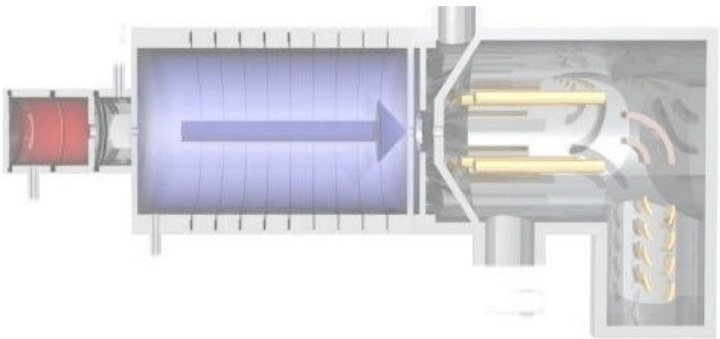

Editors: A. Hansel, T. D. Märk

universität innsbruck

innsbruck university press

PROTON TRANSFER REACTION – MASS SPECTROMETRY

PTR-MS

THE SOLUTION FOR ONLINE TRACE GAS ANALYSIS

Interested in an
ultra-sensitive trace gas detector?

Looking for a
customized real-time VOC
monitoring solution?

We have
Expertise in PTR-MS since 1998.

We are
the world's leading producer
of PTR-MS online mass spectrometry
instruments.

We have
over 100 satisfied customers.

**We wish you an interesting
PTR-MS Conference 2007!**

www.PTRMS.COM

IONICON
ANALYTIK

A-6020 Innsbruck • Technikerstrasse 21a • Telefon: +43 / 512 / 50 74 800 • Fax: +43 / 512 / 50 79 818 • Mail: info@ptrms.com • Internet: www.ptrms.com

CONFERENCE SERIES

*i*up • *innsbruck* university press

www.uibk.ac.at/iup

Local Organizing Committee:
Armin Hansel (Chairman)
Tilmann Märk
Armin Wisthaler
Jürgen Dunkl
Manuela Löffler
Ralf Schnitzhofer
Jens Herbig

Vizerektorat für Forschung
Leopold-Franzens-Universität Innsbruck
Christoph-Probst-Platz, Innrain 52
A-6020 Innsbruck, Austria
www.uibk.ac.at/iup

Book editors: Armin Hansel, Tilmann Märk
Organization: Jens Herbig, Ralf Schnitzhofer
Publishing staff: Carmen Drolshagen, Jasmine Luger
Cover design: Carmen Drolshagen
Produced: Book on Demand

ISBN-10: 3-902571-03-9
ISBN-13: 978-3-902571-03-8

3rd International Conference on Proton Transfer Reaction Mass Spectrometry and Its Applications

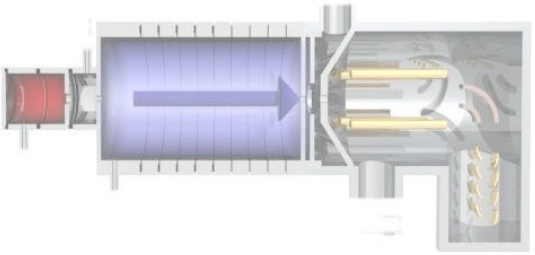

Contributions

Editors:
Armin Hansel
Tilmann Märk

Institut für Ionenphysik und Angewandte Physik
der Leopold-Franzens-Universität Innsbruck
Technikerstr. 25
A-6020 Innsbruck, Austria

Obergurgl, Austria
January 27 - February 01, 2007

PROTON TRANSFER REACTION – MASS SPECTROMETRY

Ultra-Sensitive Real-Time VOC Detector

HIGHSENSITIVITY
PTR-MS

- **very low detection limit (pptv-range)**
- **real time measurement**
- **online monitoring**

- Mass range: 1 - 512 amu (up to 2048 amu on request)
- Detection limit: 5 pptv
- Heatable inlet and reaction chamber

NEW AUTO - PERFORMANCE - CONTROL unit available in 2007:

- Automatic transmission measurement
- Software integrated ion source and SEM check
- Calibration with different gas standards available

Real-time applications of PTR-MS:

- environmental research
- food & flavor science
- cleanroom air analysis
- dangerous substance detection
- indoor air - "sick building syndrome" control

www.PTRMS.COM

IONICON
ANALYTIK

A-6020 Innsbruck • Technikerstrasse 21a • Telefon: +43 / 512 / 50 74 800 • Fax: +43 / 512 / 50 79 818 • Mail: info@ptrms.com • Internet: www.ptrms.com

THE SOLUTION FOR ONLINE TRACE GAS ANALYSIS

Automated Customized Real-Time Monitoring

> **small dimensions and low weight**
> **easy to handle**
> **short start-up time**

COMPACT
PTR-MS

- Mass range: 1 - 300 amu
- Detection limit: 500 pptv
- Heatable inlet and reaction chamber

NEW customized VOC monitoring solution available in 2007:

- Customized user interface
- Automated calibration and performance checks
- Alarm levels for selected compounds
- Reliable monitoring of production plants

Real-time applications of PTR-MS:

- incineration process monitoring
- chemical production plant surveillance
- selected/total VOC concentration monitoring
- offices, planes, cars, trains - VOC pollution quantification
- quality control without sample pretreatment

www.PTRMS.COM

IONICON
ANALYTIK

A-6020 Innsbruck • Technikerstrasse 21a • Telefon: +43 / 512 / 50 74 800 • Fax: +43 / 512 / 50 79 818 • Mail: info@ptrms.com • Internet: www.ptrms.com

PROVIDING TRACE GAS SOLUTIONS FOR BIOTECHNOLOGY AND MEDICINE

Zero-Air Generation and Gas Calibration

- > simple, automated PTR-MS calibration
- > VOC-free (zero-air) generation
- > portable, standalone device

  - > Calibration range: 0.3-75 ppbv
  - > Humidity range: 25-95 % rH (at ambient temperature)
  - > Zero-air flow: 0.25-1.50 l min^{-1}

GAS CALIBRATION UNIT

Available in 2007

Versions available:

- > Basic
  - > calibrations at ambient/cylinder air humidity
- > Standard
  - > calibrations for variable dry → humid conditions

Gas standards:

- > internal, refillable gas canister
- > different standard gas mixtures available

Further details of the gas calibration unit may be found in the conference contributions, abstract: Singer *et al.*

WWW.IONIMED.COM

IONIMED ANALYTIK

Technikerstrasse 21a • A-6020 Innsbruck • Austria • Tel.: +43 512 507 4810 • Fax.: +43 512 507 9818 • Email: office@ionimed.com

Contents

Foreword 1

1. Opening Lecture

The role of chemical ionization in understanding the atmosphere
F. L. Eisele, D. J. Tanner, R. L. Mauldin, D. R. Hanson, and Hans Friedli 4

2. Advanced Aerosol Characterization

Laboratory studies on the properties and processes of complex organic aerosols
Yinon Rudich, Elad Dinar, Ilya Taraniuk, Ali Abo Riziq, Ellen R. Graber, Tatu Anttila and Thomas Mentel 10

On-line characterisation of gaseous and particulate organic analytes using atmospheric pressure chemical ionisation mass spectrometry
Thorsten Hoffmann, Jörg Warnke, Christopher Reinnig, Rolf Bandur, Sven Hoffmann, Bettina Warscheid 15

Development and first deployment of an aerosol collection/thermal-desorption PTR-ITMS instrument for the measurement of aerosol organic species
Troy Thornberry, Daniel M. Murphy, David S. Thomson and Edward R. Lovejoy 20

Secondary organic aerosol formation from isoprene: results from laboratory and field experiments
Magda Claeys 25

Examples of particle analysis by mass spectrometry from PSI smog chamber experiments
J. Dommen, A. Metzger, A. Gascho, K. Gaeggeler, M.R. Alfarra, A.S.H. Prevot, M. Kalberer, D. Gross, A. Brunner and U. Baltensperger 27

Chemical Ionization Mass Spectrometry Applied to the Study of Atmospheric Nanoparticles
J. N. Smith, G. J. Rathbone, F. L. Eisele and P. H. McMurry 31

3. New Developments in Chemical Ionization Mass Spectrometry (CIMS)

Applications of Chemical Ionization Mass Spectrometry to Atmospheric Chemistry
L. Gregory Huey, David J. Tanner, Saewung Kim, Robert Stickel, Steven Sjostedt, Oscar Vargas, Anne Case, Andrew Turnipseed and John B. Nowak 38

Atmospheric Monitoring With Chemical Ionisation Reaction Time-of-Flight Mass Spectrometry (CIR-TOF-MS)
Paul S. Monks, Kevin P. Wyche, Robert S. Blake, Chris Whyte and Andrew M. Ellis 41

The Direct Analysis in Real Time (DARTtm) ion source
Robert B. Cody 47

In situ measurements of gas- and condensed-phase HNO_3 in the upper troposphere and lower stratosphere
Peter J. Popp 48

4. PTR-MS: Measurements of Anthropogenic VOCs

Emissions and Chemistry of Atmospheric VOCs: New Insights From Three Summers of Airborne and Ship-Based Measurements
Joost de Gouw, Carsten Warneke 54

Measurement of benzene and toluene emissions in the urban environment: Is this distribution controlled by vehicle emissions?
Berk Knighton 59

Operational Optimization of CFC destruction facility by means of PTR-MS and its modified method
Akio Shimono, Toshihide Hikida and Makoto Naganuma 63

5. PTR-MS: Measurements of Biogenic VOCs

The Forest as a Chemical Reactor: Natural Compounds Have Profound Impacts on Earth's Atmosphere
Allen H. Goldstein, Rupert Holzinger, Anita Lee and Nicole Bouvier-Brown 70

Volatile organic compounds emitted from natural landscapes measured by PTR-MS
Thomas Karl 75

Measuring ecosystem scale VOC emissions by PTR-MS
J. Rinne, R. Taipale, C. Spirig, T.M. Ruuskanen, T. Markkanen, T. Vesala, A. Brunner, C. Ammann, A. Neftel, T. Douffet, Y. Prigent, P. Durand, M. Kulmala 76

Comparison of different approaches to measure VOC exchange over grassland by PTR-MS
A. Neftel, C. Ammann, A. Brunner, M. Jocher, C. Spirig, B. Davidson, J. Rinne and J. Dommen 80

Emission of biogenic volatile organic compounds (BVOCs) from vegetation
Francesco Loreto 85

Better insight in regulation, biosynthesis and function of isoprene emission using PTR-MS analysis
Jörg-Peter Schnitzler, Maaria Loivamäki, Markus Teuber, Katja Behnke and David Andres-Momtaner 86

6. PTR-MS: Instrument Development

The NIES PTR-TOFMS instrument: design, performance and application
Hiroshi Tanimoto, Satoshi Inomata, Nobuyuki Aoki, Yasuhiro Sadanaga, Jun Hirokawa . . . 92

Development of a High Resolution PTR-TOFMS
Martin Graus, Markus Müller, Armin Wisthaler and Armin Hansel 97

Proton-transfer reaction Ion Trap Mass Spectrometry for applications in medical sciences
Frans J.M. Harren, Elena Crespo, Simona M. Cristescu, Pieter Zanen, Marco M.L. Steeghs 102

O_2^+ as primary reagent ion in the PTR-MS instrument: detection of gas-phase ammonia
Michael Norman, Armin Wisthaler and Armin Hansel 104

7. PTR-MS: Applications in Food Science

PTR-MS in food science and technology: a review
Franco Biasioli 110

General overview: Applications of PTR-MS in food research at Nestlé
Christian Lindinger, Philippe Pollien, Santo Ali, Jean-Claude Spadone, Fabien Robert . . . 116

Targeting the qualitative, quantitative and temporal aspects of retronasal aroma perception: a challenge for time-intensity profiling?
Andrea Buettner, Montserrat Mestres 118

8. Contributed Papers (Posters)

Automated Taste-Aroma Delivery System for Simultaneous Analytical and Physiological Recordings
Julie Hudry, Boris Reynaud, Santo Ali, Nicolas Antille, Johannes le Coutre 124

Ion/molecule reaction studies in support of the detection of sesquiterpenes by CIMS
Crist Amelynck, Niels Schoon, Elke Debie and Patrick Bultinck 127

Assessing truffle origin by PTR-MS fingerprinting and comparison with GC-MS for the headspace analysis
Eugenio Aprea, Silvia Carlin, Giuseppe Versini, Tilmann D. Märk and Flavia Gasperi 132

Discrimination of Different Wine Varieties through Direct Headspace Analyses by PTR-MS
Renate Spitaler, Nooshin Araghipour, Tomas Mikoviny, Armin Wisthaler, Josef Dalla Via, Tilmann D. Märk 136

Does the emission of oxygenated plant volatiles reflect stress induced membrane damages?
Csengele Barta, Federico Brilli, Alessio Fortunati and Francesco Loreto 140

VOC emissions of white clover triggered by ozone
Aurelia Brunner, Christof Ammann, Markus Jocher, Christoph Spirig and Albrecht Neftel 141

Headspace Analysis of In Vitro Cultured Cells using PTR-MS
C. Brunner, B. Thekedar, L. Keck, U. Oeh and C. Hoeschen 146

Analysis of Lactones by Proton Transfer Reaction - Mass Spectrometry (PTR-MS). Fragmentation Patterns and Detection Limits
Katja Buhr, Andrea Buettner and Peter Schieberle 149

Differentiation of monoterpenes by Collision Induced Dissociation with a Proton-transfer reaction Ion Trap Mass Spectrometer (PIT-MS)
Marco M.L. Steeghs, Elena Crespo, Cor Sikkens, Simona M. Cristescu and Frans J.M. Harren 154

Real time analysis by Chemical Ionisation in a High Resolution Mass Spectrometer
Christophe Dehon, Michel Heninger, Pierre Boissel, Joel Lemaire, Stephane Pasquiers, Nicole Simiand, Pierre Tardiveau, Francois Jorand, Helene Mestdagh 156

Predicting Consumer Freshness Perceptions of Cakes by Using Descriptive Sensory Analysis and Headspace Volatile Composition
Samuel Heenan, Jean-Pierre Dufour, Conor Delahunty, Winna Harvey 161

PTR-MS measurements of traffic-related emissions: Annual variations of the toluene/benzene ratio
Jürgen Dunkl, Ralf Schnitzhofer, Jonathan Beauchamp, Armin Wisthaler and Armin Hansel 166

Interactions between BVOC emission and ozone uptake in forest species*
Silvano Fares, Francesco Loreto and Jürgen Wildt 170

Characterisation of organosulfates from the photooxidation of isoprene in ambient PM2.5 aerosol by LC/ESI-linear ion trap MS
Yadian Gómez, Reinhilde Vermeylen, Willy Maenhaut and Magda Claeys 171

Customized solution for chemical plant monitoring
G. Hanel, A. Jordan, E. Hartungen, S. Haidacher, R. Schottkowsky, L. Märk T. D. Märk 173

Measurements of biogenic volatile organic compounds above a sub-arctic wetland in northern Sweden
Thomas Holst, Sean Hayward, Anna Ekberg and Almut Arneth 174

Qualitative and quantitative detection of Mycotoxin in cereals
E. Hartungen, A. Jordan, L. Märk, T. D. Märk 178

Development of new PTR ion sources for soft and selective ionization
Satoshi Inomata, Hiroshi Tanimoto and Nobuyuki Aoki 180

Aldehyde measurements and estimation of contribution from photochemical production in urban atmosphere
Shungo Kato, Masumi Ideguchi and Yoshizumi Kajii 185

Correct equations for concentrations in the drift tube of a PTR-MS and potential implications for the calculated concentrations
Lothar Keck, Uwe Oeh and Christoph Hoeschen 187

Coupling a FTICR mass spectrometer with a Proton Transfer Reaction ion source
Joël Lemaire, Laurent Clochard, Christophe Dehon, Hélène Mestdagh, Pierre Boissel, Gérard Mauclaire and Michel Heninger 191

Novel approach to study aroma release kinetics
Mateus M-L., Lindinger C., Liardon R., Blank I. 195

Isoprene Photooxidation Product Study using Proton-Transfer-Reaction Mass Spectrometry (PTRMS) and a coupling of Gas Chromatography and PTRMS
Axel Metzger, A. Brunner, A. Gascho, J. Dommen and Urs Baltensperger 200

Emission of volatile organic compounds from bacterial cultures
Tomas Mikoviny, Michael Bunge, Nooshin Araghipour, Rosa Margesin, Franz Schinner, Armin Wisthaler and Tilmann D. Märk 204

Rapid Testing of Olive Oil Quality Using SIFT-MS
Daniel B. Milligan, Brett M. Davis, Senti T. Senthilmohan, Paul F. Wilson and Murray J. McEwan 208

Differentiation of monoterpenes by Collision Induced Dissociation with a Proton-transfer reaction Ion Trap Mass Spectrometer (PIT-MS)
Marco M.L. Steeghs, Elena Crespo, Cor Sikkens, Simona M. Cristescu, Frans J.M. Harren 212

Measurement of VOC fluxes above bare soil by PTR-MS
Martina Müsch, Jochen Tschiersch 215

Coacervates for aroma modulation
Philippe Pollien, Fabien Robert, Christian Lindinger, Santo Ali and Jean-Claude Spadone 216

Disjunct eddy covariance measurements of biogenic volatile organic compound fluxes from a boreal Scots pine forest
Risto Taipale, Janne Rinne, Taina M. Ruuskanen, Maija Kajos, Hannele Hakola, Heidi Hellén and Markku Kulmala 218

Monitoring herbivore induced VOC emissions from plants
A. Schaub, J. Beauchamp, R. Mumm, M. Dicke and A. Hansel 223

Vertical Distribution of Air Pollutants in the Inn Valley Atmosphere in Winter 2006
Ralf Schnitzhofer, Michael Norman, Jürgen Dunkl, Armin Wisthaler, Alexander Gohm, Friedrich Obleitner and Armin Hansel 227

Dynamic Gas Dilution System for Accurate Calibration of Analytical Instruments such as PTR-MS
Wolfgang Singer, Jonathan Beauchamp, Jens Herbig, Jürgen Dunkl, Ingrid Kohl and Armin Hansel 232

Detection of processed animal proteins in feedstuffs: evaluation of PTR-MS
Saskia van Ruth, Leo van Raamsdonk, Nooshin Araghipour and Jennifer Colineau 238

Can PTR-MS Measure Propylene Quantitatively in the Atmosphere?
Carsten Warneke, Joost de Gouw, Dan Welsh-Bon, William C. Kuster 243

In-Situ Evidence for Free-Troposheric Longrange Transport of a Siberian Forest Fire Plume to the North Pole Region
Armin Wisthaler, Erik Swietlicki, Michael Tjernström, Armin Hansel and Caroline Leck 247

9. Index of Authors 252

Foreword

PTR-MS (Proton Transfer Reaction - Mass Spectrometry) is a relatively new technology developed at the Institute of Ion Physics and Applied Physics at the University of Innsbruck in the 1990's. PTR-MS has been found to be an extremely powerful and promising technology for the detection of volatile organic compounds (VOC) at ultra low concentrations (pptv) in gaseous media, such as air. PTR-MS has been successfully employed in many fields of research, including atmospheric chemistry, environmental research, food and flavour technology. In 1998 the spin-off company Ionicon Analytik GmbH (www.ptrms.com) was founded to provide this technique to a growing user community. In 2004 Ionimed Analytik GmbH (www.ionimed.com) was founded to provide trace gas solutions for biotechnology and medicine. Today more than 100 instruments are in use throughout the world, including noted multinational companies and renowned research institutions working in the field of environmental science, food technology and medicine.

The intent in initiating and to organize the 1st International PTR-MS Conference in January 2003 in Igls, Austria was to bring together active scientists and technologists involved in real-world mass spectrometric measurements of VOC from both academia and industry. The 3rd PTR-MS conference continues this biennial series to provide a forum for researchers dedicated to the further development of PTR-MS with particular focus on the implementation of new sophisticated mass spectrometric techniques. To promote the development and application of chemical ionization for on-line gas-phase and particulate-phase analysis that go beyond PTR-MS. To foster the application of PTR-MS to various scientific disciplines with particular focus on environmental sciences, biology and food science.
The conference aims to bring together an outstanding group of scientists from Academia and Industry to enhance communication and discussion within the PTR-MS community and to stimulate the exchange of ideas and expertise with other chemical ionization mass spectrometry communities.
We would like to thank Jürgen Dunkl, Jens Herbig, Manuela Löffler, Ralf Schnitzhofer and Armin Wisthaler who worked very hard to organise this conference. Special thanks go to IONIMED ANALYTIK, IONICON ANALYTIK, PFEIFFER VACUUM AUSTRIA and WINN (West Austrian Initiative for Nano Networking) who financially supported the Conference.

Armin Hansel

Tilmann Märk

Innsbruck, December 2006

1. Opening Lecture

The role of chemical ionization in understanding the atmosphere

F. L. Eisele,[1,2], D. J. Tanner[2], R. L. Mauldin[1], D. R. Hanson[1], and Hans Friedli[1]

[1] *Atmospheric Chemistry Division, National Center for Atmospheric Research, Boulder, Colorado, USA, eisele@ucar.edu*

[2] *Earth and Atmospheric Sciences, Georgia Institute of Technology, Atlanta, Georgia, USA*

Abstract

The application of chemical ionization mass spectrometry to atmospheric studies has led to its use over a large dynamic range of reaction times and incorporates a wide variety of different types of chemical reactions. In some cases, the atmosphere itself is used as a chemical ionization source and reaction vessel, while in others the ionization and ion chemistry are fully constrained. In many cases, the compound of interest can be directly ionized while in others, it most be converted into a compound that will form a stable ion. In some cases the formation of stable terminal ions is both desirable and enhanced through ion molecule reactions while still other studies require the separation of successive ion assisted growth reactions from single step proton exchange reactions. All of the above scenarios are encountered in investigations of the composition of the earth's atmosphere. A representative subset of these different techniques will be discussed along with a brief history and a perspective of how they relate to PTR-MS.

Introduction

Chemical ionization (CI) and the ion molecule reactions that result can provide a powerful tool for identifying and quantifying neutral atmospheric species and, in some extreme cases, possibly controlling their concentration. The uses of chemical ionization mass spectrometry (CIMS) span a broad range of operating conditions, making the technique quite versatile. It can be applied over a wide range of parameter space where reaction times range from less than 10^{-3} to 10^{3} seconds, at pressures of less than a torr up to or above an atmosphere, and with a wide range of reactant ions. Different applications of CI are required to address different types of questions, which in turn will lead to quite different instrument designs and measurement approaches. Several of these techniques will be compared with a focus on the use of CIMS for the study of difficult to measure trace atmospheric compounds and for the study of aerosol nucleation.

Experimental Methods and Discussion

Nature's CI experiments

Cosmic rays cause ionization throughout the atmosphere, with photo-ionization contributing greatly in the ionosphere, and radioactive compounds such as radon adding significantly to the ionization of the lower troposphere. Once formed, ions can react for time scales of 10^{3} seconds before being lost to particle surfaces or by ion-ion recombination. During this time, ions typically

react to successively form more and more energetically stable complexes. Since in the lower atmosphere ions can undergo tens of trillions of collisions during their lifetime, their final identity can be determined by a single collision with a trace compound in the low parts per quadrillion by volume (ppqv) concentration range. Thus, the identification of natural terminal ion species provides an extremely sensitive detection method for compounds such as strong acids and bases, which form very stable ions in the negative and positive ion spectra, respectively. Interestingly some of the first mass spectrometric measurements of atmospheric ions were carried out in the ionosphere, which was difficult to reach but where ions make up a much larger fraction of the total gas [1]. By the later 1970s measurements moved down to the stratosphere where ion concentration dropped substantially but the complexity of the ion chemistry increased [2]. Finally, by the early 1980s measurements of mass spectra were possible in the troposphere even at ground level where ions made up only about one part in 10^{17} air molecules [3] and the ion chemistry becomes more complex and variable. Initially, such measurements were focused on understanding the local ion chemistry, but soon such observations also became a tool for determining neutral concentrations. In some cases neutral concentrations were derived from models that used measured ambient ion concentration as an input [4]. New more precise and portable measurement techniques that constrained the ion chemistry and reaction time were also developed [5].

Negative ions and CIMS measurement of sulfuric acid

Measurements of sulfuric acid are a good example of one of these new techniques. Sulfuric acid is typically only present in the atmosphere at concentrations below 1 part per trillion by volume (pptv) and condenses on surfaces on contact. It is therefore best measured at ambient pressure where diffusion can limit wall contact and the number of ion-molecule collisions is large. The use of a highly selective ion molecule reaction to form a very stable ion product results in little to no chemical background signal. A proton exchange reaction between the reactant ion NO3- and gas phase H_2SO_4, where sulfuric acid is one of a small number of acids in the atmosphere (higher acidity than HNO3) that will transfer a proton to NO3-, is ideally suited to this measurement. Once formed the HSO_4^- core ion will not react further except to form clusters. Using the reaction geometry shown in figure 1, the product to reactant ion ratio along with a well defined reaction time, in this case about 0.1 s, provides a measure of sulfuric acid concentrations.

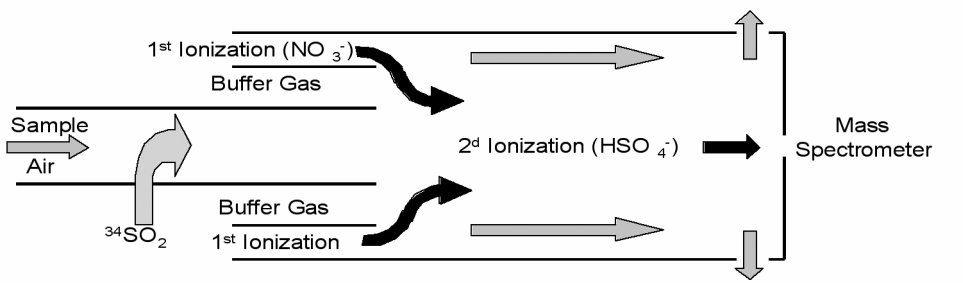

Figure 1: Geometry used to separate primary and secondary ionization for sulfuric acid and OH (SO_2 addition) measurements. Green and black arrows show neutral and ion motion respectively.

Chemical conversion followed by 2 stage CIMS to measure OH

A modification of the sulfuric acid measurement can then make possible a sensitive measure of the atmospheric OH radical. Sampling this radical involves some of the same difficulties encountered in the measurement of sulfuric acid, including concentrations only in the 1-10 ppqv range and rapid OH loss to sample tube walls, but in the case of OH the loss is by reaction rather than condensation. The OH measurement has the added problems that OH does not directly form an ion that is stable in sampled air and also OH can be formed at concentrations above ambient by the direct application of chemical ionization to an air sample. Chemically converting each OH molecule into one isotopically labeled sulfuric acid molecule as shown in equation 1 solves the first problem. The H_2SO_4 concentration, which is equal to the initial OH concentration, is then subsequently measured as described above. The latter problem of OH production by the CI process itself is largely solved by geometrically separating the neutral gas flow where the initial ionization takes place, i.e. where both NO_3^- and OH are formed, and the second ionization region where NO_3^- reacts with the sampled air containing $H_2{}^{34}SO_4$. Once NO_3^- is formed in the outermost gas flow as shown in figure 1, these ions, but not the neutral gas flow, are moved by electric fields to the central sampled air flow where OH is converted into H_2SO_4 and subsequently reacts with NO3- to form HSO_4^-. By adding additional steps (not shown) to this technique the measurement of HO_2 and RO_2 are also made possible.

(1) OH $+{}^{34}SO_2+M \rightarrow$ multi-step$\rightarrow H_2{}^{34}SO_4+M$

Multi-step ion chemistry to measure SO_2

Sulfur dioxide, a precursor of sulfuric acid, can be measured by several techniques, but one interesting method involves an O^- exchange from a compound such as CO_3^- to convert SO_2 into SO_3^-. A second stabilizing ion-molecule reaction between SO_3^- and O_2 then leads to the SO_5^- ion which is less likely to react further in sampled air prior to mass analyzes [6,7].

Positive ions and PTR-MS

PTR-MS is a powerful new tool which is capable of measuring a wide variety of organics and other compounds [8]. Water typically forms fairly stable ion clusters in the positive spectrum that can increase the proton affinity of a reactant ion sufficiently to prevent its reaction with most organics. The PTR-MS technique is unique in that it makes use of reduced pressure combined with ion drift/collisions in strong electric fields to minimize the attachment of water molecules to the reactant ion. This makes possible direct proton exchange between reactant ions such as H_3O^+ and a variety of organic compounds that have proton affinities above water but below that of water clusters. The sensitivity of PTR-MS is typically limited to the mid to high pptv range, and very low volatility/polar/sticky compounds are difficult to get into the instrument.

Proton-plus-water cluster transfer for low concentration/polar compounds

While PTR-MS largely avoids the problems caused by water clusters, there are many compounds including a number of organics that will react with a hydrated ion even though their proton affinity is below that of the ion cluster. For a number of fairly polar organics these reactions appear to proceed at atmospheric pressure by transferring a proton plus several water molecules to the polar organic. Presumably the proton affinity of the resulting organic/water cluster is higher than the initial water cluster alone. While more limited in application, this technique could offer

more sensitivity and less wall losses for the measurement of, for example, aerosol nucleation and growth precursors.

Ion cluster measurements and ion induced nucleation

While HSO_4^- appears to be a terminal ion species in the atmosphere, in the sense that it does not lose its charge to other compounds, it can continue to react by clustering, particularly with other acids. Under controlled conditions, this cluster formation processes can be used as a measurement technique where the concentration of a compound of interest which forms a cluster is determined from the concentration ratio of the ion cluster/reactant ion [9,10]. The atmosphere may carry this cluster growth one step further. It might use an ion's ability to stabilize molecular clusters to allow serial cluster growth resulting in clusters sufficiently large to form critical nuclei, i.e. clusters that even after they are neutralized, are sufficiently large/stable to grow into particles. The problems associated with studying this process are largely caused by the difficulty of mass identifying weakly bound ion clusters at ambient concentrations during short nucleation events.

Measurement of prenucleation neutral molecular clusters

The opposite problem exists for studying neutral clusters by CIMS. To measure neutral clusters using CIMS, ion induced clustering must be minimized and clearly separated from the process of neutral cluster charging. This can be accomplished by designing a measurement scheme where the interaction time between reactant ions and pre-existing neutral clusters can be varied over a wide range. This means that while the time available for charging any individual pre-existing neutral cluster varies, it varies in the same manner for all such clusters, thus the ratio of any two clusters charged by this technique should be time independent. This is not true for the serial growth of ion induced clusters, allowing their contribution to be separated out [11].

References

[1] R. S. Narcisi and A. D. Bailey, Mass Spectrometric Measurements of Positive Ions at Altitudes from 64 to 112 Km, Journal of Geophysical Research, 70, 3687-3700 (1965).

[2] F. Arnold, H. Bohringer, and G. Henschen, Composition measurements of stratospheric positive ions, Geophysical Research Letters, 5, 653-656 (1978).

[3] M. D. Perkins and F. L. Eisele, First Mass Spectrometric Measurements of Atmospheric Ions at Ground Level, Journal of Geophysical Research, 89, 9649-9657 (1984).

[4] F. Arnold, R. Fabian, G. Henschen, and W. Joos, Stratospheric trace gas analysis from ions: H_2O and HNO_3, Planetary and Space Science, 28, 681-685 (1980).

[5] F. L. Eisele and D. J. Tanner, Ion-assisted tropospheric OH measurements, Journal of Geophysical Research, 96, 9295-9308 (1991).

[6] F. L. Eisele and H. Berresheim, High-Pressure Chemical Ionization Flow Reactor for Real-Time Mass Spectrometric Detection of Sulfur Gases and Unsaturated Hydrocarbons in Air, Analytical Chemistry, 64, 283-288 (1992).

[7] O. Mohler, T. Reiner, and F. Arnold, The formation of SO_5^- by gas phase ion-molecule reactions, Journal of Chemical Physics, 97, 8233-8239 (1992).

[8] W. Lindinger, A. Hansel, and A. Jordan, Review On-line monitoring of volatile organic compounds at pptv levels by means of Proton-Transfer-Reaction Mass Spectrometry (PTR-MS) Medical applications, food control and environmental research, International Journal of Mass Spectrometry and Ion Processes, 173, 191-241 (1998).

[9] L. G. Huey, E. J. Dunlea, E. R. Lovejoy, D. R. Hanson, R. B. Norton, F. C. Fehsenfeld, and C. J. Howard, Fast time response measurements of HNO3 in air with a chemical ionization mass spectrometer, Journal of Geophysical Research, 103, 3355-3360 (1998).

[10] R. L. Mauldin III, D. J. Tanner, and F. L. Eisele, A New CIMS Technique for the Fast Measurement of Gas Phase Nitric Acid in the Atmosphere, Journal of Geophysical Research, 103, 3361-3367 (1998).

[11] F. L. Eisele and D. R. Hanson, First Measurements of Prenucleation Molecular Clusters, Journal of Physical Chemistry A, 104, 830-836 (2000).

2. Advanced Aerosol Characterization

Laboratory studies on the properties and processes of complex organic aerosols

Yinon Rudich[1], Elad Dinar[1], Ilya Taraniuk[1], Ali Abo Riziq[1], Ellen R. Graber2, Tatu Anttila[3], ‡ and Thomas Mentel[3]

[1]Department of Environmental Sciences, Weizmann Institute of Science, Rehovot 76100, Israel, yinon.rudich@weizmann.ac.il

[2]Institute of Soil, Water and Environmental Sciences, Volcani Center, A.R.O., Bet Dagan 50250, Israel

[3]Institute for Tropospheric Chemistry, Research Center Jülich, Jülich Germany

‡current address: Research and Development, Finnish Meteorological, Institute, 00101 Helsinki, Finland

Abstract

Aerosol particles affect climate in several direct and indirect manners. The direct climatic effect is via scattering and absorption of radiation and the indirect effect is mostly by affecting the properties of clouds and precipitation. These climatic effects impose one of the largest uncertainties in our understanding of the climate system. Recent studies have shown that organic matter, natural and anthropogenic, is dominating the tropospheric aerosol mass and affects its properties. We will discuss laboratory studies that focus on studying the properties and processes of organic aerosols especially their interaction with vapor pressure, physical properties, optical properties and density. We will emphasize the experimental approach and highlight the increased complexity of the studied systems.

Introduction

Atmospheric aerosols influence climate and human health on regional and global scales.[1-3] The climatic effect of aerosols is among the largest uncertainties in understanding Earth's climate and in predictions of future climatic changes.[4] Aerosols are also implicated in serious health consequences; however, the role of aerosol chemical composition in those health effects remains uncertain. Some aerosols are directly emitted from various stationary and mobile sources (***primary aerosols***) such as combustion and biomass burning,[5] vegetation,[6] ocean surfaces[7] and deserts.[8] Aerosol mass also forms in the atmosphere (***secondary aerosols, SOA***) through reactions that transform volatile organic and inorganic species into low vapor pressure compounds that can condense on existing particles. Organic particulate matter can also be directly emitted to the atmosphere, such as from the ocean surface or in biogenic aerosols.[7,11] In many environments, a major fraction of the particulate mass is composed of organic compounds.[12,13] These organics significantly influence aerosol properties; therefore they directly modulate the role aerosols play in the environment.

More then 4 decades ago, Went [14] suggested that photochemical oxidation of primary volatile and semivolatile organic compounds can produce secondary polymers of high carbon content that

may be involved in cloud droplet and haze particle formation. Recent studies of rural and urban particles [15,16], fogwater [17], marine particulate samples [18], and biomass burning aerosols [19] concluded that 20 to 70 wt% of the WSOC fraction consists of high molecular weight polycarboxylic acids [20]. These compounds, consisting of a heterogeneous mixture of structures containing aromatic, phenolic and acidic functional groups [16,21-23], have certain similarities to humic substances (HS) from terrestrial and aquatic sources. Therefore, these aerosol-associated compounds are referred to in the atmospheric chemistry literature as HUmic-LIke Substances (HULIS). Accumulating evidence shows that HULIS may form in atmospheric particulate matter via photooxidation of primary biogenic and anthropogenic precursors, or may be directly emitted from soils, vegetation, biomass burning and soot automotive exhaust [24-26].

In this talk we will describe laboratory experiments with aerosols that contain significant amounts of complex organic matter. The goal of these experiments is to better understand the physical and chemical properties of these aerosols and their processes, aiming at getting a better model of the atmospheric system. Specifically we will describe experiments which contain actual atmospheric HULIS as well ad biogenic aerosols.

Experimental Methods

We will describe several experiments with humidity tandem DMA (HTDMS), with cloud simulation chamber and with cavity ring down spectrometer aiming at measuring the CCN activity, hygroscopic growth and optical properties of organic aerosols.[27-29] In addition we will describe recent experiments in plant simulation chambers. We have used several different aerosol types in these experiments:

1. Aerosols containing HULIS extracts from collected aerosol particles. The samples are composed of HULIS from fresh and aged smoke particles a swell as those extracted from pollution aerosols. The aerosols were compared to the behavior of aerosols composed of molecular weight fractionated Suwanee River Fuulvic Acid (SRFA).
2. Single component organic aerosol generated by nebulizing aqueous solutions of the studied compounds.
3. Mixtures of organic and inorganic aerosols.
4. Organic aerosols that formed by photochemical oxidation of biogenic organic compounds emitted from plants in a simulation chamber.

Results and Discussion

We studied the activation to cloud droplets and hygroscopic growth of aerosols containing atmospheric HULIS extracted from fresh, aged and pollution particles and compared their activation to size fractionated Suwannee River fulvic acid, and correlated it to the estimated molecular weight and measured surface tension. A correlation was found between CCN-activation diameter of SRFA fractions and number average molecular weight of the fraction. The lower molecular weight fractions activated at lower critical diameters, which is explained by the greater number of solute species in the droplet with decreasing molecular weight. The three aerosol-extracted HULIS samples activated at lower diameters than any of the size-fractionated or bulk SRFA. By considering number average molecular weight (M_N), measured surface tension

(ST) and activation diameters, the Köhler model was found to account for activation diameters, provided that accurate physico-chemical parameters are known.

Cavity ring down (CRD) spectrometry was used for measuring the optical properties of pure and mixed laboratory-generated aerosols. The extinction coefficient (α_{ext}), extinction cross section (σ_{ext}) and extinction efficiency (Q_{ext}) were measured for polystyrene spheres (PSS), ammonium sulphate ($(NH_4)_2(SO_4)$), sodium chloride (NaCl), glutaric acid (GA), and Rhodamine-590 aerosols. The refractive indices of the different aerosols were retrieved by comparing the measured extinction efficiency of each aerosol type to the extinction predicted by Mie theory. Aerosols composed of sodium chloride and glutaric acid in different mixing ratios were used as model for mixed aerosols of two non-absorbing materials, and their extinction and complex refractive index were derived. Aerosols composed of Rhodamine-590 and ammonium sulphate in different mixing ratios were used as model for mixing of absorbing and non-absorbing species, and their optical properties were derived. The refractive indices of the mixed aerosols were also calculated by various optical mixing rules and a core plus shell Mie model. We found that for non-absorbing mixtures, the mixing rules calculations give comparable results, with the linear mixing rule giving a slightly better fit than the others. For absorbing mixtures, the differences between the refractive indices calculated using the mixing rules and those retrieved by CRD are generally higher.

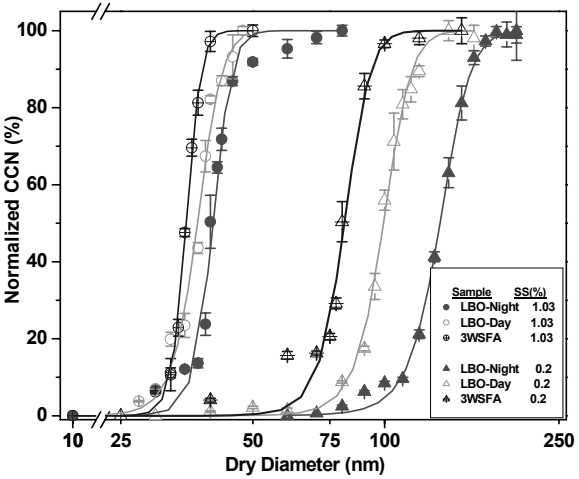

Figure 1: Activation experiments with extracted HULIS under super saturation conditions of 0.2 and 1.03%. Experiments were carried out by atomizing solution of HULIS extracted from collected wood burning smoke particles.

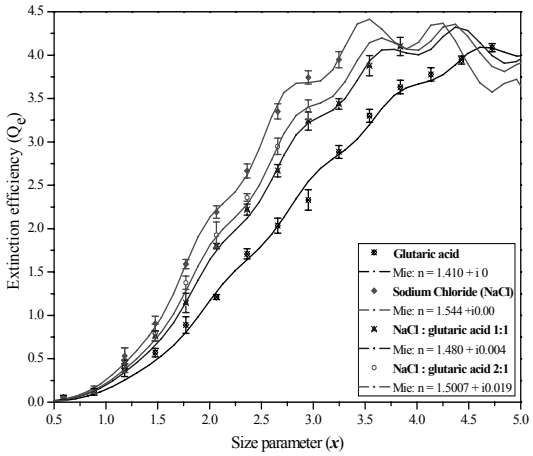

Figure 2: Extinction efficiency (Qext) as a function of size parameter (x) obtained for sodium chloride, glutaric acid, and their mixtures. The solid curves are the result of the Mie fit to the experimental points.

References

[1] Ramanathan, V.; Crutzen, P. J.; Kiehl, J. T.; Rosenfeld, D. *Science* 2001, *294*, 2119.

[2] Kaufman, Y. J.; Tanre, D.; Boucher, O. *Nature* 2002, *419*, 215.

[3] Lelieveld, J.; Crutzen, P. J.; Ramanathan, V.; Andreae, M. O.; Brenninkmeijer, C. A. M.; Campos, T.; Cass, G. R.; Dickerson, R. R.; Fischer, H.; de Gouw, J. A.; Hansel, A.; Jefferson, A.; Kley, D.; de Laat, A. T. J.; Lal, S.; Lawrence, M. G.; Lobert, J. M.; Mayol-Bracero, O. L.; Mitra, A. P.; Novakov, T.; Oltmans, S. J.; Prather, K. A.; Reiner, T.; Rodhe, H.; Scheeren, H. A.; Sikka, D.; Williams, J. *Science* 2001, *291*, 1031.

[4] Houghton, J. T.; Ding, Y. *Climate Change 2001: The Scientific Basis*, 2001.

[5] Andreae, M. O.; Rosenfeld, D.; Artaxo, P.; Costa, A. A.; Frank, G. P.; Longo, K. M.; Silva-Dias, M. A. F. *Science* 2004, *303*, 1337.

[6] Andreae, M. O.; Crutzen, P. J. *Science* 1997, *276*, 1052.

[7] Tervahattu, H.; Hartonen, K.; Kerminen, V. M.; Kupiainen, K.; Aarnio, P.; Koskentalo, T.; Tuck, A. F.; Vaida, V. *J. Geophys. Res.* 2002, *107*, art. no.

[8] Prospero, J. M. *Proc. Natl. Acad. Sci. USA* 1999, *96*, 3396.

[9] Kulmala, M. *Science* 2003, *302*, 1000.

[10] Zhang, Q.; Worsnop, D. R.; Canagaratna, M. R.; Jimenez, J. L. *Atmos. Chem. Phys.* 2005, *5*, 3289.

[11] Ellison, G. B.; Tuck, A. F.; Vaida, V. *J. Geophys. Res.* 1999, *104*, 11633.

[12] Jacobson, M. C.; Hansson, H. C.; Noone, K. J.; Charlson, R. J. *Rev. Geophys.* 2000, *38*, 267.

[13] Kanakidou, M.; Seinfeld, J. H.; Pandis, S. N.; Barnes, I.; Dentener, F. J.; Facchini, M. C.; Van Dingenen, R.; Ervens, B.; Nenes, A.; Nielsen, C. J.; Swietlicki, E.; Putaud, J. P.; Balkanski, Y.; Fuzzi, S.; Horth, J.; Moortgat, G. K.; Winterhalter, R.; Myhre, C. E. L.; Tsigaridis, K.; Vignati, E.; Stephanou, E. G.; Wilson, J. *Atmos. Chem. Phys.* 2005, *5*, 1053.

[14] Went, F. W. *Nature* 1960, *187*, 641.

[15] Samburova, V.; Szidat, S.; Hueglin, C.; Fisseha, R.; Baltensperger, U.; Zenobi, R.; Kalberer, M. *J. Geophys. Res.* 2005, *110*.

[16] Decesari, S.; Facchini, M. C.; Matta, E.; Lettini, F.; Mircea, M.; Fuzzi, S.; Tagliavini, E.; Putaud, J. P. *Atmos. Environ.* 2001, *35*, 3691.

[17] Krivacsy, Z.; Kiss, G.; Varga, B.; Galambos, I.; Sarvari, Z.; Gelencser, A.; Molnar, A.; Fuzzi, S.; Facchini, M. C.; Zappoli, S.; Andracchio, A.; Alsberg, T.; Hansson, H. C.; Persson, L. *Atmos. Environ.* 2000, *34*, 4273.

[18] Tervahattu, H.; Juhanoja, J.; Kupiainen, K. *J. Geophys. Res.* 2002, *107*, art. no.

[19] Hoffer, A.; A. Gelencser; P. Guyon; G. Kiss; O. Schmid; G. Frank; P. Artaxo; Andreae., M. O. *Atmos. Chem. Phys. Discuss.* 2005, *5*, 7341–7360.

[20] Graber, E. R.; Rudich, Y. *Atmos. Chem. Phys.* 2006, *6*, 729.

[21] Varga, B.; Kiss, G.; Ganszky, I.; Gelencser, A.; Krivacsy, Z. *Talanta* 2001, *55*, 561.

[22] Kiss, G.; Varga, B.; Galambos, I.; Ganszky, I. *J. Geophys. Res.* 2002, *107*, 8339.

[23] Gysel, M.; Weingartner, E.; Nyeki, S.; Paulsen, D.; Baltensperger, U.; Galambos, I.; Kiss, G. *Atmos. Chem. Phys.* 2004, *4*, 35.

[24] Kalberer, M.; Paulsen, D.; Sax, M.; Steinbacher, M.; Dommen, J.; Prevot, A. S. H.; Fisseha, R.; Weingartner, E.; Frankevich, V.; Zenobi, R.; Baltensperger, U. *Science* 2004, *303*, 1659.

[25] Hoffer, A.; Kiss, G.; Blazso, M.; Gelencser, A. *Geophys. Res. Lett.* 2004, *31*, L06115.

[26] Gao, S.; Ng, N. L.; Keywood, M.; Varutbangkul, V.; Bahreini, R.; Nenes, A.; He, J. W.; Yoo, K. Y.; Beauchamp, J. L.; Hodyss, R. P.; Flagan, R. C.; Seinfeld, J. H. *Environ. Sci. Tech.* 2004, *38*, 6582.

[27] Dinar, E.; Mentel, T. F.; Rudich, Y. *Atmos. Chem. Phys.* 2006, *in press*.

[28] Dinar, E.; Taraniuk, I.; Graber, E. R.; Anttila, T.; Mentel, T. F.; Rudich, Y. *J. Geophys. Res.* 2006, *In press*.

[29] Dinar, E.; Taraniuk, I.; Graber, E. R.; Katsman, S.; Moise, T.; Anttila, T.; Mentel, T. F.; Rudich, Y. *Atmos. Chem. Phys.* 2006, *6*, 2465.

On-line characterisation of gaseous and particulate organic analytes using atmospheric pressure chemical ionisation mass spectrometry

Thorsten Hoffmann[1], Jörg Warnke[1], Christopher Reinnig[1], Rolf Bandur[2], Sven Hoffmann[2], Bettina Warscheid[2]

[1] *Institute of Inorganic and Analytical Chemistry, Johannes Gutenberg-University Mainz, Germany, t.hoffmann@uni-mainz.de*

[2] *Institute of Analytical Sciences Dortmund, Germany*

Abstract

A modified atmospheric pressure chemical ionisation ion source is applied for direct analysis of volatile or low volatile organic compounds in air. The method is based on the direct introduction of the analytes in the gas phase and/or particle phase into the ion source of an commercial ion-trap mass spectrometer. Using corona discharge for the production of primary ions we demonstrate the analytical potential of on-line atmospheric pressure chemical ionisation mass spectrometry for reaction monitoring experiments. To do so, atmospherically relevant gas phase reaction are carried out in a 500 L reaction chamber and gaseous and particulate compounds are monitored in the positive and negative ion mode of the mass spectrometer. MS/MS experiments are used to identify the organic products. The technique was applied to several reaction system, e.g. for the identification of oligomeric products formed in secondary organic aerosol systems.

Introduction

Gaseous and particulate organic compounds represent key species for the understanding and control of a variety of technical and environmental processes. Areas such as industrial process analysis, medical or environmental research rely on development of analytical techniques to monitor trace amounts of organic species in complex matrices with a high time resolution. In this context, environmental chemistry is an especially challenging field, since not only hundreds of different organic compounds are emitted into the atmosphere by anthropogenic or natural sources, which directly effect air quality and impact the tropospheric oxidation capacity, but these compounds also go through several oxidation processes - which enhances the complexity of the analytical problem. For example, the reaction of volatile organic compounds (VOCs) with atmospheric oxidising species (ozone, OH-radicals) leads to the formation of less volatile products that can undergo phase transition (gas-to-particle conversion). Since often the individual concentrations of the analytes have to be known in both phases, e.g. for toxicologic or climate related studies, the necessity to differentiate between gas and particle phase further adds to the analytical challenge.

Often off-line techniques are applied for the identification and quantification of organic compounds in the gas or particle phase. However, the main drawbacks of applying off-line techniques are the high time consumption per analysis and an enhanced risk of positive or

negative artefacts during the multistep analytical procedure. Therefore, several alternative analytical approaches have been applied to improve the analysis of airborne organic compounds.

The analytical technique presented here is based on the application of a benchtop MS instrument with an atmospheric pressure inlet equipped with a modified ion source. Atmospheric pressure ionisation techniques (API) are used to enable the analysis of compounds in the gas and particle phase. Corona discharge is a widely used technique for the production of primary ions at atmospheric pressure when liquid chromatography is coupled with mass spectrometry and a number of atmospheric pressure chemical ionisation (APCI) interfaces for different mass analysers are commercially available. The technique represents a soft ionisation method, where fragmention of the analyte molecules plays a minor role and mostly intents molecular are observed. For LC-APCI-MS applications, an electrical potential (1.5 – 5 kV) is applied between a metal tip (corona discharge needle) and a metal plate, in which the inlet to the mass spectrometer is located. The extremely inhomogeneous electrical field that is formed between the needle and the plate induces a discharge current, which finally leads to the formation of primary ions, such as N_2^+, O_2^+ or, if traces of water are present, H_3O^+. Similarly, also negative primary ions, e.g. O_2^-, are formed in the discharge region. These primary ions finally react with the analyte molecules, often by proton-exchange reactions (proton-transfer or proton abstraction), and finally produce quasimolecular analyte ions, such as $[M+H]^+$ or $[M-H]^-$, in the atmospheric pressure region of the ion source.

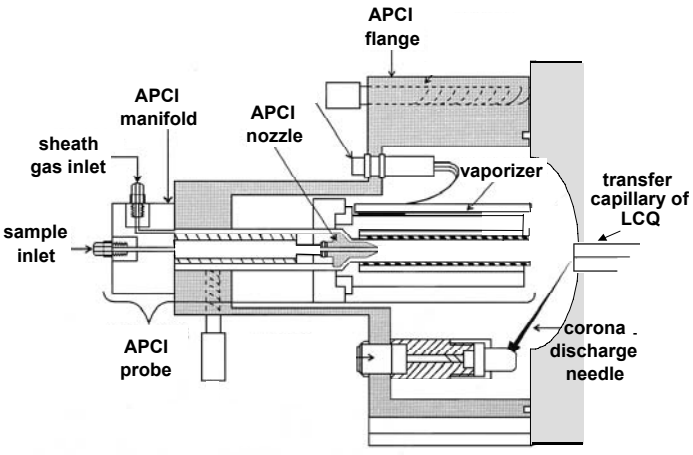

Figure 1: Schematic diagram of the experimental setup used for the on-line APCI (Atmospheric Pressure Chemical Ionisation) measurements employing corona discharge as a source for primary ions.

Experimental Methods

All experiments were performed using a Finnigan LCQ ion-trap mass spectrometer (”LCQ classic”, Thermo Finnigan, San Jose, CA) with a commercial ion transfer system for atmospheric pressure applications. For on-line APCI-MS the mass spectrometer was operated in the positive or negative ion mode. The sheath flow inlet and regulation system is part of the standard ion source for LC/MS-coupling, usually used for nebulisation of the LC-eluent. To adapt the ion source to the sample inlet system, the original APCI-source was modified by changing gas and analyte inlet lines. A sketch of the adapted APCI-source used is shown in Figure 1. Details on the ion source construction are given in Ref. [1] and [2]. The following APCI-source parameters were adjusted to ensure optimal vaporisation and ionisation conditions for analytes in air: vaporiser temperature 450°C, corona discharge voltage 3 kV, plasma current 3 µA. Capillary voltage and capillary temperature were adjusted to 6 V and 200°C, respectively.

Results and Discussions

An important advantage of APCI-MS applied as an on-line technique is its high time resolution of about 1 s. This analytical technique can therefore serve as an important tool to receive reliable information on the product distribution under rapidly changing reaction conditions. In addition, certain physico-chemical properties of compounds in air, e.g. their distribution between the gas and aerosol phase can promptly be investigated by using on-line APCI-ITMS. To demonstrate the analytical potential of APCI-MS, the formation of a C_{10}-keto-aldehyde from the gas phase ozonolysis of a biogenic VOC (alpha-pinene) is investigated here by on-line APCI-MS.

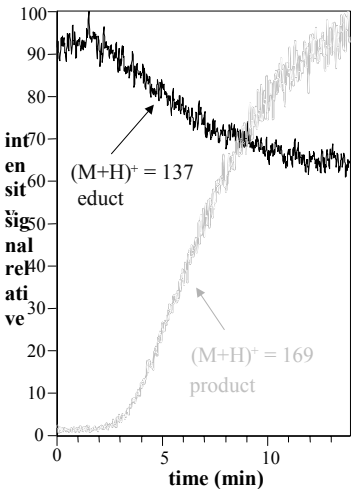

Figure 2: Positive ion traces of educt (m/z 137) and product ions (m/z 169) after starting gas phase ozonolysis by mixing ozone into the hydrocarbon filled reaction chamber at t = 2.

Figure 2 shows traces of both $[M+H]^+$ ions of the educt alpha-pinene (m/z 137) and the product pinonaldehyde (m/z 169). As can be seen in the figure, after the introduction of ozone into the

chamber an instantaneous decrease of the signal intensity of the educt as well as the of the reaction product is clearly visible. After about 3 min the product pinonaldehyde was observed.

The example discussed above demonstrate that a modified atmospheric pressure chemical ionisation source can be utilised to perform real-time measurements of gaseous organic compounds. However, using an activated charcoal diffusion denuder (efficiency > 0.99) in front of the ion source to remove gas phase hydrocarbons, also the chemical composition of organic aerosol particles can be investigated by the mass spectrometric on-line system. The consecutive measurement with and without the denuder enables the investigation of gas/particle partitioning of the individual compounds.

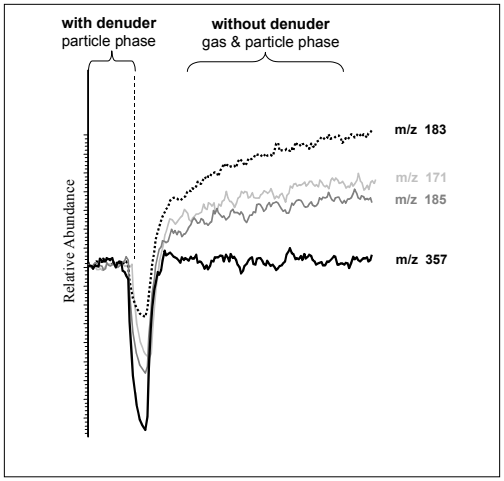

Figure 3: Positive ion traces of educt (m/z 137) and product ions (m/z 139) after starting gas phase ozonolysis by mixing ozone into the hydrocarbon filled reaction chamber at t = 2.

As an example, Figure 3 shows the mass traces of selected m/z-ratios from the alpha-pinene-ozone-reaction system. The mass traces shown were recorded in the negative ion mode. The measurements were performed in a dynamic reaction chamber when the reaction reached steady-state conditions. To illustrate the relative distribution of the individual compounds between gas and particle phase, the intensity of the 4 mass-to-charge ratios were normalisied to the same value when the denuder was installed. After removing the denuder, the intensity of the organic acids with a lower molecular weight (m/z 171, 183, 185) immediately increased, demonstrating that an additional amount of these compounds reach the MS when also the gas phase was allowed to enter the ion source. M/z 183 is a keto-carboxylic acid, m/z 171 and m/z 185 are diacids, thus explaining the relative behaviour of these 3 acids. The exact structure of m/z 357 is still not completely understood, however, it is obviously a very low volatile compounds (dimerisation product) that is only present in the particle phase.

References

[1] B. Warscheid and T. Hoffmann, Direct analysis of highly oxidised organic aerosol constituents by on-line ion trap mass spectrometry in the negative ion mode, Rapid Commun. Mass Spectrom. 16, 496-504, (2002).

[2] T. Hoffmann, R. Bandur, S. Hoffmann and B. Warscheid, On-line characterisation of gaseous and particulate organic analytes using atmospheric pressure chemical ionisation mass spectrometry, Spectrochimica Acta B 57, 1635-1648, (2002).

Development and first deployment of an aerosol collection/thermal-desorption PTR-ITMS instrument for the measurement of aerosol organic species

Troy Thornberry[1,2], Daniel M. Murphy[1], David S. Thomson[1,2], and Edward R. Lovejoy[1]

[1] NOAA Earth System Research Laboratory, Boulder, Colorado, USA, troy.thornberry@noaa.gov

[2] Cooperative Institute for Research in Environmental Sciences, University of Colorado, Boulder, Colorado, USA

Abstract

A new instrument that utilizes the PTR-MS technique to probe the organic composition of atmospheric aerosols has been developed. Aerosols are collected by impaction and then thermally desorbed into a carrier gas that transports the organic analyte molecules into the drift tube. Ions are detected using an ion trap mass spectrometer. The instrument was deployed for the first time during summer 2006 in the Texas Air Quality Study aboard R.V. *Ronald H. Brown.*

Introduction

Organic material has been observed to comprise a significant fraction of aerosol mass in many regions of the troposphere [1,2], but detailed measurements of the individual species that comprise the organic fraction have been limited in spatial extent and temporal resolution [3]. The organic compounds that make up the organic fraction of atmospheric aerosol have the potential to affect the radiative and microphysical properties of the aerosol, with concomitant impacts on the role of the aerosol in climate forcing through direct and indirect effects [4,5]. Knowledge of the organic species present in atmospheric aerosols is needed to understand their effect on aerosol properties as well as to resolve outstanding questions about important organic aerosol sources and formation mechanisms [6-8], and to elucidate the role of aerosols in the chemistry of the atmosphere through their interaction with gas-phase compounds [9,10]. The measurement of aerosol organic compounds poses a significant experimental challenge due to the complexity and large number of organic species, and the low concentration at which individual species are present. The PTR-MS technique has proved to be a useful tool in the study of atmospherically important volatile organic compounds (VOCs). Its ability to sensitively detect and quantify the concentrations of many common VOCs has led to an increased understanding of the sources, transport, chemical transformations, and losses processes of these compounds through both laboratory and field experiments [11]. A logical extension of the technique is application to semi-volatile and condensed-phase organic species in the atmosphere. This has previously been implemented in laboratory and smog chamber settings [12,13], but has not generally had sufficient sensitivity for ambient measurements.

Experimental Methods

This work describes the development of a new instrument that uses the PTR-MS method to attempt to speciate the organic compounds present in ambient atmospheric aerosol. A schematic of the instrument as it was recently deployed is shown in Figure 1.

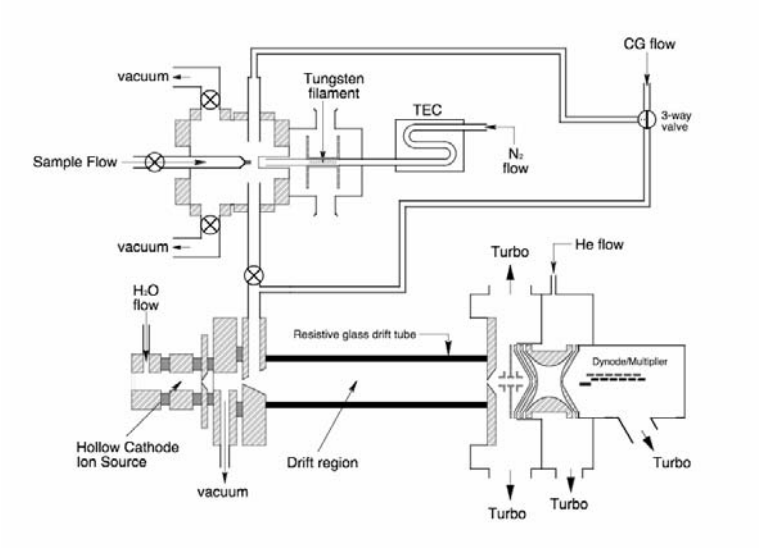

Figure 1: Schematic of the AOS-PTR-ITMS instrument showing the aerosol collection/desorption chamber and the PTR-ITMS with resistive glass drift tube.

Aerosol Collection/Desorption

In order to reach a desired sensitivity for individual organic species in the low ng m^{-3} range, aerosol collection was used to concentrate aerosol mass for analysis. Aerosol collection was accomplished by direct impaction of aerosols in a ~1.5 standard liter per minute (slpm) sample flow onto a cooled target. The aerosol inlet chamber, transfer line, and drift tube were all heated to > 135°C to reduce adsorption of desorbed compounds. The aerosol target was cooled to ambient/sub-ambient temperature by flowing nitrogen gas that had been passed through a thermoelectric cooler against the reverse side of the target. To desorb the organic material, the temperature of the aerosol target was rapidly raised (~ 10 sec) to 150-160°C by heating the nitrogen stream resistively with a tungsten coil. The efficiency of the aerosol collection as a function of aerosol diameter is dependent on the nozzle geometry. During the TexAQS study, the nozzle used was circular with a diameter of 0.5 mm. This led to a small size cut-point near 500 nm. The presence of an upstream 1 μm cut-point impactor meant that the sampled aerosol size range was only 0.5-1 μm.

PTR-ITMS

The PTR-ITMS instrument developed here is similar to the ion trap based PTR-MS instrument previously reported by Warneke et al. [14] with several modifications. The drift tube used was a single piece resistive lead glass tube (Burle Electro-Optics, Inc., Sturbridge, MA, USA), 25 cm long with an ID of 2.35 cm. The increased length required a higher voltage be applied to the inlet end of the drift tube in order to achieve declustering, however the increase required was significantly reduced when the drift tube was heated. The use of an ion trap as the mass spectrometric analyzer was dictated by the goal of continuously measuring the entire mass spectrum while desorbing the analytes rapidly in order to maximize the concentration in the carrier gas and shorten the sampling/analysis cycle time. The upper limit of the ion trap mass scan was 367 Thomsons.

Operation During TexAQS

During the recent deployment on board R.V. *Ronald H. Brown*, the instrument was operated on an alternating cycle of one ten-minute ambient sample and one five-minute background sample with the sample valve closed. The need for the frequent background determinations was motivated by high instrumental background signals arising from the presence of rubber seals in the heated inlet chamber, transfer line, and drift tube. The difference between sample and background conditions resulted in some masses having negative baselines.

Results and Summary

Much of the time during the TexAQS campaign a combination of low sub-micron particle number (often ~ 300 cm^{-3}) or a small size distribution (aerosol mass mode ~100 nm) resulted in undetectably low levels of aerosol organics in the particle size range sampled. Signals significantly above detection limit were observed during several periods when aerosol loading increased in the 0.5-1 μm size range and AMS measurements indicated appreciable organic mass. One interval was an extended period from August 30 – September 4 with a high photochemistry episode occurring on September 2. Time series for several different masses are shown in Figure 2

for this period. The different masses are seen to exhibit significantly different temporal behaviors indicating varying composition of the aerosol organic fraction. These results and instrument performance will be presented.

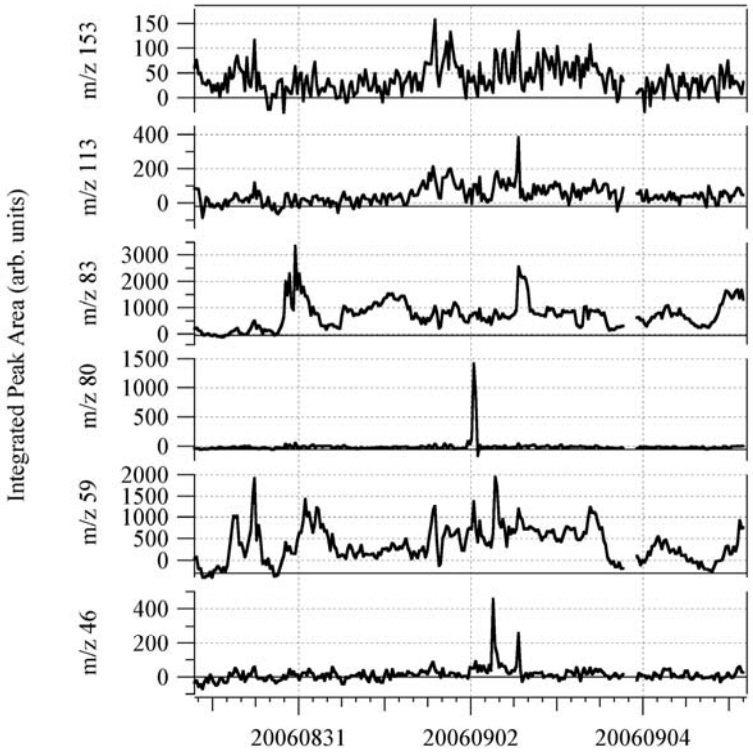

Figure 2: Time series of several masses observed by the AOS-PTR-ITMS during its initial deployment aboard R.V. Ronald. H. Brown during the summer 2006 TexAQS campaign.

References

[1] J. H. Seinfeld and J. F. Pankow, Organic atmospheric particulate material, Ann. Rev. Phys. Chem. 54, 121-140 (2003).

[2] D. M. Murphy, et al., Single-particle mass spectrometry of tropospheric aerosol particles, J. Geophys. Res.-Atmospheres 111, Art. No. D23S32 (2006).

[3] S. Fuzzi, et al., Critical assessment of the current state of scientific knowledge, terminology, and research needs concerning the role of organic aerosols in the atmosphere, climate, and global change, Atmos. Chem. Phys. 6, 2017-2038, (2006).

[4] T. Novakov and J. E. Penner, Large contribution of organic aerosols to cloud-condensation-nuclei concentrations, Nature 365, 823-826, (1993).

[5] U. Lohmann, and C. Leck, Importance of submicron surface-active organic aerosols for pristine Arctic clouds, Tellus B 57, 261-268, (2005).

[6] R. Volkamer, et al., Secondary organic aerosol formation from anthropogenic air pollution: Rapid and higher than expected, Geophys. Res. Lett. 33, Art. No. L17811, (2006).

[7] C. L. Heald, et al., A large organic aerosol source in the free troposphere missing from current models, Geophy. Res. Lett., 32, Art. No. L18809, (2005).

[8] M. Kalberer, M. Sax, and V. Samburova, Molecular Size Evolution of Oligomers in Organic Aerosols Collected in Urban Atmospheres and Generated in a Smog Chamber, Env. Sci. Tech. 40, 5917-5922, (2006).

[9] C. L. Badger, et al., Reactive uptake of N_2O_5 by aerosol particles containing mixtures of humic acid and ammonium sulfate, J. Phys. Chem. A, 110, 6986-6994, (2006).

[10] D. G. Nash, M. P. Tolocka, and T. Baer, The uptake of O-3 by myristic acid-oleic acid mixed particles: evidence for solid surface layers, PCCP 8, 4468-4475, (2006).

[11] J. A. de Gouw and C. Warneke, Measurements of volatile organic compounds in the Earth's atmosphere using proton-transfer–reaction mass spectrometry, Mass Spec. Rev., in press.

[12] J. D. Hearn and G. D. Smith, A chemical ionization mass spectrometry method for the online analysis of organic aerosols, Anal. Chem. 76, 2820-2826, (2004).

[13] J. Dommen, A. Gascho, M. Steinbacher, Measurement of gas phase and aerosol composition in a smog chamber with a PTR-MS, presented at the 2nd International Conference on Proton Transfer Reaction Mass Spectrometry and Its Applications, (2005).

[14] C. Warneke, J. A. de Gouw, E. R. Lovejoy, P. C. Murphy, and R. Fall, Development of proton-transfer ion trap-mass spectrometry: On-line detection and identification of volatile organic compounds in air, J. Am. Soc. Mass Spec. 16, 1316-1324, (2005).

Secondary organic aerosol formation from isoprene: results from laboratory and field experiments

Magda Claeys

University of Antwerp (Campus Drie Eiken), Department of Pharmaceutical Sciences, Universiteitsplein 1, BE-2610 Antwerp, Belgium magda.claeys@ua.ac.be

Abstract

For a long time it was thought that isoprene, which is emitted in large amounts by the terrestrial vegetation (estimated at about 500 Tg/year on a global scale) does not give rise to secondary organic aerosol (SOA) formation. However, recent field observations of certain aerosol compounds, i.e., diastereoisomeric 2-methyltetrols and 2-methylglyceric acid, attributable to isoprene oxidation, and the experimental observation that isoprene under highly acidic conditions can lead to the formation of oligomeric, humic-like substances through heterogeneous reactions, re-opened the issue of SOA formation from isoprene. In this lecture, results will be presented from recent laboratory chamber studies that were performed in collaboration with the groups of J. Seinfeld (California Institute of Technology, Pasadena, CA, USA) and E. Edney and T. Kleindienst (US Environmental Protection Agency, Research Triangle Park, NC, USA).

In a first study [1], the chemical composition of SOA from the photooxidation of isoprene under different NO_x conditions was studied using a wide range of mass spectral techniques. Oligomerization was observed to be an important SOA formation pathway in all cases; however, the nature of the oligomers depends strongly on the NO_x level, with acidic products formed under high NO_x conditions only. Evidence is presented of particle-phase esterification reactions in SOA, where the further oxidation of the isoprene gas-phase oxidation product methacrolein under high-NO_x conditions produces oligoesters containing 2-methylglyceric acid as a key monomeric unit. Under low-NO_x conditions hemiacetal dimers are formed from C_5 alkene triols and 2-methyltetrols; these compounds are also found in Amazonian wet season aerosol, demonstrating the atmospheric relevance of these low-NO_x chamber experiments.

In a second study [2], the chemical composition of SOA from the photooxidation of isoprene, in the presence or absence of sulfate seed aerosol, is investigated using electrospray-mass spectrometry techniques. Evidence is presented for the formation of sulfate esters of 2-methyltetrols, 2-methyltetrol nitrate derivatives, and 2-methylglyceric acid. These compounds are also found in ambient aerosol collected at several locations in the southeastern U.S. and at K-puszta, Hungary. It is likely that this pathway is important in the formation of humic-like substances in ambient aerosol.

References

[1] J.D. Surratt, S.M. Murphy, J.H. Kroll, N.L. Ng, L. Hildebrandt, A. Sorooshian, R. Szmigielski, R. Vermeylen, W. Maenhaut, M. Claeys, R.C. Flagan, and J.H. Seinfeld, Chemical composition of secondary organic aerosol formed from the photooxidation of isoprene, Journal of Physical Chemistry A 110, 9665-9690 (2006).

[2] J.D. Surratt, J.H. Kroll, T.E. Kleindienst, E.O. Edney, M. Claeys, A. Sorooshian, N.L. Ng, J.H. Offenberg, M. Lewandowski, M. Jaoui, R.C. Flagan, and J.H. Seinfeld, Evidence for organosulfates in secondary organic aerosol, Environmental Science and Technology, in press.

Examples of particle analysis by mass spectrometry from PSI smog chamber experiments

J. Dommen[1], A. Metzger[1], A. Gascho[1], K. Gaeggeler[1], M.R. Alfarra[1], A.S.H. Prevot[1], M. Kalberer[2], D. Gross[3], A. Brunner[4] and U. Baltensperger[1]

[1] Paul Scherrer Institut, Laboratory of Atmospheric Chemistry, CH-5232 Villigen, Switzerland, josef.dommen@psi.ch

[2] Department of Chemistry and Applied Biosciences, ETH Zurich, CH-8092 Zurich, Switzerland

[3] Department of Chemistry, Carleton College, Northfield, Minnesota 55126, USA

[4] Research Station Agroscope Reckenholz-Tänikon ART, Zürich, Switzerland

Abstract

Mass spectrometry has evolved as a strong tool for the characterization of atmospheric aerosols. Smog chamber experiments are often used to test new instrumentation and investigate aerosol formation under controlled conditions. Several different mass spectrometric techniques were operated at the PSI smog chamber to measure the gas and particle phase of photooxidation reaction systems with different precursors. We present here the measurement capabilities of various mass spectrometers used to measure the particle phase and compare the results obtained. For higher mass peaks the off-line laser desorption/ionization MS and the on-line TSI single particle Aerosol Time of Flight MS matched up quite well. With a modified version of the IONICON PTR-MS semi-volatile species from the particle phase were measured. Aerosols were also trapped directly on a pre-concentration trap of a GC and then measured with a GC-PTR-MS. This allowed to differentiate between isobaric masses and observe their partitioning behavior.

Introduction

Ambient aerosol particles have a variety of important impacts; visibility reduction, impacts on climate and adverse health effects. These effects are governed by their chemical composition and physical properties. Organic compounds account for 20-90 % of the total fine particle mass concentration in a wide variety of atmospheric environments [1]. The formation of secondary organic aerosol (SOA) has recently received much attention. It has been estimated that the major SOA precursors are biogenic origin but anthropogenic contribution to SOA formation can be important in polluted regions [1]. Isoprene, monoterpenes and sesquiterpenes, are believed to have an important role in SOA formation in rural and remote areas [2, 3, 4], but in urban areas aromatic hydrocarbons play a significant or even dominant role [5]. SOA is formed from reactions of volatile organic compounds with hydroxyl radicals, ozone and nitrate radicals where the resultant low vapor pressure oxidation products partition between gas and aerosol phase.

Compounds identified so far from the organic fraction of the particles are mainly oxygenated compounds like aldehydes, ketones and organic acids, e.g. [6, 7]. Recent studies have shown that a substantial fraction of organic aerosol mass is composed of oligomers [8, 9]. The heterogeneous

reactions of relatively volatile carbonyls in the aerosol phase are estimated to have great importance on the formation of high molecular weight products via oligomerization [8, 10]. Surratt et al. [9] proposed that under high-NOx conditions particle phase esterification is a key process in oligomerization while under low-NOx conditions organic peroxides may contribute significantly. However, this fraction of organic aerosol mass and the process of oligomerization is not well understood. It is expected that oligomerization reactions affect a number of other aerosol properties such as optical parameters, hygroscopic growth, and cloud condensation nuclei potential, which is crucial for the role of aerosol in the global climate change. The composition of SOA on the molecular level is difficult to analyze, and traditional studies are only able to resolve a small fraction of the entire organic particle mass. Chemical mechanisms associated with SOA formation are also still poorly understood. One of the main reasons for this is that traditional methods for organic particle analysis, such as filter or impactor sampling with subsequent solvent extraction and gas chromatography/mass spectrometry for compound separation and identification, are very time-consuming and are unable to provide sensitivity and time resolution needed to study aerosol formation in detail.

Recently, fast online methods for VOC determinations in particles by mass spectrometric methods have been developed. At the PSI smog chamber several research groups gathered to perform joint experiments with such new instruments. The goal of this effort was to test the potential of various mass spectrometric techniques for the investigation of the chemical composition of SOA and the formation of oligomers therein.

The presentation will give an overview of some measurements and present first results. The focus will lie on a comparison of the different techniques.

Experimental Methods

The following instruments/systems were involved:

(MA)LDI-MS

SOA particles were sampled on impactor plates for 1-4 h. After sampling, the SOA was directly measured without further preparation using a TOF-MS (Axima-CFR, Kratos/Shimadzu, Manchester, U.K.) in the positive ion mode. Laser desorption was carried out with a nitrogen laser, operating at 337 nm.

TSI Single particle Aerosol Time of Flight Mass Spectrometer (ATOFMS, TSI 3800)

The aerosol time-of-flight mass spectrometer is a single particle mass spectrometer designed to sample individual aerosol particles in real time. Particle-laden air is sampled into the source of the bipolar time-of-flight mass spectrometer where a pulse of a Nd:YAG laser is used for desorption and ionization of the particles. The interaction of the particle with the laser beam generates both positive and negative ions, which are accelerated into the respective flight tubes of the instrument. Thus, from each particle that successfully interacts with the desorption/ ionization laser, complete positive and negative ion mass spectra are generated.

Aerodyne Aerosol Mass Spectrometer

The instrument utilises an aerodynamic lens to produce a collimated particle beam that impacts on a porous tungsten surface heated typically to 550^{o}C under high vacuum (~ 10^{-8} Torr), causing the

non-refractory fraction of the particles to flash vaporise. The vapour plume is immediately ionised using a 70 eV electron impact (EI) ionisation source, and a quadrupole mass spectrometer (QMA 410, Balzers, Liechtenstein) is used to analyse the resultant ions with unit mass-to-charge (*m/z*) resolution.

Proton-transfer-reaction MS (PTR-MS) and GC-PTR-MS

A commercial PTR-MS instrument (IONICON Analytik GmbH, Innsbruck, Austria) was used to measure molecular constituents of particles in an aerosol. The inlet system of the instrument was modified to make the lines as short as possible to minimize losses of organic compounds. First, the gas phase is stripped off by a charcoal denuder. Then the aerosols are thermally evaporated in a coiled stainless steel tube heated to 200 °C.
For a better identification of the masses detected by PTR-MS, measurements with gas-chromatographic methods were performed. GC-MS analyses were performed on aerosol samples taken onto Tenax/Carbopak B cartridges and a second PTR-MS was coupled to a GC-FID system. Details about the GC methods are presented by Davidson et al. [11].

Ion Chromatography-MS

The sampling system is a wet effluent diffusion denuder/ aerosol collector (WEDD/AC). It consists of a glass denuder rinsed with water to strip the gas phase while the particles are grown in heated water vapor under supersaturated conditions and impacted in a maze impactor. The gas or particle containing liquid sample is collected and concentrated before chromatographic analysis. The analysis of the concentrated ions on an IonPac AS11-HC column switched between the two-concentrator columns. Detection was done with a conductivity detector and a single quadrupole mass detector (Dionex, MSQ^{TM}) in series.

Results

Chamber studies by Laser desorption ionization MS (LDI-MS) have shown that a substantial fraction of the organic aerosol mass is composed of oligomers [8]. This off-line method needs relatively large amounts of aerosol mass and time resolution is thus restricted. A real-time detection of oligomers in secondary organic aerosols has been carried out with an aerosol time-of-flight mass spectrometer (ATOFMS) [12]. In SOA particles from α-pinene photooxidation ions were observed in the single-particle mass spectra up to 750 Da. These high-mass ions occur with a characteristic spacing of 14 and 16 Da, indicative of oligomeric species. A comparison between the (matrix-assisted) laser desorption/ ionization mass spectra and those of the ATOFMS was done. We cannot compare the peak positions directly since ionization procedures of the two methods are different. However, after reconstruction of the spectra the peaks of the two mass spectrometric techniques match up well.

A modified version of the IONICON PTR-MS was used to measure volatile organic species in the aerosol phase. Several mass peaks could be observed which appeared when the particles started to grow. For a further identification of these peaks we used a GC-PTRMS to separate isobaric species. To do that, particles were directly sampled on the pre-concentration trap of the GC interface. In SOA from trimethylbenzene photooxidation several compounds could be separated for the m/z 113 peak which partition differently between gas and particle phase.

References

[1] M. Kanakidou, J.H. Seinfeld, S. N. Pandis, I. Barnes, F.J. Dentener, M.C. Facchini, R. Van Dingenen, B. Ervens, A. Nenes, C.J. Nielsen, E. Swietlicki, J.P. Putaud, Y. Balkanski, S. Fuzzi, J. Horth, G.K. Mootgat, R. Winterhalter, C.E.L. Myhre, K. Tsigaridis, E. Vignati, E.G. Stephanou and J. Wilson, Organic aerosol and global climate modelling: a review, Atmospheric Chemistry and Physics 5, 1053-1123, (2005).

[2] R.J. Griffin, D.R. Cocker III, J.H. Seinfeld and D. Dabdub, Estimate of global atmospheric organic aerosol from oxidation of biogenic hydrocarbons, Geophysical Research Letters 26, 2721-2724, (1999).

[3] T. Hoffman, J.R. Odum, F. Bowman, D. Collins, D. Klockow, R.C. Flagan and J.H. Seinfeld, Formation of organic aerosols from the oxidation of biogenic hydrocarbons, Journal of Atmospheric Chemistry 26, 189-222, (1997).

[4] B. Bonn and G.K. Moortgat, Sesquiterpene ozonolysis: origin of atmospheric new particle formation from biogenic hydrocarbons, Geophysical Research Letter 30, 1585-1588, (2003).

[5] S. Pandis, R.A. Harley, G.R. Cass and J.H. Seinfeld, Secondary organic aerosol formation and transport Atmospheric Environment 26A, 2269-2282, (1992).

[6] H.J.L. Forstner, R.C. Flagan and J.H. Seinfeld, Secondary organic aerosol from the photooxidation of aromatic hydrocarbons: Molecular composition, Environmental Science and Technology 31, 1345-1358, (1997).

[7] M. Glasius, M. Duane and B.R. Larse, Determination of polar terpene oxidation products in aerosols by liquid chromatography-ion trap mass spectrometry, Journal of ChromatographyA 833, 121-135, (1999).

[8] M. Kalberer, D. Paulsen, M. Sax, M. Steinbacher, J. Dommen, A.S.H. Prevot, R. Fisseha, E. Weingartner, V. Frankevich, R. Zenobi and U. Baltensperger, Identification of polymers as major components of atmospheric organic aerosols, Science 303, 1659-1662, (2004).

[9] J.D. Surratt, S.M. Murphy, J.H. Kroll, N.L. Ng, L. Hildebrandt, A. Sorooshian, R. Szmigielski, R. Vermeylen, W. Maenhaut, M. Clayes, R.C. Flagan and J.H. Seinfeld, Chemical composition of secondary organic aerosol formed from the photooxidation of isoprene, Journal of Physical Chemistry A 110, 9665-9690, (2006).

[10] M. Jang, N.M. Czoschke, S. Lee and R.M. Kamens, Heterogenous atmospheric aerosol production by acid catalyzed particle-phase reactions, Science 298, 814-817, (2002).

[11] B. Davidson, A. Brunner, C. Ammann, C. Spirig, M. Jocher, A. Neftel, Cut induced VOC emissions from agricultural grasslands, Submitted to Plant Biology (2006).

[12] D.S. Gross, M.E. Gälli, M. Kalberer, A.S.H. Prevot, J. Dommen, M.R. Alfarra, J. Duplissy, K. Gaeggeler, A. Gascho, A. Metzger, and U. Baltensperger, Real-Time Measurement of Oligomeric Species in Secondary Organic Aerosol with the Aerosol Time-of-Flight Mass Spectrometer, Analytical Chemistry 78, 2130-2137, (2006).

Chemical Ionization Mass Spectrometry Applied to the Study of Atmospheric Nanoparticles

J. N. Smith[1], G. J. Rathbone[1], F. L. Eisele[1], and P. H. McMurry[2]

[1] *National Center for Atmospheric Research, Boulder, Colorado, USA, jimsmith@ucar.edu*

[2] *Department of Mechanical Engineering, University of Minnesota, Minneapolis, Minnesota, USA*

Abstract

The Thermal Desorption Chemical Ionization Mass Spectrometer is a unique instrument for determining the chemical composition of atmospheric particles as small as 6 nm in diameter. This is made possible in large part to an ion source that operates at atmospheric pressure, thus eliminating the source of signal loss in conventional aerosol mass spectrometers that require that particles enter the vacuum chamber before analysis. Atmospheric pressure chemical ionization within the TDCIMS ion source involves cluster formation with water, however laboratory studies show that it can be a highly sensitive and soft ionization technique. A demonstration of the instrument performance of the TDCIMS is presented from a recent study of aerosol formation in Mexico City, where 8-10 nm particles were observed to contain methyl ammonium.

Introduction

The application of mass spectrometry to the study of the chemical composition of aerosol has brought about a revolution in atmospheric chemistry [1]. For example, the ability to study, in real-time, the composition of individual particles has allowed for the identification of chemical tracers that can be used for studying the formation and transport of pollutants. Most aerosol mass spectrometers require that particles are transferred into vacuum, where a subsequent desorption step leads to gas phase species that are ionized using convention mass spectrometer ion sources such as electron impact. The strength of this arrangement lies in its ability to apply very mature ion chemistry theory to the interpretation of the resulting mass spectra. A significant weakness, however, is encountered when these techniques are applied to the study of nanoparticles, which we define as particles smaller than 50 nm in diameter. The cubic relationship of particle mass to size, combined with high diffusive losses in transferring nanoparticles into vacuum, leads to minute sample sizes and a lack of sensitivity to particles smaller than 20 nm.

Seven years ago, we developed a instrument that overcomes the challenges of measuring nanoparticle composition by collecting and analyzing particles at atmospheric pressure. The Thermal Desorption Chemical Ionization Mass Spectrometer (TDCIMS), uses recently developed techniques for charging, size separating, and collecting nanoparticles together with a unique atmospheric pressure thermal desorption/chemical ionization technique that allows for the study of ambient particles as small as 6 nm in diameter. The ionization scheme used in TDCIMS is closely related to the highly sensitive chemical ionization schemes that are currently used to measure gas phase species such as sulfuric acid [2].

The purpose of this document is to summarize the current TDCIMS instrument and to summarize ongoing research aimed at understanding the unique chemistry that occurs within the ion source region. An example of the application of the technique is provided from a recent study of particle formation in Mexico City.

Experimental Method

A brief description of the TDCIMS instrument is presented here, whereas a detailed description can be found in recent publications (see [3] and references cited therein). Ambient particles are first charged using a unipolar charger [4]. Next, charged particles are size-selected using a nanometer Differential Mobility Analyzer (nano-DMA; model 3085, TSI, Inc.) located directly downstream of the charger. Up to 3 sets of charger/nano-DMA pairs can be combined in parallel in order to increase delivered particle mass. Charged particles are then introduced into the electrostatic precipitator: a cylindrical chamber that contains a collection wire that is biased to a high voltage (usually 4000 V) and located on the axis of the chamber (figure 1). Charged particles cross flow streamlines, through a clean N_2 buffer gas that isolates the collection wire from contamination from the ambient gas, and are collected on the tip of the wire. Once a sufficient amount of particles are collected, usually 10-100 pg over a period of 5-10 min, the wire is transferred into the ion source region of the chemical ionization mass spectrometer. A current pulse or ramp is applied to the wire to resistively heat it in order to thermally desorb the compounds in the collected particles. The ion source consists of an Am241 radioactive foil at atmospheric pressure, which emits α-particles that ionize the buffer gas mixture to form H_3O^+, O_2^- and CO_3^-, and clusters of these with H_2O, as the primary stable ions. These ions react with the compounds evaporated from the aerosol to ionize the compounds, and electrostatic lenses direct these ions into the collision cell where the ions are de-clustered. The ions are finally detected using a triple quadrupole mass spectrometer (Extrel CMS).

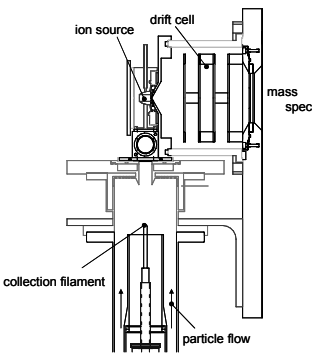

Figure 1: Diagram of particle collection and ionization regions of the TDCIMS.

Results and Discussion

Ion Source Chemistry

As mentioned previously, a unique feature of the atmospheric pressure thermal desorption scheme employed in the TDCIMS is the participation of molecular clusters, most specifically water, in the ion source chemistry. The presence of these clusters is unavoidable, and would normally lead to a limited set of compounds that could be successfully ionized by proton transfer from water because of the increase in proton affinity of the $H_3O^+(H_2O)_n$ cluster. Figure 2a demonstrates this increase in the endothermicity of the proton transfer reaction for the case of acetone ionization, and suggests that the protonation reaction likely occurs by an initial association step, which is followed by a declustering step that removes the excess water molecules from the newly formed adduct. Note that at ambient pressure and room temperature, the cluster size is estimated to be in the range of 3-5 water molecules. Figure 2b shows the instrument response to a calibration gas consisting of 3 ketones. The H_3O^+ ion is also plotted, representing the total reagent ion since it declustered just prior to measurement. As the plot shows, when $[H_3O^+]$ is comparable to that of the analyte, the instrument response to the analyte is determined by the competition between all other compounds present in the gas: species with higher proton affinity such as 2-heptanone will exhibit more of an ideal linear response compared with acetone, which has a proton affinity that is about 8 kcal/mol lower. However when $[H_3O^+]$ is greater than the total reagent compound concentration, the response appears to be linear as shown in the lower plot of figure 2b where the concentration of the protonated acetone appears to be linear over the lowest gas concentrations. These results and others using aldehydes, amines, and organic acids show that (a) in most cases the atmospheric ion chemistry employed by the TDCIMS is both sensitive and non-destructive and (b) instrument response can be linear under conditions where the reagent gas concentration is greater than that of the analytes.

Representative Ambient Aerosol Measurements

An example of measurements of ambient nanoparticles will be provided from a recent campaign in Mexico City. On 18 March we monitored 15 – 200 amu positive ions in 8 – 10 nm diameter particles during a new particle formation event that began at ~17:00 GMT (13:00 local time). During this experiment we applied a linear current ramp to the wire containing collected particles, thus providing a means for isolating species contained in particles from those that have partitioned to the walls of the ion source. Figure 3a shows the resulting ion signal for ammonium (18 amu), where no significant difference is seen between the ion signal obtained during particle collection (dashed trace) and that obtained when no particles were collected (solid trace). By contrast, dimethyl ammonium (46 amu) shows a sharp well-defined peak during particle collection that is absent when particles were not collected (figure 3b). The background levels of ammonium and dimethyl ammonium seen in figure 3 are background signals that develop over time as the desorbed gases deposit to surfaces. As figure 3b shows, the use of a temperature ramp is effective in separating the signal for gases desorbed from particles from that desorbed by walls, etc. This observation of dimethylamine in particles formed from nucleation is similar to some of the earliest measurements of the composition of particles formed by nucleation in the Finnish boreal forest [5], where dimethyl amine was the only species that could be positively identified as being enriched in newly formed particles.

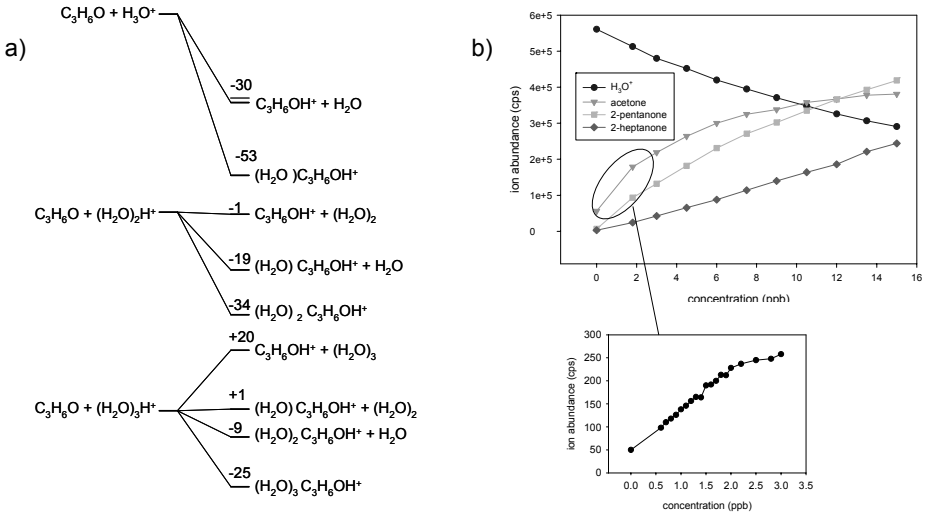

*Figure 2: (a) Reaction energies (in kcal/mol) for the acetone- $H_3O^+(H_2O)_n$ system, calculated using HF/6-31G** geometries with MP2/6-31G** single point energies. (b) Instrument response for a mixture of 3 ketones.*

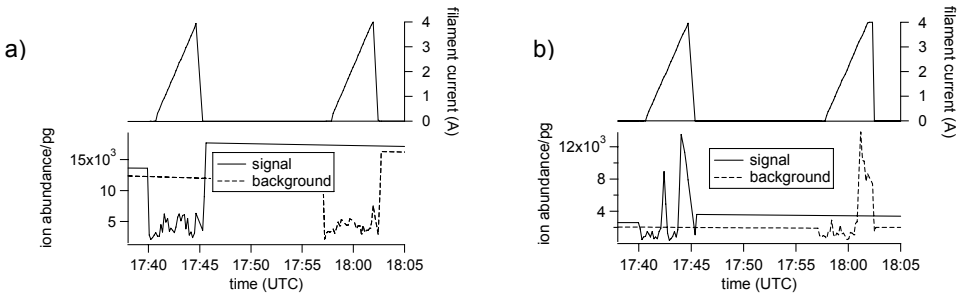

Figure 3: (a) (top) current ramp applied to wire. (bottom) TDCIMS ion signal for ammonium (18 amu). (b) same as (a) for dimethyl ammonium (46 amu).

Acknowledgements

This research was supported by the Office of Science (BER), U.S. Department of Energy, Grant No. DE-FG-02-05ER63997 and by the NOAA Atmospheric Composition and Climate Program under grant NA05OAR4310101.

References

[1] D.G. Nash, T. Baer, and M.V. Johnston, Aerosol mass spectrometry: An introductory review, Int. J. Mass Spectrom. 258, 2-12, (2006).

[2] F.L. Eisele, and D.J. Tanner, Measurement of the gas phase concentration of H2SO4 and methane sulfonic acid and estimates of H2SO4 production and loss in the atmosphere, J. Geophys. Res. 98, 9001-9010, (1993).

[3] J.N. Smith, K.F. Moore, F.L. Eisele, D. Voisin, A.K. Ghimire, H. Sakurai, and P.H. McMurry, The chemical composition of atmospheric nanoparticles during nucleation events in Atlanta, J. Geophys. Res. - Atmos. 110, D22S03, (2005).

[4] D.-R. Chen, and D.Y.H. Pui, A high efficiency, high throughput unipolar aerosol charger for nanoparticles, J. Nanoparticle Res. 1, 115-126, (1999).

[5] J.M. Makela, S. Yli-Koivisto, V. Hiltunen, W. Seidl, E. Swietlicki, K. Teinila, M. Sillanpaa, I.K. Koponen, J. Paatero, K. Rosman, and K. Hameri, Chemical composition of aerosol during particle formation events in boreal forest, Tellus B 53, 380-393, (2001).

3. New Developments in Chemical Ionization Mass Spectrometry (CIMS)

Applications of Chemical Ionization Mass Spectrometry to Atmospheric Chemistry

L. Gregory Huey[1], David J. Tanner[1], Saewung Kim[1], Robert Stickel[1], Steven Sjostedt[1], Oscar Vargas[1], Anne Case[1], Andrew Turnipseed[2], and John B. Nowak[3,4]

[1] *School of Earth and Atmospheric Science, Georgia Institute of Technology, Atlanta, GA, USA, greg.huey@eas.gatech.edu*

[2] *Atmospheric Chemistry Divsion, NCAR, Boulder, CO, USA*

[3] *Cooperative Institute for Research in Environmental Sciences, University of Colorado, Boulder, CO, USA.*

[4] *Chemical Sciences Division, Earth System Research Laboratory, NOAA, Boulder, CO, USA*

Abstract

During the last seven years our research group has developed chemical ionization mass spectrometric (CIMS) techniques for the measurement of a wide range of atmospheric species. In this presentation, I will discuss CIMS data from five field campaigns: eddy flux measurements of PANs in Duke Forest; HO_x and sulfuric acid observations from both Mexico City and Houston, Texas; gas-phase ammonia measurements from the Atlanta Nucleation Experiment; and pernitric acid (HO_2NO_2), HCl, and SO_2 measurements from the NASA DC-8 during INTEX A and B. These data highlight the unique selectivity, sensitivity, and fast time response of CIMS. The PAN measurements were performed with an integration period of 0.25 s (4 Hz) to allow us to measure fluxes by eddy covariance. The fast time response of the Atlanta ammonia measurements (1 min) allowed us to examine its role in particle nucleation as well as test our understanding of urban ammonia sources. Finally, the sensitivity of the CIMS is crucial for the high time and spatial resolution measurements of species found in low concentrations (< 100 pptv) such as HO_x, H_2SO_4, HCl and HO_2NO_2.

Introduction

The focus of this presentation is to demonstrate the versatility of chemical ionization mass spectrometry (CIMS) as an analytical tool for the measurement of trace atmospheric gases. Four different CIMS methods (PANs and N_2O_5; NH_3; OH, RO_2, and H_2SO_4; and SO_2, HO_2NO_2, and HCl) will be described and representative field data for each will be presented.

Experimental Methods

All of the chemical ionization measurement techniques employ the same differentially pumped quadrupole mass spectrometer. Important common features include an actively pumped collisional dissociation chamber (CDC) and octopole ion guides. Different ion molecule reactors can be attached to this assembly. The PANs, NH_3, and SO_2 measurements are carried out with low pressure (10-30 torr) ion molecule reactors while the H_2SO_4 measurements utilize an ambient pressure reactor. Examples of the low and ambient pressure systems are shown in Figures 1 and 2, respectively. Each of the methods has been described in recent publications [1-6].

Results and Discussion

Results from a variety of field campaigns at various stage of analysis will be shown. For example, ammonia data from the 2002 ANARCHE campaign in Atlanta strongly indicates that current air quality models may under predict gas phase ammonia levels during the day. More recent HO_x data from the 2006 Texas Air Quality and MILAGRO studies will be examined to contrast ozone production in these environments.

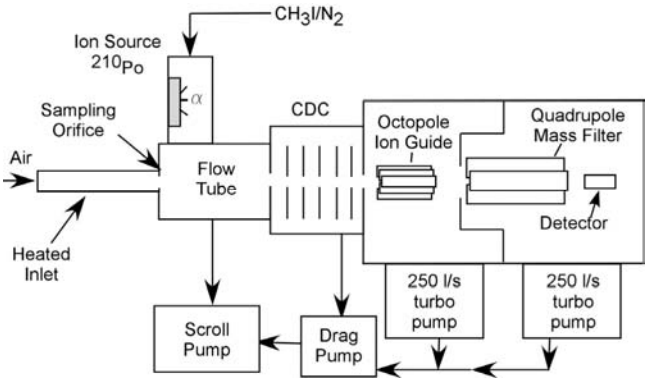

Figure 1: CIMS instrument with a low pressure flow tube used to measure PANs and N_2O_5.

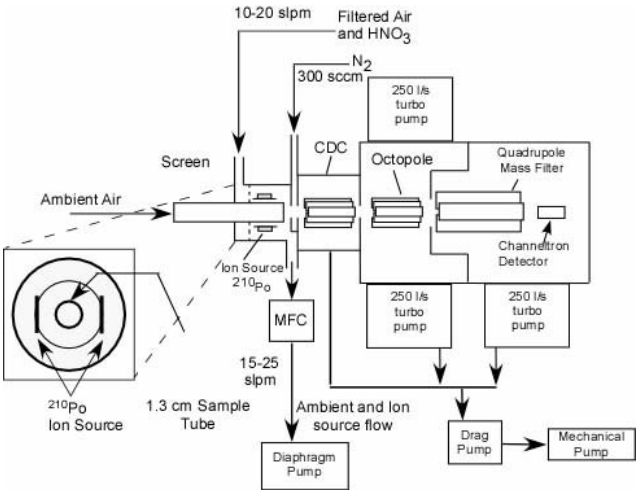

Figure 2: CIMS instrument with an atmospheric pressure flow tube used to measure OH, RO_2, and H_2SO_4. Figure taken from S. Sjostedt thesis.

References

[1] J. B. Nowak, L.G. Huey, A.J. Russell, D. Tian, J.A. Neuman, D. Orsini, S.J. Stostedt, A.P. Sullivan, D.J. Tanner, R.J. Weber, A. Nenes, E. Edgerton, and F.C. Fehsenfeld, Analysis of Urban Gas-phase Ammonia Measurements from the 2002 Atlanta Aerosol Nucleation and Real-time Characterization Experiment (ANARChE), Journal Geophysial Research – Atmospheres 111 (D17), doi: 10.1029/2006JD007113, (2006).

[2] A. Turnipseed, L.G. Huey, E. Nemitz, R. Stickel, J. Higgs, D. Tanner, D. Slusher, J. Sparks and A. Guenther, Eddy Covariance Fluxes of Peroxyacetyl Nitrate (PAN) and NOy to a Coniferous Forest, Journal Geophysial Research – Atmospheres 111, (D9), Art. No. D09304, (2006).

[3] D.L. Slusher, L.G. Huey, D.J. Tanner, F.M. Flocke and J.M. Roberts, A CIMS Technique for the simultaneous measurement of peroxyacyl nitrates and dinitrogen pentoxide, Journal Geophysial Research – Atmospheres 109, D19315, doi:10.1029/2004JD004670, (2004).

[4] D. L. Slusher, S.J. Pitteri, B.J. Haman, D.J. Tanner and L.G. Huey, A Chemical Ionization Technique for Measurement of Pernitric Acid in the Upper Troposphere and the Polar Boundary Layer, Geophysical Research Letters 28, 3875, (2001).

[5] L.G. Huey, D.J. Tanner, D.L. Slusher, J.E. Dibb, R. Arimoto, G. Chen, D. Davis, M.P. Buhr, J.B. Nowak, R.L. Mauldin III, F.L. Eisele and E. Kosciuch, CIMS measurements of HNO_3 and SO_2 at the South Pole during ISCAT 2000, Atmospheric Environment 38, 5411-5421, (2004).

[6] S. Sjostedt, L.G. Huey, et al., Observations of Hydroxyl and the Sum of Peroxy Radicals at Summit, Greenland During Summer 2003, Atmospheric Environment., in press, (2006).

Atmospheric Monitoring With Chemical Ionisation Reaction Time-of-Flight Mass Spectrometry (CIR-TOF-MS)

Paul S. Monks[1], Kevin P. Wyche[1], Robert S. Blake[1], Chris Whyte[1] and Andrew M. Ellis[1]

[1]Department of Chemistry,University of Leicester, Leicester, UK, P.S.Monks@le.ac.uk

Abstract

The technique of Chemical Ionisation Reaction (CIR) ionisation has been successfully coupled for the first time to Time-of-Flight Mass Spectrometry (TOF-MS) and has been applied to the measurement of a range of trace atmospheric volatile organic compounds (VOCs) and oxygenated volatile organic compounds (OVOCs) (Blake *et al.*, 2003 and Wyche *et al.,* 2005). Initial results have demonstrated the instrument to be capable of recording the entire mass spectrum in "*real-time"* (*ca.* 1 minute) with sensitivities in the order of 0.1 counts $ppbV^{-1}$ s^{-1}.

Introduction

The use of chemical ionisation reaction mass spectrometry utilising the hydronium ion as the primary chemical ionisation (CI) reagent, for fast real time measurement of trace volatile organic compounds and oxygenated volatile organic compounds has a wide array of applications. Examples include the monitoring of atmospheric species and pollution episodes (*e.g.* Hewitt *et al.*, 2003), medical diagnostics *via* breath analysis (*e.g.* Lirk *et al.,* 2004) and forensic investigations.

Standard PTR-MS instruments employ quadrupole mass spectrometers (*e.g.* Hansel *et al.,* 1995) which suffer from several drawbacks such as relatively low mass resolution ($m/\Delta m = 100$), limited mass range (generally poor transmission above 1000 Da) and since they essentially act as mass filters, the inability to capture the entire mass spectrum in a given instant. In an attempt to avoid these problems a PTR system has been successfully coupled to a Time-of-Flight (TOF) mass spectrometer, which benefits from a mass resolution ($m/\Delta m$) in excess of 1000 Da, a theoretically limitless mass range and most significantly is able to observe all mass channels simultaneously (Blake *et al.,* 2003). However, as the system has the ability to function just as successfully with chemical ionisation reagents other than proton donating species, we term this technique *Chemical Ionisation Reaction Time-of-Flight Mass Spectrometry* (CIR-TOF-MS). Other reagent ions typically employed include NO^+, O_2^+ and NH_4^+ (Blake *et al.,* 2006).

The new University of Leicester CIR-TOF-MS has been applied to the monitoring of atmospheric volatile organics in the contemporary urban boundary layer and has recently taken part in several key environment chamber studies. The CIR-TOF-MS has also been applied to the monitoring of VOC emissions from drying paint films in the indoor environment and accelerant traces at arson scenes as well being developed as a medical diagnostic tool for human breath analysis.

Experimental Methods

The University of Leicester CIR-TOF-MS instrument (shown schematically in Figure 1) is described in detail elsewhere (Blake *et al.*, 2003). In brief, the ion source/drift tube assembly (constructed in house) consists of a series of seven stainless steel electrodes separated by insulating spacers. The drift region is operated at a relatively high pressure (~8 - 10 mbar) in order to optimise the ion yield. Hence under standard operating drift tube voltages, an *E/N* ratio (where *E* = electric field strength and *N* = gas number density) of around 150 Td is achieved (1 Townsend (Td) = 10^{-17} V cm^2). Unlike in conventional PTR–MS, our system employs a radioactive ion source to generate the CI reagent (^{241}Am which emits α particles with energy of the order 5 MeV). The benefits of using a radioactive ion source include the lack of settling time required after a change in internal conditions, including a change in the supply of reagent gas. The time-of-flight mass spectrometer, supplied by Kore technology (Ely, UK), is orthogonal in design with a duty cycle of approximately 3% for a mass scan of 0-100 Daltons. The instrument has a mass resolution in excess of 1000.

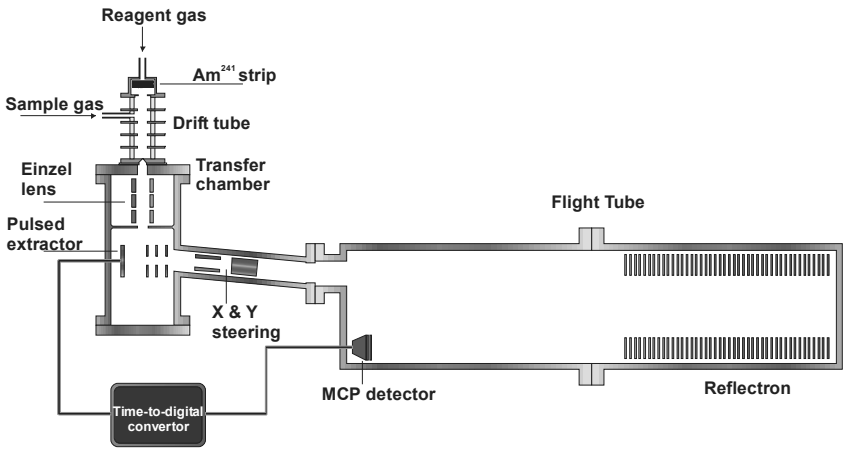

Figure 1: Schematic diagram of the Chemical Ionisation Reaction Time-of-Flight Mass Spectrometer (CIR-TOF-MS) showing the major components

Results

4.1 Chemical Ionisation Reaction-Mass Spectrometry (CIR-MS)

Figure 2 displays the raw CIR-MS mass spectrum recorded in the absence of sample, when NO^+ was employed as the primary reagent ion as an alternative to hydronium. The data presented in figure 2 clearly demonstrates that the CIR-MS instrument is capable of generating a clean source of primary ions other than proton transfer species. Similar spectra are obtained for the other CI reagents (see Wyche *et al.*, 2005 and Blake *et al.*, 2006).

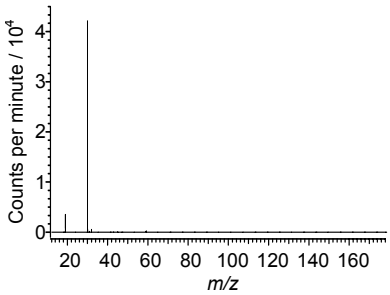

Figure 2: Raw mass spectrum taken using NO+ as the primary reagent ion in the absence of an analyte.

Inspection of Figure 3 reveals that the mass spectra for acetone and propanal generated with the hydronium ion as the CI reagent are virtually identical, both dominated with large $[MH]^+$ peaks. This epitomises the problem of isobaric compound identification in a PTR-MS instrument, it is near impossible to identify which spectrum belongs to the aldehyde and which the ketone. In dramatic contrast to this, when NO^+ is employed as the CI reagent, the mass spectra for these test compounds change markedly. As is common with ketones (and similar to the results of the SIFT-MS of Smith and Španěl), acetone was observed to form an ion/molecule association complex (*m/z* = 88), whereas its aldehyde counterpart did not. In contrast propanal appears to occupy mass channels at the opposite end of the spectrum, with small M^+ and $[M\text{-}H]^+$ mass peaks as well as large peaks at *m/z* = 29 and 27. Typically it was found that saturated ketones generally react with NO^+ reagent ions to form ion/molecule association complexes, with a number of fragment ions observed in lighter mass channels, whose abundance increase with increasing chain length. Conversely aldehydes generally fragment more extensively, typically producing formyl, alkyl and acylium ions.

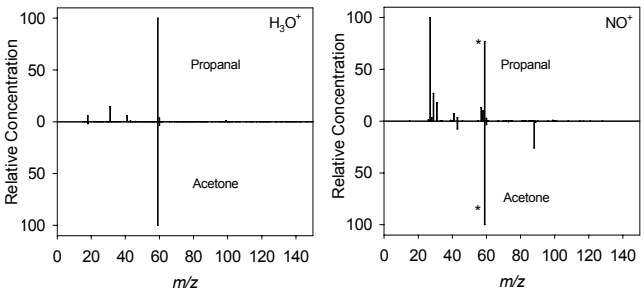

Figure 3: Processed mass spectra for acetone and propanal, generated with either H3O+ or NO+ ions as the CI reagent. Stared peak are present as a consequence of residual water contamination.

Because of the unique and compound specific spectral differences or "fingerprints" which can be derived from the use of two or more different reagent ions, it becomes possible to discriminate between isobaric compounds during on-line measurement. This observation was found to apply

even to structural isomers (Wyche *et al.,* 2005). In more recent work by our group, we have been able to demonstrate the benefits of using an expanded range of reagent ions for VOC detection in the CIR-MS technique (Blake *et al.,* 2006).

4.2 Atmospheric Monitoring

During January 2005 the CIR-TOF-MS took part in the ACCENT sponsored OVOC measurement intercomparison held at the SAPHIR atmospheric simulation chamber (Jülich, Germany) (for details regarding the chamber itself see Karl *et al.,* 2004). The intercomparison campaign comprised 5 separate experiments during which a series of 14 different atmospherically significant OVOCs were monitored at three distinct concentrations levels under various humidities and ozone content.

Figure 4 displays the "*real-time*" data obtained from the chamber by the CIR-TOF-MS for the OVOC acetaldehyde (circles) plot along side theoretical chamber acetaldehyde concentrations (blue line). The theoretical concentrations were derived from the knowledge of the amount of OVOC initially injected into SAPHIR. Inspection of figure 4 reveals the high quality of CIR-TOF-MS measurement, with all three measuring periods and both dilution phases clearly captured, with the instrument tracking theoretical values throughout. CIR-TOF-MS average 1 minute accuracy, precision and signal to noise ratio in this instance were as good as 12.5%, 15.4% and 8:1 respectively. Full details regarding the performance and validation of the CIR-TOF-MS technique during the SAPHIR OVOC intercomparison can be found in Wyche *et al.,* 2006.

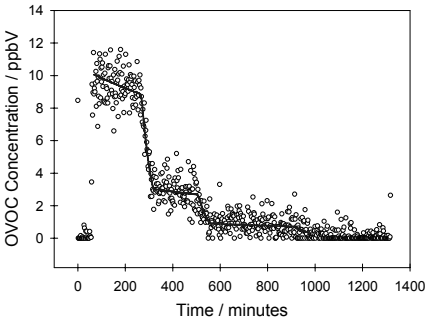

Figure 4: Real-time monitoring of acetaldehyde (circle points) along with theoretically derived mixing ratios (blue line) obtained during the Jülich OVOC intercomparison

In order to demonstrate the quality of CIR-TOF-MS data acquisition and to further exemplify the sensitivity of the instrument to trace compounds during real-time measurement, example VOC data recorded during urban air sampling is presented in Figure 5. Air from outside of the University was extracted into the CIR-TOF-MS *via* a Teflon sampling tube over a one week period. Leicester is a typical moderate U.K. city with a population of around 300,000 people and the sample site is located approximately 1 mile from the city centre, hence substantial quantities of volatile organic species are expected. Figure 5 shows the temporal profile recorded over a week period for acetone.

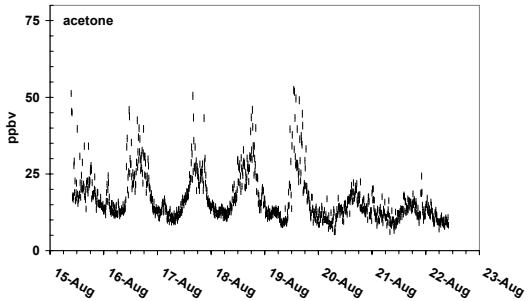

Figure 5: Monitoring the urban atmosphere, the temporal trace for acetone (a) over a one week period.

Conclusions

The CIR-TOF-MS technique is highly versatile, providing ppbV detection sensitivities on minute time scales. The potential benefits of employing the TOF-MS are considerable, with the sample matrix being probed in more depth and detail than has been possible previously.

Methods are described for advancements in the CIR-TOF-MS technique utilising ion beam multiplexing in a Hadamard Transform instrument. Encoding the ion beam in this manner in the TOF-MS system will improve the instrument sensitivity by an order of magnitude.

References

Blake, R. S., C. Whyte, C. O. Hughes, A. M. Ellis and P. S. Monks: (2004) Demonstration of proton-transfer reaction time-of-flight mass spectrometry for real-time analysis of trace volatile organic compounds, *Analytical Chemistry* 76(13): 3841-3845

Blake, R. S., K. P. Wyche, A. M. Ellis and P. S. Monks: (2006) Chemical ionization reaction time-of-flight mass spectrometry: Multi-reagent analysis for determination of trace gas composition, *International Journal Of Mass Spectrometry* 254(1-2): 85-93

Hansel, A., A. Jordan, R. Holzinger, P. Prazeller, W. Vogel and W. Lindinger: (1995) Proton-Transfer Reaction Mass-Spectrometry - Online Trace Gas-Analysis At The ppb Level, *International Journal Of Mass Spectrometry* 150: 609-619

Hewitt, C. N., S. Hayward and A. Tani: (2003) The application of proton transfer reaction-mass spectrometry (PTR-MS) to the monitoring and analysis of volatile organic compounds in the atmosphere, *Journal Of Environmental Monitoring* 5(1): 1-7

Karl, M., T. Brauers, H. P. Dorn, F. Holland, M. Komenda, D. Poppe, F. Rohrer, L. Rupp, A. Schaub and A. Wahner: (2004) Kinetic Study of the OH-isoprene and O3-isoprene reaction in the atmosphere simulation chamber, SAPHIR, *Geophysical Research Letters* 31(5)

Lirk, P., F. Bodrogi and J. Rieder: (2004) Medical applications of proton transfer reaction-mass spectrometry: ambient air monitoring and breath analysis, *International Journal Of Mass Spectrometry* 239(2-3): 221-226

Smith, D., A. M. Diskin, Y. F. Ji and P. Spanel: (2001) Concurrent use of H_3O^+, NO^+, and O-2($^+$) precursor ions for the detection and quantification of diverse trace gases in the presence of air and breath by selected ion-flow tube mass spectrometry, *International Journal Of Mass Spectrometry* 209(1): 81-97

Wyche, K. P., R. S. Blake, K. A. Willis, P. S. Monks and A. M. Ellis: (2005) Differentiation of isobaric compounds using chemical ionization reaction mass spectrometry, *Rapid Communications In Mass Spectrometry* 19(22): 3356-3362

Wyche, K. P., R. S. Blake, A. M. Ellis, P. S. Monks, R. Koppman, T. Brauers and E. Apel: (2006) Performance of Chemical Ionisation Reaction Time-of-Flight Mass Spectrometry (CIR-TOF-MS) for the Measurement of Atmospherically Significant Oxygenated Volatile Organic Compounds, *Atmospheric Chemistry and Physics Discussions,* 6, 10247-10274.

The Direct Analysis in Real Time (DART^{tm}) ion source

Robert B. Cody

JEOL USA, Inc., 11 Dearborn Road, Peabody, MA, 03801 United States.

Abstract

The Direct Analysis in Real Time (DART^{tm}) ion source was constructed and tested in early 2003 and introduced as a commercial product in 2005. DART is now in use for a wide range of small-molecule applications in industrial, academic and government laboratories around the world. The source permits near instantaneous analysis of gases, liquids, solids, and materials on surfaces in open air at ground potential. Although the DART ionization mechanism is based upon atmospheric pressure reactions of metastable atoms and molecules, one of the most important modes of operation involves proton transfer reactions. The majority of DART applications have been in the analysis of liquids, solids and materials on surfaces, making DART a complementary technique to traditional PTRMS. An overview of the DART ion source and its applications will be presented in this talk.

In situ measurements of gas- and condensed-phase HNO_3 in the upper troposphere and lower stratosphere

Peter J. Popp[1,2]

[1] *Chemical Sciences Division, NOAA Earth Systems Research Laboratory, 325 Broadway, Boulder, CO 80305 USA Peter.J.Popp@noaa.gov*

[2] *Cooperative Institute for Research in Environmental Sciences, University of Colorado, Boulder, CO 80307 USA*

Abstract

The NOAA chemical ionization mass spectrometer (CIMS) onboard the NASA WB-57F high-altitude research aircraft measures HNO_3 with two independent channels of detection that allow a determination of the amount of HNO_3 in the condensed phase. This instrument has been used to demonstrate the heterogeneous production of HNO_3 in the plume of a solid-fuel rocket motor and to quantify the uptake of HNO_3 by subtropical cirrus cloud particles. More recent measurements over the eastern Pacific Ocean in January of 2004 have revealed a new category of HNO_3-containing particles in the tropical lower stratosphere. These particles are most likely composed of nitric acid trihydrate (NAT). The small number density of these NAT particles implies a slow or highly selective nucleation process, and microphysical trajectory models suggest the particles grow over a 6-14 day period in air that remains close to the tropical tropopause. Understanding the formation of NAT particles in the tropics could improve our understanding of stratospheric nucleation processes in polar regions and, therefore, dehydration and denitrification. A preliminary analysis of HNO_3 uptake in subvisual cirrrus clouds near the tropical tropopause will also be presented.

Introduction

Particles affect chemical composition and climate forcing in the upper troposphere and lower stratosphere[1-4]. For example, ice formation in the tropopause region regulates stratospheric humidity through particle sedimentation and controls the radiative properties of high clouds[5]. Polar stratospheric clouds, when composed of nitric acid trihydrate (NAT; $HNO_3 \cdot 3H_2O$), sediment and denitrify the lower stratosphere in winter and thereby enhance photochemical ozone destruction[6-8]. Theoretical efforts have had limited success in identifying and quantifying atmospheric nucleation processes, in part, because of incomplete knowledge of aerosol composition and how composition affects nucleation. This in turn limits our current understanding of how global change might alter future cloudiness, stratospheric dehydration, and ozone amounts.

Observations of ambient aerosol from ground-based, airborne, and space-borne platforms under a wide range of conditions are providing key guidance in completing our understanding of microphysical processes. In situ observations made on airborne platforms are particularly effective because they offer high spatial resolution with quantitative detail. By induction, in situ observations can be used to reveal features of atmospheric aerosol processes that would otherwise

be inaccessible. An important example of the guiding role of observations is the discovery of large NAT particles in the Arctic winter stratosphere using airborne instruments[9,10]. Proof of their existence has led to a refined and more comprehensive view of how NAT particles denitrify the stratosphere and how atmospheric conditions can affect denitrification[6,11]. However, the nucleation process for these large particles remains an unsolved microphysical puzzle.

Here we present evidence for a new category of nitric acid-containing particles that nucleate and grow in the tropical lower stratosphere. In contrast to the background liquid sulfate aerosol, these particles are solid, much larger (1.7-4.7 μm vs. 0.1 μm), and significantly less abundant ($<10^{-4}$ cm^{-3} vs. 10 cm^{-3}). The particles are assumed to be composed of NAT, although they grow under substantially different conditions than NAT particles found in polar regions. First, gas-phase HNO_3 values observed in the tropical lower stratosphere were typically 0.1 ppbv or lower, which is 10 to 100 times less than that available for particle growth in the polar stratosphere. Second, the particles grow at temperatures much closer to the frost point. In the tropics, NAT saturation conditions occur within +1.5 K of the frost point while the difference can exceed +6 K in the polar lower stratosphere. Third, the new particles grow in a narrow layer (a few hundred meters) near the tropopause where NAT saturation conditions are favorable. In the polar vortex, NAT growth occurs over a 5-10 km vertical extent in the low temperature region of the polar stratosphere.

Experimental Methods

The tropical NAT particles were detected in situ with a chemical ionization mass spectrometer (CIMS) onboard the NASA WB-57F high-altitude research aircraft. The CIMS instrument measures HNO_3 with two independent channels of detection connected to separate forward- and downward-facing inlets[12]. The forward-facing inlet samples both gas- and particle-phase HNO_3. Particles are inertially stripped from the airstream sampled by the downward-facing inlet, effectively yielding a measure of only gas-phase HNO_3. Thus, the difference in the signal between the two channels allows a determination of the amount of HNO_3 in the particle phase[12,13]. When particle concentrations are low enough ($< \sim 10^{-3}$ cm^{-3}), individual HNO_3-containing particles can be detected as peaks above the background gas-phase value in the time series of HNO_3 measurements. The frequency of these peaks in the time series and the known sampling volume of the CIMS instrument directly yield the ambient particle concentration[9].

Results and Discussion

HNO_3-containing particles were observed on two flights over the eastern tropical Pacific Ocean in January 2004. The flights originated and ended in San Jose, Costa Rica, (10° N) while reaching the Galapagos Islands (1° S) or as far as 3° south of the equator. The most intense period of particle observations occurred on 29 January over a 300 km (30 min.) flight segment (marked by X in Fig. 1). Individual HNO3-containing particles are identified in Fig. 1A as peaks throughout the segment. The detection of several individual particles is shown in Fig. 1E. During the 30 min. interval, a total of 59 particles were observed, yielding an average particle concentration of $6 \cdot 10^{-5}$ cm^{-3}. Overall, particles were found over a narrow range of flight altitudes (18 ± 0.1 km) and temperatures (190 ± 2 K), and over a broad geographic extent (1100 km) between 3° S and 7° N latitude. Microwave temperature profiles show that the cold-point

tropopause was typically 0.5 to 1 km below the observed particles (Fig. 1C). The two halves of the time series in Fig. 1 contrast the flight segment where particles are detected with one of similar length at lower altitude. The latter shows no evidence of particles and further shows the agreement between the two CIMS detection channels in the absence of HNO_3-containing particles.

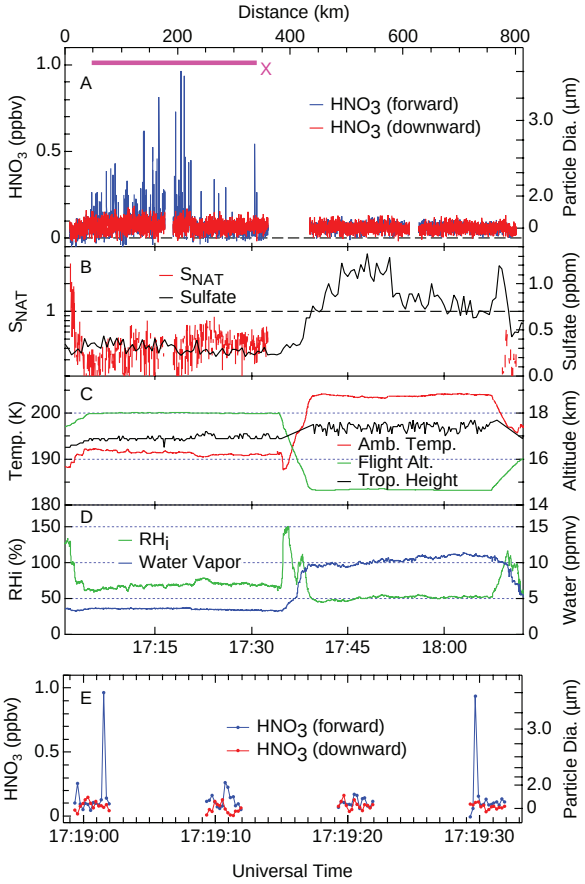

Figure 1: Time series measurements of the HNO_3 mixing ratios observed from the forward- and downward-facing CIMS channels (blue and red lines in (A), respectively) during the flight of 29 January 2004. The purple bar in (A) represents a 300 km flight segment in which HNO_3-containing particles were observed. Also shown are calculated values of S_{NAT} and measured sulfate mass mixing ratios (panel B); ambient temperature, flight altitude and cold-point tropopause height (panel C); and measured water vapor and calculated values of relative humidity with respect to ice (RH_i) (panel D). Panel (E) is a 35-s flight segment expanded from

panel A that shows HNO_3-containing particles as peaks in forward-facing CIMS channel (blue line) and the absence of peaks in the downward-facing CIMS channel (red line).

NAT is the most reasonable assumption for the composition of the sampled particles. NAT is the most stable HNO_3 condensate at the observed levels of HNO_3 and water vapor, and is known to form at low temperatures in the polar winter stratosphere. Because of their low number density and thermodynamic considerations, the observed particles are unlikely to be supercooled ternary solution (STS) composed of H_2SO_4, HNO_3, and water. Ice particles with HNO_3 on the surface or in the bulk are also unlikely due to the large particle sizes (50-200 μm or greater) required. With NAT composition assumed, particle diameters are shown with the right hand axes in Figs. 1A,E. When all particles are examined from both flights, sizes range from 1.7 to 4.7 μm in diameter.

Several important implications follow from the observations of tropical NAT particles and inferred formation conditions. First, it seems reasonable to speculate that the tropical and polar NAT particles nucleate with a common process since low NAT particle concentrations are observed in both regions. Second, ice particles might form via a similar nucleation process and with the same nuclei as tropical NAT particles. Third, the observations and trajectory analysis of tropical NAT particles imply that these particles might be a common feature of the tropical tropopause region. Fourth, at the number concentrations and sizes observed, tropical NAT particles will not be observable in satellite extinction measurements.

References

[1] Baker, M.B. Cloud microphysics and climate. *Science* 276, 1072-1078 (1997).

[2] Lawrence, M.G., Crutzen, P.J. The impact of cloud particle gravitational settling on soluble trace gas distributions. *Tellus* 50B, 263-289 (1998).

[3] McFarquhar, G.M., Heymsfield, A.J., Spinhirne, J., Hart, B. Thin and subvisual tropopause tropical cirrus: Observations and radiative impacts. *J. Atmos. Sci.* 57, 1841-1853 (2000).

[4] Jensen, E.J., Pfister, L. Transport and freeze-drying in the tropical tropopause layer. *J. Geophys. Res.* 109, 10.1029/2003JD004022 (2004).

[5] Jensen, E.J., Toon, O.B., Pfister, L., Selkirk, H.B. Dehydration of the upper troposphere and lower stratosphere by subvisible cirrus clouds near the tropical tropopause. *Geophys. Res. Lett.* 23, 10.1029/96GL00722 (1996).

[6] Davies, S. *et al.* 3-D microphysical model studies of Arctic denitrification: Comparison with observations. *Atmos. Chem. Phys. Disc.* 5, 347-393 (2005).

[7] Rex, M. et al. Prolonged stratospheric ozone loss in the 1885/96 Arctic winter. *Nature* 389, 835-838 (1997).

[8] Gao, R.S. *et al.* Observational evidence for the role of denitrification in Arctic stratospheric ozone loss. *Geophys. Res. Lett.* 28, 2879-2882 (2001).

[9] Fahey, D.W. *et al.* The detection of large HNO_3-containing particles in the winter arctic stratosphere. *Science* 291, 1026-1031 (2001).

[10] Northway, M.J. *et al.* An analysis of large HNO_3-containing particles sampled in the Arctic stratosphere during the winter of 1999/2000. *J. Geophys. Res.* 107, 10.1029/2001JD001079 (2002).

[11] Mann, G.W. *et al.* Factors controlling Arctic denitrification in cold winters of the 1990s. *Atmos. Chem. Phys.*, 3, 403-416 (2003).

[12] Popp, P.J. *et al.* Nitric acid uptake on subtropical cirrus cloud particles. *J. Geophys. Res.* 109, 10.1029/2003JD004255 (2004).

[13] Gao, R.S. *et al.* Evidence that nitric acid increases relative humidity in low-temperature cirrus clouds. *Science* 303, 516-520 (2004).

4. PTR-MS: Measurements of Anthropogenic VOCs

Emissions and Chemistry of Atmospheric VOCs: New Insights From Three Summers of Airborne and Ship-Based Measurements

Joost de Gouw[1,2], Carsten Warneke[1,2]

[1] *NOAA Earth System Research Laboratory, Boulder, Colorado, USA, Joost.deGouw@noaa.gov*

[2] *Cooperative Institute for Research in Environmental Sciences, University of Colorado, Boulder, Colorado, USA*

Abstract

The development and use of PTR-MS has led to significant new insights into the emissions, chemistry and loss processes of volatile organic compounds (VOCs) in the atmosphere. It is the aim of this work to review our most recent results from airborne and ship-based VOC measurements, with a particular focus on VOCs in urban air.

Introduction

In the summers of 2002, 2004 and 2006 we deployed a PTR-MS instrument onboard the NOAA research vessel *Ronald H. Brown* and onboard the NOAA WP-3D research aircraft. In 2002, we studied the long-range transport of air masses across the Pacific Ocean towards the U.S. West coast using the NOAA WP-3D [1,2]. Later that summer, we did measurements in the framework of the New England Air Quality Study from the *Ronald H. Brown* [3-5]. In 2004, we returned to the northeastern U.S. with the NOAA WP-3D aircraft, and studied the air quality in the region, and the onset of trans-Atlantic transport [6-8]. Finally, in 2006, we studied ozone chemistry in Houston, Texas, as part of the Texas Air Quality Study and sampled the emissions of numerous industrial sources from the NOAA WP-3D.

Over the course of these studies, much has been learned about the sources, chemistry and loss processes of atmospheric VOCs. The sampled air masses varied from (1) fresh and aged biomass burning plumes, (2) fresh and aged urban plumes, and (3) fresh and aged industrial plumes, to (4) air masses impacted by biogenic emissions. In this work, we will review our findings, and focus in particular on the sources and chemical evolution of oxygenated VOCs in urban air.

Experimental Methods

The VOC measurements in this work were mostly made by proton-transfer-reaction mass spectrometry (PTR-MS). Additional data were obtained by gas chromatographic methods, both on-line and from canister sampling, and detailed inter-comparisons with the PTR-MS results have been made with generally favorable results [3,6]. Also, we have developed a PTR-MS with an ion trap mass spectrometer for on-line quantification and identification of atmospheric VOCs [9,10]. Much of our research on the sensitivity and selectivity of PTR-MS for different atmospheric VOCs will be reviewed in a forthcoming issue of *Mass Spectrometry Reviews* [11].

Results and Discussion

Over the course of the 3 summers, the NOAA WP-3D sampled numerous urban plumes, and two examples are given in Fig. 1. A nighttime flight was conducted on August 7-8, 2004, which allowed urban air to be sampled with a minimum of processing during the transport. Fig. 1 shows part of the flight track with the gray scale indicating the measured mixing ratio of CO. Enhanced CO was observed southeast of New York City, and a back-trajectory leads back to the city and shows that the transport time was ~4 hours. The plume was observed at 2:15 am UTC or 10:15 pm local time, and thus the observed pollutants were emitted around 6:15 pm, and transported at a time when the atmospheric oxidation by OH and NO_3 is at a minimum [4]. On August 14, 2004, a plume from New York City was intercepted to the east during a daytime flight. The back-trajectory in Fig. 1 shows that the plume had been transported for ~24 hours.

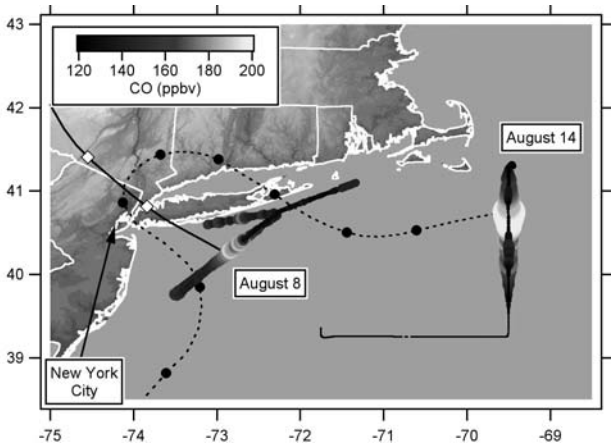

Figure 1: Sampling locations of two urban plumes from New York City. The plumes were observed on August 8 and 14, 2004, at night and day, respectively. The map shows part of the flight tracks of the NOAA WP-3D with the gray scale indicating the measured mixing ratio of CO. The black curves show back-trajectories with 1 symbol per 4 hr. (CO data are courtesy of John Holloway).

Figure 2 shows the results from the PTR-MS measurements in the two urban plumes. The urban plumes are readily discerned from forest fire plumes by the absence of acetonitrile (Fig. 2C). In addition, the ratios between the aromatic VOCs are quite distinct: toluene is dominant in the unprocessed urban plume (Fig. 2A).

The night- and daytime plumes from New York City show some striking chemical differences. The highest enhancement ratios of aromatic VOCs are observed in the nighttime plume. For toluene and in particular the higher aromatics, much lower values are seen in the daytime plume, explained by reactions with OH during the transport. In contrast, the enhancement ratios of the oxygenated VOCs are much lower in the nighttime plume than in the daytime plume. This is

particularly the case for acetone, acetic acid and MEK, and to a lesser extent for acetaldehyde (Fig. 2B+C). These observations are largely consistent with the evolution of aromatic and oxygenated VOCs in urban plumes inferred from ship-based measurements in 2002 [5]: aromatics are removed from the atmosphere in reactions with OH, whereas oxygenated VOCs are also photo-chemically produced.

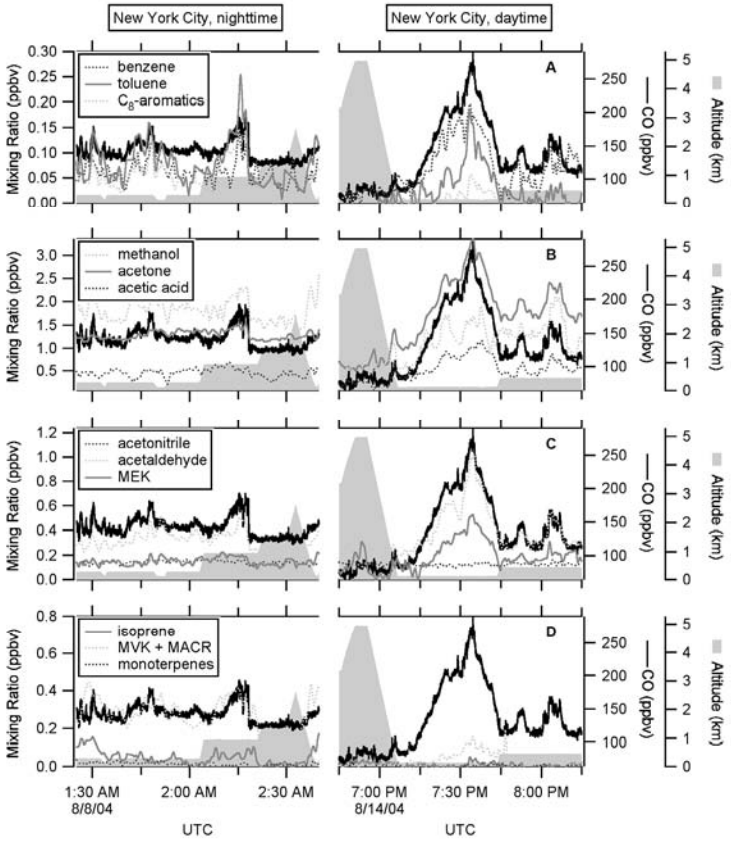

Figure 2: PTR-MS measurement results from a relatively unprocessed, nighttime plume (left panels) and a well-processed, daytime plume (right panels) from New York City. (CO data are courtesy of John Holloway).

The levels of biogenic VOCs were low but not zero in the urban plumes (Fig. 2D). This could be due to emissions from urban vegetation. Biogenic emissions are not limited to city boundaries, and as a result, the correlation with CO is not as good as for the anthropogenic VOCs. During the

nighttime flight, the levels of MVK + MACR were much higher than those of their precursor, isoprene. This indicates a high degree of photochemical processing of the biogenic emissions, as expected for emissions that take place mainly during the day and are measured during the night. The levels of biogenic VOCs were even lower in the daytime plume, which was exposed to much higher concentrations of OH radicals during the transport.

In this work, our observations in urban plumes will be described in more detail. Direct emissions of oxygenated VOCs as well as photochemical formation have been quantified and our observations compared with emissions inventories, and with detailed photochemical box models, respectively. Direct emissions of most oxygenated VOCs are much higher than emissions inventories indicate. On the other hand, box models are capable of reproducing the observed secondary formation of oxygenated VOCs with the exception of acetic acid.

Results obtained in fresh and aged forest fire plumes, industrial plumes, and air masses impacted by biogenic emissions will be presented and compared with the urban plumes in Figs. 1 and 2. Finally, we will discuss our observations of VOCs in the clean atmosphere, including the free troposphere, and the marine boundary layer, where ocean uptake of several VOCs was inferred from the data.

References

[1] J.A. de Gouw, C. Warneke, D.D. Parrish, J.S. Holloway, M. Trainer, F.C. Fehsenfeld, Emission sources and ocean uptake of acetonitrile (CH_3CN) in the atmosphere, Journal of Geophysical Research 108, 4329, doi:10.1029/2002JD002897 (2003).

[2] J.A. de Gouw, et al., Chemical composition of air masses transported from Asia to the U.S. West Coast during ITCT 2K2: Fossil fuel combustion versus biomass-burning signatures, Journal of Geophysical Research 109, D23S20, doi:10.1029/2003JD004202 (2004).

[3] J.A. de Gouw, P.D. Goldan, C. Warneke, W.C. Kuster, J.M. Roberts, M. Marchewka, S.B. Bertman, A.A.P. Pszenny, W.C. Keene, Validation of proton transfer reaction-mass spectrometry (PTR-MS) measurements of gas-phase organic compounds in the atmosphere during the New England Air Quality Study in 2002, Journal of Geophysical Research 108, 4682, doi:10.1029/2003JD003863 (2003).

[4] C. Warneke, et al., Comparison of daytime and nighttime oxidation of biogenic and anthropogenic VOCs along the New England coast in summer during the New England Air Quality Study 2002, Journal of Geophysical Research 109, D10309, doi:10.1029/2003JD004424 (2004).

[5] J.A. de Gouw, et al., Budget of organic carbon in a polluted atmosphere: Results from the New England Air Quality Study in 2002, Journal of Geophysical Research 110, D16305, doi:10.1029/2004JD005623 (2005).

[6] J.A. de Gouw, et al., Volatile organic compounds composition of merged and aged forest fire plumes from Alaska and western Canada, Journal of Geophysical Research 111, D10303, doi:10.1029/2005JD006175 (2006).

[7] C. Warneke, et al., Biomass burning and anthropogenic sources of CO over New England in the summer 2004, Journal of Geophysical Research 111, D23S15, doi:10.1029/2005JD006878 (2006).

[8] C. Warneke, et al., Determination of urban VOC emissions ratios and comparison with inventories, Journal of Geophysical Research, submitted.

[9] C. Warneke, J.A. de Gouw, E.R. Lovejoy, P.C. Murphy, W.C. Kuster, R. Fall, Development of proton-transfer ion trap-mass spectrometry: on-line detection and identification of volatile organic compounds in air, Journal of the American Society of Mass Spectrometry 16, 1316-1324 (2005).

[10] C. Warneke, S. Kato, J.A. de Gouw, P.D. Goldan, W.C. Kuster, M. Shao, E.R. Lovejoy, R. Fall, F.C. Fehsenfeld, Online volatile organic compound measurements using a newly developed proton-transfer ion-trap mass spectrometry instrument during New England Air Quality Study-Intercontinental Transport and Chemical Transformation 2004: performance, intercomparison, and compound identification, Environental Science & Technology 39, 5390-5397 (2005).

[11] J.A. de Gouw, C. Warneke, Measurements of volatile organic compounds in the Earth's atmosphere using proton-transfer–reaction mass spectrometry, Mass Spectrometry Reviews, in press.

Measurement of benzene and toluene emissions in the urban environment: Is this distribution controlled by vehicle emissions?

Berk Knighton[1]

[1]*Department of Chemistry, Montana State University, Bozeman, USA*
bknighton@chemistry.montana.edu

Abstract

The distribution or ratio of benzene and toluene measured in an air sample is a commonly reported quantity. In vehicle exhaust it is an important indicator of the quality of the vehicle's emission control system. In atmospheric science it can be used to derive the photochemical age of the air mass providing that the starting distribution of these two compounds is known. While the ratio of these compounds in an urban environment might be expected to be controlled predominately by vehicular emissions there is emerging evidence that this may not be the case. During the 2003 and 2006 Mexico City Metropolitan Area (MCMA) field campaigns, a PTR-MS was deployed on-board the Aerodyne mobile laboratory and made continuous measurements as it traveled throughout the region. It was consistently noted that the benzene to toluene ratio was observed to be higher on-road where the measurements are dominated by vehicle emissions, than at stationary urban sampling sites. Is this counterintuitive result real or simply a measurement artifact? Inter-comparison of the on-road PTR-MS measurements with other vehicle tail pipe emission and tunnel studies suggest that the PTR-MS results are robust. This implies that vehicle emissions alone do not define the distribution of benzene and toluene in the MCMA urban environment. Examination of the data reported in other studies suggests that this result is not unique to Mexico City. One possible explanation is solvent based toluene emissions, but is there really enough solvent borne toluene to alter the ambient concentration distribution in the urban airshed? Mobile PTR-MS measurements from the US and Mexico will be presented and discussed in an attempt to address this important question.

Introduction

Vehicle exhaust emissions are typically thought to be the dominant source of aromatic hydrocarbons in polluted urban environments. It would then be expected that the distribution of these aromatic compounds in an unprocessed urban air mass should closely resemble that being emitted from vehicle tailpipes. A very different result was obtained from the results of the 2003-MCMA field campaign, where it was observed that fleet averaged benzene to toluene ratio was 0.48 [1] while a ratio of 0.23 was obtained by measurements made at stationary sites within the urban core [2]. The result seems counterintuitive. How can on-road measurements be so different from measurements made at stationary sites that are located only meters from major roadways? A problem with the PTR-MS measurements used to make the fleet averaged measurement in 2003 might explain the apparent discrepancy. The urban ratio of 0.23 is similar to that expected for gasoline vehicles operating without any exhaust emission control system, suggesting that older model vehicles are responsible for most of the pollution. Emissions dominated by heavily polluting older vehicles however, are not supported by tunnel studies conducted in Mexico City where benzene to toluene ratios of 0.42 and 0.35 were observed [3]. The tunnel study results are

similar to the PTR-MS derived fleet average value and provide some support for the PTR-MS measurement. US measurements show a similar disparity between the vehicle emission and urban airshed benzene to toluene ratio. The average urban US ambient measurements [4] indicate a ratio of 0.44 while US tunnel studies [5] provide ratios of 0.61 and 0.78. Collectively these measurements suggest that the ambient concentrations of benzene, toluene or both are not controlled solely by vehicle emissions. In this presentation evidence is provided that suggests that solvent sources of toluene are significantly influencing the distribution of benzene and toluene in urban ambient atmospheres.

Experimental Methods

The PTR-MS used in this study has been modified to operate on board the Aerodyne mobile laboratory [2]. Different data acquisition modes were used for on-road and stationary site sampling. On-road measurements required high resolution and 9 ion masses were monitored at 0.1 sec per mass resulting in an a measurement cycle of approximately 1.5 seconds. Stationary monitoring employed an alternating acquisition mode. The instrument was programmed to switch between a selected set of 10 ion masses (1 sec per mass) for 24 cycles followed by full mass scans from 20–160 amu (0.1 sec per mass) for 12 cycles. In both on-road and stationary sampling modes, ions corresponding to methanol (m/z 33), acetaldehyde (m/z 45), acetone (m/z59), benzene (m/z 79), toluene (m/z 93), C2-benzenes (m/z 107), C3-benzenes (121) were measured and concentrations are calculated using calibration factors. The final benzene concentration has been corrected for contributions from the fragmentation of ethylbenzene and propylbenzene [2].

Carbon monoxide was measured by tunable infrared laser differential absorption spectroscopy. Concentrations are determined by fitting the measured rotational-vibrational transmission spectrum to a Voight line shape model using known line strength parameters.

Results

Figure 1 shows time series trends and correlation scatter plots for benzene and CO observed during on-road and fixed site sampling. The signals are highly correlated in both sampling modes, although there is more scatter in the on-road data due to the variations in vehicle engine type and extent of emission control. The similarity in slopes infers that vehicular emissions are a dominating source of CO and benzene. Solvent sources of benzene including evaporative emissions from gasoline are observed, but these emissions appear to be relatively unimportant in comparison to vehicle exhaust emissions. The fixed site correlation scatter plot shows a few gasoline evaporative emission events as small vertical rays in the correlation scatter plot where the benzene concentration increases without any change in the CO concentration.

A correlation scatter plot comparing the benzene and toluene concentrations measured on-road versus that observed at the fixed sampling sites is shown in Figure 2. The magnitude and correlation of the signals indicates that the on-road concentrations of benzene and toluene are dominated by vehicular emissions. The linear regression line for the on-road data has been fit to all of the data, but assumes a zero intercept and is biased downward because of toluene solvent plumes (which are obscured by the fixed site data). The correct on-road benzene to toluene ratio will be higher than the slope (0.42) and is similar to the 0.48 value observed in 2003 [1]. The benzene to toluene ratio observed at the fixed sites is substantially lower, a result which is thought to be from the enrichment in ambient toluene concentration from solvent sources. The circled region in Figure 2 highlights the

section of the scatter plot where solvent related sources of toluene are clearly evident. The line shown for the fixed site data was given a slope of 0.23 on the basis of a previous study [2] and is included to further illustrate the influence of solvent borne toluene.

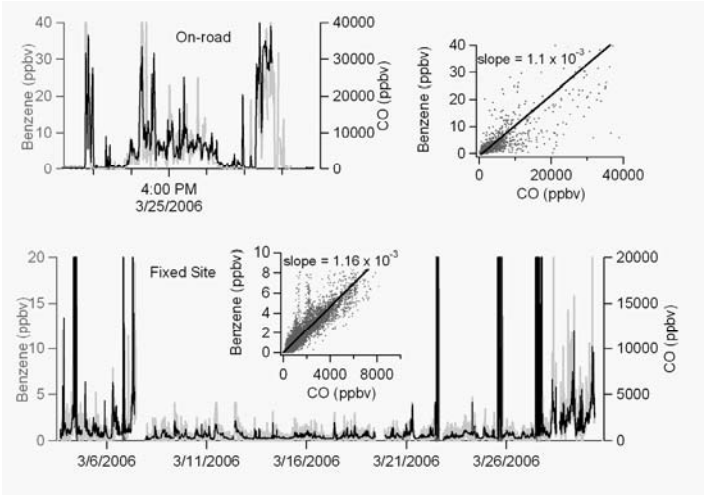

Figure 1: Time series trends and correlation scatter plots for benzene and CO observed during on-road and fixed site sampling.

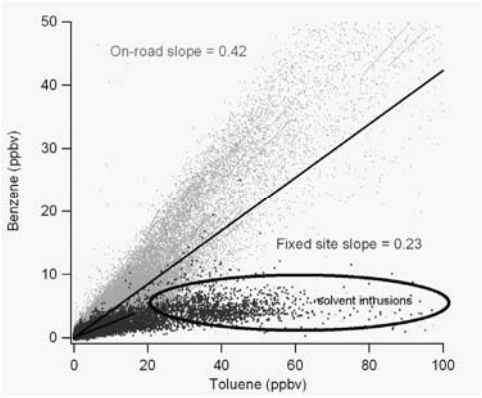

Figure 2: Comparison of the benzene to toluene concentrations observed on-road versus at fixed sampling sites.

Discussion

While Figure 2 clearly shows the influence on solvent based toluene on the measurements made during the 2006 Mexico City field campaign, how representative is this data set and where are the solvent sources of toluene? This data appears to be quite representative of Mexico City as similar results were observed in field campaigns conducted there in 2002 and 2003. Mobile exploration of toluene sources reveals that the bulk of these sources appear to be related to painting. Evaporative emissions from gasoline are not as important as expected and only appear to be significant in the immediate vicinity of gasoline fueling stations. Also, because gasoline contains other aromatic components, like benzene, solvents emissions for this source are not recognized as solvent toluene in this study. Street line painting and autobody repair facilities are major toluene sources while residential house painting also contributes but is more minor. Unidentified sources are also important as it is not unusual to pull up to an intersection and note unusually high levels of toluene with no apparent source nearby. My experience in the US has been more limited, but in the few studies that I have participated in toluene plumes have also been observed. While the data implicating the importance solvent sources of toluene may not be overwhelming, the evidence for a missing source of toluene is more persuasive. The disparity between the distribution of benzene and toluene in the ambient urban environment and that observed in vehicle emission studies and tunnel studies provides a compelling argument for a missing source of toluene. As vehicle emissions get cleaner their importance to urban air pollution should diminish and so non-combustion emission sources may start to have a more important contribution to the hydrocarbon burden in urban atmospheres.

References

[1] M. Zavala, S. C. Herndon, R. S. Slott, E. J. Dunlea, L. C. Marr, J. H. Shorter, M. Zahniser, W. B. Knighton, T. M. Rogers, C. E. Kolb, L. T. Molina, M. J. Molina, Characterization of on-road vehicle emissions in the Mexico City Metropolitan Area using a mobile laboratory in chase and fleet average modes during the MCMA-2003 field campaign, Atmospheric Chemistry and Physics Discussions. 6, 4689-4725 (2006).

[2] T. M. Rogers, E. P. Grimsrud, S. C. Herndon, J. T. Jayne, C. E. Kolb, E. Allwine, H. Westberg, B. K. Lamb, M. Zavala, L. T. Molina, M. J. Molina, W. B. Knighton, On-road measurements of volatile organic compounds in the Mexico City metropolitan area using proton transfer reaction mass spectrometry, International Journal of Mass Spectrometry, 218, 26-37, (2006).

[3] V. Mujica, J. Watson, E. Vega, E. Reyes, M. E. Ruiz, J. Chow, Receptor model source apportionment of nonmethane hydrocarbons in Mexico City, The Scientific World Journal. 2, 844-860, (2002).

[4] D. D. Parish, M. Trainer, V. Young, P. D. Goldan, W. C. Kuster, B. T. Jobson, F. C. Feshenfeld, W. A. Lonneman, R. D. Zika, C. T. Farmer, D. D. Reimer, M. O. Rogers, Internal consistency tests for evaluation of measurements of anthropogenic hydrocarbons in the troposphere, Journal of Geophysical Research 103, 22339-22359, (1998).

[5] W. R. Pierson, A. W. Gertler, N. F. Robinson, J. C. Sagebiel, B. Zielinska, G. A. Bishop, D. H. Stedman, R. B. Zweidinger, W. D. Ray, Real-world automotive emissions - Summary of studies in the Fort McHenry and Tuscarora Mountain Tunnels, Atmospheric Environment, 30, 2233-2256, (1996).

Operational Optimization of CFC destruction facility by means of PTR-MS and its modified method

Akio Shimono[1], Toshihide Hikida and Makoto Naganuma[1]

[1]Sanyu Plant Service Co., Ltd., 1-8-21 Hashmotodai, Sagamihara-shi, Kanagawa-ken, 229-1132 Japan (a.shimono@g-sanyu.co.jp)

Abstract

We have applied the conventional PTR-MS technology via proton transfer reaction to on-line monitoring of various volatile organic compounds emitted from incinerators including the approved facilities for the destruction of discarded chlorofluorocarbon (CFC) compounds. For the purpose of real-time monitoring of the CFC destruction efficiency, the modified method by using O_2^+ as the primary ion was proposed. The improved sensitivities for CFCs was successfully demonstrated at an approved CFC destruction facility employing a rotary kiln incinerator designed for hazardous waste incineration. The advantages and the limitations of this modified method were also discussed.

Introduction

Certain CFCs are recognized as Ozone Depleting Substances (ODS) as well as they show strong greenhouse effects. The release of chemically stable CFCs to ambient air has significantly contributed on stratospheric ozone depletion which still continues. The practice of proper collection, recovery, and destruction is a crucial nationwide task. Based on the report prepared by UNEP Ad hoc Technical Advisory Committee on ODS destruction facilities [1], several CFC destruction technologies were proposed and are put in practical use in Japan, including rotary kiln incinerators, cement kilns, gaseous/fume oxidation, liquid injection incineration, plasma pyrolysis, catalytic dehydrohalogenation. Among these, the destruction by rotary kiln incinerators has important advantages of cost-effectiveness and popularity, because existing waste incinerators are available and no specific maintenance technology is required. The rotary kiln incinerators in service which Japanese Government approves as the CFC destruction facilities are originally designed for the incineration of various types of industrial wastes including such wastes as containing halogenated compounds.

We reported the first attempt to apply PTR-MS instruments to on-line monitoring of volatile organic compounds (VOCs) occurred in incinerator flue gases [2]. We have demonstrated that the concentration of m/z 129 which is detected by PTR-MS and corresponds to the mixture of naphthalene and chlorophenol is an appropriate index of dioxins formed in waste incineration in the significant presence of chlorine containing species. We have laid importance on the simultaneous monitoring of benzene and other alkylbenzenes. Villinger et al [3] reported that the toluene-to- benzene ratio varied with the transient engine states in their automobile exhaust measurements, and that the toluene-to-xylene ratio was almost stable. They concluded that benzene was formed in combustion process, whereas toluene and xylene originated from unburnt fuel. Though they considered that benzene was formed from demethylation of other alkylbenzenes existing in supplied fuel, we observed benzene spikes in incinerator flue gases

without any relation to the feeding of aromatic species. Those benzene spikes may indicate that the benzene formation from the reaction of acetylene with C_4, and C_5 radicals [4], or the self-recombination of propargyl radicals [5], which many combustion chemists have ever been interested in. Such benzene spikes were also observed in automobile exhausts employing a course of chasis dynamo experiments. Our findings will be discussed elsewhere in detail. We have also observed the characteristic naphthalene formation based on the similar mechanism both in incinerator flue gases and in automobile exhausts. These facts shows the feasibility of combustion diagnostics via on-line monitoring by using PTR-MS as well as it is a powerful tool for emission monitoring of undesired toxic trace species.

In the meanwhile, some rotary kiln incinerators in service for hazardous waste management have played significant roles on the activity of discarded CFC destruction. The requirement of real-time monitoring of residual CFC concentrations which are converted to the destruction efficiencies have been emerged because those incinerators also burn various types of other wastes under the condition that the collected and thus feed quantities of wastes could hardly be maintained constant. In our preliminary results, CFCs escaped from decomposition and remained in flue gases could be detected by PTR-MS. However it was certain that the sensitivity for CFC species is 2 orders of magnitude lower compared with that for ordinary oxygenated organics. Japanese Government specifies the regulatory standard for the destruction efficiency for CFCs of 99% or 99.9% according to the destroyed amount at approved CFC destruction facilities. It was still hard to assess the destruction efficiency especially by using the compact version of PTR-MS instrument, in view of the compliance with the higher goal at 99.99% which the report of the Fourth Meeting of the Parties to the Montreal Protocol suggested, and which corresponds to the residual CFCs in flue gases at several tens ppb under typical conditions. Thus the limitation to the detection of CFCs remained in flue gases was an issue on the application of PTR-MS instruments to CFC destruction facilities. The proton affinities for such halogen-substituted saturated hydrocarbons are much less than that for water. Their chemical ionization seems to be driven by halogen subtraction.

Experimental

The sensitivities for CFCs, halons, and other chlorine-substituted saturated hydrocarbons by means of a high sensitivity version of PTR-MS instrument and a compact version of PTR-MS instrument were investigated by comparison with known concentrations of their standard gases in terms of estimated reaction rate constants. The typical figures at 10^{-11} cm^3/s level suggested the possibility that these species reacted with a few % of O_2^+ existing as an impurity of primary ions. Then we examined the use of pure oxygen as the primary ion source. In order to supply slightly pressurized oxygen with 99.99% purity from cylinders to the existing ion source section, an additional line equipped with a mass flow controller was connected to the inlet to the ion source section through a tee connector for switching between the proton transfer reaction ionization and the chemical ionization by using O_2^+. The O_2^+ formation was stable and the sensitivities by means of this modified method were also investigated in a similar manner.

The modified method using O_2^+ was implemented on the compact version of PTR-MS instrument working as an on-line flue gas monitor at a rotary kiln incinerator facility approved as the CFC destruction facility depicted before [2]. The main CFC species discarded and thus destroyed in the rotary incinerator was HCFC-22 (chlorodifluoromethane). The typical feed rate for HCFC-22 was 20 kg/h corresponding to approximately 2% of the total waste loading. The temperature at the exit

of rotary kiln was kept above 950˚C by the operational control. This temperature above 950˚C corresponds to the temperature in the flame zone higher than 1200˚C, where the gases of CFC species are directly injected. A series of long-term continuous measurements of HCFC-22 concentration remained in flue gases were performed at the CFC destruction facility with the simultaneous monitoring of possible byproducts including $CHCl_3$, CCl_4 and other several species. The experimental destruction of halon-1311 was also conducted and the residual halon-1311 in flue gases was monitored by the modified method. The flue gas was sampled just before the stack and passed through a cyclone separator coupled with an auto-balancing trap for the only removal of supersaturated and then condensed water particles. Then the sampling line was heated up to 105 ˚C and the sampled gas was introduced into the instrument without any further pretreatment. The effect of the additional humidity reduction by a thermoelectric cooling unit down to 5 ˚C was also investigated.

Results and Discussion

The conditions of the ion source section for the modified method was similar to the conditions for the conventional PTR-MS except that oxygen is supplied at 2.0 sccm. The O_2^+ production by the modified method was typically 2 x 10^{-7} A at drift voltage of 500V for the compact version of PTR-MS instrument. For most of hydrocarbons (described as M) such as butene, acetone, acetonitrile, methylethylketone and benzene, the chemical ionization by O_2^+ mainly produced M^+ ions through charge transfer reaction, where as the main products from these species by the conventional PTR-MS were $(M+H)^+$ ions. It also applied to the case of halogen-substituted unsaturated hydrocarbons including dichlorobenzene, vinyl chloride, and trichloroethylene. In the case of halogen-substituted saturated hydrocarbons including chloroform, carbon chloride, 1,2-dichloroethane, 1,1,1-trichloroethane, CFC-11 (trichlorofluoromethane), CFC-12 (dichloro-difluoromethane), CFC-113 (trichlorotrifluoroethane), HCFC-22 (chlorodifluoromethane), halon-1301 (bromotrifluoromethane), halon-1211 (bromochlorodifluoromethane), the main products for both methods were $(M-X)^+$, where X denotes one halogen atom. On the other hand, the sensitivities for these species by the conventional PTR-MS were 2 orders of magnitude lower than that by the chemical ionization by O_2^+. The preliminary results showed that the reaction rate constants for these species with the chemical ionization by O_2^+ were roughly within the order of 10^{-9} cm^3/s. The O_2^+ concentration in the conventional PTR-MS was maintained at around 2%. Thus it is considered that the signal intensity for these species are simply contributed by O_2^+ concentration. By employing the chemical ionization by O_2^+, the nominal masses of the product ions for halogen-substituted saturated hydrocarbons appeared in odd numbers, which could be conveniently separated from most of other hydrocarbons.

When we applied the chemical ionization by O_2^+ to actual incinerator flue gases, the significant numbers of H_3O^+ and $H_3O^+ \cdot H_2O$ ions were generated because the water content in flue gases amounted to 20 to 30% under the water vapor saturated conditions at around 70˚C. Typically the O_2^+ production dropped to 7 x 10^{-8} A and the almost same amount of H_3O^+ was generated. From other experiments, it was clear that the O_2^+ strongly correlated with absolute humidity. This may implies that water vapor goes backward into the source drift region of the ion source section and then competes with O_2 for the ionization. However, the ratio of product ions to O_2^+ ions were not affected by water vapor at least in the case of CFC-11, CFC-12, CFC-113, HCFC-22, halon1211, and halon1301. Additionally these ratios had linear relationship with the concentration of these species. Thus the quantitative analysis for halogen-substituted saturated hydrocarbons by the chemical ionization by O_2^+ was possible. The first result of long-term on-line continuous

monitoring of the residual HCFC-22 for longer than 2 months was shown in Fig. 1. The measurement was conducted without any further treatment of water vapor. The measured concentration approximately below 30 ppb corresponds to the destruction efficiency higher than 99.99%. Therefore the result indicates that the complete destruction of CFCs by rotary kiln incinerators are quite feasible.

For better signal-to-noise ratio, when the chemical ionization by O_2^+ is employed for such applications, the suppression of O_2^+ reduction and H_3O^+ production is significant. The effect of the additional humidity reduction by a thermoelectric cooling unit down to 5 ˚C was tested on-line. O_2^+ production became twice as much as H_3O^+ production. Still, this may lead to the adverse effect that some part of the object species for measurements is removed by condensation if the boiling point of the species is low. Further work is required in order to improve the modified method as the unique on-line monitoring tool for CFC destruction facilities.

Conclusions

The modified ionization method by using O_2^+ coupled with PTR-MS instruments were proposed and tested for on-line monitoring of CFCs in flue gases at a rotary kiln incinerator where discarded CFCs were destroyed. The improved sensitivities for CFCs compared with the conventional PTR-MS technology were observed and the control of destruction efficiency for CFCs above 99.99% was demonstrated.

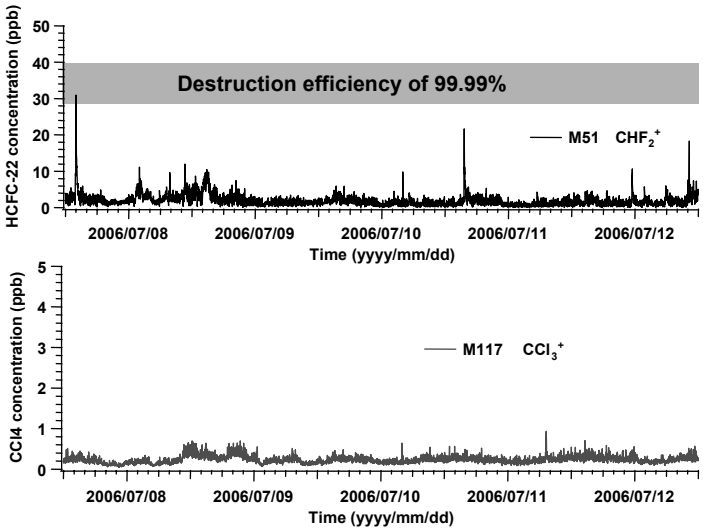

Figure 1: Time trend of the concentrations of HCFC-22 and possible its destruction byproduct, CCl_4

References

[1] Documents of the 4th Meeting of the Prties 23-25 November 1992. Copenhagen, UNEP/OzL.Pro.4/4, Report of the Ad hoc Technical Advisory Committee on ODS destruction Technologies, 1992

[2] Shimono, A. and Naganuma, M., 2nd International Conference on Proton Transfer Reaction Mass Spectrometry and its Applications; Contributions, 56-59(2005)

[3] Villinger, J., Federer, W., Resch, R., Lubich, M., Sejkora, W. and Dornauer, A., SAE technical paper series 931027, 1993

[4] Frenklich M. and Wang, H., *J. Phys. Chem.* 98, 11465-11489(1994)

[5] Miller, J. A. and Melius, C. F., *Combust. Flame* 91, 21-39(1992)

5. PTR-MS: Measurements of Biogenic VOCs

The Forest as a Chemical Reactor: Natural Compounds Have Profound Impacts on Earth's Atmosphere

Allen H. Goldstein[1], Rupert Holzinger[1, 2], Anita Lee[1,3], and Nicole Bouvier-Brown[1]

[1] *Department of Environmental Science, Policy, and Management, University of California at Berkeley, Berkeley, California, USA, corresponding author email ahg@nature.berkeley.edu*

[2] *Institute for Marine and Atmospheric Research, University of Utrecht, Utrech, The Netherlands*

[3] *United States Environmental Protection Agency, San Francisco, California, USA*

Abstract

Volatile Organic Compounds (VOCs) naturally produced and emitted by plants play important roles in the chemistry of the atmosphere, with terpenes and isoprene affecting regional air quality, atmospheric radiation, and global climate through secondary organic aerosol formation. We have conducted extensive field measurements of biogenic VOCs, and their oxidation products, in a California pine forest at the Blodgett Forest Research Station. Measurements of concentrations and forest-atmosphere interactions have been made using automated in-situ chromatography techniques as well as a fast response Proton-Transfer-Reaction Mass Spectrometer (PTR-MS) coupled to micrometeorological flux techniques. Field measurements of vertical concentration profiles through the forest canopy and fluxes above the canopy reveal the secondary production of large amounts of previously unreported compounds. We also performed terpene oxidation experiments in smog chambers to show that the products of these reactions are consistent with those compounds detected in and above the forest. In addition, we can show that about half the ecosystem scale ozone flux in summer is actually due to chemical reactions occurring between terpenoid compounds and ozone within the forest canopy. Taken together, this information suggests that the flux of terpenes leaving the forest canopy represents only a fraction of the terpenoid compounds actually emitted, and the rest is chemically processed within the forest canopy. Branch enclosure measurements confirm many BVOCs are emitted that are not typically observed above the forest, presumably due to their high reactivity and thus very short atmospheric residence times. The implication of our research is that the source of secondary aerosols from biogenic terpene oxidation is likely much larger than previously estimated, and much larger than all anthropogenic sources combined. We have also observed fine aerosol growth events which we believe are related to the terpene oxidation occurring in the forest canopy. Similar observations of aerosol growth events, non-stomatal ozone deposition, and missing OH reactivity at forested sites around the world suggest unmeasured highly reactive BVOC emission is common and not unique to our measurement site. These highly reactive BVOCs represent a previously unquantified carbon loss from ecosystems and a major source of secondary organic aerosols, oxidized gas phase organics, and OH radicals to the atmosphere.

Introduction

The Blodgett forest site on the western slope of the Sierra Nevada Mountains of California (38.90O N, 120.63O W, 1315m elevation) is located 75 km downwind (northeast) of Sacramento where it receives anthropogenically impacted air masses rising from the valley below during the day[*Lamanna and Goldstein*, 1999]. At night the wind usually shifts towards the west and air masses descending from the sparsely populated Sierra Nevada are advected to the site. The plantation is owned and operated by Sierra Pacific Industries (SPI) and was planted with Pinus ponderosa L. in 1990, interspersed with a few individuals of Douglas fir, white fir, California black oak, and incense cedar. Average tree height was 4.8 (median) in 2003 and the canopy height was defined to be 6.4m, a height exceeded by 20% of the trees. The understory was composed primarily of manzanita (Arctostaphylos spp.) and whitethorn (Ceonothus cordulatus) shrubs. A sketch of the experimental setup is given in Figure 1. Air was sampled through 6 individual gas inlets. Inlet A was used to sample air from 12.5m for eddy-covariance flux measurements of total monoterpenes, methylbutenol, and selected terpene oxidation products. This inlet was located at the top of the tower, adjacent to the sonic anemometer. Air was pulled at 10 L min^{-1} through a 2 μm Teflon particulate filter, and brought down, using ¼ inch ID Teflon tubing, to the instruments in a temperature controlled container. Inlets B-F were used to sample vertical gradients at height-levels within (1.1, 3.1, 4.9m) and above (8.75, 12.5m) the canopy. The 5 gradient inlets each consisted of 30m PFA tubing (ID ~4mm) protected by a Teflon filter (PFA holder, PTFE membrane, pore size 2μm); a sample flow of 1 liter per minute was maintained at all times through each sample tube.

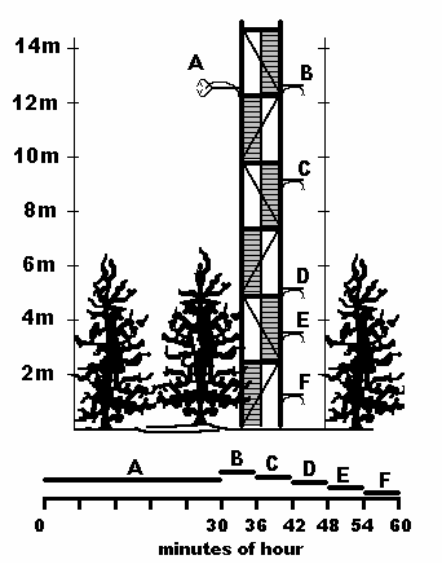

Figure 1: Experimental Setup: high flow inlet A was used for flux measurements; VOC-gradients were measured by sampling from 5 individual inlets (B-F) positioned at 1.1, 3.1, 4.9, 8.75, and 12.5m above ground. Canopy height was 6.4 m. (from [Holzinger et al., 2005])

In addition to the canopy scale flux and gradient measurements, branch enclosures were used to observe the BVOC emissions directly before any atmospheric oxidation could occur. Sampling from the branch enclosure included 3 methods: PTRMS, in-situ GC-FID, and Solid Phase Micro Extraction (SPME) fibers which were later analyzed by GC-Ion Trap-MS.

Controlled smog chamber reaction studies were performed at the California Institute of Technology in collaboration with Professor John Seinfeld and his research group ([*Lee et al.*, 2006a; *Lee et al.*, 2006b; *Ng et al.*, 2006; *Varutbangkul et al.*, 2006]). The ozone oxidation of 10 terpenes, and the photooxidation of 16 terpenoid compounds were conducted individually at the Caltech Indoor Chamber Facility under atmospherically relevant HC:NOx ratios to monitor the time evolution and yields of SOA and gas-phase oxidation products using PTR-MS. Several oxidation products were calibrated in the PTR-MS, including formaldehyde, acetaldehyde, formic acid, acetone, acetic acid, nopinone, methacrolein + methyl vinyl ketone; other oxidation products were inferred from known fragmentation patterns, such as pinonaldehyde; and other products were identified according to their mass to charge (m/z) ratio.

Results & Discussion

Vertical gradients of mixing ratios of volatile organic compounds at Blodgett Forest revealed large quantities of previously unreported oxidation products of short lived biogenic precursors. The emission of biogenic precursors must be in the range of 13–66μmolm−2 h−1 to produce the observed oxidation products. That is 6–30 times the emissions of total monoterpenes observed above the forest canopy on a molar basis. These reactive precursors constitute a large fraction of biogenic emissions at this site, and are not included in current emission inventories. When oxidized by ozone they should efficiently produce secondary aerosol and hydroxyl radicals [*Holzinger et al.*, 2005].

During the controlled smog chamber reaction studies of terpenoid compound oxidation, numerous unidentified products were formed, and the evolution of first- and second-generation products was clearly observed. SOA yields from the different terpenes ranged from 1 to 68%, and the total gas-plus particle-phase products accounted for 50–100% of the reacted carbon (Figure 2). The carbon mass balance was poorest for the sesquiterpenes, suggesting that the observed products were underestimated or that additional products were formed but not detected by PTR-MS. Several second-generation products from isoprene photooxidation, including m/z 113, and ions corresponding to glycolaldehyde, hydroxyacetone, methylglyoxal, and hydroxycarbonyls, were detected. The detailed time series and relative yields of identified and unidentified products aid in elucidating reaction pathways and structures for the unidentified products. Many of the unidentified products from these experiments were also observed within and above the canopy of the Ponderosa pine plantation at Blodgett Forest, confirming that many products of terpene oxidation can be detected in ambient air using PTR-MS, and are indicative of concurrent SOA formation[Lee et al., 2006b].

During an intensive field campaign in summer 2005 we measured ecosystem fluxes of the sum of methyl-butenol (MBO), total monoterpenes, and an oxidation product with our eddy-covariance system. The compounds were detected by PTR-MS at molecular weights of 69, 137, and 113 amu; typical fluxes were 4-18, 2-6, 0.4-1.5 μmol m2 h-1 for MBO, monoterpenes, and the oxidation product, respectively. These are the first canopy scale fluxes of any terpene oxidation

products, and they show that even this one oxidation product (113 amu) has a flux equivalent to approximately 25% of the total terpenes observed to escape from the forest canopy.

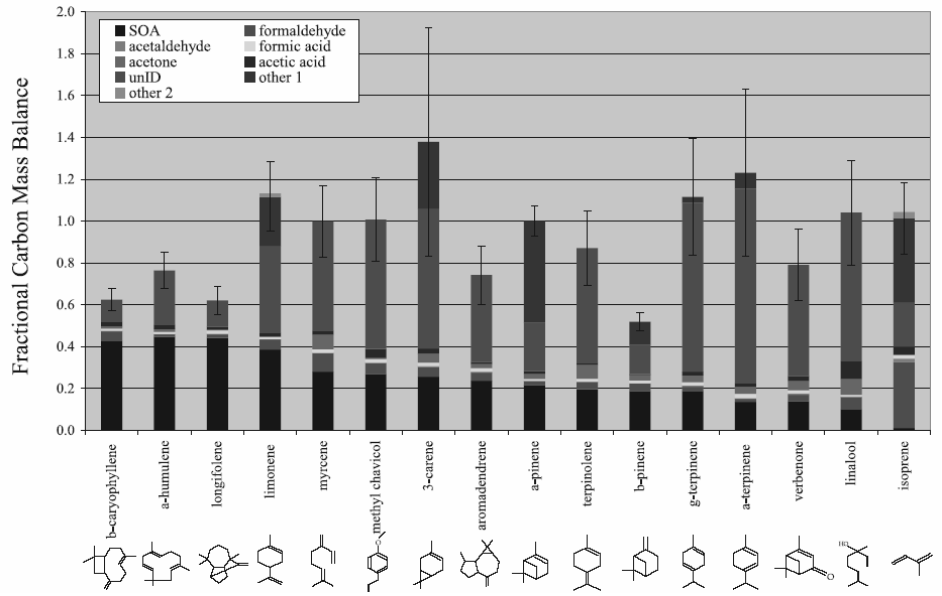

Figure 2: Carbon mass balance of terpene oxidation products. Other 1 = nopinone and MACR + MVK from b-pinene and isoprene, respectively, and limononaldehyde, caronaldehyde, pinonaldehyde, terpinaldehyde, and a-terpinaldehyde, from limonene, 3-carene, a-pinene, g-terpinene, and a-terpinene, respectively. Other 2 = limonaketone from limonene and 3-methyl furan from isoprene (from [Lee et al., 2006b]).

References

Holzinger, R., A. Lee, K.T. Paw, and A.H. Goldstein, Observations of oxidation products above a forest imply biogenic emissions of very reactive compounds, *Atmospheric Chemistry and Physics*, *5*, 67-75, 2005.

Lamanna, M.S., and A.H. Goldstein, In situ measurements of C-2-C-10 volatile organic compounds above a Sierra Nevada ponderosa pine plantation, *Journal of Geophysical Research-Atmospheres*, *104* (D17), 21247-21262, 1999.

Lee, A., A.H. Goldstein, M.D. Keywood, S. Gao, V. Varutbangkul, R. Bahreini, N.L. Ng, R.C. Flagan, and J.H. Seinfeld, Gas-phase products and secondary aerosol yields from the ozonolysis of ten different terpenes, *Journal of Geophysical Research-Atmospheres*, *111* (D7), 2006a.

Lee, A., A.H. Goldstein, J.H. Kroll, N.L. Ng, V. Varutbangkul, R.C. Flagan, and J.H. Seinfeld, Gas-phase products and secondary aerosol yields from the photooxidation of 16 different terpenes, *Journal of Geophysical Research-Atmospheres*, *111* (D17), 2006b.

Ng, N.L., J.H. Kroll, M.D. Keywood, R. Bahreini, V. Varutbangkul, R.C. Flagan, J.H. Seinfeld, A. Lee, and A.H. Goldstein, Contribution of first- versus second-generation products to secondary organic aerosols formed in the oxidation of biogenic hydrocarbons, *Environmental Science & Technology*, *40* (7), 2283-2297, 2006.

Varutbangkul, V., F.J. Brechtel, R. Bahreini, N.L. Ng, M.D. Keywood, J.H. Kroll, R.C. Flagan, J.H. Seinfeld, A. Lee, and A.H. Goldstein, Hygroscopicity of secondary organic aerosols formed by oxidation of cycloalkenes, monoterpenes, sesquiterpenes, and related compounds, *Atmospheric Chemistry and Physics*, *6*, 2367-2388, 2006.

Volatile organic compounds emitted from natural landscapes measured by PTR-MS

Thomas Karl

National Center for Atmospheric Research

Abstract

The emission of biogenic volatile organic compounds (VOC) is recognized as the largest terrestrial source of reactive carbon to the atmosphere [Guenther et al., 2000]. Predicting the role of the biosphere in the behavior of the earth system and understanding the interaction between ecosystems and the atmosphere is becoming an increasingly important part of atmospheric science. It is suggested that landuse change will have a profound impact on the distribution of biogenic VOC emissions. In addition, recent reports ([Kurpius and Goldstein, 2003], [Holzinger et al., 2004],[Di Carlo et al., 2004]) hypothesize large biogenic emissions, that could offset the HOx balance and the ozone flux budget above various ecosystems. These studies suggest large hitherto unknown sources of reactive organic compounds that have yet to be identified. This presentation will summarize results obtained recently from PTR-MS flux measurements during CELTIC (Chemical Emission, Loss and Transport within Canopies) field experiments (DukeForest, NC, 2003, Amazon, BR,

2004 and Prophet Tower, MI, 2005, Niwot Ridge, 2006) and address uncertainties that will have to be considered in future field campaigns and modeling exercises.

References

Di Carlo, P., W.H. Brune, M. Martinez, H. Harder, R. Lesher, X.R. Ren, T.

Thornberry, M.A. Carroll, V. Young, P.B. Shepson, D. Riemer, E. Apel, and C.

Campbell, Missing OH reactivity in a forest: Evidence for unknown reactive biogenic VOCs, Science, 304 (5671), 722-725, 2004.

Guenther, A., C. Geron, T. Pierce, B. Lamb, P. Harley, and R. Fall, Natural emissions of non-methane volatile organic compounds; carbon monoxide, and oxides of nitrogen from North America, Atmospheric Environment, 34 (12-14), 2205-2230, 2000.

Holzinger, R., A. Lee, K.T. Paw U, and A.H. Goldstein, Observations of oxidation products above a forest imply biogenic emissions of very reactive compounds, Atmos. Chem. Phys. Disc., 4, 5345-5365, 2004.

Kurpius, M.R., and A.H. Goldstein, Gas-phase chemistry dominates O-3 loss to a forest, implying a source of aerosols and hydroxyl radicals to the atmosphere, Geophysical Research Letters 30 (7), -, 2003.

Measuring ecosystem scale VOC emissions by PTR-MS

J. Rinne[1], R. Taipale[1], C. Spirig[2], T.M. Ruuskanen[1], T. Markkanen[3], T. Vesala[1], A. Brunner[2], C. Ammann[2], A. Neftel[2], T. Douffet[4], Y. Prigent[4], P. Durand[5], M. Kulmala[1]

[1] *University of Helsinki, Finland, janne.rinne@helsinki.fi*

[2] *Research Station Agroscope Reckenholz-Tänikon ART, Zürich, Switzerland*

[3] *Bayreuth University, Germany*

[4] *CNRM – MétéoFrance, Toulouse, France*

[5] *Laboratoire d'Aerologie, Toulouse, France*

Abstract

The disjunct eddy covariance (DEC) method has during the past few years been applied for volatile organic compound (VOC) flux measurements above vegetation canopies. The variants of this technique are shortly reviewed together with their characteristics. The disjunct eddy sampling causes uncertainty to the measured flux which can be estimated using various methods. Results of the recent method intercomparison experiments show good correspondence between DEC and conventional continuously sampling eddy covariance method.

Introduction

During the past decade proton transfer reaction – mass spectrometry has been applied to measure ecosystem scale VOC emissions using micrometeorological eddy covariance techniques [1]-[5]. These techniques are based on the measurement of rapid variations in VOC concentrations and vertical wind velocity. As these techniques rely in resolving the variations in time-scales of one second or less, the fast response PTR-MS is particularly suitable for these measurements.

Experimental Methods

In the traditional, continuously sampling eddy covariance method both vertical wind velocity and trace gas concentration are measured continuously with fast response instruments. As a large part of the flux is carried by high frequency eddies, instruments with response times higher than one second are utilized. The flux, F, is calculated as the covariance between vertical wind speed, w, and VOC concentration, c,

$$F = \frac{1}{t_2 - t_1} \int_{t_1}^{t_2} w' c' \, dt \,, \qquad (1)$$

where the primes denote difference from time average. This method is in wide use to measure fluxes of carbon dioxide, water vapor and ozone between surface and the atmosphere. It has also been used to measure fluxes of VOCs, especially isoprene.

Disjunct eddy covariance technique was first applied to VOC flux measurements in order to overcome the requirement of fast response VOC analyzer. This technique utilizes grab samplers,

which take in an air sample in less than a second. This air sample is then analyzed before next sample is taken, usually in 10-30 seconds. The flux is then calculated as a covariance of the disjunct time series,

$$F = \frac{1}{N}\sum_{i=1}^{N} w'_i \, c'_i \,, \qquad (2)$$

where w_i is the vertical wind velocity recorded at the moment the air sample was taken into the sampler [2].

The fast response PTR-MS is capable for flux measurements using the traditional continuously sampling eddy covariance method. However, as the PTR-MS measures only one mass at the time, only a flux of one compound at a time could be measured. Using the basic idea of disjunct eddy covariance this limitation can be overcome. In this variant of the disjunct eddy covariance method different masses are measured sequentially with a short dwell time [3]. Therefore, even when the air is sampled continuously, disjunct time series is created for the concentration of each mass, and Equation (2) can be used to calculate the flux.

In spectral space the flux of a compound equals to the integral of the co-spectra of the vertical wind speed and the concentration of the compound. The disjunct eddy covariance techniques rely on the aliasing of the co-spectra from the frequencies between the Nyquist frequency and the cut-off frequency due to the sensor response time to the lower frequencies (Figure 1). Thus the integral of the aliased co-spectra yields the same result as the non-aliased spectra of the continuous time series. The highest resolved frequency is defined by the response time of the instruments.

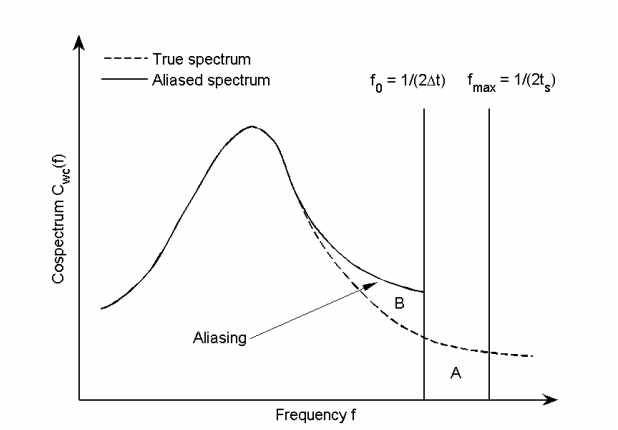

Figure 1: Effect of disjunct eddy sampling on the co-spectrum of vertical wind and concentration of the trace gas. f_0 is the Nyquist frequency, Δt sampling interval, f_{max} highest frequency contributing to the measured flux, and t_s the response time of the analyzer.

Results

The DEC method has been successfully used for VOC flux measurements above vegetation canopies. Recent intercomparison campaigns show in general good correlation with the fluxes measured by disjunct eddy covariance and conventional continuously sampling eddy covariance techniques [6]-[7]. The fluxes measured by the DEC-PTR-MS technique often show the vegetation to emit significant amounts of non-terpenoid compounds, in addition to terpenoids [3]-[5], [8].

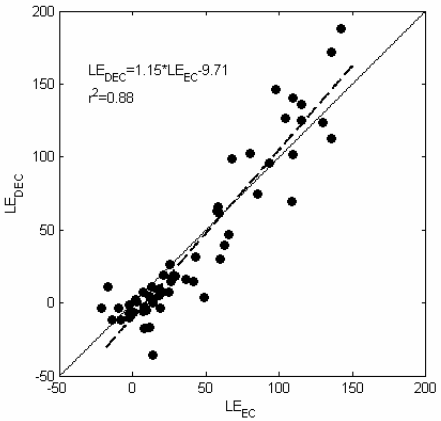

Figure 2: Result of a field intercomparison of latent heat fluxes measured by a disjunct eddy covariance system with grab samplers and an infra red gas analyzer (LE_{DEC}), and by conventional eddy covariance system with krypton hygrometer (LE_{EC}) [6].

Discussion

The DEC methods shortly reviewed provide a powerful tool for measurements of ecosystem – atmosphere trace gas exchange. However, there still remain issues affecting the data quality which need to be further examined. These include the flux uncertainty and biases due to the disjunct eddy sampling and data processing methods. Also the effect of chemical degradation on the measured fluxes needs to be further studied. As the results of the recent method intercomparison experiments which will be reviewed show, the DEC method with PTR-MS can be used to obtain reliable data on VOC emission fluxes. Finally, some aspects of the data interpretation and future prospects will be discussed.

References

[1] T. Karl, A. Guenther, A. Jordan, R. Fall, and W. Lindinger, Eddy covariance measurement of biogenic oxygenated VOC emissions from hay harvesting. Atmospheric Environment 35, 491-495, (2001).

[2] H. J. I. Rinne, A. B. Guenther, C. Warneke, J. A. de Gouw, and S. L. Luxembourg. Disjunct eddy covariance technique for trace gas flux measurements, Geophysical Research Letters 28, 3139–3142, (2001).

[3] T. G. Karl, C. Spirig, J. Rinne, C. Stroud, P. Prevost, J. Greenberg, R. Fall, and A. Guenther, Virtual disjunct eddy covariance measurements of organic trace compound fluxes from a subalpine forest using proton transfer reaction mass spectrometry, Atmospheric Chemistry and Physics 2, 279-291, (2002).

[4] C. Warneke, S. L. Luxembourg, J. A. de Gouw, H. J. I. Rinne, A. B. Guenther, and R. Fall, Disjunct eddy covariance measurements of oxygenated volatile organic compound fluxes from an alfalfa field before and after cutting, Journal of Geophysical Research 107, D8, 10.1029/2001JD000594, (2002).

[5] C. Spirig, A. Neftel, C. Ammann, J. Dommen, W. Grabmer, A. Thielmann, A. Schaub, J. Beauchamp, A. Wisthaler, and A. Hansel, Eddy covariance flux measurements of biogenic VOCs during ECHO 2003 using proton transfer reaction mass spectrometry Atmospheric Chemistry and Physics 5, 465-481, (2005).

[6] J. Rinne, T. Douffet, Y. Prigent & P. Durand, Field comparison of disjunct and conventional eddy covariance techniques for trace gas flux measurements, Submitted to Environmental Pollution, (2006).

[7] C. Ammann, A. Brunner, C. Spirig, and A. Neftel, Technical note: Water vapour concentration and flux measurements with PTR-MS, Atmospheric Chemistry and Physics 6, 4643-4651, (2006).

[8] R. Taipale, J. Rinne, T. M. Ruuskanen, M. Kajos, H. Hakola, H. Hellén, and M. Kulmala, Disjunct eddy covariance measurements of biogenic volatile organic compound fluxes from a boreal Scots pine forest, this issue (2007).

Comparison of different approaches to measure VOC exchange over grassland by PTR-MS

A. Neftel[1], C. Ammann[1], A. Brunner[1], M. Jocher[1], C. Spirig[1], B. Davidson[2], J. Rinne[3] and J. Dommen[4]

[1] *Research Station Agroscope Reckenholz-Tänikon ART, Zürich, Switzerland, albrecht.neftel@art.admin.ch*

[2] *Lancaster University, England*

[3] *University of Helsinki, Finland*

[4] *Paul Scherrer Institut, Villigen, Switzerland*

Abstract

The development of the PTR-MS technique greatly enhanced the possibilities to measure VOC exchange over biological systems, from the small scale using dynamic chambers up to the ecosystem level using a variety of eddy covariance techniques. We present an intercomparison of different approaches for the measurement of VOC fluxes above a managed grassland site. Dynamic chambers and several variants of the eddy correlation technique were applied in combination with PTR-MS measurements to determine the VOC exchange both during growing phases and after cuts of the grassland. Methanol was continuously emitted during the undisturbed growing phases, whereas emissions of acetaldehyde, acetone and a whole suite of other carbonyls and alcohols could only be observed after cutting or during hay drying. The combination of PTR-MS and gas chromatographic techniques allowed the identification of various compounds that could only ambiguously be detected by PTR-MS alone. While all flux measurement methods proved suitable for detecting VOC fluxes at this site, there are advantages and drawbacks of the different methods that will be discussed.

Introduction

The application of the proton transfer reaction – mass spectrometry in field and laboratory studies during the past decade yielded many very successful results and enlarged our knowledge of VOC exchange fluxes between the biosphere and the atmosphere. On the ecosystem scale, VOC exchange has been measured by application of various eddy covariance techniqeues [1-6].

There are two independent limitations to the applicability of PTR-MS for flux measurements. First there are instrumental limitations like sensitivity, time resolution and fragmentation of product ions. Secondly, limitations of the flux measurement technique need to be considered. In the case of eddy covariance approaches for measurements on the ecosystem scale, micrometeorological difficulties due to topography and intermediate or missing turbulence may exist. For measurements with chambers, potential influences of the chambers on the enclosed system and resulting artifacts in the VOC exchange need to be considered. On the other hand, chambers may

be advantageous in terms of detection limits for very small VOC fluxes, since they allow relatively long integration times.

The application of different flux measurement approaches in parallel is a promising way to overcome the limitations of the single methods and to study the advantages and drawbacks of different techniques. We therefore conducted a flux measurement intercomparison above a grassland field using both dynamic chambers and different eddy covariance techniques. The measurements were done in several phases, covering both grass cut events and undisturbed growing phases.

Experimental Methods

Site

Measurements were performed at the Swiss CarboEurope grassland site in Oensingen during summer 2005. The field has a size of 104 m x 146 m and had been split into two different regimes: an intensively managed part (intensive, INT) and an extensively managed part (extensive, EXT). The intensive part is cut four times a year and is fertilised after each cut, the extensively managed field is cut three times a year and is not treated with any fertilizer. The intensive field is composed mainly of three species (two graminoids, one legume), the extensive part has a higher diversity (six graminoids, four forbs, two legumes).

VOC Analysis

The PTR-MS used here corresponds to the PTR-MS-HS type, featuring three turbo pumps for increased sensitivity and a drift tube (equipped with Teflon rings) optimized for fast time response and minimal interactions with polar compounds . The air was sampled in the middle of the field, close to the sonic anemometer. A pump pulled the air through a 30 m long Teflon tube to the inlet of the PTR-MS. The PTR-MS was running under the following conditions: pressure drift tube: 2.1 mbar, pressure detection: 2.4x10-5 mbar, E/N: 122Td, drift tube temperature: 45°C.

The VOC fluxes were calculated using the eddy covariance method (EC). Details of the measurement system and flux calculations can be found in Ammann et al.[3] and Rinne et al. [7]. A mass scan before and during a test cut indicated the relative abundance of the ion masses. Based on these results, six masses were selected and measured continuously for the flux calculation with the EC method. The integration time for a single compound was 50 (for m21 and m37) to 200 ms (for all other compounds), resulting in a measurement of each compound every 0.7 to 1.3 s. In addition to EC measurements, an automated dynamic chamber system was used to determine VOC fluxes. The lower demands of the chamber system with respect to time resolution allowed the continuous monitoring of roughly 20 ion masses.

For a better identification of the masses detected by PTR-MS, occasional measurements with gas-chromatographic methods were performed. GC-MS analyses were performed on samples taken onto Tenax/Carbopak B cartridges and a second PTR-MS was coupled to a GC-FID system. Details about the GC methods are presented by Davidson et al. [8].

Results

Flux measurements

Figure 1 shows VOC fluxes measured after the cut of the extensive field on 1 June 2005 (11:30 LT): methanol, acetaldehyde, and acetone. The daytime average over the four days after the cut are 0.50 µg m^{-2} s^{-1}, 0.17 µg m^{-2} s^{-1}, and 0.10 µg m^{-2} s^{-1}, respectively, for the three clearly identified compounds. Because of weak turbulence and small fluxes during the night, no valid flux data could be obtained for these periods.

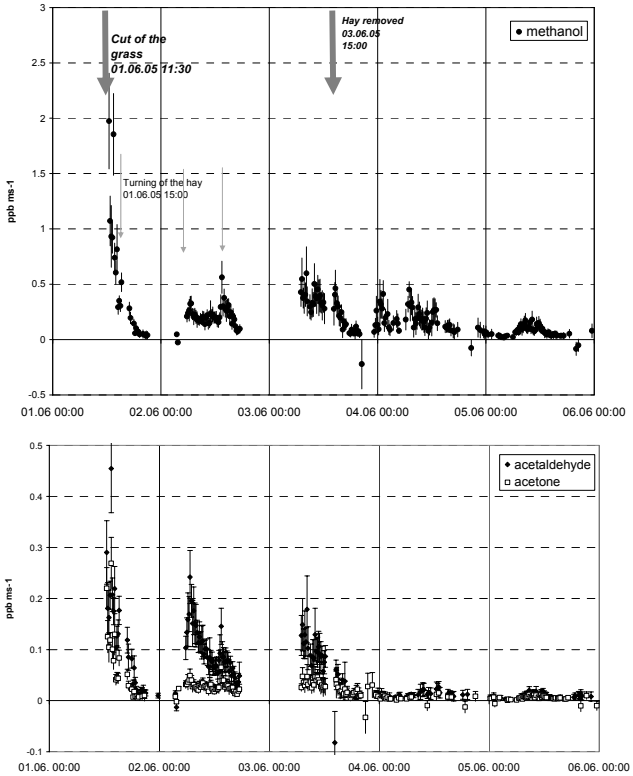

Figure 1: VOC fluxes after a cut on the extensive field on June 1 2005.

Several daily maxima of the fluxes were associated with hay turning to support the drying process. After the hay was removed, the emissions of acetaldehyde, acetone, m81 and m83 declined to very low values. In the following only methanol and m73 fluxes showed values significantly different from zero.

Figure 2 shows the methanol fluxes obtained with different variants of the eddy covariance technique in combination with the PTR-MS. These fluxes were observed on the intensive field during a non-disturbed growing phase, three weeks before the next cut. All methods agreed within the typical uncertainties of this type of measurement. Again, no consistent fluxes could be detected during the nights.

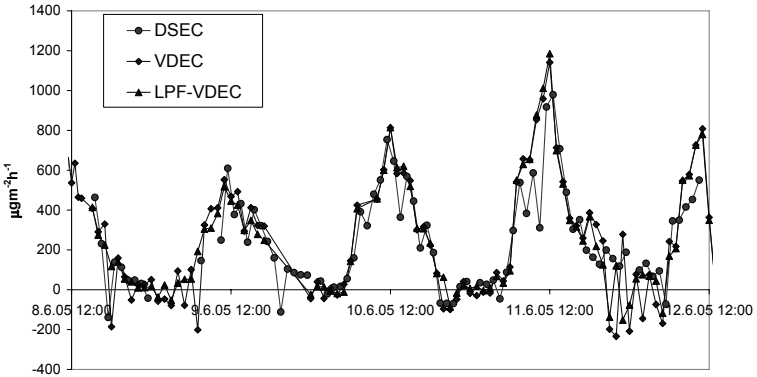

Figure 2: Methanol fluxes measured with different eddy covariance techniques: DSEC = disjunct sampling eddy covariance, VDEC= virtual disjunct eddy covariance, LPF-VDEC = low pass filtering virtual disjunct eddy covariance.

Figure 3 shows a third period of flux measurements, comparing the dynamic chamber results with those of the EC method. It demonstrates that the chambers used here are a viable alternative for flux measurements over a grassland system. Note that the chambers detected slight deposition of methanol during the night.

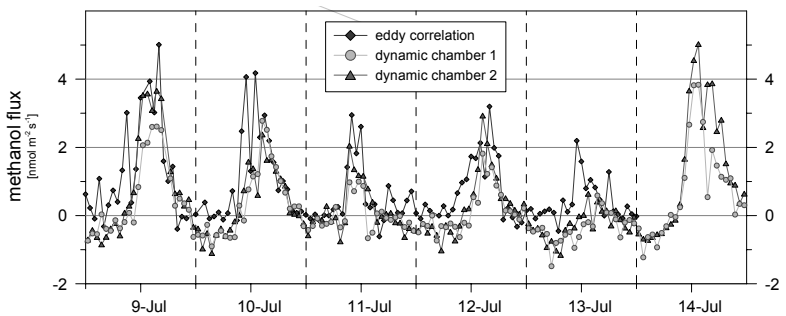

Figure 3: Diurnal exchange of methanol over a grassland as obtained from chambers and eddy correlation measurements..

Discussion

The grassland site investigated here provided very favorable conditions to compare the different flux measurement approaches that essentially turned out to be equivalent. Whenever a flux of a specific mass can be measured with either one of the approaches it can also be measured with the others. Deposition fluxes could only be traced with the dynamic chambers but are prone to be influenced by the chambers themselves mainly due to dew formation on the chamber walls.

References

[1] Holzinger, R., Lee, A., McKay, M. & Goldstein, A. H. Seasonal variability of monoterpene emission factors for a Ponderosa pine plantation in California. Atmospheric Chemistry And Physics 6, 1267-1274 (2006).

[2] Warneke, C. et al. Disjunct eddy covariance measurements of oxygenated VOC fluxes from an Alfalfa field before and after cutting. Journal of Geophysical Research 107, 10.1029/2001JD000594 (2002).

[3] Ammann, C., Brunner, A., Spirig, C. & Neftel, A. Technical note: Water vapour concentration and flux measurements with PTR-MS. Atmospheric Chemistry And Physics 6, 4643-4651 (2006).

[4] Spirig, C. et al. Eddy covariance flux measurements of biogenic VOCs during ECHO 2003 using proton transfer reaction mass spectrometry. Atmospheric Chemistry and Physics 5, 465-481 (2005).

[5] Karl, T. G. et al. Virtual disjunct eddy covariance measurements of organic compound fluxes from a subalpine forest using proton transfer reaction mass spectrometry. Atmospheric Chemistry and Physics 2, 279-291 (2002).

[6] Karl, T. et al. Eddy covariance measurements of oxygenated volatile organic compound fluxes from crop harvesting using a redesigned proton-transfer-reaction mass spectrometer. Journal of Geophysical Research 106, 24157-24167 (2001).

[7] Rinne, J., Taipale R, Spirig, C., Ruuskanen, T.M., Markkanen, T.M., Vesala, T., Brunner A., Ammann, C., Neftel, A., Douffet, T., Prigent, Y., Durand, P., and Kulmala, M. Measuring ecosystem scale VOC emissions by PTR-MS. This issue (2007).

[8] Davison, B., Brunner, A., Ammann, C., Spirig, C., Jocher, M., Neftel, A.: Cut induced VOC emissions from agricultural grasslands. Submitted to Plant Biology (2006).

Emission of biogenic volatile organic compounds (BVOCs) from vegetation

Francesco Loreto

CNR – Istituto di Biologia Agroambientale e Forestale, Via Salaria Km. 29, 300, 00016 Monterotondo Scalo (Roma), Italy, francesco.loreto@ibaf.cnr.it

Summary

Plants emit in the atmosphere volatile hydrocarbons of different metabolic origin. Volatile isoprenoids (isoprene and monoterpenes) are emitted in large quantities and at a very large metabolic cost for plants. They also influence the chemistry of the troposphere. In perturbed environments with substantial loads of anthropogenic compounds, volatile isoprenoids can power the formation of ozone, photochemical smog, and particulate. Crucial to improve models and algorithms of isoprenoid emission and to predict their contribution to chemical reaction in the atmosphere, is the knowledge of the biochemical and ecological bases of isoprenoid formation. It is shown how interdisciplinary studies and technological progresses, including the use of PTR-MS technology, have driven to a) the preparation of detailed inventories of isoprenoid emitters, b) the discovery of a novel biochemical pathway from which volatile isoprenoids are formed, c) the understanding of environmental control on isoprenoid biosynthesis and emission, in turn leading to the preparation of an emission algorithm based on the response to light and temperature, d) the comprehension of functional roles of isoprenoids in plants. It is suggested that these new scientific finding could lead to improved models for predicting isoprenoid emissions and their impact on biosphere-atmosphere interactions.

Better insight in regulation, biosynthesis and function of isoprene emission using PTR-MS analysis

Jörg-Peter Schnitzler, Maaria Loivamäki, Markus Teuber, Katja Behnke and David Andres-Momtaner

Institut für Meteorologie und Klimaforschung (IMK-IFU), Forschungszentrum Karlsruhe GmbH, Garmisch-Partenkirchen, Germany, joerg-peter.schnitzler@imk.fzk.de

Abstract

Trees produce a wide spectrum of volatile organic compounds (VOCs) such as isoprene and monoterpenes. Recently much progress was made to elucidate the metabolic pathway leading to isoprene, to get insight in the regulation of its formation and to understand the biological function of this highly volatile and reactive compound. For all these facets of research, PTR-MS have been shown to be an excellent analytical technique.

The presentation will summarize actual work using PTR-MS as tool for fast functional screening of transgenic plants manipulated in isoprene biosynthesis and the analysis of metabolic intermediates such as DMADP and enzyme activities. Furthermore, labelling experiments with ^{13}C will demonstrate the flexible utilisation of different carbon sources for isoprene formation when plants experience environmental stress. Finally, data with transgenic plants will be present giving proof that isoprene emission can be involved in the thermal protection of leaves.

Introduction

Numerous plants emit volatile organic compounds (VOCs) in response to light and temperature changes or other abiotic stresses (Kreuzwieser et al. 1999). Low molecular weight terpenes such as isoprene (C5) and monoterpenes (C10) are released in substantial amounts from woody plants in a light- and temperature-dependent manner and have significant impact on atmospheric chemistry since they contribute to ozone and secondary organic aerosol formation in the presence of anthropogenic pollutants (Atkinson 2000). Furthermore, isoprenoid emissions contribute to the regulation of atmospheric hydroxyl radical (·OH) concentration and influence the atmospheric residence time of methane, an important greenhouse gas (Thompson 1992). The physiological role of such terpene emissions is still not completely understood. Terpene emissions are believed to improve the thermotolerance of photosynthetic tissues since they are likely to intercalate in thylakoid membranes of chloroplasts and may stabilize them at high temperatures (Loreto et al. 1998, Sharkey et al. 2001). Moreover, there is increasing evidence showing that terpene volatiles exhibit antioxidant activities *in planta* by quenching reactive oxygen species (Loreto and Velikova 2001, Loreto et al. 2001, Loreto et al. 2004). The increasing scientific interest in plant VOC biochemistry, physiology, and ecology has led to a considerable interest in real time measurement of VOCs like PTR-MS (Tholl et al. 2006).

PTR-MS can be combined with additional equipment for parallel measurements of other stress physiological parameters such as photosynthetic activity (e.g. Schnitzler et al. 2004, Graus et al. 2004). Sensitive, fast and fully automated VOC analysis systems are also of increasing importance in biochemical studies to elucidate plant VOC biosynthesis and metabolic intermediates (Nogués et al. 2006). In addition, molecular functional genomics approaches for

dissecting plant VOC biosynthesis pathways demand time efficient techniques for volatile product analysis of recombinant enzymes or high throughput volatile metabolite profiling of mutant and transgenic plant lines.

Experimental Methods

Functional screening of transgenic plants with a head space analysis system and PTR-MS

Single leaves or leaf discs were placed in 2 ml vials filled with 200 µl mineral water, allowed to stabilise for 30 min, sealed gastight and incubated under controlled light and temperature for a certain time period. For transfer of sample into the PTR-MS, the head space was transferred into a 10 ml injection loop by flushing the vials with 10 ml N_2. Subsequently, the samples were injected into the MS with a high flow rate of 250 ml min^{-1}. Isoprene or monoterpenes were detected at m69 and m137, respectively. System calibration was performed using vials containing calibration gas. For data analysis, count readings were exported, processed, and imported into chromatography software for classical peak analysis.

Determination of isoprene emission from Grey poplar (*Populus* x *canescens*) shoots

The measurement of isoprene emission from shoot culture containers was performed with an adapted head space analysis system using PTR-MS (for details see Loivamäki et al. 2006). The measurements were performed on two gas-tight culture containers in parallel, each containing 6-7 cell cultured shoots aged 6 - 8 weeks partially with a developed root system. Clean air adjusted to a dew point of 28 °C was flushed at 500 ml min^{-1} into the containers and from the outlet air 100 ml min^{-1} was pumped into the PTR-MS to analyze volatiles. Measurements were performed on each container alternatively (automatically switched each 3 min with 60 s stabilization time). To avoid drying of the plants used to a confine environment, H_2O was added carefully on the surface of the solid medium at the beginning and once during the experiment. The first 24 - 48 hours of the experiments were used to flush excess of isoprene previously accumulated in the containers during the development of the plants and to let the plants adapt to the constant gas stream. After the isoprene level appears stable, isoprene emission was measured over a LD day-night cycle. At 22:00 of the following day one container was placed in continuous light and the other in continuous darkness and emissions were measured during three virtual day-night cycles. For calibration of the PTR-MS a gas standard (11 compounds with 1.05 ppmv each, Apel-Riemer, Denver, USA) with a continuous flow (20 ml min^{-1}) was diluted into the cuvette gas stream and flushed through an empty container for half an hour at the beginning and at the end of each experiment.

Results and Discussion

Circadian rhythm of isoprene emission in Grey poplar

Emission of isoprene from the poplar shoot cultures followed a clear diurnal pattern under light-dark (LD) conditions (Fig. 1A), being low overnight and high and stable over the day. When the shoots were placed in continuous darkness (Figure 1B) isoprene emission dropped down very fast after switching off the light and subsequently declined with a slower rate over the following three

days. Remarkably, isoprene emission of the shoot cultures does occur, even if at low rate, under darkness. Under continuous light (Fig. 1A) we detected fluctuating isoprene emission rates with a 24 hours period between two peaks, therefore defining a circadian rhythm. Under light-light (LL) conditions isoprene emission displayed clear daily changes at the third and forth day after onset of continuous illumination (Fig. 3C). At these days, emission was as its strongest (around time 86 h) approx. 20 % higher than the emission as its lowest (around time 78 h) during the previous 24 h cycle and approx. 30 % higher (at around 114 h) than the lowest (at around 100h) emission in the last 24 h cycle. The highest rate of emission occurred always in the subjective afternoon showing switched circadian rhythm phase of isoprene emission under continuous illumination.

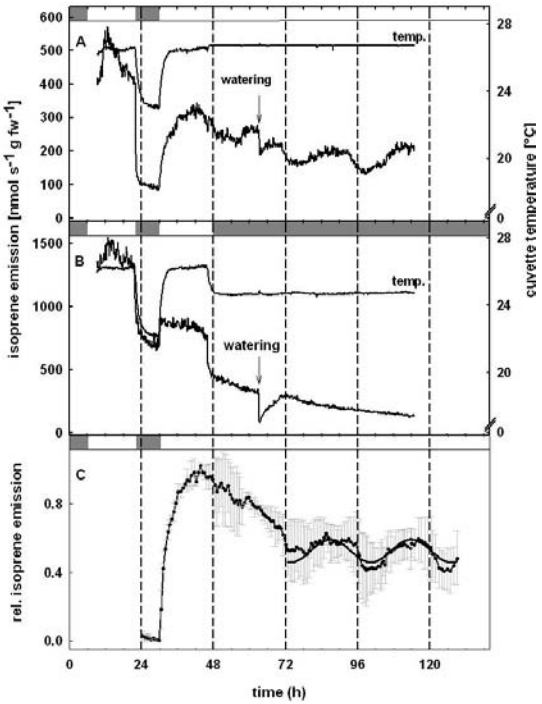

Figure 1: Circadian rhythm of isoprene emission in Grey poplar (A) continuous light, (B) continuous dark ness, (C) relative isoprene emission (n = 3 cultures +/s SD)

In "field" conditions, isoprene emission from poplars was known to present daily variations, linked to temperature and light intensity (Mayrhofer et al. 2005). Our results on poplar shoot cultures grown under controlled conditions confirm this by showing that during night isoprene emission of the shoots is indeed dramatically reduced but not zero. As in darkness no new carbon is fixed, this continuous emission of isoprene testifies for another carbon source than photosynthesis (see Schnitzler et al. 2004). The plants were grown on medium, which contains

sucrose. These artificial growing conditions (compared to soil) could therefore explain this unusual nightly emission of isoprene, the sucrose being a potential carbon source.

Functional screening of isoprene emitting Arabidopsis

There has been growing research focusing on isoprene. It is known that volatile isoprenoids emitted by vegetation have various meanings, i.e. in plant defence, but also in atmospheric chemistry. However, the physiological function of isoprene for the plant itself is still unknown. Aim of the presented work is therefore to study proposed biological functions of isoprene formation in transgenic *Arabidopsis thaliana*, a species which is *per se* a non emitter of isoprene. Plants have been transformed with different constructs of the isoprene synthase gene (*PcISPS*) from Grey poplar in order to introduce isoprene emission into this model plant species. The presented data (Fig. 2) show our selection of transgenic lines using functional emission screening with PTR-MS.

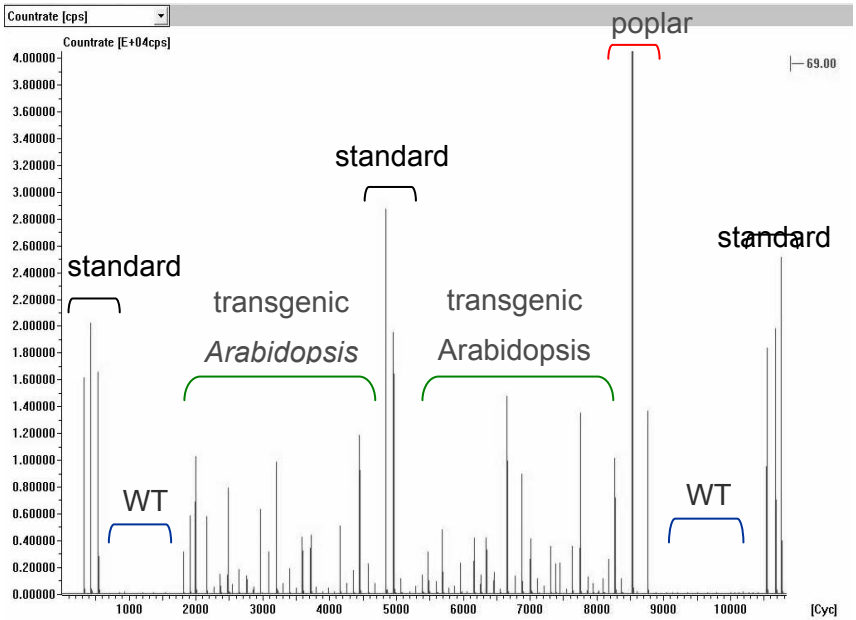

Figure 2: Fast functional emission screening of transgenic Arabidopsis leaves using PTR-MS of head space.

This head space analysis was found to allow a high throughput screening of transformants e.g. *Arabidopsis* with a minimal expense of time. In addition, this technique was found also to be a versatile tool for the analysis of isoprene and monoterpene synthase activities as well as the quantification of metabolic intermediates.

References

[1] R. Atkinson, Atmospheric chemistry of VOCs and NOx. *Atmospheric Environment* 34, 2063-2101, (2000).

[2] M. Graus, J.-P. Schnitzler, A. Hansel, C. Cojocariu, H. Rennenberg, A. Wisthaler, and Kreuzwieser, Transient release of oxygenated VOC during light-dark transitions, Plant Physiology 135, 1967-1975, (2004).

[3] J. Kreuzwieser, J.-P. Schnitzler, and R. Steinbrecher, Biosynthesis of organic compounds emitted by plants, Plant Biology 1, 149-159 (1999).

[4] M. Loivamäki, S. Louis, G. Cinege, I. Zimmer, R.J. Fischbach, and J.-P. Schnitzler, Circadian rhythms of isoprene biosynthesis in Grey poplar leaves, Plant Physiology, in press, (2006).

[5] F. Loreto and V. Velikova, Isoprene produced by leaves protects the photosynthetic apparatus against ozone damage, quenches ozone products, and reduces lipid peroxidation of cellular membranes, Plant Physiology 127, 1781-1787, (2001).

[6] F. Loreto, A. Forster, M. Durr, O. Csiky, and GT. Seufert, On the monoterpene emission under heat stress and on the increased thermotolerance of leaves of *Quercus ilex* L. fumigated with selected monoterpenes, Plant Cell and Environment 21, 101-107, (1998).

[7] F. Loreto, M. Mannozzi, C. Maris, P. Nascetti, F. Ferranti, and S. Pasqualini, Ozone quenching properties of isoprene and its antioxidant role in leaves, Plant Physiology 126, 993-1000, (2001).

[8] S. Mayrhofer, M. Teuber, I. Zimmer, S. Louis, R.J. Fischbach, and J.-P. Schnitzler, Diurnal and seasonal variation of isoprene biosynthesis-related genes in *Populus* x *canescens* leaves, Plant Physiology 139, 474-484,(2005).

[9] I. Nogués, F. Brilli, and F. Loreto, Dimethylallyl diphosphate and geranyl diphosphate polls of plant species characterized by different isoprenoid emissions, Plant Physiology 141, 721-730, (2006).

[10] J.-P. Schnitzler, M. Graus, J. Kreuzwieser, U. Heizmann, H. Rennenberg, A. Wisthaler, and A. Hansel, Contribution of different carbon sources to isoprene biosynthesis in poplar leaves, Plant Physiology 135, 152-160, (2004).

[11] T.D. Sharkey, X.Y. Chen, and S. Yeh, Isoprene increases thermotolerance of fosmidomycin-fed leaves, Plant Physiology 125, 2001-2006, (2001).

[12] D. Tholl, W. Boland, A. Hansel, F. Loreto, U.S.R. Röse, and J.-P. Schnitzler, Practical approaches to plant volatile analysis, The Plant Journal 45, 540-560, (2006).

[13] A.M. Thompson, The oxidizing capacity of the Earth's atmosphere: probable past and future changes, Science, 256, 1157-1165, (1992).

6. PTR-MS: Instrument Development

The NIES PTR-TOFMS instrument: design, performance and application

Hiroshi Tanimoto[1], Satoshi Inomata[2], Nobuyuki Aoki[2], Yasuhiro Sadanaga[2], Jun Hirokawa[3]

[1] *Asian Environment Research Group, National Institute for Environmental Studies, Tsukuba, Japan, tanimoto@nies.go.jp*

[2] *Atmospheric Environment Division, National Institute for Environmental Studies, Tsukuba, Japan, ino@nies.go.jp*

[3] *Faculty of Environmental Earth Science, Hokkaido University, Sapporo, Japan*

Abstract

A proton transfer reaction – time-of-flight mass spectrometer (PTR-TOFMS) has been developed for real-time measurements of volatile organic compounds in air. The instrument is designed to be operated with a hollow cathode discharge ion source and an ion drift tube at relatively high pressures. Each component of the system, the ion source, the drift tube, the ion transfer region, and the time-of-flight mass spectrometer were characterized in detail by a number of laboratory experiments. The optimized instrumental configuration enables us to gain hydronium (H_3O^+) ions intensities of ~7 $\times 10^5$ counts for 1-min integration at a drift tube pressure of ~5 torr. It also suppresses background signals and interferences from sample air (NO^+ and O_2^+), which undergo reactions with volatile organic compounds. The detection limits for propene, acetaldehyde, acetone, isoprene, benzene, toluene, and p-xylene are calculated to be in the range of sub-ppbv for a 1-min integration time. A good linear response at trace levels was confirmed, but a slight sensitivity dependence on water vapor content was revealed. We find that the instrument can be used for on-line monitoring to detect large variations from emission sources in real-time.

Introduction

The proton transfer reaction (PTR) ionization is one of chemical ionization (CI), which enables soft ionization of chemical species that have a proton affinity higher than that of the reagent species (i.e., water in many cases). The PTR from hydronium ions (H_3O^+) occurs with many VOCs except low-molecular weight nonmethane hydrocarbons (NMHCs), and produces predominantly protonated ions with less fragmentation than electron-impact ionization (EI). The PTR-MS instrument was first reported by the group at Innsbruck University [1] who coupled a hollow cathode discharge ion source and a drift tube with a quadrupole mass spectrometer (QMS). This development allows on-line measurements of VOCs at parts per trillion by volume (pptv) levels without any pre-concentration; such instruments are now used to identify the speciation of VOCs and quantify their mixing ratios in environmental, medical, and food applications [2].

Recently, applications of the PTR ionization method to other mass spectrometric detection techniques, including time-of-flight mass spectrometers (TOFMS), have been reported. The TOFMS has the advantage of high mass resolution, leading to explicit identification of compounds of interest. Proton transfer reaction – time-of-flight mass spectrometer (PTR-TOFMS) instruments with a high mass resolution ($m/\Delta m$ >1000) have been reported, coupled with

radioactive and hollow cathode ion sources [3,4]. However, the sensitivity of this discharge-based instrument was less than that of current PTR-QMS instruments. Also, a large amount of NO^+ and O_2^+ ions were produced, likely due to the back-diffusion of air from the drift tube to the hollow cathode ion source [4].

Experimental Methods

We have developed a PTR-TOFMS instrument for simultaneous and real-time detection of VOCs that play important roles in the formation of ozone and secondary organic aerosols in air. These species include unsaturated (alkene, diene), oxygenated (aldehyde, ketone, alcohol), and aromatic hydrocarbons. Our PTR-TOFMS instrument is a combination of a custom-built ion source/drift tube and an orthogonal time-of-flight mass spectrometer, consisting of four components: (1) the ion source, (2) the drift tube, (3) the ion transfer chamber, and (4) the time-of-flight mass spectrometer (Figure 1). The hollow cathode discharge ion source was designed and built in our laboratory to be coupled with an ion drift tube operated at a pressure of ~5 torr, which is higher than typical conditions. More details on the instrument are described in our recent papers [5,6].

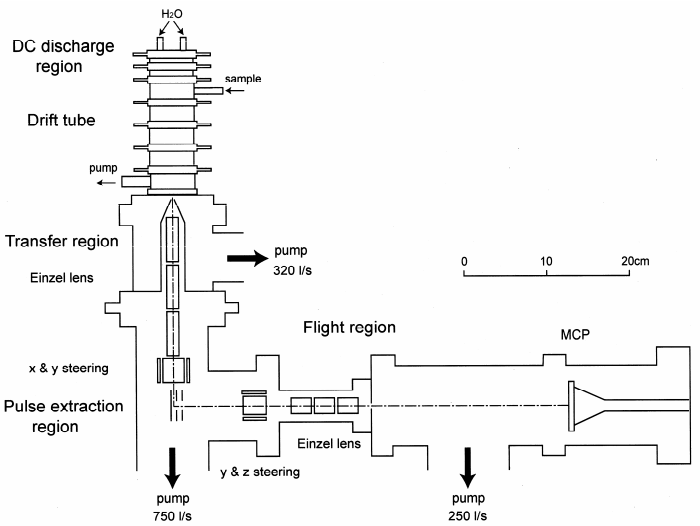

Figure 1: Schematic diagram of the NIES PTR-TOFMS instrument. The discharge ion source, drift tube, ion transfer region, pulse extraction region, and flight region are illustrated.

Results and Discussion

Figure 2 shows distributions of the hydronium ions and its cluster ions as a function of the E/N ratio in the drift tube. The E/N ratio acts as an indicator of the collision energy of the ion – molecule reactions in the drift cell. The H_3O^+ ions constitute more than 90% of the total hydronium ions above 100 Td, and reach 98% at 160 Td. In contrast, the concentration of $H_3O^+ \bullet H_2O$ ions gradually decreases from 8% at 100 Td to 2% at 160 Td. The $H_3O^+ \bullet (H_2O)_2$ ions constitute only less than 0.2% of the total intensity in the range of 100–160 Td. The absolute signal of H_3O^+ ions increases from 5×10^5 to 7×10^5 counts with the increase in the E/N value in the range from 100 to 160 Td by 1-min integration at a repetition rate of 10 kHz. The signals of the protonated ions ($VOC \bullet H^+$) for benzene, toluene, and p-xylene produced by PTR ionization are also displayed as a function of the E/N ratio. The ion intensity for benzene, toluene, and p-xylene substantially increases with E/N values from 100 to 140 Td, reaching the maximum around 130 – 140 Td, very likely because of the increase in the absolute amount of H_3O^+ ions [5]. The intensity of these species gradually decreases above 140 Td, suggesting that fragmentations occur at high E/N ratios. The ion intensity for isoprene drastically decreases with the increase in E/N values from 100 to 160 Td, implying that fragmentation reactions take place with isoprene more effectively (not shown in the figure).

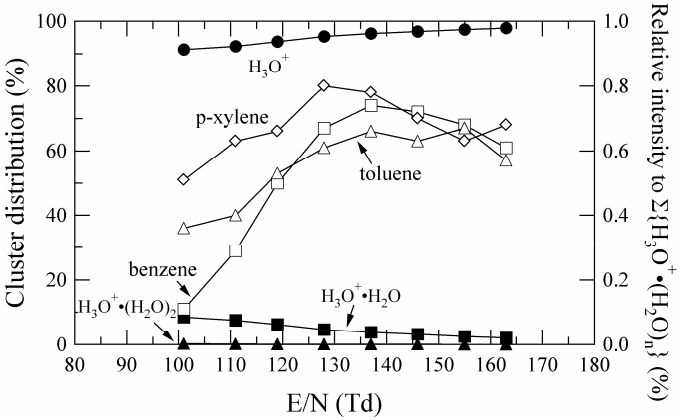

Figure 2: Dependence of the $H_3O^+ \bullet (H_2O)_n$ (n=0, 1, 2) cluster ion distributions on the E/N ratio in the drift tube (left axis). The dependence of the protonated ions for benzene, toluene, and p-xylene is also shown (right axis). The drift tube pressure is 5 torr, and E inlet is 400 V/cm. [Tanimoto et al., 2006]

Figure 3 shows a mass spectrum of the standard gas containing propene, acetaldehyde, acetone, isoprene, benzene, toluene, and p-xylene at the mixing ratios of 10 ppbv. Corresponding to $VOC \cdot H^+$ ions, peaks at m/z = 69, 79, 93, and 107 appear and their intensities are enhanced at m/z = 43, 45, and 59 by proton transfer reactions. Figure 3 also shows the difference between the mass

spectra of sample and background measurements. The ion intensities around m/z = 19, 37, and 55 showed negative values due to losses of H_3O^+ and $H_3O^+(H_2O)_{1-2}$ by proton transfer reactions. Also, the signals around m/z = 30 (NO^+) and m/z = 32 (O_2^+) showed slight negative values due to the ion-molecule reactions of these ions with VOCs sampled. The ion counts obtained for propene, acetaldehyde, acetone, isoprene, benzene, toluene, and p-xylene at 10 ppbv are 260, 1520, 2290, 520, 810, 1010, and 1020 counts, respectively, over 6×10^5 scans (10 kHz repetition, 1-min integration). A linear response in the range from 10 to 200 ppbv was confirmed, and the sensitivity (counts/ppbv) was determined for each species. The detection limits for these VOCs with our PTR-TOFMS instrument are estimated to be at the sub-ppbv levels for 1-min integration, depending on speciation of VOCs [5,6].

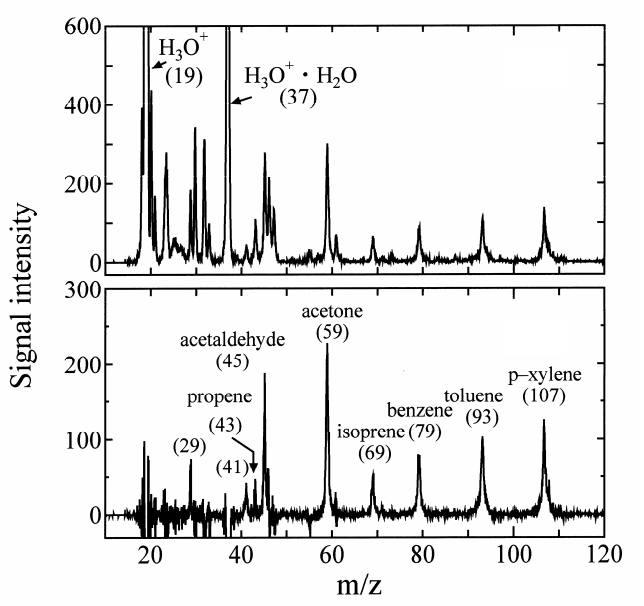

Figure 3: (upper panel) Sample mass spectrum obtained from standard gas measurements. The standard gases measured were seven VOCs at 10-ppbv mixing ratios. The spectrum was integrated during 1-min at a repetition rate of 10 kHz. (lower panel) Difference between the sample and the background mass spectra. [Inomata et al., 2006]

References

[1] A. Hansel, A. Jordan, R. Holzinger, P. Prazeller, W. Vogel, and W. Lindinger, Proton-transfer reaction mass-spectrometry – Online trace gas analysis at the ppb level, Intern. J. Mass Spectrom. Ion Processes, 149/150, 609-619, (1995).

[2] W. Lindinger, A. Hansel, and A. Jordan, On-line monitoring of volatile organic compounds at pptv levels by means of Proton-Transfer-Reaction Mass Spectrometry (PTR-MS): Medical applications, food control and environmental research, Intern. J. Mass Spectrom. Ion Processes, 173, 191-241, (1998).

[3] R.S. Blake, C. Whyte, C.O. Hughes, A.M. Ellis, and P.S. Monks, Demonstration of proton-transfer reaction time-of-flight mass spectrometry for real-time analysis of trace volatile organic compounds, Anal. Chem., 76, 3841-3845, DOI: 10.1021/ac0498260, (2004).

[4] C.J. Ennis, J.C. Reynolds, B.J. Keely, and L.J. Carpenter, A hollow cathode proton transfer reaction time of flight mass spectrometer, Intern. J. Mass Spectrom., 247, 72-80, DOI: 10.1016/j.ijms.2005.09.008, (2005).

[5] S. Inomata, H. Tanimoto, N. Aoki, J. Hirokawa, and Y. Sadanaga, A novel discharge source of hydronium ions for proton transfer reaction ionization: Design, characterization, and performance, Rapid Comm. Mass Spectrom., 20, 1025-1029, (2006).

[6] H. Tanimoto, N. Aoki, S. Inomata, J. Hirokawa, and Y. Sadanaga, Development of a PTR-TOFMS instrument for real-time measurements of volatile organic compounds in air, submitted manuscript, (2006).

Development of a High Resolution PTR-TOFMS

Martin Graus[1], Markus Müller[1], Armin Wisthaler[1], and Armin Hansel[1]

[1] Institute of Ion Physics and Applied Physics / Ion Molecule Reactions and Environmental Physics, University of Innsbruck, Innsbruck, Austria
martin.graus@uibk.ac.at

Abstract

A PTR type ionisation chamber was coupled to a high resolution time of flight mass spectrometer (TOF-MS) resulting in a powerful analytical device for on-line trace gas analysis. The instrument was optimised and characterised using a dynamically diluted VOC gas mixture. A mass resolving power of 4000 (FWHM) can be achieved allowing for mass peak separation of isobaric ions. At one minute integration time a typical detection limit of a few tens to a few hundreds of pptv was reached.

In this paper the performance of the recently developed high resolution PTR-TOFMS will be presented and discussed. In addition first application results will be shown.

Introduction

Proton transfer reactions (PTR) for chemical ionisation are well studied and using them in a drift tube reaction cell as employed in PTR-MS technology is a well established ionisation method. Conventional PTR-MS uses quadrupole mass spectrometry (q-MS) and has been available for more than ten years [1]. Sensitivity, detection limit, gas sampling method and time resolution of PTR-MS have improved significantly since its early days [2]. PTR-MS has found manifold applications in atmospheric chemistry [3, 4, 5, 6], biology [7, 8, 9] and other scientific fields where the monitoring of organic trace compounds is desired [10]. Ever increasing requirements for more and more complex applications, however, have revealed limitations originating from the mode of operation of the q-MS, such as duty cycle and poor compound identification.

The ability of PTR-MS equipped with a q-MS to separate two ion species is usually limited to $\Delta m \cong 1$. The identification capability with such a poor mass resolving power is very much restricted. Monitoring of VOCs in complex air matrices often results in a mass spectrum with ion signals on almost every single mass. Such a spectrum consists of a superposition of MH^+ mother ions, fragment ions and their isotopes. Identification and also quantification of specific trace gases from such a mass spectrum becomes increasingly difficult.

Several groups have reported the coupling of a chemical ionisation cell to a TOF-MS [11, 12, 13]. PTR-TOFMS is a promising approach to overcome the limitations addressed above having the following advantages:

- TOF-MS has virtually no limitation of the mass range.
- With TOF-MS full mass spectra are recorded within a fraction of a second. This substantially improves the duty cycle of a PTR-TOFMS in comparison to conventional PTR-MS technology.

- TOF-MS technology in compact designs is becoming available with a mass resolving power that allows the separation of isobaric species.

Here we present a PTR-TOFMS system that provides for all three advantages. A prototype was developed at the University of Innsbruck in a cooperation project with Ionicon Analytik Ges.m.b.H.

System Description

The PTR-TOFMS combines the well established PTR ionisation method with a novel TOF-MS system. The continuous ion beam from the reaction chamber (drift tube) is transferred through a differentially pumped ion optic towards the pulser. Ions are extracted from the continuous beam orthogonally with short pulses at a typical rate of 33 kHz into the flight region. All ions gain the same kinetic energy

$$E_{kin} = U_{acc} \cdot q_{ion} = \frac{m \cdot v^2}{2}$$

resulting in a mass dependent velocity

$$v(m) \propto \frac{1}{\sqrt{m}}$$

and thus the time of flight of the ions correspond to their respective masses

$$ToF_m \propto \sqrt{m} \ .$$

The ions are reversed in the reflectron which allows for the correction of peak broadening in the time of flight spectrum due to unfavourable starting conditions and enables a longer flight path in a compact design. Single ions are detected upon their impact on the multi-channel plates and counted by a time to digital converter (TDC). The time of flight spectra of a number of single extraction are added up to enable reasonable statistics on the resulting spectrum. Assuming an extraction rate of 33 kHz a spectrum comprise over 48.000 entries that are stored on a computer for further evaluation and data treatment. Figure 1 shows the principal building blocks of our PTR-TOFMS.

The data acquisition software controls the pulser timing, handles the incoming data and allows for data displaying and some online data manipulation such as averaging, zooming, single peak fit, extraction and displaying of time series of mass signals. Further data evaluation is done off-line using home build procedures coded in IGOR Pro® (WaveMetrics).

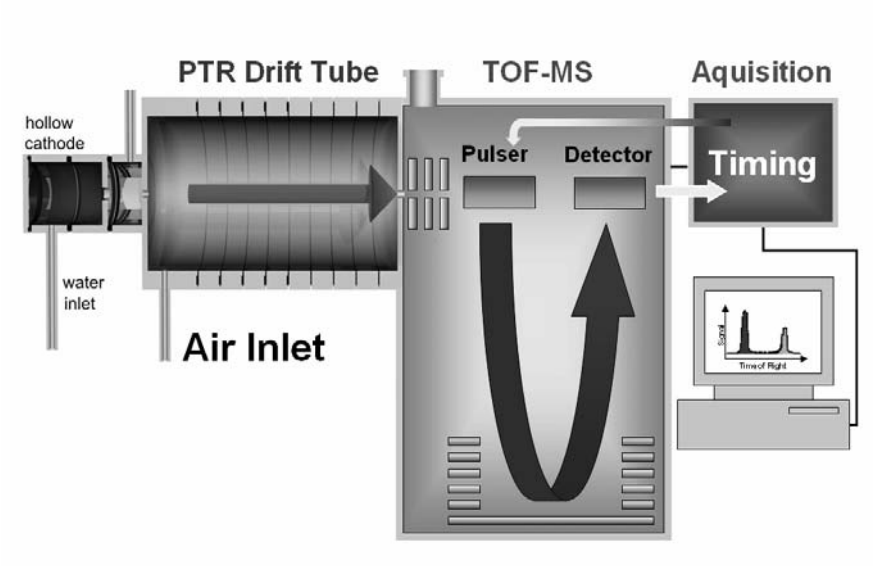

Figure 1: Schematic representation of the Innsbruck PTR-TOFMS: (1) Ionisation chamber (drift tube), (2) Mass analyser (TOF-MS), and (3) ion detection, timing, and data acquisition.

System Performance

The performance of the PTR-TOFMS was assessed by applying a calibrated VOC gas mixture containing a suite of carbonyls, alcohols and terpenes dynamically diluted to a range of 3 to 30 ppbv. In several steps sensitivity, limit of detection, mass resolution and mass accuracy were improved significantly by doing both, optimisation of the geometry of the hardware and tuning all voltages of the ionisation chamber and the TOF-MS system. An overview of the mentioned performance parameters will be given in the conference presentation as well as in the conference contribution by Müller *et al*. Data examples from first applications will be presented.

Acknowledgement

The development of this PTR-TOFMS prototype is a cooperation of the Leopold Franzens University of Innsbruck and Ionicon Analytik Ges.m.b.H. as our industrial partner in the consortium. We thank Ionicon, and in particular Alfons Jordan, Gernot Hanel and Stefan Haidacher for their support. The TOF-MS system was funded by the University of Innsbruck („Uni Infrastruktur 2004“ Programms, GZ.10.220/2-VII/2004). The project is financially supported by the Austrian Research Funding Association (FFG; Basisprogramm – Brückenschlag 1, P.-Nr. 810074)

References

[1] Hansel, A., Jordan, A., Holzinger, R., Prazeller, P., Vogel, W. and Lindinger, W., 1995. Proton transfer reaction mass spectrometry: on-line trace gas analysis at the ppb level. International Journal of Mass Spectrometry and Ion Processes 149-150, 609-619.

[2] Hansel, A., Jordan, A., Warneke, C., Holzinger, R. and Lindinger, W., 1998. Improved detection limit of the proton-transfer reaction mass spectrometer: on-line monitoring of volatile organic compounds at mixing ratios of a few pptv. Rapid Communications in Mass Spectrometry 12, 871-875.

[3] Wisthaler, A., Hansel, A., Dickerson, R. R. and Crutzen, P. J., 2002. Organic trace gas measurements by PTR-MS during INDOEX 1999. Journal of Geophysical Reserch 107, 8024.

[4] de Gouw, J. A., Goldan, P. D., Warneke, C., Kuster, W. C., Roberts, J. M., Marchewka, M., Bertman, S. B., Pszenny, A. A. P. and Keene, W. C., 2003. Validation of proton transfer reaction-mass spectrometry (PTR-MS) measurements of gas-phase organic compounds in the atmosphere during the New England Air Quality Study (NEAQS) in 2002. Journal of Geophysical Reserch 108, 4682.

[5] Lee, A., Goldstein, A. H., Kroll, J. H., Ng, N. L., Varutbangkul, V., Flagan, R. C. and Seinfeld, J. H., 2006. Gas-phase products and secondary aerosol yields from the photooxidation of 16 different terpenes. Journal of Geophysical Reserch 111, D17305.

[6] Spirig, C., Neftel, A., Ammann, C., Dommen, J., Grabmer, W., Thielmann, A., Schaub, A., Beauchamp, J., Wisthaler, A. and Hansel, A., 2005. Eddy covariance flux measurements of biogenic VOCs during ECHO 2003 using proton transfer reaction mass spectrometry. Atmospheric Chemistry and Physics 5, 465-481.

[7] Karl, T., Fall, R., Rosentiel, T. N., Prazeller, P., Larsen, B., Seufert, G. and Lindinger, W., 2002. On-line analysis of the $^{13}CO_2$ labeling of leaf isoprene suggests multiple subcellular origins of isoprene precursors. Planta 215, 894–905.

[8] Fall, R., Karl, T., Hansel, A., Jordan, A. and Lindinger, W., 1999. Volatile organic compounds emitted after leaf wounding: On-line analysis by proton-transfer-reaction mass spectrometry. Journal of Geophysical Reserch 104, 15963-15974.

[9] Schnitzler, J.-P., Graus, M., Kreuzwieser, J., Heizmann, U., Rennenberg, H., Wisthaler, A. and Hansel, A., 2004. Contribution of Different Carbon Sources to Isoprene Biosynthesis in Poplar Leaves. Plant Physiology 135, 152-160.

[10] Lindinger, W., Hansel, A. and Jordan, A., 1998. Proton-transfer-reaction mass spectrometry (PTR-MS): on-line monitoring of volatile organic compounds at pptv levels. Chemical Society Review 27, 347-375.

[11] Blake, R. S., Whyte, C., Hughes, C. O., Ellis, A. M. and Monks, P. S., 2004. Demonstration of Proton-Transfer Reaction Time-of-Flight Mass Spectrometry for Real-Time Analysis of Trace Volatile Organic Compounds. Anal. Chem. 76, 3841-3845.

[12] Ennis, C. J., Reynolds, J. C., Keely, B. J. and Carpenter, L. J., 2005. A hollow cathode proton transfer reaction time of flight mass spectrometer. International Journal of Mass Spectrometry 247, 72-80.

[13] Inomata, S., Tanimoto, H., Aoki, N., Hirokawa, J. and Sadanaga, Y., 2006. A novel discharge source of hydronium ions for proton transfer reaction ionization: design, characterization, and performance. Rapid Communications in Mass Spectrometry 20, 1025-1029.

Proton-transfer reaction Ion Trap Mass Spectrometry for applications in medical sciences

Frans J.M. Harren[1], Elena Crespo[1], Simona M. Cristescu[1], Pieter Zanen[2], Marco M.L. Steeghs[1]

[1] *Life Science Trace Gas Facility, Molecular and Laser Physics, Institute for Molecules and Materials, Radboud University, Nijmegen, The Netherlands.*

[2] *Department of Pulmonology, University Medical Center, Utrecht, The Netherlands*

Abstract

In recent years, it has become apparent that there is a need to overcome the disability of conventional PTR-MS to identify the volatile organic compounds (VOCs) under analysis, without compromising its sensitivity or time resolution. A successful approach to do so is to replace the quadrupole mass filter with a quadrupole ion trap mass spectrometer [1]. Here we present a new Proton-transfer reaction Ion Trap Mass Spectrometer (PIT-MS) (figure 1; [2]), which has been developed from a commercially available ion trap system. Most of the advantages of the PIT-MS have been shown in literature [1-4]. We explore the capabilities of this system and its advantages over the conventional PTR-MS system. We find the optimal kinetic energy parameter E/N (95 Td) for the proton-transfer reaction to be significantly lower than for the conventional Proton-Transfer Reaction Mass Spectrometer (PTR-MS) (120 Td). The lower degree of fragmentation upon proton-transfer is identified as an additional advantage of the use of an ion trap mass spectrometer. The PIT-MS system is tested in a comparison with our PTR-MS on measurements of VOCs emitted from an Elstar apple. In this example, we show the advantages and the problems related to the use of Collision Induced Dissociation (CID) analysis for the identification of VOCs.

Furthermore, we present the measurement of VOC breath profiles as an indicator for the lung disease COPD. Chronic obstructive pulmonary disease is a non-curable disease for which the risk groups are well defined. Screening could allow early-stage identification of the disease. Breath analysis using PTR-MS is fast, easy, non-invasive and involves no risk to the patient. The goal of this project is to explore the capability of measuring exhaled VOCs to replace or complement pulmonary function tests in the detection of severe and especially mild emphysema found on high-resolution computed tomography in (recently quitted) heavy smokers. Current and former male smokers participated in a population based lung cancer screening trial. Computed tomography scans, pulmonary function tests and breath sample collection were performed on 431 subjects. This is the first attempt to discriminate between patients with and without disease, without prior selection of a control group of healthy subjects and under “uncontrolled” conditions (no restrictions on food, diet, exercise etc). In contrast, our control group consists of “healthy smokers” with the same background. Using bootstrapped stepwise forward logistic regression, we identified specific breath profiles as a potential tool for diagnosis of emphysema, airflow limitation and/or gas-exchange impairment. The exhaled breath profile provides comparable results to pulmonary function tests in detecting emphysema and the combination of both leads to an improved diagnostic quality.

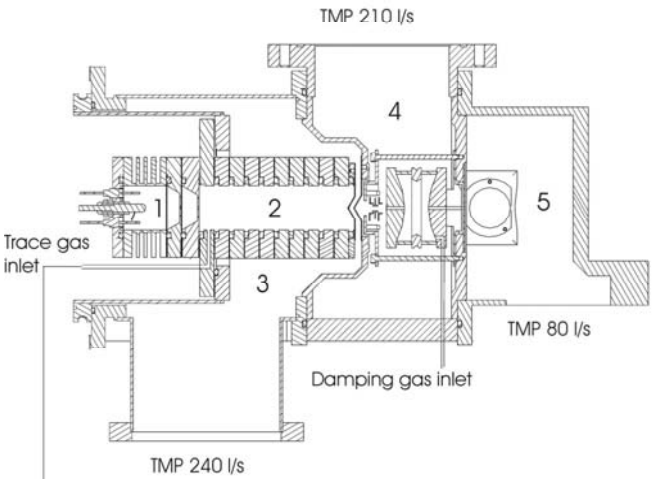

Figure 1: Nijmegen PIT-MS with 1) H3O+ ion source, 2) drift tube, 3) buffer chamber, 4) ion trap chamber and (5) detector chamber.

References

[1] C. Warneke, J.A. de Gouw, E.R. Lovejoy, P.C. Murphy and W.C. Kuster, Development of Proton-Transfer Ion Trap-Mass Spectrometry: On-line Detection and Identification of Volatile Organic Compounds in Air, Journal of the American Society for Mass Spectrometry 16, 1316-1324 (2005)

[2] M.M.L. Steeghs, C. Sikkens, E. Crespo, S.M. Cristescu and F.J.M. Harren, Development of a Proton-transfer reaction Ion Trap Mass Spectrometer: Online detection and analysis of volatile organic compounds, International Journal of Mass Spectrometry *in press*

[3] C. Warneke, S. Rosen, E.R. Lovejoy, J.A. de Gouw and R. Fall, Two additional advantages of proton-transfer ion trap mass spectrometry, Rapid communications in mass spectrometry 18 (1), 133-134 (2004)

[4] P. Prazeller, P.T. Palmer, E. Boscaini, T. Jobson, M. Alexander, Proton transfer reaction ion trap mass spectrometer, Rapid communications in mass spectrometry 17 (14), 1593-1599 (2003)

O_2^+ as primary reagent ion in the PTR-MS instrument: detection of gas-phase ammonia

Michael Norman[1*], Armin Wisthaler[1] , and Armin Hansel[1]

[1]*Institute of Ion and Applied Physics; Innsbruck University, Austria, armin.wisthaler@uibk.ac.at*

[*]*current affiliation: Environment and Health Administration, Stockholm City, Stockholm, Sweden*

Abstract

Oxygen (O_2) was used as a source gas in a conventional PTR-MS instrument to produce O_2^+ as chemical ionization (CI) reagent instead of H_3O^+. The use of O_2^+ as CI reagent allows for fast, highly sensitive and specific measurements of ammonia (NH_3) via the electron transfer reaction $O_2^+ + NH_3 \rightarrow NH_3^+ + O_2$. Instrument linearity was tested in the in the 2-to-2000 ppbv range. The 2σ detection limit was found to be ~90 pptv for a 1s signal integration time at dry conditions, slightly deteriorating with increasing humidity. The time response, defined by a $1/e^2$ decay in the calibration signal, ranged from 30s to 45s. Excellent agreement was obtained in intercomparison measurements of atmospheric NH_3 with two other NH_3 sensors based on liquid chemistry. The PTR-MS instrument was capable of detecting fast changes (<30 s) in ambient NH_3 concentrations.

Introduction

Ammonia (NH_3) is the most abundant alkaline gas in the atmosphere. It plays an important role in neutralizing acidic gases and particles and it influences formation and composition of particles. Anthropogenic sources like livestock waste, application of fertilizers and biomass burning are estimated to be larger than natural sources from soils and oceans [1]. It is anticipated that the increased use of three-way catalysts in automobiles will lead to increased NH_3 emissions in urban areas [2]. There are, however, large uncertainties in the atmospheric NH_3 budget mainly due to the lack of highly sensitive, accurate and fast analytical techniques. Chemical ionization mass spectrometry (CIMS) has the potential for fast and highly sensitive NH_3 measurements. Selected ion flow tube mass spectrometry (SIFT-MS) has been used for on-line NH_3 detection [3], but the low sensitivity of this technique limits its applicability for atmospheric measurements. More sensitive CIMS techniques were recently developed by two groups: the NOAA-CDS atmospheric pressure ionization instrument [4] and the Georgia Tech low pressure flow tube reactor [5]. Previous NH_3 measurements by PTR-MS were compromised by a large instrumental background caused by intrinsic NH_3 formation. NH_3 is believed to be produced from H_2O and N_2 in the plasma ion source. Herein we propose the use of a PTR-MS instrument that uses O_2^+ as precursor ions for fast and accurate measurements of atmospheric NH_3.

Experimental Methods

The instrument used in this study was a standard PTR-MS instrument build at the University of Innsbruck [6,7]. Pure oxygen (O_2, purity 5.2) was fed to the ion source instead of water vapor, forming O_2^+ primary reagent ions. Relative abundances of H_3O^+, $H_3O^+(H_2O)$, NO^+ and NO_2^+ ions were below 5 %, respectively. O_2^+ (recombination energy: 12.07 eV) reacts at collision rate with NH_3 (ionization energy: 10.07 eV) via electron transfer:

$$O_2^+ + NH_3 \rightarrow NH_3^+ + O_2$$

This reaction scheme has been proposed earlier for the detection of NH_3 via SIFT-MS [4]. The only product ion observed here was NH_3^+, detected at m/e=17. In a drift tube, the formation of $NH_3^+(H_2O)_{n=1,2}$ cluster ions -as observed in SIFT-MS flow tubes [8]- is effectively prevented by the application of an electric field. In the absence of water in the ion source (which partially leaks into drift tube) the drift voltage necessary to prevent hydration can be reduced to 450 V (E/N ~110 Td) leading to an increased ion residence time and thus an increased sensitivity. Potential interferences from OH^+ and CH_5^+ ions (both would also be detected at m/e=17) can be excluded. Both OH^+ and CH_5^+ ions rapidly react with H_2O (present at % levels in ambient air) and are thus not expected to be present in the drift tube. NH_3^+ ions do not react with any of the major components of air and secondary reactions do not need to be considered [9]. The applicability of O_2^+ ions for the detection of other trace gases than NH_3 (e.g. benzene, toluene, xylene) is currently under investigation.

Results and discussion

Calibration

Two methods for generating NH_3-free air were used. One was the use of a mixed platinum/palladium (Pt/Pd) catalyst operated at 350 ºC to convert NH_3 into NO, N_2O and NO [10]. The removal efficiency was found to be ≥ 99 %. The other was the use of Whatman-41 cellulose filters coated with oxalic acid. The NH_3 collection efficiency of two scrubber filters placed in series has been reported to be 98 % [11]. Gas-phase concentrations of NH_3 were created using a permeation device with an estimated permeation rate of 51-55 ng NH_3 min^{-1} at 30 ºC. The permeation tube was kept in a temperature controlled (30 ºC) oven and was continuously flushed with NH_3-free air. NH_3 concentrations in the 2-to-2000 ppbv range were generated via one or two stage dilution with NH_3-free air. The instrument was observed to have a linear response to NH_3 concentrations over the whole tested range with a normalized sensitivity of 3.6 cps per ppbv NH_3 (normalized to $1 \cdot 10^6$ cps O_2^+ ions). The relatively low sensitivity may be partly explained by the fact that ion extraction from the drift tube and ion injection into the quadrupole MS were not optimized for ions with low m/e values. An exemplary calibration curve is shown in Figure 1.

Instrumental background and detection limit

The instrumental background was determined by monitoring the signal at m/e = 17 when sampling air from the Pt/Pd catalyst. The observed background signal was slightly humidity-dependent increasing from ~300pptv at dry conditions to ~900 pptv at humid conditions. The 2σ detection limit at dry conditions was 90 pptv for a 1s signal integrations time and deteriorated slightly with humidity. The detection limit of the modified PTR-MS instrument is comparable to

numbers reported for other CIMS instruments [4]; it is greatly improved compared to SIFT-MS instruments.

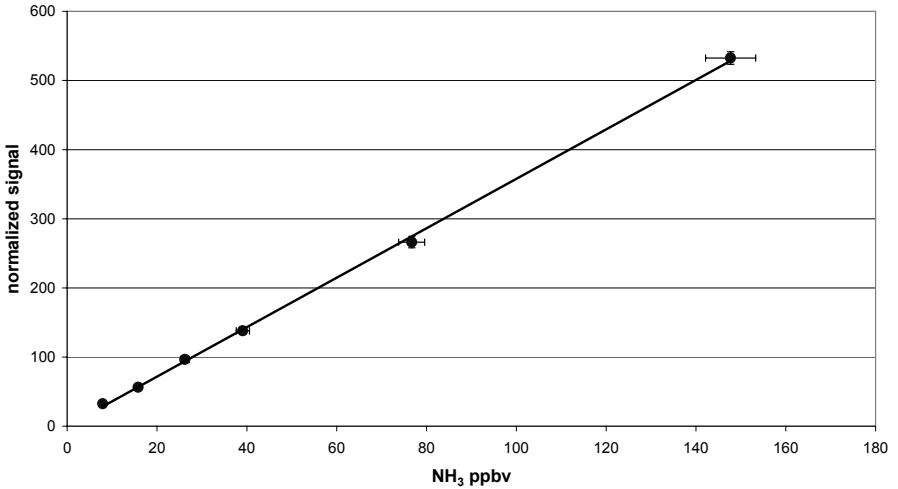

Figure 1: Calibration curve of the PTR-MS instrument for NH_3 using O_2^+ as precursor ion. The signal is normalized to an O_2^+ signal of $1 \cdot 10^6$ cps. The vertical bars represent the observed variability of the m/e=17 signal at each concentration and the horizontal bars represent the uncertainty in the permeation rate of the NH_3 source.

Response time

The time response, defined by a $1/e^2$ decay in the calibration signal, ranged from ~30s (@ ~1.2 ppmv NH_3) to ~45s (@ ~20 ppb NH_3). The observed time response is on the same order as observed for other CIMS instruments [4].

Field test

The instrument was tested at the Oensingen (CH) field site within the framework of the NitroEurope project. The modified PTR-MS instrument sampled air via a capillary inlet from a 17 m long, ½" OD PFA tube flushed with ~ 15 SLPM of air from an intensely treated grass field. Fast changes in NH_3 concentrations were observed due to turbulent transport of NH_3-rich air from the soil surface. The obtained data indicate that the modified PTR-MS instrument can monitor fast changes (<30 s) in gas phase NH_3 concentrations and that it even might be used for eddy covariant NH_3 flux measurements. NH_3 time series were in excellent agreement with data from liquid-chemistry based NH_3 instruments, i.e. the GRAEGOR (Gradient analyzer for gases and aerosols) and the AiRRmonia (Automated ammonia analyzer).

Conclusion

We have shown that the conventional PTR-MS instrument can be easily modified to use O_2^+ as precursor ions which allows for fast and accurate measurements of atmospheric NH_3.

References

[1] A. F. Bouwman, D. S. Lee, W. A. Asman, F. J. Dentener, K. W. van der Hoek and J. G. J. Olivier,. A global high resolution emission inventory for ammonia. Global. Biogeochem. Cyc., 11, 561-587, (1997).

[2] C. Perrino,M. Catrambone,A. Di Menno Di Bucchianico, and I. Allegrin, Gaseous ammonia in the urban area of Rome,Italy and its relationship with traffic emissions. Atmospheric Environment 36, 5385–5394, (2002).

[3] P. Spanel, S. Davis and D. Smith, 1998. Quantification of ammonia in human breath by selected ion flow tube analytical method using H_3O^+ and O_2^+ precursor ions. Rapid. Commun. Mass Spectrom. 12, 763-766.

[4] J. B. Nowak, L. G. Huey, A. G. Rusell, D. Tian, J. A. Neumann, D. Orsini, S. J. Sjostedt, A. P. Sullivan, D. J. Tanner, R. J. Weber, A. Nenes, E. Edgerton and F. C. Fehsenfeld, 2006. Analysis of urban gas-phase ammonia measurements from the 2002 Atlanta aerosol nucleation and real-time characterization experiment (ANARChE). J. Geophys. Res, vol. 111, (2006)

[5] J. B. Nowak, L. G. Huey, F. L. Eisele, D. J. Tanner, R. L. Mauldin III, C. Cantrell, E. Kosciuch and D. D. Davis, 2002. Chemical ionization mass spectrometry technique for detection of dimethylsulfoxide and ammonia. J. Geophys. Res., 107, D18, 4363, (2002).

[6] A. Hansel, A. Jordan, R Holzinger, P. Prazeller, W. Vogel and W. Lindinger, 1995. Proton transfer reaction mass spectrometry: On-line trace gas analysis at the ppb level. Int. J. Mass Spec. Ion. Proc., 149/150, 609-619, (1995).

[7] W. Lindinger, A. Hansel, A. Jordan, Proton-transfer reaction mass spectrometry (PTR–MS): on-line monitoring of volatile organic compounds at pptv levels. Chemical Society Review 27, 347–375, (1998).

[8] P. Spanel and D. Smith, Selected-ion flow tube studies of the reaction of H_3O^+, NO^+, and O_2^+ with several amines and some other nitrogen-containing molecules. Int. J, Mass Spect., 176, 203-211, (1998).

[9] V. G. Anicich and W. T. Huntress, JR, A survey of ion-molecule reactions for use in modeling the chemistry of planetary atmospheres, cometary comae and interstellar clouds. Astrophys. J. Suppl. Ser., 62, 553-672, (1986).

[10] L. Gang, Catalytic oxidation of ammonia to nitrogen. Technische Universiteit Eindhoven, ISBN 90-386-2653-3, NUGI 813, (2002).

[11] P. Quinn and T. Bates, Collection efficiencies of a tandem sampling system for atmospheric aerosol particles and gaseous ammonia and sulfur dioxide. Environ. Sci. Technol., 23, 736-739, (1989).

7. PTR-MS: Applications in Food Science

PTR-MS in food science and technology: a review

Franco Biasioli

Iasma Research Center, Agrifood Quality Department, via E. Mach, 1 - 38010 San Michele all'Adige (TN), Italy, franco.biasioli@iasma.it

Applications of PTR-MS in food science and technology have been proposed and investigated since the very beginning of its history together with environmental and medical applications [1]. They cover roughly one fourth of the total PTR-MS activity (apparatus and papers).

Almost every process that takes place in food affects the emission of organic volatile compounds (VOCs) that often play a key role in the perception of food characteristics. Thus, the capability of PTR-MS to monitor VOCs in real time, with high sensitivity and quantitatively, provides a tool for product and process characterization in food research.

With my contribution I hope to start a discussion on the potential of PTR-MS in the overabundance of traditional or innovative competitive methods rapidly increasing in their performances. As literature suggests, PTR-MS applications in food science and technology can be grouped in the following classes shortly introduced below: i) rapid product characterization, ii) real time monitoring of VOCs for process characterization and, in particular, iii) during food consumption, and iv) measurements of fundamental parameters like fragmentation patterns and partition coefficients for food relevant compounds.

"While identification of compounds in many cases can be done unambiguously, it should be emphasized that PTR-MS primarily has its strength in monitoring fast concentration changes of compounds rather than in compound analysis". On this note of Lindinger *et al.* [2] relies the success of PTR-MS in environmental science, where spectrometric peaks can often be related to single compounds [3]. This is not the case for food because a single product can emit hundreds of different VOCs. Nevertheless PTR-MS static or semi-static headspace characterization has been used in several studies both to classify products according to their VOCs fingerprint [4, 5] or to relate this fingerprint to other parameters: cultivar of fruit [6] and thus genetic information [7, 8], sensory attributes both in real [9-12] and model [13, 14] systems, presence of defects or degradation [15-18], ageing and post harvest storage [19, 20]. Here the interesting properties of PTR-MS are: the direct inlet of the headspace mixtures that warrants a genuine measurement without altering the sample, the rapidity that allows the collection of several data and thus of a robust statistics [6] and the detection of trace compound that could be difficult with other methods [21]. The methods described in [2] to increase the dimensionality of PTR-MS spectra (comparison of fragmentation patterns and their dependence on energy, isotopic ratios or partition coefficients) have been exploited, e.g., for coffee by Yeretzian et al. [22] but it turned out that separation methods are often necessary [23, 24]. Application of data mining techniques to PTR-MS spectra, alongside introducing to the PTR-MS community standard methods as principal component analysis, partial least squares regression and classification, random forest, support vector machines, etc. [5, 9, 12, 25, 26], brought also fundamental results concerning the optimum way to use the anonymous PTR-MS fingerprinting [27].

After the direct monitoring of coffee roasting [28] it was clear that monitoring of processes, even in difficult situations where relatively high humidity or temperature can not be avoided, is probably the application that better fits PTR-MS potential. The problem of compound identification as been partly overcame by the comparison as, e.g., in the works of van Ruth and coworkers [21, 24] or by the coupling, as proposed by Nestlè research centre [29], of PTR-MS with GC. This allowed the relatively safe identification of compounds while preserving the salient and unique features of PTR-MS. By this latter approach it was possible to monitor important reactions taking place during food processing as Maillard reactions or acrylamide and furan formation [30-32]. Metabolic or catabolic pathways in plants, fruits, meat can be considered as further examples of processes relevant for food science successfully monitored by PTR-MS [2, 18, 33-35].

In vivo release of flavor compounds during food consumption attracted a lot of attention to investigate the mechanisms underlying flavor perception and PTR-MS is particularly suited for this application where VOCs of interest are often known and at high concentrations [36, 37]. This is usually used to measure the effect of texture or oral processing on the dynamic of flavor release [38-44]. Other virtuosities include the sampling of the air "in" the nose, the coupling with other techniques and the simulation of mastication by artificial mouths [13, 45-50]. In-vivo measurements provide also information on single consumers. This allows, on one hand, the control of the high variability in oral processing protocols [38] and, on the other, it opens the way to a "consumer-centric" investigation of flavour perception [51].

With the exception of the coupling with GC [32], food science community seems, in my opinion, more oriented to applications of commercial PTR-MS than to the implementation of new instrumental developments. Waiting for the availability of hyphenated systems (e.g. time-of-flight, ion trap), studies on PTR-MS fundamentals concentrates on the measurement of relevant parameters like, e.g., fragmentation patterns and their dependence on instrumental settings [52, 55] or partition coefficients and Henry law constants [56].

In conclusion, PTR-MS has widened the possibility of a food research laboratory. By itself, without the coupling with GC or other spectrometric methods, it provides a rapid and non-invasive fingerprint that can be used to classify products and to correlate VOCs profile with other important characterisation of food. The time evolution of this profile allows the monitoring of rapid changes in concentration occurring during food processing or during food consumption. The coupling of PTR-MS with GC separation allows in few cases the unambiguous interpretation of spectrometric peaks and as been successfully applied in few cases. Hyphenating PTR-MS with other spectrometric techniques, further developments in automatic sampling and data analysis and visualization, and the availability of data on parameters relevant for food applications (e.g. fragmentation patterns and partition coefficients) will further extend its potential and eventually make it suited for industry applications.

References

[1] Lindinger, W., *et al.* On-line monitoring of volatile organic compounds at pptv levels by means of Proton-Transfer-Reaction Mass Spectrometry (PTR-MS) Medical applications, food control and environmental research (1998) Int J Mass Spectrom Ion Proc, 173 (3), 191

[2] Lindinger, W., *et al.* Environmental, food and medical applications of proton-transfer-reaction mass spectrometry (PTR-MS), Advances in Gas-Phase Ion Chemistry, 4, 1–35.

[3] Warneke, C., *et al.* Validation of atmospheric VOC measurements by proton-transfer-reaction mass spectrometry using a gas-chromatographic preseparation method, (2003) Environmental Science and Technology, 37 (11), 2494-2501

[4] Boscaini, E., *et al.* Characterization of wine with PTR-MS (2004) Int J Mass Spectrom, 239 (2-3), 215-219

[5] Biasioli, F., *et al.*. Coupling Proton Transfer Reaction-Mass Spectrometry with Linear Discriminant Analysis: A Case Study (2003) J Agric Food Chem, 51 (25), 7227-7233

[6] Granitto P.M., *et al.*. Rapid and non-destructive identification of strawberry cultivars by direct PTR-MS headspace analysis and data mining techniques, Sensor Actuat B-Chem, in press

[7] Carbone, F., *et al.* Development of molecular and biochemical tools to investigate fruit quality traits in strawberry elite genotypes (2006) Mol Breeding, 18 (2), 127-142

[8] Zini, E., *et al*. QTL mapping of volatile compounds in ripe apples detected by proton transfer reaction-mass spectrometry (2005) Euphytica, 145 (3), 269-279

[9] Gallardo-Escamilla, F.J., *et al.* Influence of starter culture on flavor and headspace volatile profiles of fermented whey and whey produced from fermented milk (2005) J Dairy Sci, 88 (11), 3745-3753

[10] Gallardo-Escamilla, F.J., *et al.* Sensory characteristics and related volatile flavor compound profiles of different types of whey (2005) J Dairy Sci, 88 (8), 2689-2699

[11] Biasioli, F., *et al.* Correlation of PTR-MS spectral fingerprints with sensory characterisation of flavour and odour profile of "Trentingrana" cheese (2006) Food Qual Prefer, 17 (1-2), 63

[12] Gasperi, F., *et al.* The mozzarella cheese flavour profile: A comparison between judge panel analysis and PTR-MS (2001) J Sci Food Agric, 81 (3), 357

[13] Van Ruth, S.M., *et al.* Volatile flavor analysis and sensory evaluation of custard desserts varying in type and concentration of carboxymethyl cellulose (2004) J Agric Food Chem, 52 (26), 8105-8110

[14] Roberts, D.D., *et al.* Comparison of nosespace, headspace, and sensory intensity ratings for the evaluation of flavor absorption by fat (2003) J Agric Food Chem, 51 (12), 3636-3642

[15] Shaker, E.S. Antioxidative effect of extracts from red grape seed and peel on lipid oxidation in oils of sunflower (2006) Food Sci Technol, 39 (8), 883-8

[16] Aprea, E., *et al.* Proton transfer reaction-mass spectrometry headspace analysis for rapid detection of oxidative alteration of olive oil (2006) J Agric Food Chem, 54 (20), 7635

[17] Jaksch, D., *et al.* The effect of ozone treatment on the microbial contamination of pork meat measured by detecting the emissions using PTR-MS and by enumeration of microorganisms (2004) Int J Mass Spectrom, 239 (2-3), 209-214

[18] Mayr, D., *et al.* Detection of the spoiling of meat using PTR-MS (2003) Int J Mass Spectrom, 223-224, 229-235

[19] Aprea, E., *et al.* Assessment of Trentingrana cheese ageing by PTR-MS and chemometrics (2007) Int Dairy J, 17 (3), 226-234

[20] Boschetti, A., *et al.* PTR-MS real time monitoring of the emission of volatile organic compounds during postharvest aging of berryfruit (1999) Postharvest Biol Tec, 17 (3), 143

[21] Boscaini, E., *et al.* Gas chromatography-olfactometry (GC-O) and proton transfer reaction-mass spectrometry (PTR-MS) analysis of the flavor profile of Grana Padano, Parmigiano Reggiano, and Grana Trentino cheeses (2003) J Agric Food Chem, 51 (7), 1782-1790

[22] Yeretzian, C., *et al.* Analysing the headspace of coffee by proton-transfer-reaction mass-spectrometry (2003) Int J Mass Spectrom, 223-224, 115-139

[23] Van Ruth, S.M., *et al.* Comparison of volatile flavour profiles of kidney beans and soybeans by GC-MS and PTR-MS (2005) Food Science and Technology Research, 11 (1), 63-70

[24] Van Ruth, S., *et al.* Evaluation of three gas chromatography and two direct mass spectrometry techniques for aroma analysis of dried red bell peppers (2003) Int J Mass Spectrom, 223-224, 55-65

[25] Van Ruth, S.M., *et al*. Characterisation of the volatile profiles of infant formulas by PTR-MS and gas chromatography-mass spectrometry (2006) Food Chem, 98 (2), 343-350

[26] Biasioli, F., *et al.* Fingerprinting mass spectrometry by PTR-MS: Heat treatment vs. pressure treatment of red orange juice - A case study (2003) Int J Mass Spectrom, 223-224, 343-353

[27] Granitto, P.M., *et al.* Recursive feature elimination with random forest for PTR-MS analysis of agroindustrial products (2006) Chemometr Intell Lab, 83 (2), 83-90.

[28] Yeretzian, C., *et al.* On-line monitoring of coffee roasting by Proton-Transfer-Reaction Mass-Spectrometry (2000) ACS Sym Ser, 763, 112-123

[29] Lindinger, C *et al.* Unambiguous identification of volatile organic compounds by proton-transfer reaction mass spectrometry coupled with GC/MS (2005) Anal Chem, 77 (13), 4117

[30] Mär̈k, J., *et al.* Quantitation of furan and methylfuran formed in different precursor systems by PTR-MS (2006) J Agric Food Chem, 54 (7), 2786-2793

[31] Pollien, P., *et al.* Proton Transfer Reaction Mass Spectrometry, a Tool for On-Line Monitoring of Acrylamide Formation in the Headspace of Maillard Reaction Systems and Processed Food (2003) Anal Chem, 75 (20), 5488-5494

[32] Robert, F., *et al.* Acrylamide formation from asparagine under low-moisture Maillard reaction conditions. 1. Physical and chemical aspects in crystalline model systems (2004) J Agric Food Chem, 52 (22), 6837-6842

[33] Fall, R. *et al.* Volatile organic compounds emitted after leaf wounding: On-line analysis by proton-transfer-reaction mass spectrometry (1999) J Geophys Res-Atmos, 104 (D13), 15963

[34] Boamfa, E.I., *et al.* Trace gas detection from fermentation processes in apples; An intercomparison study between proton-transfer-reaction mass spectrometry and laser photoacoustics (2004) Int J Mass Spectrom, 239 (2-3), 193-201

[35] Mayr, D., *et al.* Rapid detection of meat spoilage by measuring volatile organic compounds by using PTR-MS (2003) Appl Environ Microb, 69 (8), 4697-4705

[36] Roberts, D., *et al.* Flavor release: A rationale for its study (2000) ACS Sym Ser, 763, 1-6.

[37] Fay, L.B., *et al*. Novel mass spectrometry methods in flavour analysis (2001) Chimia, 55 (5), 429-434.

[38] Aprea, E., *et al.* In vivo monitoring of strawberry flavour release from model custards: Effect of texture and oral processing (2006) Flavour Frag J, 21 (1), 53-58

[39] Mei, J.B., *et al.* Influence of strawberry yogurt composition on aroma release (2004) J Agric Food Chem, 52 (20), 6267-6270

[40] Hansson, A., *et al.* The influence of gel strength on aroma release from pectin gels in a model mouth and in vivo, monitored with proton-transfer-reaction mass spectrometry(2003) J Agric Food Chem, 51 (16), 4732-4740

[41] Boland, A.B., *et al.* Influence of the texture of gelatin gels and pectin gels on strawberry flavour release and perception (2006) Food Chem, 96 (3), 452-460

[42] Mestres, *et al.* A. Release and perception of ethyl butanoate during and after consumption of whey protein gels: Relation between textural and physiological parameters (2006) J Agric Food Chem, 54 (5), 1814-1821

[43] Van Ruth, S.M., *et al.* In vitro and in vivo volatile flavour analysis of red kidney beans by proton transfer reaction-mass spectrometry (2004) Food Res Int, 37 (8), 785-791

[44] Mayr, D., *et al.* Breath-by-breath analysis of banana aroma by proton transfer reaction mass spectrometry (2003) Int J Mass Spectrom, 223-224, 743-756

[45] Frasnelli, J., *et al.* Intranasal concentrations of orally administered flavours (2005) Chem Senses, 30 (7), 575-582

[46] Mestres, M., *et al.* Aroma release and retronasal perception during and after consumption of flavored whey protein gels with different textures. 1. In vivo release analysis (2005) J Agric Food Chem, 53 (2), 403-409

[47] Van Ruth, S.M., *et al.* Influence of saliva on temporal volatile flavour release from red bell peppers determined by proton transfer reaction-mass spectrometry (2003) Eur Food Res Technol, 216 (3), 220-223

[48] Van Ruth, S.M., *et al.* Influence of mastication rate on dynamic flavour release analysed by combined model mouth/proton transfer reaction-mass spectrometry (2004) Int J Mass Spectrom, 239 (2-3), 187-192

[49] Boland, A.B., *et al.* Influence of gelatin, starch, pectin and artificial saliva on the release of 11 flavour compounds from model gel systems (2004) Food Chem, 86 (3), 401-411

[50] Hansson, A., *et al.* The influence of gel strength on aroma release from pectin gels in a model mouth and in vivo, monitored with proton-transfer-reaction mass spectrometry (2003) J Agric Food Chem, 51 (16), 4732-4740

[51] C. Yeretzian, *et al.* Individualization of Flavor Preferences: Toward a Consumer-centric and Individualized Aroma Science, Compr Rev Food Sci F - Vol. 3, 2004 pp. 152-159 [62]

[52] Buhr, K., *et al.* Analysis of volatile flavour compounds by Proton Transfer Reaction-Mass Spectrometry: Fragmentation patterns and discrimination between isobaric and isomeric compounds (2002) Int J Mass Spectrom, 221 (1), 1-7

[53] Tani, A., *et al.* Measurement of monoterpenes and related compounds by proton transfer reaction-mass spectrometry (PTR-MS)(2003) Int J Mass Spectrom, 223-224, 561-578

[54] Pollien, P., *et al.* Liquid-air partitioning of volatile compounds in coffee: Dynamic measurements using PTR-MS (2003) Int J Mass Spectrom, 228 (1), 69-80

[55] Hartungen, E.V., *et al.* Proton-transfer-reaction mass spectrometry of carboxylic acids: Determination of Henry's law constants and axillary odour investigations (2004) Int J Mass Spectrom, 239 (2-3), 243-248

[56] E. Aprea et al., PTR-MS study of esters in water and water/ethanol solutions: fragmentation patterns and partition coefficients (2006) Int. J. Mass Spectrom. In press

General overview: Applications of PTR-MS in food research at Nestlé

Christian Lindinger, Philippe Pollien, Santo Ali, Jean-Claude Spadone, Fabien Robert

Nestlé Research Center, Vers-chez-les-Blanc, 1000 Lausanne 26, Switzerland

Abstract

Since our first application of PTR-MS in 2001 multiple improvements in sensitivity, accuracy, automated measurements and software tools can be reported. Diverse developments and implementations of versatile interface systems allow using the PTR-MS in applications like:

- Monitoring the kinetics of aroma compound release from diverse food matrices
- On-line measurements of nose-space concentration during consumption of food (aroma compounds released into the nasal cavity)
- Unambiguous chemical characterization of on-line PTR-MS spectra by coupling GC-MS with PTR-MS

The rate of aroma release in time and intensity varies strongly from case to case. As an example, measuring the head-space of coffee obtained by pouring hot water on soluble coffee powder, the concentration of several aroma compounds and the relative humidity of the sample gas are exceeding the limits of PTR-MS specifications. Furthermore, the observed release kinetic is very quick and has therefore to be analyzed with a high time resolution. An interface providing a defined dilution, a quick gas exchange and an adaptation of the humidity of the sample gas is indispensable for such analysis. In many cases, the range in concentration of different compounds varies over several orders of magnitude. Aroma compounds of interest might often be present in traces of a few ppt while other dominating compounds exceed the tenth of ppm level. Therefore the dilution of the sample gas has to be adapted carefully. Fortunately PTR-MS shows outstanding advantages covering a linear range nearly over five orders of magnitude and broad acceptance of humidity of the sample gas. Nevertheless a strong influence of molecular fragmentation patterns depending on the humidity of the sample gas can be observed, and has to be controlled in order to obtain reproducible data. An automatic standardization of the PTR-MS settings influencing the compound fragmentation has been implemented for better comparison of datasets obtained by different PTR-MS. This novel approach was presented at the last PTR-MS conference in 2005. Since this time several improvements in reproducibility and automation are achieved and discussed in detail.

Due to the lack of identification using PTR-MS, a simultaneous trapping of sample gas on Tenax traps during the on-line release measurements and the trap-desorption on a GC-column coupled to MS and PTR-MS simultaneously, overcomes this deficit. This development was shown at the second PTR-MS conference. Recent improvements in coupling the GC-column outlet directly to a second drift-tube inlet show advantages in:

- Better controlling of the dilution of the column effluent introduced to the PTR-MS drift tube with nitrogen or air (necessary because of using He as carrier gas)

- Capability of controlling the humidity content of the GC separated analyte to obtain similar results in fragmentation pattern as observed during the on-line release measurements
- Defined pressure conditions at the column outlet of the GC

A further improvement is achieved by using a TOF-MS as GC detector. A time resolution of up to 50 spectra per second allows for a de-convolution of multiple overlapping GC-peaks and therefore a better identification of very complex mixtures.

Many applications benefits directly from this versatile infrastructure as the 2 following ones:

(1) Aroma perception during consumption event is changing upon time. Psychophysics study such as time-intensity are very time consuming and difficult. Moreover, psychophysics study does not always allow understanding the physico-chemical phenomenon behind. We used recently PTR-MS to investigate the kinetic of release of various encapsulated system. PTR-MS allow a rapid and direct comparison in aroma release of the different systems.

(2) To obtain a deeper understanding of the interpretation of aroma and flavor profiles by human brain, the cortical representation of gustatory or olfactory stimuli are studied by electroencephalographic (EEG) studies. Simultaneous recordings of swallowing, breathing, aroma release and brain response are performed using electromyographic sub mental electrodes, a flow transducer, PTR-MS and electroencephalography (EEG); respectively. By hyphenating these techniques, this method offers great opportunities in the field of flavor research by giving a rich picture of the processing of information, from the sensory input to brain integration and perception. PTR-MS ensure a perfect control of the aroma released upon time.

Targeting the qualitative, quantitative and temporal aspects of retronasal aroma perception: a challenge for time-intensity profiling?

Andrea Buettner[1], Montserrat Mestres[1]

[1] *Deutsche Forschungsanstalt fuer Lebensmittelchemie, Lichtenbergstr. 4, D-85748 Garching, Germany, e-mail: Andrea.Buettner@gmail.de*

[2] *Facultat d'Enologia, Dept Química Analítica i Orgànica, Universitat Rovira i Virgili, C/Ramón y Cajal 70, 43005 Tarragona, Spain*

Abstract

The temporal dynamics and qualitative and quantitative aspects of retronasal aroma perception were investigated to elucidate the relationship between the molecular and the perceptive level during and after administration of chemical stimuli. The basic principle was to apply precisely defined odorous and taste stimuli, while measuring the temporal release characteristics of the odorants using proton-transfer reaction mass spectrometry (PTR-MS). In parallel, the sensory response to the stimuli was investigated. Subjects indicated the time course of their sensations, while specifically rating the qualitative and quantitative aspects of their sensations. Cross-linking of the analytical data with time-resolved sensory evaluation revealed not only drastic differences in sensory intensity rating but also extensive variation in the corresponding sensory temporal resolution as a function of tastant addition.

Introduction

One of the driving forces for consumer preference is the perception of aroma and taste attributes during consumption of foods. Tastants are released within the oral cavity during mastication while odorants need to travel along the retronasal path via the pharynx into the nasal cavity. There they elicit the characteristic chemosensory impressions associated with a certain food product.

The temporal aspect of these processes has soon been regarded in flavor research (1). To seize the perception of individuals in a time-resolved manner, sensory descriptive approaches such as Time Intensity Profiling and theoretical models for the prediction of temporal sensory perception have been developed (2, 3, 4).The Time Intensity Profiling technique evolved to be a useful tool for the rating of subjective food flavor perception, being further developed until today by a broad range of scientists both in academy and industry. It has also become evident that interactions between different modalities such as taste and aroma, but also specific consumption patterns can considerably influence subjective sensory ratings (5, 6, 7, 8, 9, 10).

The aim of the present study was to cross-link individual perception both with chemoanalytical studies to elucidate interaction phenomena between different sensory modalities. This involves a specified time-resolved sensory analysis together with on-line observation of the respective aroma release patterns in vivo. The key goal of the study was to cross-link the analytical and sensory findings in a highly indiviualized approach.

Experimental Methods

Preparation of Gels

Gels with 4 %, and 10 % protein concentration, respectively, were freshly prepared and flavoured with ethyl butanoate according to the procedure described in (11). Gels contained either no tastants, or 2.5 %salt or 10 % sugar, respectively. Gelling was allowed for 15 hours at room temperature in open-ended syringes with a inner diameter of 18 mm. Prior to analysis they were freshly cut into cylinder-shaped samples of 2 mL. Samples were then applied immediately for analysis and were kept at 4 °C between sessions. The samples were singly presented to the sensory panel for retronasal evaluation.

Sensory analysis

Sensory analyses were performed in a sensory panel room at 21±1 °C at three different sessions. The samples (2 mL) were taken into the oral cavity and chewed for 30 sec with closed lips and without swallowing. Then, panelists were instructed to swallow the entire bolus and, after that, to continue chewing for 60 sec. The different gels were presented in triplicates to the panelists 3 samples of each type of gel). The order of the gels was randomised with a 15 min break between samples and, after each evaluation, the panelists rinsed the oral cavity with tap water. No information about the purpose of the experiment or the exact composition of the samples was given to the panelists.

Panelists were *not* specifically trained to produce TI curves but should indicate during the whole chewing procedure the moments of intense aroma perception (ethyl butanoate) by raising their thumbs. End of subjective aroma perception should be indicated by raising the whole hand. Intensity rating was performed on a seven-point scale from 0 (not perceivable) to 3 (highly intense aroma impression). In addition, taste intensity was rated for each sample.

Breath sampling

In parallels to sensory evaluation, nosespace air was sampled with two glass tubes fitted into the nostrils (10). The transfer line was a heated silo steel capillary with an inner diameter of 0.5 mm. A small fraction of 15 sccm was introduced into the drift tube of the PTR-MS (Compact PTR-MS, Ionicon, Innsbruck, Austria). The tubes were heated at 50 °C, to prevent condensation along the sampling line.

During the whole gel chewing sequence, as described above, the nosespace volatile concentration was measured simultaneously by using real-time PTR-MS. By resting the nostrils at the glass tubes, the tidal breath flow from the nostril was directly sampled without disturbance of the normal breathing or gel consumption pattern. PTR-MS data was always recorded together with the sensory evaluation by the panelists and their respective manual aroma indications as described above. Panelists were not allowed to look at any time at the data recording system and had no visual, acustical or other indication on when odor signals were detected by the MS system. Acetone, isoprene (both as indicators for the panelists' breathing patterns) and ethyl butanoate were analyzed in the selected ion mode (masses 49, 69 and 117, respectively). Peak counting was performed on the basis of 10% of the maximum peak intensity level as related to I max.

Results and Discussion

When comparing the sensory rating for the soft (4 % protein content) and hard (10 % protein content) gel, the perception of both taste attributes, sweet and salty, was considerably reduced in the hard gels (Fig. 1a), which is well in line with numerous other reports relevant to the field.

Rating of the aroma impression of ethyl butanoate reached the highest intensity score (intensity 3) for the soft gel without sugar or salt addition, but was significantly reduced in the hard non-tastant gel (Fig. 1b). Characteristic differences in the release profiles between the soft and hard gels without tastant addition can be quoted to be responsible for the observed differences in aroma intensity perception as described elsewhere (10).

However, when comparing the hard gel without and with sugar addition, no distinct differences in ethyl butanoate release were observable by means of PTR-MS for these gels (data not shown). This can be attributed to the fact, that both gels were chewed in similar ways due to their similarity in texture (data not shown), so that release profiles were consistent. Nevertheless, aroma rating was higher for the sweet gel, and, consequently, seemed to be influenced by the sensory perception of the sweet taste on a purely perceptive level. The same effect might be true under different conditions also for soft gel system, but could not be documented in this case as ethyl butanoate intensity rating was already at maximum for the non-sweetened gel. On the other hand, saltiness drastically decreased ethyl butanoate perception in both the soft and the hard gel. Again, this sensory decrease could not be correlated with any difference in the respective release patterns. These findings support the idea of congruent and incongruent sensory modalities as discussed previously. That means sweetness perception enhances fruity aroma notes while the "incongruent" salty taste leads to reduction of the fruit aroma perception.

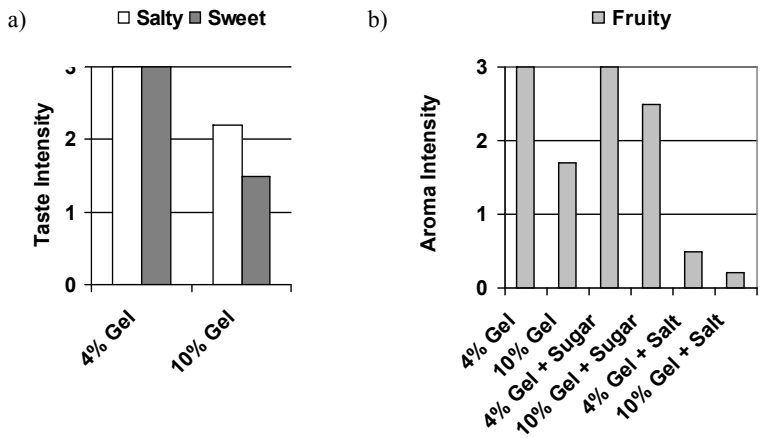

Figure 1: a) Perception of salt (2.5 %) and sugar (10 %) in gels of different gel hardness and b) aroma intensity rating for gels with and without tastant addition.

Apart from these purely qualitative and quantitative findings, this study predominantly focused on the aspect of temporal resolution. By utilizing a time-resolved concept in direct coupling with PTR-MS monitoring for each single panelist, it was possible to document that subjects were highly effective in sensorically indicating even singular ethyl butanoate aroma pulse events (as monitored by means of PTR-MS) during the course of gel consumption (cf. 10). However, this ability was significantly reduced in combination with salty taste. Interestingly, this partial loss in temporal resolution for the ethyl butanoate perception also occurred when sweet gels were consumed. It might be that the continuous tastant stimulation (following the classical time-intensity shape) reduces our ability to differentiate between individual retronasal aroma pulses.

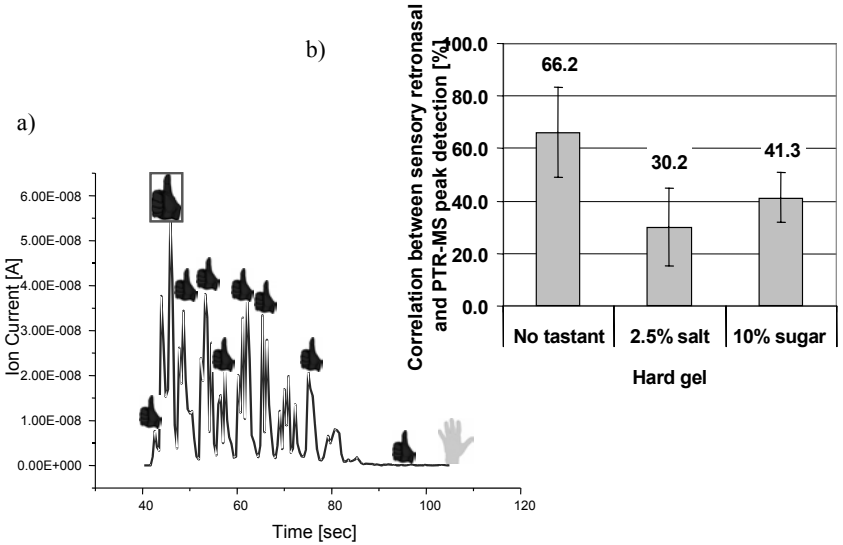

Figure 1: a) Characteristic PTR-MS release profile of ethyl butanoate, and respective sensory aroma pulse indication by hand sign; b) Correct sensory retronasal identification of ethyl butanoate aroma pulse for non-tasting and tasting gels.

References

[1] S. Kelling, B. Halpern, Taste judgments and gustatory stimulus duration : simple taste reaction times,. Chem. Senses 12, 543-562, (1987).

[2] G. Birch, S. Munton, Use of the „SMURF“ in taste analysis, Chem. Senses 6, 45-52, (1981).

[3] W. Lee, R. Pangborn, Time-intensity: the temporal aspects of sensory perception, Food Technol. 11, 71-78 (1986).

[4] O. Overbosch, S. de Jong, A theoretical model for perceived intensity in human taste and smell. II. Temporal integration and reaction times, Physiol. Behav. 45, 607-613, (1989).

[5] J. Maga, Flavor potentiators, CRC Crit. Rev. Food Sci. Nutr. 18, 231, (1983).

[6] H. Lawless, Sensory interactions in mixtures, J. Sens. Stud. 1, 259-274, (1986).

[7] R. Frank, J. Byran, Taste-smell interactions are tastant and odorant dependent, Chem. Senses 13, 445-455, (1988).

[8] J. Davidson, R. Linforth, T. Hollowood, A. Taylor, Effect of sucrose on the perceived flavor intensity of chewing gum, J. Agric. Food Chem. 47, 4336-4340 (1999).

[9] A. Buettner, A. Beer, C. Hannig, M. Settles, Observation of the swallowing process by application of videofluoroscopy and real-time magnetic resonance imaging – consequences for aroma perception. Chem. Senses 26, 1211-1219, (2001).

[10] M. Mestres, N. Moran, A. Jordan, A. Buettner, Aroma release and retronasal perception during and after consumption of flavored whey protein gels with different textures. J. Agric. Food Chem. 53, 403-409 (2004).

[11] K. Weel, A. Boelrijk, A. Alting, P. van Mil, J. Burger, H. Gruppen, A. Voragen, G. Smit, Flavor release and perception of flavored whey protein gels, J. Agric. Food Chem. 50, 5149-5155, (2002).

8. Contributed Papers (Posters)

Sorted by name of presenting authors.

Automated Taste-Aroma Delivery System for Simultaneous Analytical and Physiological Recordings

Julie Hudry, Boris Reynaud, Santo Ali, Nicolas Antille, Johannes le Coutre

Nestlé Research Center, Vers-chez-les-Blanc, 1000 Lausanne 26, Switzerland

Abstract

The aim of the present investigation was to develop of an automated taste-aroma delivery system for simultaneous real-time measurements of swallowing, nasal airflow, aroma release and chemosensory cortical responses. The system was developed in order to investigate taste-aroma integration under "pseudo-natural" conditions with consequent amount of liquid, whole-mouth stimulation and in-mouth retronasal stimulation after swallowing.

Introduction

Flavor perception is a complex combination of peripherally distinct sensory inputs including markedly taste and smell. During eating or drinking of food, tastants directly activate taste receptors on the tongue whereas volatiles are released into the oral cavity and transported to the olfactory receptors in the nasal cavity. This transport of volatiles, or retronasal olfaction, occurs with the airflows associated with chewing, swallowing and breathing. In the timing of flavor integration, complete flavor perception may occur after retronasal stimulation.

Previous electroencephalographic (EEG) studies of the cortical representation of gustatory or olfactory stimuli have delivered tastants to the mouth in very small quantities or stimulated olfaction orthonasally (measured by PTR-MS).

Experimental Methods

Schematic of the experimental procedure.

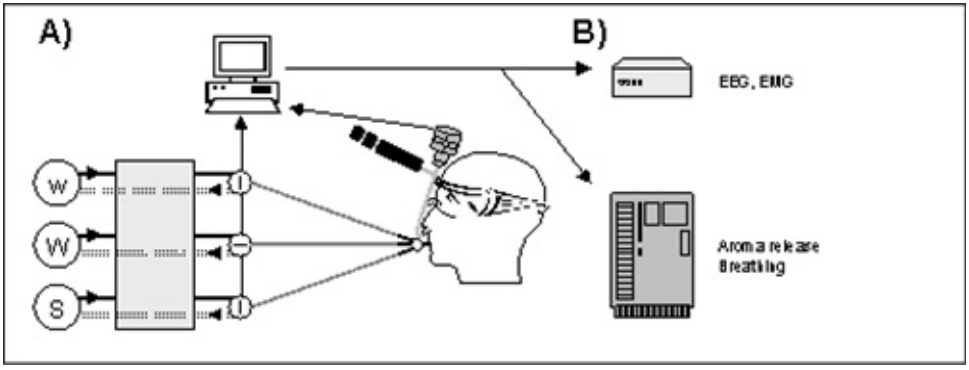

Results

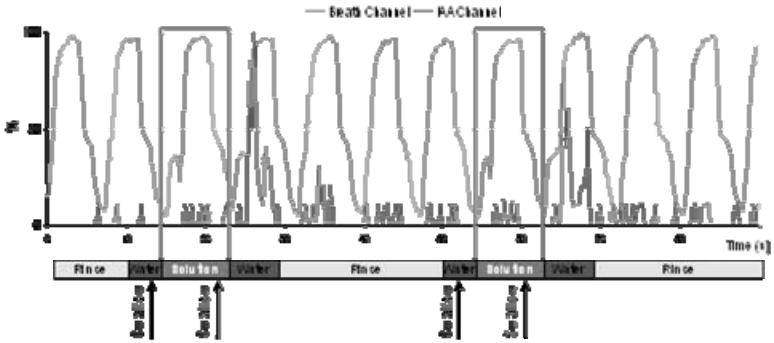

Figure 1: On-line nose-space PTR-MS measurement and simultaneous event time line. Upper part: PTR-MS isoamyl acetate (IAA) volatile channel and PTR-MS endogenous breathing acetone channel. The main volatile peak appears after delivery of the solution, once the solution has been swallowed and during exhalation. Lower part: Diagram of the experimental paradigm, with the swallow cued immediately before and after solution delivery.

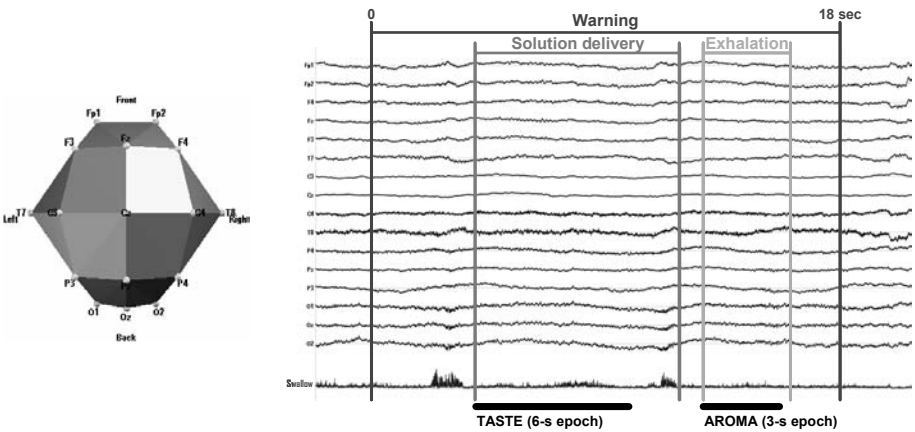

Figure 2: Raw EEG data and triggers - Left: Topographic location of EEG electrodes. Right: 6-s (taste) and 3-s (aroma) artifact-free digitized epochs were extracted through a hanning window and transformed into the frequency domain in 1-Hz bins by FFT. The 1-Hz bins were combined into the following relative spectral magnitude bands: theta (4-7 Hz), lower alpha (8-9 Hz), upper alpha (10-12 Hz), beta (13-29 Hz) and gamma (30-150 Hz). Epochs with artifacts and

frequencies below 4 Hz were eliminated. Swallowing signals were collected from submental electromyographic (EMG) electrodes.

Discussion

- The present study aimed to develop a method for studying the integration and cortical representation of complex stimuli containing both taste and aroma, by using conditions closer to the common consumption of liquid beverages.
- The method comprises an automated taste-aroma delivery system with an operating software controlling simultaneously stimulus delivery, in-mouth aroma release and physiological recordings.
- The operating system allows the precise control of taste-aroma stimulations (timing, amount, concentration) as well as the monitoring of physiological parameters (breathing, swallowing) triggering retronasal aroma onsets.
- By combining classical analytical, sensory and EEG techniques, this method offers great opportunities in the field of flavor research by giving a full picture of the processing of information, from the stimuli to the brain integration and perception.

Ion/molecule reaction studies in support of the detection of sesquiterpenes by CIMS

Crist Amelynck[1], Niels Schoon[1], Elke Debie[2], and Patrick Bultinck[2]

[1] *Belgian Institute for Space Aeronomy, Ringlaan 3, B-1180 Brussels, Belgium, crist.amelynck@bira-iasb.oma.be*

[2] *Ghent University, Department of Inorganic and Physical Chemistry, Krijgslaan 281, S3, B-9000 Gent, Belgium*

Abstract

The ion/molecule reactions of H_3O^+ ions with a series of sesquiterpenes have been studied in view of their detection by CIMS. For all sesquiterpenes multiple product ions have been observed, but the protonated molecular parent ion is always the major ion species with yields ranging from 30 to 94 %. All reactions proceed at the collision rate, which is calculated to be close to 3×10^{-9} cm^3 $molecule^{-1}$ s^{-1}. Preliminary studies indicate that NO^+ may also be a potential reagent ion for sesquiterpene detection.

Introduction

It is well-established that large amounts of volatile organic compounds (VOC) are emitted by terrestrial vegetation. Isoprene (C_5H_8) and the monoterpenes ($C_{10}H_{16}$) are generally found to be the biogenic VOCs (BVOCs) with the highest emission rates, but oxygenated BVOCs and sesquiterpenes ($C_{15}H_{24}$) are also known to be emitted directly by vegetation. Quantification of sesquiterpene emissions is an experimental challenge because of their low vapor pressure and their ability to react very rapidly with atmospheric oxidants (mainly O_3), resulting in atmospheric lifetimes of only a few tens of seconds for some compounds. Important efforts have been carried out lately to develop and improve analytical techniques for sesquiterpene detection and quantification [1]. PTR-MS instrumentation has also been used recently to measure sesquiterpene concentrations, e.g. in smog chamber studies of sesquiterpene ozonolysis [2] and in VOC emission studies from herbivore infested branches [3]. In principle a PTR-MS instrument can be used to derive sesquiterpene concentrations from ion/molecule reaction rate constants, reaction time and product ion distributions, provided these are accurately known. In this paper we report preliminary results from a selected ion flow tube (SIFT) study of H_3O^+/sesquiterpene reactions, as well as calculated collision rate constants for these reactions. The latter are based upon density functional theory calculations of polarizabilities and electric dipole moments.

Methods

Selected ion flow tube studies

The ion/molecule reactions were studied in a selected ion flow tube reactor at room temperature and at 150 Pa. A schematic representation of the instrument is given in Figure 1. H_3O^+ precursor ions (and others) are produced in a microwave discharge in a mixture of air and water vapor, mass selected in a first quadrupole filter and injected in a flow tube reactor. The ions in the flow tube are convectively transported by a helium buffer gas flow towards the mass spectrometer inlet,

where they are sampled, mass-analyzed by a second quadrupole filter and detected by a secondary electron multiplier which is operated in the pulse counting mode. More detailed information about the instrument can be found in [4]. To avoid differential diffusion of the product ions when performing product ion distributions, sesquiterpenes were introduced right in front of the mass spectrometer inlet. Introduction of stable sesquiterpene flows was accomplished by sending a helium flow over a reservoir containing liquid sesquiterpene which was kept at a constant temperature (usually 298 K). The tubing between the reservoir and the flow tube was made of stainless steel and kept at 373 K. Mass discrimination measurements of the spectrometer were carried out regularly to account for detector deteriorations.

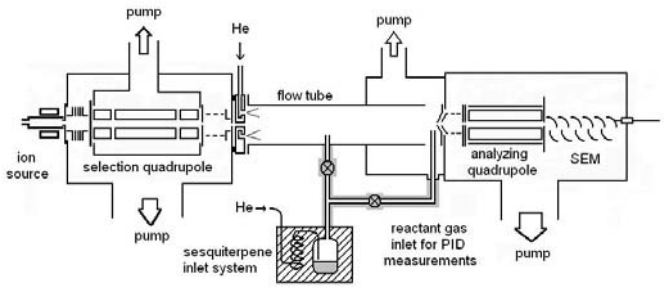

Fig. 1: schematic representation of the SIFT apparatus

Density functional theory calculations

Collision rate constants k_C of the H_3O^+/sesquiterpene reactions were obtained with the parameterized equation of Su and Chesnavich [5,6]. Polarizabilities and electric dipole moments were calculated using density functional theory (DFT). The hybrid B3LYP functional was employed, which has a good performance in combination with the aug-cc-pVDZ basis set. The sesquiterpenes were subjected to a thorough conformational analysis (MMFF random search in combination with an MM3/MM4 stochastic search) to find all possible conformations within an energy barrier of 4 kcal/mol from the lowest energy configuration. All these conformations were taken into account when calculating an average collision rate constant. All DFT calculations were carried out with the Gaussian'03 software [7] in a distributed computer environment.

Results and discussion

An overview of the product ion distribution of the reactions of H_3O^+ precursor ions with β-caryophyllene, α-humulene, longifolene and α-cedrene, obtained at thermal conditions with the SIFT instrument is given in Table 1. The reactions of H_3O^+ with α-cedrene and longifolene mainly result in the protonated parent molecule (>80 %). Non-dissociative proton transfer is less efficient for the reactions with β-caryophyllene and α-humulene. Multiple fragment ions are observed and these can be divided in 2 groups of which all elements are separated by a CH_2 unit (14 u). One group contains ions with masses 81, 95, 109, 123 and 137 u. The other group contains

ions with masses 121, 135 and 149 u. It should be noted that the ions with mass 81 and 137 u from the first group are also characteristic for the reactions of H_3O^+ with monoterpenes.

β-caryophyllene			**α-humulene**		
m/z	*Product ion*	*%*	*m/z*	*Product ion*	*%*
81	$C_6H_9^+$	4	81	$C_6H_9^+$	2
95	$C_7H_{11}^+$	9	95	$C_7H_{11}^+$	7
109	$C_8H_{13}^+$	10	109	$C_8H_{13}^+$	7
121	$C_9H_{13}^+$	3	121	$C_9H_{13}^+$	2
123	$C_9H_{15}^+$	7	123	$C_9H_{15}^+$	7
135	$C_{10}H_{15}^+$	8	135	$C_{10}H_{15}^+$	4
137	$C_{10}H_{17}^+$	7	137	$C_{10}H_{17}^+$	2
149	$C_{11}H_{17}^+$	16	149	$C_{11}H_{17}^+$	9
205	$C_{15}H_{25}^+$	30	205	$C_{15}H_{25}^+$	54
others		6	others		6
longifolene			**α-cedrene**		
m/z	*Product ion*	*%*	*m/z*	*Product ion*	*%*
95	$C_7H_{11}^+$	3	109	$C_8H_{13}^+$	2
109	$C_8H_{13}^+$	3	205	$C_{15}H_{25}^+$	94
149	$C_{11}H_{17}^+$	5	others		4
205	$C_{15}H_{25}^+$	83			
others		6			

Table 1: Product ion distributions of H_3O^+/sesquiterpene reactions. Only products with yields ≥ 2 % are listed. The m/z value refers to the first isotope of the product ions, but all isotopes are included in the yields.

From Table 1 it is clear that H_3O^+ precursor ions are certainly useful for sesquiterpene detection, but they cannot be used to distinguish between different isomers. Therefore, as is frequently done in SIFT-MS studies, the potential of NO^+ and O_2^+ precursor ions for sesquiterpene detection will be studied in detail in the near future. Preliminary results already indicate that NO^+ also seems to be a suitable CIMS reagent, but O_2^+/sesquiterpene reactions are less useful due to extensive fragmentation.

Because of the low vapor pressure and the stickiness of the sesquiterpenes, absolute rate constant measurements are difficult to perform. However, by simultaneously introducing H_3O^+, NO^+ and O_2^+ precursor ions in the flow tube reactor and by monitoring the count rates of the these three ions at controlled (but not measured) sesquiterpene concentrations in the reactor, the rate constant ratios of the NO^+/sesquiterpene and O_2^+/sesquiterpene reactions with respect to the H_3O^+/sesquiterpene reaction could be obtained. For all sesquiterpenes and within experimental error, the relative rate constant ratios thus obtained were found to scale linearly with the

reciprocal of the square root of the reduced mass of the ion/sesquiterpene system, which is a good indication that all reactions proceed at the collision limit.

The collision rate constants k_C of the H_3O^+/sesquiterpene reactions were subsequently obtained with the parameterized theory of Su and Chesnavich. Polarizabilities (α) and electric dipole moments (μ_D) of the sesquiterpenes, required for calculating these collision rate constants, were determined using B3LYP/aug-cc-pVDZ and are shown in Table 2. The second column of this table refers to the number of rotamers that were found and taken into account when averaging the molecular parameters and the collision rate constants. Previous experiments by the authors have shown that collision rate constants, calculated in this way for a large variety of chemical species, generally agree quite well with experimentally derived absolute rate constants obtained with the SIFT apparatus.

compound	# config.	μ_D (D)	α (Å^3)	k_C (10^{-9} cm^3 molecule^{-1} s^{-1})
β-caryophyllene	9	0.65	26.6	3.1
α-humulene	4	0.24	27.4	3.0
longifolene	2	0.94	25.9	3.2
α-cedrene	2	0.21	25.3	2.9

Table 2: averaged polarizabilies and electric dipole moments (from B3LYP/aug-cc-pVDZ calculations) and thermal averaged Su-Chesnavich collision rate constants.

From the data presented above it can be concluded that H_3O^+ precursor ions are useful for the sensitive detection of sesquiterpenes, due to the high reaction rate constants and the fact that reactions (at least at thermal energies) mainly result in a non-dissociative proton transfer product. We are well aware that the SIFT-MS method is not sufficiently sensitive for ambient sesquiterpene detection, but the method could be used in experimental set-ups (e.g. smog chambers or fast flow reactors) for dedicated experiments, where sesquiterpene concentrations can be much larger. Because of the higher ion energies in drift tube experiments compared to SIFT conditions, H_3O^+/sesquiterpene product ions in a PTR-MS instrument will be subjected to even more fragmentation. However, product ion distributions at thermal conditions in a SIFT will already give an indication about some of the fragments that can be expected in PTR-MS experiments. Because of the rather small electric dipole moments, the collision rate constants of H_3O^+/sesquiterpene reactions are not expected to be much affected by the electric fields which are typically applied in a PTR-MS drift tube.

References

[1] D. Helmig, J. Ortega, A. Guenther, J.D. Herrick, and C. Geron, Atm. Environ. 40, 4150-4157, 2006.

[2] A. Lee, A.H. Goldstein, M.D. Keywood, S. Gao, V. Varutbangkul, R. Bahreini, N.L. Ng, R.C. Flagan, and J. Seinfeld, J.Geophys. Res., Vol. 11, D07302, doi: 10.1029/2005JD006437, 2006.

[3] A. Schaub et al., Geophysical Research Abstracts, EGU General Assembly 2006, Vienna, Austria, abstract number EGU06-A-07408.

[4] N. Schoon, C. Amelynck, L. Vereecken and E. Arijs, Int. J. Mass Spectrom. 229, 231-240, 2003.

[5] T. Su, W.J. Chesnavich, J. Chem. Phys. 76, 5183-5185, 1982.

[6] T. Su, J. Chem. Phys. 89, 5355, 1988.

[7] M.J. Frisch et al., Gaussian ’03, Revision B.05, Gaussian Inc., Wallingford, CT, 2004.

Assessing truffle origin by PTR-MS fingerprinting and comparison with GC-MS for the headspace analysis

Eugenio Aprea[1], Silvia Carlin[1], Giuseppe Versini[1], Tilmann D. Märk[2] and Flavia Gasperi[1]

[1] *IASMA RESEARCH CENTER, Agrifood Quality Department, via E. Mach, 1 - 38010 San Michele all'Adige (TN), Italy, eugenio.aprea@iasma.it*

[2] *Institut für Ionenphysik und Angewandte Physik, Universität Innsbruck, Technikerstr. 25, 6020, Innsbruck, Austria*

Abstract

PTR-MS spectra of the headspace of white truffles were used as fingerprint to evaluate the possibility to discriminate the samples according to their origin. PTR-MS analysis allows a rapid and simple measurement of the headspace of whole truffle, avoiding sample alteration or damage, in this way the sample is available for further uses (more analysis, consume, commerce). Furthermore, the comparison with GC-MS for the identification of volatile compounds allows the exploiting of the analytical information embedded in the PTR-MS spectra.

Introduction

White truffle (*Tuber magnatum Pico*) is a subterranean fungus belonging to the order Tuberales and is highly appreciated for its unique and characteristic aroma, if is found mainly in Italy [1] and in some regions of southern France. As truffles are considered delicacy, their prices can be very high and it is interesting to develop methods that allow an objective evaluation of their aroma and to ascertain their origin.

We investigate the feasibility of a simple, rapid and non destructive analysis of truffles volatiles by means PTR-MS comparing headspace of white truffles coming from different Italian regions. The analysis of PTR-MS spectra by data mining techniques has been tested in several works [2-8] showing the usefulness and robustness of this approach. PTR-MS fingerprint is not completely anonymous but contains useful analytical information because the single masses recorded can often be related to specific compounds and the intensity of the signals are proportional to their concentrations [9]. Even if, PTR-MS is not a separation technique, the comparison with GC-MS allows the identification of several peaks [10].

Experimental Methods

Samples

Eighteen white truffles (*T. magnatum Pico*) from 6 different Italian regions (Langhe, Lazio, Marche, Molise, Toscana, Umbria) were collected in 2006 by "Centro Nazionale Studi Tartufo" in Alba. All the samples were checked by microscopy to ascertain the specie and the homogeneity of ripening degree.

Headspace analysis

A whole truffle (weight: 8.2 - 22.0 g, average 13.3 g) was introduced in a cap closed glass vessel. After 45 min of equilibrium at 25 °C the volatiles compounds were measured by a commercial version of the High-Sensitivity PTR-MS (IONICON Analytik GmbH). The headspace mixture was continuously extracted for less than 5 min at about 10 cm^3/min (corresponding to the acquisition of five complete spectra ranging from m/z 20 to m/z 240). To avoid possible systematic memory effects from one measurement to the next, the apparatus was flushed with outdoor air for 10-11 min between measurements.

The means of the last three of the five spectra acquired were used as fingerprints of the truffles. The spectra were subjected to the Principal Component Analysis (PCA) computed by means the software The Unscrambler 8.5 (CAMO PROCESS AS, OSLO, Norway).

The same vessels and the same equilibrium conditions, above reported, were employed for SPME/GC-MS headspace determination. After 20 min of the fiber enrichment (50/30 μm DBV/CAR/PDMS; SUPELCO), the volatiles were desorbed and injected in a Perkin-Elmer AutoSystem XL gas chromatography coupled with a TurboMass Gold (Perkin-Elmer, Norwalk CT) mass spectrometer operated in electronic ionization mode (m/z 30-300). Separation was achieved on an HP-Innowax fused-silica capillary column (30 m, 0.2 mm ID, 0.2 mm film thickness Agilent Technologies). Time of analysis for each samples was of 128 min.

Fragmentation patterns

In order to obtain PTR-MS fragmentation patterns, the main compounds identified by GC-MS were measured following the procedure described in Aprea et al. [11]. Dimethyl sulfide (99%), dimethyl sulfoxide (≥99.5%), dimethyl disulfide (99+%), p-cymene (99%), 2-acetyl-5-methylfuran (98%), benzothiazole (95%), bis(methylthio)methane (99%), tris(methylthio) methane (98%) with the purity reported in parentheses, were purchased from Sigma-Aldrich.

Results and discussion

Fingerprinting

Figure 1 reports the plot of first 3 PCA scores of PTR-MS data. It is shown that the samples are partly separated according their origin. Truffles from Langhe, Marche, Umbria and Toscana are well separated from the others, those from Lazio and Molise are more scattered and partly overlapped. Even if the reduced number of samples, the possibility to use the PTR-MS fingerprinting to ascertain the origin of truffles is promising, providing a non destructive method

that does not alter the sample in any way preserving the truffles for further analysis or for the consume.

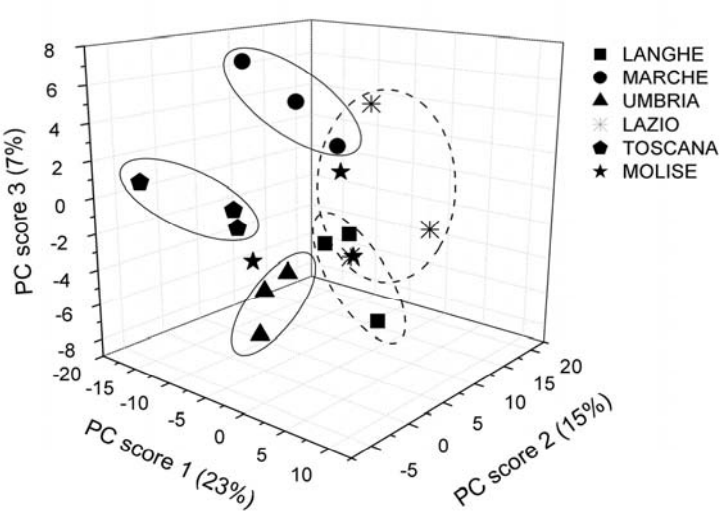

Figure 1: Plot of the first three PCA scores for the analysis of the six truffle proveniences. Samples from Langhe, Lazio, Umbria and Toscana appear separated according the place of origin. In parentheses the explained variance.

Headspace composition

The fragmentation pattern of pure standards and the comparison of gas-chromatograms allowed the identification of the most important compounds present in the headspace of truffles. The PTR-MS spectrum is dominated by the signal at m/z 63 ranging from 76 % to 84 % of the total ion counts (average values of three samples belonging to the same origin group) and was attributed to protonated dimethyl sulfide. The second most intense signal was recorded at m/z 61, attributed to the protonated bis(methylthio)methane, it ranges from 2 % to 6 % (average values of three samples belonging to the same origin group). Many other signals are relevant for the spectra, even if their relative contribution to the total headspace composition is lower. One-way ANOVA analysis on PTR-MS data indicates that there are significant differences (95%), among origin classes, for m/z 49 (methanethiol), m/z 63 (dimethyl sulfide), m/z 61 (bis(methylthio)methane), m/z 115 (dihydro-3,5-dimethyl-2(3H)-furanone), m/z 143 (2,4-octanedione), m/z 93 (p-cymene), m/z 79 and m/z 95 (sum of dimethyl disulfide, dimethyl sulfoxide, dimethyl sulfone).

Conclusions

A rapid, simple and not destructive measurement of the headspace of truffles can be archived by PTR-MS. The acquired spectra were used as fingerprint of the samples showing a partial discrimination of analyzed samples according their origin. The comparison of GC-MS for the

identification of headspace components allows the attribution of single compounds to the PTR-MS signals, so that time consuming GC analysis can be restricted to a preliminary phase and the fast and cheaper PTR-MS measurements can be used for extensive sampling campaigns.

References

[1] G. Giovanetti, Ecologia e produzione di Tuber magnatum in Italia, L'Informatore Agrario, 39 (37), 27463-27466 (1983).

[2] F. Gasperi, G. Gallerani, A. Boschetti, F. Biasioli, A. Monetti, E. Boscaini, A. Jordan, W. Lindinger and S. Iannotta, The Mozzarella cheese flavour profile - a comparison between Judge Panel analysis and Proton Transfer Reaction-Mass Spectrometry, Journal of Science of the Food and Agriculture, 81(3), 357-363, (2001).

[3] F. Biasioli, F. Gasperi, E. Aprea, L. Colato, E. Boscaini, and T.D. Märk, Fingerprinting mass spectrometry by PTR-MS: heat treatment vs. pressure treatment of red orange juice - a case study, International Journal of Mass Spectrometry, 223-224 (1/3), 343-353 (2003).

[4] F. Biasioli, F. Gasperi, E. Aprea, D. Mott, E. Boscaini, D. Mayr and T.D. Märk, Coupling Proton Transfer Reaction-Mass Spectrometry with Linear Discriminant Analysis: a case Study, Journal of Agriculture and Food Chemistry, 51(25), 7227-7233, (2003).

[5] F. Biasioli, F. Gasperi, D. Mott, E. Aprea, F. Marini and T.D. Märk, Characterisation of strawberry genotypes by Proton Transfer Reaction Mass Spectrometry spectral fingerprinting: a three years study, Acta Horticulturae, 708, 497-500, (2006).

[6] F. Biasioli, F. Gasperi, E. Aprea, I. Endrizzi, V. Framondino, F. Marini, D. Mott and T.D. Märk, Correlation of PTR-MS spectral fingerprints with sensory characterisation of flavour and odour profile of "Trentingrana" cheese, Food Quality and Preferences, 17(1-2), 63-75, (2006).

[7] E. Aprea, F. Biasioli, F. Gasperi, D. Mott, F. Marini and T.D. Märk, Assessment of Trentingrana cheese ageing by Proton Transfer Reaction-Mass Spectrometry and Chemometrics, International Dairy Journal, 17, 226–234, (2007).

[8] P.M. Granitto, F. Biasioli, E. Aprea, D. Mott, C. Furlanello, T.D. Märk and F. Gasperi, Rapid and non-destructive identification of strawberry cultivars by direct PTR-MS headspace analysis and data mining techniques, Sensors and Actuators B, (in press), doi:10.1016/j.snb.2006.03.047.

[9] A. Hansel, A. Jordan, R. Holzinger, P. Prazeller, W. Vogel and W. Lindinger, Proton transfer reaction mass spectrometry: on-line trace gas analysis at the ppb level, International Journal of Mass Spectrometry, 149-150, 609-619 (1995).

[10] C. Lindinger, P. Pollien, S. Ali, C. Yeretzian, I. Blank, and T.D. Märk, Unambiguous Identification of Volatile Organic Compounds by Proton-Transfer Reaction Mass Spectrometry Coupled with GC/MS, Analytical Chemistry, 77, 4117-4124, (2005).

[11] E. Aprea, F. Biasioli, , G. Sani, C. Cantini, T.D. Märk and F. Gasperi, PTR-MS headspace analysis for rapid detection of oxidative alteration in olive oil. Journal of Agriculture and Food Chemistry, 54, 7635-7640, (2006).

Discrimination of Different Wine Varieties through Direct Headspace Analyses by PTR-MS

Renate Spitaler [1, §], Nooshin Araghipour [2, §], Tomas Mikoviny [2], Armin Wisthaler [2], Josef Dalla Via [1, §], Tilmann D. Märk [2, *]

[1] *Research Centre for Agriculture and Forestry Laimburg, I-39040 Pfatten, Italy*

[2] *Institut für Ionenphysik, Universität Innsbruck, Technikerstrasse 25, A-6020 Innsbruck, Austria*

[§] *contributed equally to this work*

Abstract

The main aim of this work was to improve the capabilities of PTR-MS for fast and sensitive screening of wine headspace in order to categorize different wines according to grape variety, growing location, harvesting time and enological practices. Multivariate statistics were applied to discriminate between different wine varieties. A direct correlation between aroma and genetic profile confirmed that the study of VOCs is a useful tool to distinguish between different wines in variety characterization.

Introduction

The aroma profile of wines depends on grape variety, ripening conditions and wine making procedures. In the literature more than 800 aroma compounds have been reported in wines, including higher alcohols, aldehydes, ketones, esters, acids and monoterpenes [1]. Such complex aromas are difficult to standardise because of the influence of different factors affecting the volatile composition of wine; these include fruit genotype, environmental influence on the vineyard (soil, climate), fruit maturity and enology procedure conditions during fermentation until refinement of the final product through barrel and bottle-aging [2,3]. Fast, low-cost methods for on-site assessment of quality, origin and history of raw and final products are therefore of great interest to the wine industry.

Experimental Methods

A previous study using PTR-MS for analyses of alcoholic beverages [4] has been improved for direct headspace analyses of wine. The new set-up exhibited satisfactory time stability and reproducibility. The wine used in this study was produced from two different varieties of grapes – *Pinot Noir* and *Cabernet Sauvignon* – with different growing locations, harvesting times, enological practices and aging processes. Principal components analysis (PCA) was used to discriminate investigated wine samples

For evaluation purposes relative signal intensities of protonated ethanol on m/z 47^+ (the second most abundant ion) was kept at 10% of the hydronium (H_3O^+) primary ion, which was constant for all measured samples in keeping with standard experimental practice. To achieve this primary ion signal ratio a higher dilution of wine sample headspace air to dilution air was chosen (1:40)

whereby compounds at lower mixing ratios could potentially fall under the PTR-MS detection threshold. However, a high sensitivity PTR-MS instrument with a very low limit of detection [1] was used in these measurements and provided reasonable results in this respect.

PTR-MS analyses of *Cabernet Sauvignon* (CS) and *Pinot Noir* (PN) samples produced the same qualitative pattern of signals. For each wine sample analyzed the total ion counts were calculated as the sum of intensities of all signals contained in the absolute quantification matrix. This matrix was subjected to one-way ANOVA (α=0.05) analysis in order to detect whether any significant differences existed between the different analyzed samples. Following the procedure outlined in [5] a second data matrix was produced, subsequently referred to as the "relative quantification matrix", in which every variable of the absolute quantification matrix was represented as a percentage of the respective total ion count.

Principal component analyses (PCA) were performed with the absolute as well as with the relative quantification data matrices. Only factors with eigenvalues ≥ 1 were extracted. From the absolute quantification matrix, four factors were extracted.

Results

PCA was applied to those masses selected from the absolute quantification matrix showing significant variance with ANOVA. The analysis of the complete absolute quantification matrix resulted in a good discrimination of *Pinot Noir* from *Cabernet Sauvignon* samples. The plot of the PCA factor 2 versus factor 3 resulted in two well-separated, whereas the plot of factor 1 versus factor 3 did not allow differentiation of the two wine varieties (figure not shown).

PCA was performed with the complete set of 22 variables. The scatter plot of the first versus the second principal component factors allowed for discrimination of the two wine varieties (Figure 2a). Similarly, the scores for the second and the third principle component factors form two well-separated clusters for both varieties (Figure 2b). In Figure 2a, those samples containing the highest volatile contents (PN22, CS41, CS42) are clustered separately from the other samples. This is an indication of the impact of ecological factors on the chemical composition of wine like growing location (which, in the present case, is mainly due to the different altitudes of the growing sites) and the harvesting date. In both wine varieties the highest amounts of volatiles were observed in the wines collected at the higher altitude on the later harvesting date.

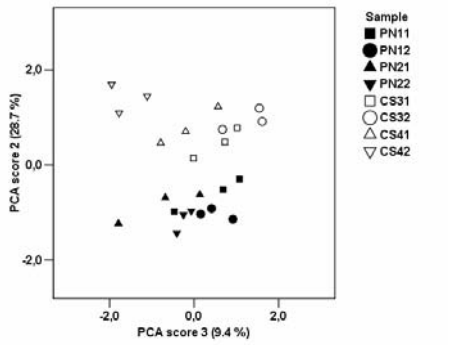

Figure 1: Scatter plot of the scores for the first versus the second principal component obtained from the absolute quantification matrix. Lower growing sites are represented by squares and circles, higher growing sites by triangles. The last digits of the sample acronyms indicate the harvesting date: 1 = earlier, 2 = later harvest.

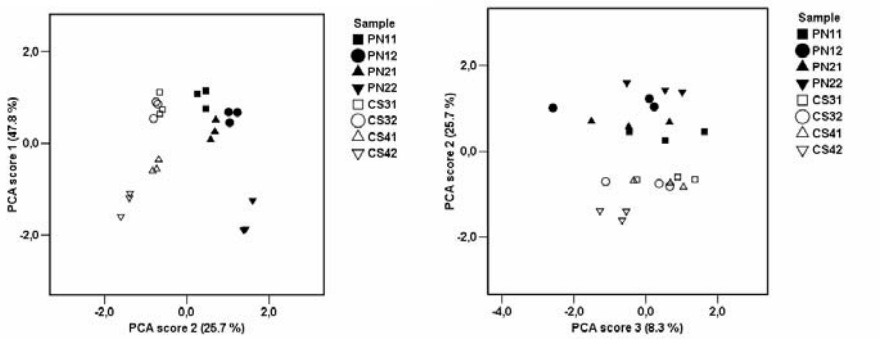

Figure 2a (left): Scatter plot of the scores for the first versus the second principal components obtained from the relative quantification matrix.

Figure 2b (right): Scatter plot of the scores for the second versus the third principal component obtained from the relative quantification data matrix.

Lower growing sites are represented by squares and circles, higher growing sites by triangles. The last digits of the sample acronyms indicate the harvesting date: 1 = earlier, 2 = later harvest.

Discussion

These results are in good agreement with the ratings by members of a tasting panel who examined samples of the same wines. According to this panel the *Pinot Noir* wine from the higher growing site, as well as the *Cabernet Sauvignon* wines from both locations, exhibited a higher aroma complexity when grapes were collected on a later date, probably due to the extended period of grape maturation [6].

The presented data show that volatile component patterns in South Tyrolean (North Italian) *Pinot Noir* and *Cabernet Sauvignon* wines are similar. Wine sample discrimination by means of PCA based on absolute quantification data was successful when applied to a selection of variables showing significant variance according to one-way ANOVA. In contrast, PCA based on relative quantification results allowed a good delimitation of the two investigated wine varieties even when the complete set of variables was evaluated. Furthermore, evaluation of the relative data set emphasized the distinction of samples showing extreme characteristics.

References

[1] Aznar, M.; Lopez, R.; Cacho, J. F.; Ferreira, V.:J. Agric. Food Chem., 49, 2924 (2001)

[2] A. Delcroix, Z. Günata, J.C. Sapis, J.M. Salmon, C.Bayonove, Am. J. Enol. Vitic. 45:3 - 291, (1994).

[3] Riccardo Flamini, Mass Spectrometry Reviews 22,4 -218, (2003).

[4] E. Boscaini, T. Mikoviny, A. Wisthaler, E. von Hartungen, T. D. M¨ark: Int. J. Mass Spectrom. 239 – 215, (2004).

[5] C. Zidorn, H. Stuppner, Taxon 50 – 115, (2001).

[6] A. Hansel, A. Jordan, R. Holzinger, P. Prazeller, W. Vogel, W. Lindinger, Int. J. Mass Spectrom. Ion Process. 149/150 – 609, (1995).

Does the emission of oxygenated plant volatiles reflect stress induced membrane damages?

Csengele Barta[1], Federico Brilli[1], Alessio Fortunati[1] and Francesco Loreto[1]

1-Istituto di Biologia Agro-Ambientale e Forestale, Consiglio Nazionale delle Ricerche (IBAF-CNR), Rome, Italy, corresponding author: csengele.barta@ibaf.cnr.it

Abstract

Several plant species re-emit a fraction of their assimilated carbon into the atmosphere in the form of a wide range of biogenic volatile organic compounds (BVOCs). Oxygenated BVOCs such as methanol, acetaldehyde, and C-6 aldehydes and alcohols are emitted in large quantities, especially under environmental stress conditions. The emission of C-6 oxygenated BVOCs is thought to depend on the breakdown of membrane unsaturated fatty acids, but there is no conclusive evidence of a straight correlation between emission and damage. The suitability of biochemical, destructive, assays to assess stress-induced membrane damages in plants is discussed and the development of a suitable, non-destructive, marker is needed. We have studied whether online, proton transfer mass spectrometry (PTR-MS) measurements of C-6 oxygenated BVOCs reflect stress induced membrane-alteration status of plant cells, being a good, non-invasive indicators of oxidative stress. Under various stress conditions, such as photoinhibition, heat stress or the combination of the above, large and sustained bursts of C-6 oxygenated BVOCs were observed. These emissions were associated to stress induced membrane damage, measured by thiobarbituric acid reactive substances (TBARS) accumulation. However, different stress conditions induced different BVOC emission patterns. The compound mostly associated with membrane damage was E-(2)-hexenal. E-(2) hexanal emission in all cases anticipated membrane damage detected by biochemical methods. Therefore E-(2) hexanal emission may be considered as an early signal of oxidative membrane cleavage. BVOC analysis by PTR-MS may be a tool to characterize plant response to environmental stresses and to assist in selection of stress-resistant germoplasm.

VOC emissions of white clover triggered by ozone

Aurelia Brunner, Christof Ammann, Markus Jocher, Christoph Spirig, and Albrecht Neftel

Research Station Agroscope Reckenholz-Tänikon ART, Zürich, Switzerland, aurelia.brunner@art.admin.ch

Introduction

One of the major challenges in tropospheric chemistry is the summer smog. It is characterized by high ozone mixing ratios during hot summer days. The ozone in the troposphere is an outcome of the reactions of nitrogen oxides and volatile organic compounds (VOC) under the influence of sunlight. High ozone levels can be toxic for men and cause damage to plants. Since 1996 the UNECE ICP-Vegetation [1] conducts a bio-monitoring of pollutant impacts on plants with the participation of most European countries. Two white clover clones (*trifolium repens L.* cv. Regal), which have different ozone sensitivities, are grown and harvested according to a standard protocol. The influence of ozone on the plants is evaluated by comparing the biomass and the visible leaf injuries of the two clover clones. In this study we performed ozone fumigation experiments in climate chambers using these two white clover clones. The environmental conditions in the climate chambers mostly resembled summer conditions in central Switzerland. The aim of this experiment was to investigate whether high ozone mixing ratios lead to enhanced VOC emissions of the plants.

Experimental Methods

Plant material

The ozone fumigation experiments were conducted with two white clover clones (*trifolium repens L.* cv. Regal), an ozone-sensitive (NC-S) and an ozone-resistant (NC-R) one [2], which were kindly provided by the ICP-Vegetation Coordination Centre at the CEH Bangor, UK. 50 clover cuttings (25 NC-R and 25 NC-S) were plant in 1.1 L pots filled with peat soil and they were well watered. After 3 weeks of growing in the greenhouse, the plants were repotted in groups of five into 40 L pots, resulting in 5 pots with 5 NC-S and 5 NC-R plants, respectively. One week later they were cut down to 7 cm above ground level and left to regrow for another 4 weeks in the greenhouse. The greenhouse growing conditions during these 8 weeks were (day/night): 22/18°C air temperature, 40/70% relative humidity. During 16 h of the day (06:00-22:00) lights were on (Philips Son T plus 400W). After eight weeks the pots (3 of each clone) were moved from the greenhouse to the climate chambers where the ozone fumigation experiment took place. During the experiment each pot was watered with 1 L per day. After each experiment the plants were cut down to 7 cm above ground. The total leaf area was determined by means of a portable area meter in combination with a transparent belt conveyor accessory (LI-3000C and LI-3050C, Li-COR, Lincoln NE, USA). The dry matter yield was determined. Two batches of each clone were grown with an interval of 2 weeks.

Experimental set-up

The ozone fumigation experiments were performed in two identical computer controlled climate chambers (Phytokammer, YORK, D), one of which was fumigated with ozone. Each chamber has

a volume of 27.7 m^3 (2.8 m x 4.5 m x 2.2 m). Air temperature, relative humidity (RH) and photo synthetically radiation (PAR, up to 1000 µE m^{-2} s^{-1}) can be prescribed and adapted every minute. The climate conditions in the chambers were set to resemble summer conditions in central Switzerland. Therefore a mean diurnal cycle of air temperature, relative humidity, and radiation values of a fair weather period of summer 2005 (19.-29.06.2005) of the CarboEurope site Oensingen [3] was simulated (see Fig.1).

A computer controlled ozone fumigation setup was installed in one of the two climate chambers. The ozone was produced by an ozone generator (model 500, Fischer GmbH, Bonn, D). The ozone mixing ratios follow a diurnal cycle (Fig. 1). The first fumigation experiment (EX1) lasted 12 days with daily ozone maximum values of 70 ppbv (1 d), 100 ppbv (2 d), 120 ppbv (3 d), and 150 ppbv (3 d). The second experiment (EX2) lasted 15 days with daily ozone maximum values of 70 ppbv (1 d), 100 ppbv (1 d), and 150 ppbv (7 d).

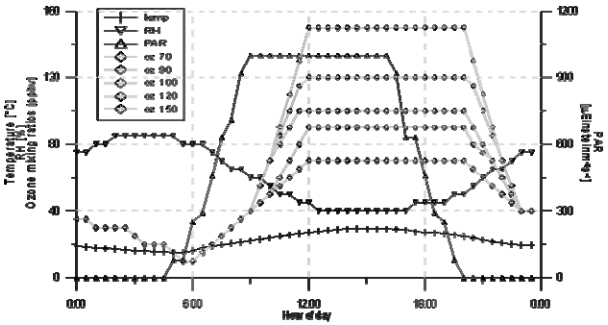

Figure 1: Diurnal cycles of air temperature, relative humidity (RH), photosynthetically active radiation (PAR) and ozone mixing ratios applied in the climate chambers.

An automatic system of six dynamic chambers, one on each 40 L pot, was used for the VOC flux measurements in the climate chambers. For detailed information about this dynamic chamber system see Pape et al. [4]. Two chamber units were operated in the climate chamber with ambient air and four of them in the ozone fumigated climate chamber. Sample air for trace gas analysis was pulled through PTFE tubes from each chamber to the analysers.

Measurements

Volatile organic compounds (VOC) were measured continuously by a proton transfer reaction mass spectrometer (PTR-MS, Ionicon GmbH, Austria) and occasionally by the combination of a GC-FID and PTR-MS. The PTR-MS technique is well described in Lindinger et al. [5]. The PTR-MS used in these experiments corresponds to the PTR-MS-HS type, featuring three turbo pumps for increased sensitivity and a drift tube (equipped with Teflon rings) optimised for fast time response and minimal interactions with polar compounds [6]. Details about the combination of PTR-MS and GC-FID are described by Davison et al. [7].

Water vapour (H_2O) and carbon dioxide (CO_2) were measured continuously by a LI 6262 (Li-Cor environmental, Lincoln NE, USA). Ozone (O_3) in the dynamic chamber system was measured continuously by a UV photometric analyser (Dasibi, Series 1008, Environmental Corp., Glendale CA, USA).

The stomatal conductance of the clover was measured by AP4 porometer (AT Delta-T Devices Ltd, Cambridge, U.K.). The measurements were usually conducted between 12:00 and 14:00 LT.

Results and discussion

Methanol fluxes

Out of more than 20 ion masses we were measuring continuously with PTR-MS, methanol (protonated ion mass 33) showed the most interesting emission pattern. Figure 2 shows the methanol flux of a resistant (re oz, NC-R) and a sensitive (se oz, NC-S) clover clone in the ozone fumigated climate chamber during the first experiment. On the first day of the experiment (no ozone fumigation) the ozone sensitive clone shows a higher methanol emission than the ozone resistant clone. On the second day this difference in the emission of the two clones is equalized. With on-going fumigation the NC-S clone emits permanently more methanol. In contrast the NC-R clone emits only slightly more methanol with increasing ozone mixing ratios. The emission pattern of both plants shows a diurnal cycle with a maximum in the early morning.

Figure 3 shows the methanol fluxes of a NC-R and a NC-S clover clone in the ozone fumigated climate chamber during the second fumigation experiment. On the first day of the fumigation (28.03.05), methanol emissions of the sensitive and resistant clone are quite similar. They follow a diurnal cycle with a maximum emission in the morning. From the second day of ozone fumigation on, the two clones show a different methanol emission. The methanol emission of the sensitive clone increases each day and night. In addition a second maximum around midday appear. After six days the emission declines. The methanol emissions of the resistant clone don't show a change until the fifth day of fumigation where an additional emission peak around midday appear.

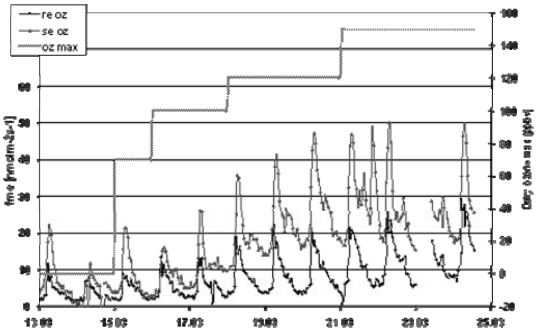

Figure 2: Methanol fluxes (fme) of an ozone-sensitive (se oz, NC-S) and an ozone-resistant (re oz, NC-R) clover clone in the ozone fumigated climate chamber during the first fumigation experiment. The dashed line indicates the daily ozone maximum.

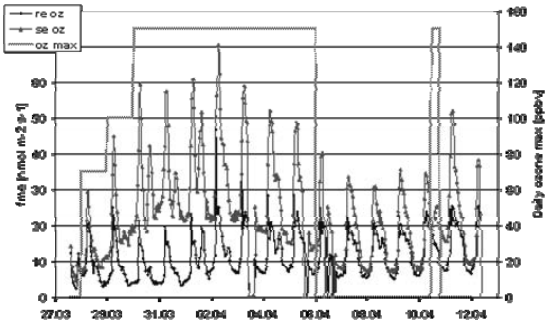

Figure 3: Methanol fluxes (fme) of an ozone-sensitive (se oz, NC-S) and an ozone-resistant (re oz, NC-R) clover clone in the ozone fumigated climate chamber during the second fumigation experiment. The dashed line indicates the daily ozone maximum.

The comparison of the methanol emissions during these two different fumigation experiments shows the different response of the plants. In EX1 the daily maximum of the ozone mixing ratio was increase from zero to 150 ppbv over a period of six days, whereas in EX2 the daily ozone maximum of 150 ppbv was reached already on the third day. The weaker reaction of the clover to the treatment in EX1 (the softer one) indicates some sort of plant adaptation to high ozone levels.

More results will be presented and discussed at the conference.

References

[1] United Nations Economic Commission for Europe International Cooperative Programme on Effects of Air Pollution on Natural Vegetation and Crops (UNECE ICP Vegetation)

[2] A. S. Heagle, J. E. Miller, B. I. Chevone, T. W. Dreschle, W. J. Manning, P.M. Mc Cool, C. Lynn Morrison, G. E. Neely, and Joanne Rebbeck, Response of a white clover indicator system to tropospheric ozone at eight locations in the united states, Water, Air and Soil Pollution 85, 1373-1378, (1995).

[3] C. Ammann, C. Flechard, J. Leifeld, A. Neftel, and J. Fuhrer, The carbon budget of newly established temperate grassland depends on management intensity, Agriculture, Ecosystems and Environment (in press).

[4] L. Pape et al., An Automated Dynamic Chamber System for Measuring Reactive Trace Gas Exchange of Grassland Ecosystems, submitted to Biogeoscience (2006).

[5] W. Lindinger, A. Hansel, and A. Jordan, On-line monitoring of volatile organic compounds at pptv levels by means of Proton-Transfer-Reaction Mass Spectrometry (PTR-MS): Medical applications, food control and environmental research, International Journal of Mass Spectrometry and Ion Processes, 173, 191-241, (1998).

[6] C. Spirig, A. Neftel, C. Ammann, J. Dommen, W. Grabmer, A. Thielmann, A. Schaub, J. Beauchamp, A. Wisthaler, A. Hansel, Eddy covariance flux measurements of biogenic VOCs during ECHO 2003 using proton transfer reaction mass spectrometry. Atmospheric Chemistry and Physics 5, 465-481 (2005).

[7] Davison, B., Brunner, A., Ammann, C., Spirig, C., Jocher, M., Neftel, A.: Cut induced VOC emissions from agricultural grasslands. Submitted to Plant Biology (2006).

Headspace Analysis of In Vitro Cultured Cells using PTR-MS

C. Brunner, B. Thekedar, L. Keck, U. Oeh and C. Hoeschen

Institute of Radiation Protection, GSF – National Research Center of Environment and Health, Ingolstädter Landstr. 1, 85758 Neuherberg, Germany, claudia.brunner@gsf.de

Abstract

In this work PTR-MS was used to analyse the specific volatile organic compounds (VOCs) emitted by retinal epithelium cells in vitro. For that purpose, these cells were cultured in a specific growth medium. Subsequently, the VOCs in the headspace of the cell culture were analysed using an online PTR-MS technique, so that the VOCs emitted (metabolic end products) or consumed (essential compound for metabolism) by the cells could be determined as a function of time. The VOC concentrations were calculated using the measured transmission function of the PTR-MS. Several emitted and consumed VOCs were detected for human retinal ephithelium cells.

Introduction

PTR-MS is widely used to detect volatile organic compounds in several different applications. Besides environmental measurements and breath gas analysis, it is also applied to study various biological samples, like in vitro cell cultures. In vitro headspace analysis of various cell lines has already been done by some research groups, for e.g. acetaldehyde was found as a marker for lung cancer cells using selected ion flow tube mass spectrometry [1].

In the frame of a larger study, human retinal ephithelium cells turned out to be useful to investigate potential effects of radiation on metabolic processes as being reflected by the VOCs in the headspace of the cells. Therefore the aim of this work was to investigate the specific organic compounds (VOCs), either produced or consumed, in the headspace of the cell culture with PTR-MS.

Experimental Methods

Retinal epithelium cells were bred in cell culture flasks of 175 cm² breeding area. This type of adherent cells is relatively easy to handle due to their low sensitivity to temperature, air conditioning and nutrition. For the breeding, fetal calf serum was added to the culture medium. However, after the cells were completely covering the ground, the culture medium with calf serum was replaced by the same medium without fetal calf serum in order to reduce the background signal.

The flasks had an inlet and an outlet at opposite ends. Synthetic air entered at the inlet of the flask and the outlet was connected to the PTR-MS. The flow rate of synthetic air through flasks was maintained at around 50 ml/min.

During the measurement the number of cells in the flask was in the range of 10^7. For the data evaluation the signals of the medium without cells were subtracted from the signals of the medium with cells.

The transmission measurements were performed with well defined concentrations of selected VOCs at ppm levels in Teflon gas sampling bags. The concentrations were obtained by injecting a defined amount of pure liquid into nitrogen as carrier gas.

Results and Discussion

To calculate the concentration of VOCs from the ion counts rates of the secondary electron multiplier, the transmission function of quadrupole mass spectrometer was determined and the result is shown in Fig. 1. The transmission function featured, somewhat unusual, a pronounced maximum in the range of mass 30 to mass 60. For the calculation of concentration only the pressure due to the sample in the drift tube was considered, i.e. the pressure due to the ion source of ~ 0.7 mbar was subtracted from the total pressure of ~2.1 mbar.

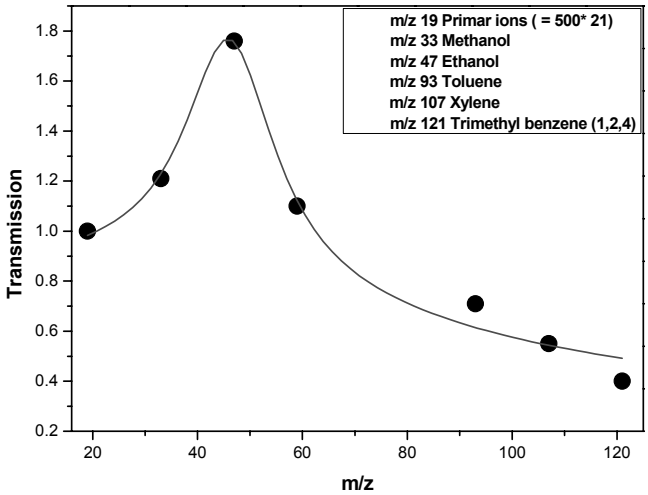

Figure 1: Transmission curve of the PTR-MS by using nitrogen as carrier gas.

The concentrations, calculated from the transmission function shown above, are displayed in Fig. 2. The concentrations refer to the changes attributed to the cells, i.e. the difference between concentrations for the medium with cells and the medium without cells. The change of concentration was found to be positive for the masses 33, 47, 59, 73 and 105 and was found to be negative for the mass mass 45. The positive differences, referring to molecules produced by the cells, could correspond to methanol (mass 33), ethanol (mass 47) and acetone (mass 59). Lacking plausible substances, mass 73 and mass 105 are not attributed to any specific molecules. The concentrations of the masses mass 43 and mass 61 in the medium with cells were slightly higher than in the medium without cells but more experiments will be necessary to obtain a better statistical significance. Mass 45 may correspond to acetaldehyde which seems to be consumed by the cells from the medium.

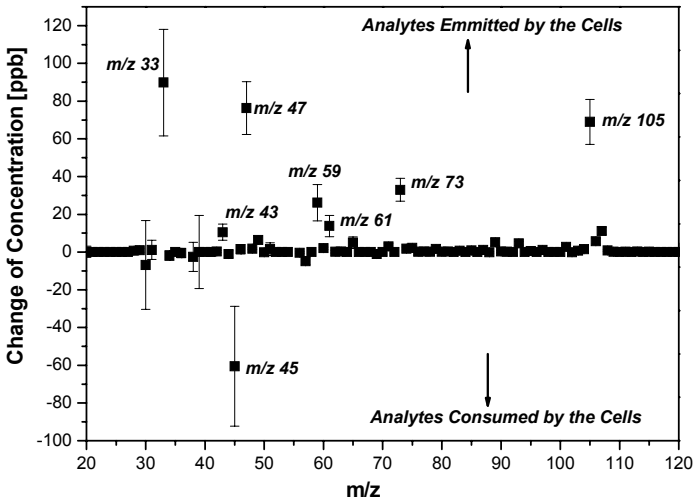

Figure 2: VOC markers produced or consumed by retinal epithelium cells.

Conclusions

Several VOC markers for human epithelium cells could be identified. The most significant markers for this cell line were m/z 33, 47, 59, 73 and 105 and some signals were tentatively attributed to specific substances. However, to identify the substances properly, measurements by gas chromatography will be necessary.

At present state only one cell line has been examined. Further experiments for various cell lines may result in the identification of other characteristic markers and eventually it might be possible to distinguish between different types of cells using headspace analysis with PTR-MS. Moreover, headspace analysis by PTR-MS could be used as a new simple method to determine whether cell cultures are dead or alive.

References

[1] Smith, D., Wang, T., Sule-Suso, J., Spanel, P., and El Haj, A., 2003, Quantification of acetaldehyde released by lung cancer cells in vitro using selected ion flow tube mass spectrometry, Rapid Communications in Mass Spectrometry, 17, 845-850 (2003).

[2] M. Steinbacher, J. Dommen, C. Ammann, C. Spirig, A. Neftel, A.S.H. Prevot, Performance characteristics of proton transfer mass spectrometer (PTR-MS) derived from laboratory and field measurements, International Journal of Mass Spectrometry 239, 117-128 (2004).

Analysis of Lactones by Proton Transfer Reaction - Mass Spectrometry (PTR-MS). Fragmentation Patterns and Detection Limits

Katja Buhr[1], Andrea Buettner[1] and Peter Schieberle[2]

[1] Deutsche Forschungsanstalt für Lebensmittelchemie, Garching, Germany, katja.buhr@lrz.tum.de

Abstract

While lactones are important aroma compounds contributing to numerous food flavors such as fruit and dairy products, their behavior in Proton Transfer Reaction - Mass Spectrometry (PTR-MS) has not been elucidated yet. As an example for lactones in general, the present study is looking into fragmentation patterns, sensitivity and detection limits of C_8- and C_9-lactones in Proton Transfer Reaction - Mass Spectrometry.

Introduction

Lactones present an important group of flavor compounds and are found in numerous foodstuffs such as fruit, dairy products and wine. For example, with their coconut-like smell, δ-octa- and δ-decalactone are character impact compounds in coconut flavor. On the other hand, γ-decalactone displays peachy odor qualities and contributes to numerous fruit flavors [1-4].

While Proton Transfer Reaction - Mass Spectrometry has proven its capacity for flavor analysis in numerous publications [4-7], the behavior of lactones has not been studied yet. In the present study, δ/γ-octalactone and δ/γ-nonalactone were chosen as representatives for the group of lactones. Their fragmentation patterns, sensitivity and detection limits at varying drift voltages were determined and implications for analysis of lactones are discussed.

Experimental Methods

Lactones were commercially obtained at p.a. grade from Aldrich, Steinheim, Germany. Aqueous solutions of individual lactones were prepared at concentrations from 0.0002, 0.002, 0.02, 0.2 and 2 mg/ml. Lactone solutions (30ml) were placed into a 300 ml Erlenmeyer flask and closed with a septum. Prior to analysis, flasks were left for 60 min at ambient temperature for equilibration.

For headspace analysis by PTR-MS (Ionicon Analytik Ges.mbH, Innsbruck, Austria), the heated nose of the instrument was pierced through the septum into the headspace of the flask. Additionally, a disposable needle was pierced through the septum in order to allow for replacement of the air continuously sampled by the instrument at 185 ml/min.

Samples were scanned for m/z 20 to m/z 220 at a constant dwell time of 0.1s while employing drift voltages of 400, 500 and 600V. Working temperatures are 130°C for the inlet system and 110°C for the drift tube.

Transmission of the ions through the quadrupole MS was considered according to the specification of the instrument. Background and transmission corrected spectra were averaged

over five measurement cycles. Presented PTR-MS spectra were obtained by normalizing the most abundant mass fragment to an intensity of 100.

Results and Discussion

Major PTR-MS fragments for the four lactones are shown in table 1. All compounds show massive fragmentation. Major ions are found at m/z 39 ($C_3H_3^+$) and m/z 55 ($C_4H_7^+$), while the molecular ion MH^+ show relative abundances of 23% and less compared to the major ion. As H_3O^+ is used as ionising agent in PTR-MS, the identity of the most abundant ions at m/z 39 and m/z 55 can be complicated by the presence of water clusters at m/z 37 $(H_2O)_2 \cdot H^+$ and m/z 55 $(H_2O)_3 \cdot H^+$. In the present case, the identity of both mass fragments was confirmed by the presence of the isotopic ions resulting from the presence of 1.1% ^{13}C for each carbon atom (δ-octalactone m/z 56(4.8); γ-octalactone m/z 56 (4.6), δ-nonalactone m/z 40 (3.1); γ-nonalactone m/z 40 (3.6)).

Compound	MW	Relative abundance[a] of major[b] ions [m/z (relative abundance)]							
δ-octalactone	142	55 (100)	39 (67)	125 (26)	59 (26)	43 (24)	**143 (23)**	41 (20)	81 (13)
		67 (12)	79 (12)	97 (11)	107 (10)				
γ-octalactone	142	55 (100)	39 (77)	43 (39)	125 (23)	41 (21)	**143 (18)**	53 (15)	83 (13)
		67 (13)	79 (13)	81 (11)	97 (11)	107 (10)			
δ-nonalactone	156	39 (100)	43 (68)	105 (60)	41 (60)	139 (50)	81 (39)	59 (35)	55 (26)
		121 (24)	**157 (22)**	97 (20)	93 (19)	69 (17)	95 (16)	79 (14)	83 (12)
γ-nonalactone	156	39 (100)	43 (88)	139 (60)	41 (60)	81 (48)	121 (29)	55 (29)	93 (22)
		97 (21)	**157 (21)**	59 (20)	67 (20)	95 (17)	69 (16)	79 (14)	83 (14)

[a] data is presented by normalising the background and transmission corrected counts per second of the most abundant mass fragment to a value of 100. All other intensities are calculated relative to the most abundant mass fragment

[b] data on mass fragments with intensities below 10 not shown

Table 1: Lactones, their molecular weight (MW) and intensities of their major ions determined by Proton Transfer Reaction - Mass Spectrometry

The present settings allowed for analysing C_8 and C_9 lactones at aqueous concentrations of 0.02 to 2.0 mg/ml. Rather than instrumental parameters, upper detection limits for analysing headspace concentrations above aqueous solutions of lactones are given by their solubility in water, which is just above 2 mg/ml for the C_8 and C_9-lactones [8]. For all of the four lactones, an aqueous solution of 0.02 mg/ml produced a signal sufficiently different from the background noise as shown for γ-nonalactone in Figure 1. Furthermore, lower detection limits are also dependent on the analyte's volatility, which decreases with increasing molecular weight. Consequently lower vapour pressures and lower solubility of C_{10} - C_{12} lactones lead to narrower concentration ranges for analysis of these lactones (data not shown). However, sensitivity for lactones can be

substantially increased by implementing lower drift voltages. When decreasing the drift voltages from 600V to 400V, the abundance of the molecular ion was increased by a factor of eight in the case of δ-octalactone and up to a factor of 28 in the case of γ-octalactone (Figure 2). A formation of water clusters $MH^+ \cdot (H_2O)$ was not observed.

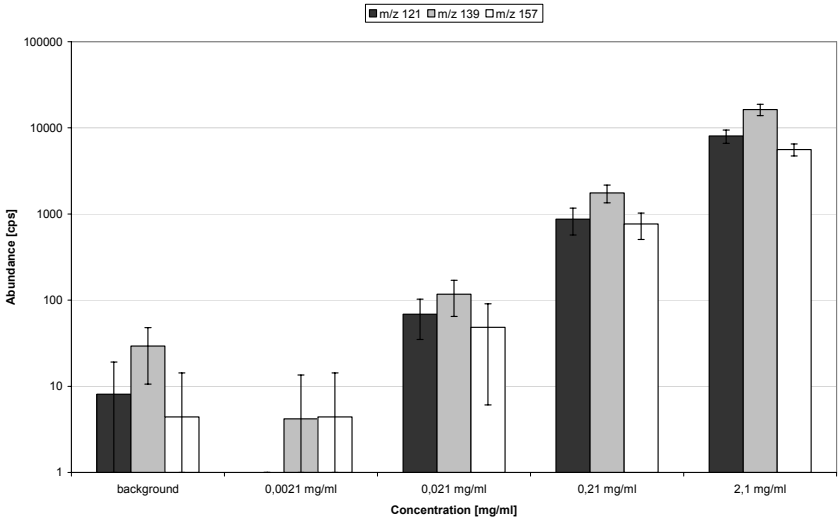

Figure 1: Sensitivity of PTR-MS for γ-Nonalactone. Abundance of molecular ion m/z 157 and fragments resulting from loss of water at m/z 139 and m/z 121 dependent on concentration of aqueous solution of γ-Nonalactone.

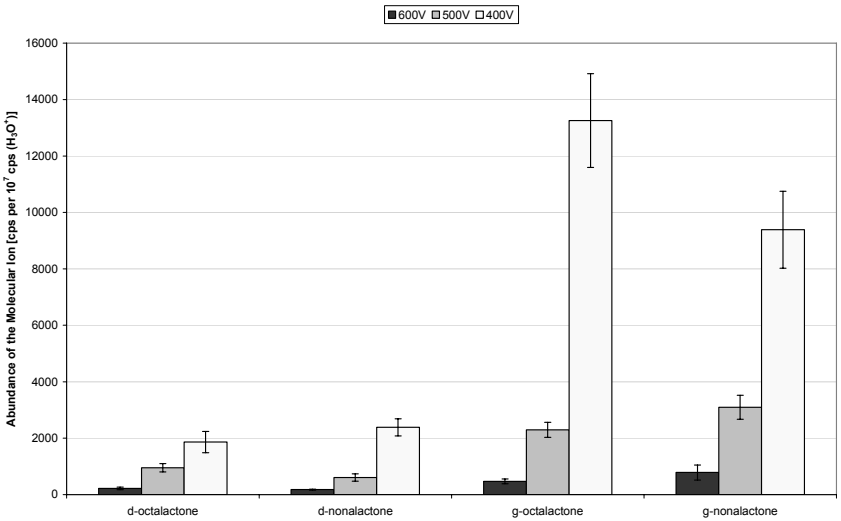

Figure 2: Analysis of Lactones by PTR-MS. Abundance of the Protonated Molecular Ion at Varying Drift Voltages. Concentration of Aqueous Lactone Solutions at 0.2 mg/ml.

The present results show first insights into behaviour of lactones in Proton Transfer Reaction - Mass Spectrometry and provide a basis for analysis of lactones in real food systems. Decrease of drift voltages present a promising approach to increase sensitivity by reducing fragmentation and thus leading to a higher abundance of the molecular ion.

References

[1] J. A. Maga, Lactones in foods, Crit Rev Food Sci 176 (8), 1-56 (1976)

[2] D. Lehmann, B. Maas, and A. Mosandl, Stereoisomeric flavour compounds LXIX: stereodifferentiation of δ(γ)-lactones C_8-C_{18} in dairy products, margarine and coconut, Z Lebensm Unters Forsch 201, 55-61 (1995)

[3] C. Derail, T. Hofmann and P. Schieberle, Differences in Key Odorants of Handmade Juice of Yellow-Flesh Peaches (Prunus persica L.) Induced by the Workup Procedure, J Agric Food Chem 47, 4742-4745 (1999)

[4] H. Guth, Identification of Character Impact Odorants of Different White Wine Varieties, J Agric Food Chem 45(8), 3022-3026 (1997)

[5] W. Lindinger, A. Hansel, A. Jordan, Online-mointoring of volatile organic compounds at pptv levels by means of Proton Transfer Reaction - Mass Spectrometry (PTR-MS). Medical applications, food control and environmental research, Int J Mass Spectrom 173, 191-241 (1998)

[6] C. Yeretzian, A. Jordan, W. Lindinger, Analysing the headspace of coffee by proton transfer reaction - mass spectrometry, Int J Mass Spectrom 223-224, 115-139 (2003)

[7] D. Mayr, T. Märk, W. Lindinger, H. Brevard, C. Yeretzian, Breath-by-breath analysis of banana aroma by proton transfer reaction - mass spectrometry, Int J Mass Spectrom 223-224, 743-756 (2003)

[8] H. Guth and R. Fritzler, Binding Studies and Computer-Aided Modelling of Macromolecule/Odorant Interactions, Chem Biodivers 1, 2001-2023 (2004)

Differentiation of monoterpenes by Collision Induced Dissociation with a Proton-transfer reaction Ion Trap Mass Spectrometer (PIT-MS)

Marco M.L. Steeghs[1], Elena Crespo[1], Cor Sikkens[1], Simona M. Cristescu[1], Frans J.M. Harren[1]

[1] *Life Science Trace Gas Facility, Molecular and Laser Physics, Institute for Molecules and Materials, Radboud University, Nijmegen, The Netherlands. e.crespo@science.ru.nl*

Abstract

The potential of Proton-Transfer Reaction Mass Spectrometry (PTR-MS) has been shown in many different fields, including atmospheric chemistry [1], medical science [2], and many biological and plant physiological fields [3]. Its high sensitivity, lack of sample preconcentration, its high time resolution, relatively low degree of fragmentation and the fact that it cannot measure the normal constituents of air, make it an excellent technique to monitor trace gas compounds in real-time. Those advantages, however, are accompanied by one disadvantage: compounds cannot be identified based on their mass only.

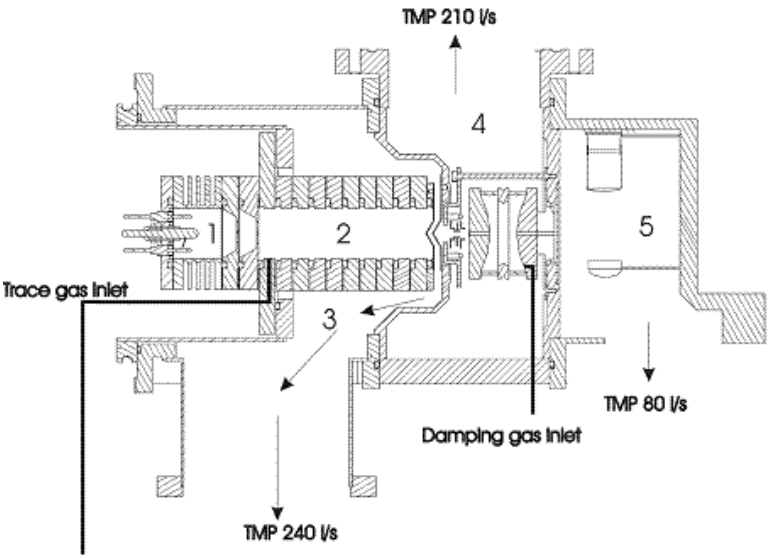

Figure 1: Nijmegen PIT-MS with 1) H3O+ ion source, 2) drift tube, 3) buffer chamber, 4) ion trap chamber and 5) detector chamber

A novel way of approaching this problem is the development of a PTR mass spectrometer based on an ion trap mass spectrometer (Figure 1; [4]). The use of an ion trap has several advantages, among which the possibility to perform collision induced dissociation (CID) is the most interesting one. CID patterns of isolated ions can be obtained that are compound-specific, which helps to identify the underlying compound. The viability of such a system and the usefulness of CID have been proven before [5]. However, the compounds for which this is shown have still fairly simple structure. Monoterpenes are very interesting biological compounds, which are similar in structure and of which many different isomers exist. Here we study the fragmentation patterns of different monoterpene species, after dissociative proton-transfer and after collision induced dissociation (CID) in our newly developed Proton-transfer reaction Ion Trap Mass Spectrometer (PIT-MS).The CID patterns of all the monoterpenes studied are found to be distinguishable, making it possible to positively identify a monoterpene solely on the basis of its CID pattern [6].

References

[1] de Gouw, J. Warneke, C. Karl, T. Eerdekens, G. Van der Veen and R. Fall, Sensitivity and specificity of atmospheric trace gas detection by proton-transfer-reaction mass spectrometry, International Journal of Mass Spectrometry, 223-224 365-382, (2003).

[2] M. Steeghs, B. Moeskops, K.van Swam, S.M. Cristescu., P.T.J. Scheepers, F.J.M. Harren, On-line monitoring of UV-induced lipid peroxidation products from human skin in vivo using proton-transfer reaction mass spectrometry, International Journal of Mass Spectrometry, *in press* , 2006.

[3] M. Steeghs, H.P. Basis, J. de Gouw, P. Goldan, W. Kuster, M. Northway, R. Fall, J.M. Vivanco, Proton-Transfer-Reaction Mass Spectrometry as a new tool for real time analysis of Root-Secreted volatile organic compounds in Arabidopsis, Plant Physiology 135, 47-58, (2004).

[4] M.M.L. Steeghs, C. Sikkens, E. Crespo, S.M. Cristescu and F.J.M. Harren, Development of a Proton-transfer reaction Ion Trap Mass Spectrometer Online detection and analysis of volatile organic compounds, International Journal of Mass Spectrometry *in press* , 2006.

[5] C. Warneke, J.A. de Gouw, E.R. Lovejoy, P.C. Murphy, W.C. Kuster and R. Fall, Development of Proton-Transfer Ion Trap-Mass Spectrometry: On-line detection and identification of volatile organic compounds in air, American Society for Mass Spectrometry 16, 1316-1324, (2004).

[6] M.M.L. Steeghs, E. Crespo and F.J.M. Harren, Collision Induced dissociation study of 10 monoterpenes for identification in trace gas measurements using the newly developed Proton-transfer reaction Ion Trap Mass Spectrometer, submitted to International Journal of Mass Spectrometry.

Real time analysis by Chemical Ionisation in a High Resolution Mass Spectrometer

Christophe Dehon[1], Michel Heninger[1], Pierre Boissel[1], Joel Lemaire[1], Stephane Pasquiers[2], Nicole Simiand[2], Pierre Tardiveau[2], Francois Jorand[2], Helene Mestdagh[1]

[1] LCP, bâtiment 350, Universite Paris-Sud 11, Orsay, France, helene.mestdagh@lcp.u-psud.fr

[2] LPGP, bâtment 210, Universite Paris-Sud 11, Orsay, France

3AlyXan, Centre Universitaire d'Orsay, Orsay, France

Abstract

A compact FTICR mass spectrometer is used for real time chemical ionization analysis of complex mixtures, as exemplified by PTRMS analysis of the output of a plasma discharge developed for depollution. To complement proton transfer ionization, chemical ionization reactions targeted towards the detection of organic sulphides are presented.

Introduction

Real-time monitoring of complex mixtures is a crucial need for environmental and industrial analysis. When associated with a smooth and selective ionization technique, the transportable FTICR mass spectrometers based on permanent magnet recently developed in the LCP group are a promising tool in this respect.

Use of FTICR brings specific advantages for mass detection: (i) mass resolution allowing isobaric separation, (ii) broad band detection: the whole mass range (10-400) can be monitored simultaneously. Since the ions are trapped in the ICR cell, this technique is very convenient for the use of chemical ionization: successive steps including mass selections, ion-molecule reactions can be performed inside the cell, allowing the use of a wide variety of reactant ions. Ion trapping also allows to perform kinetic studies so as to adjust the reaction time for chemical ionization.

Two applications are presented here: (i) real time analysis of volatile organic compounds in air at the output of a plasma discharge reactor, using proton transfer reaction from H_3O^+, (ii) selective detection of sulfur organic compounds using reactant ions prepared from dimethylether.

Real Time monitoring of a plasma reactor output

Our small FTICR apparatus has been applied to real time monitoring of pollutants present in air at trace levels and to follow their degradation after passing through a depollution system developed in the LPGP laboratory in Orsay, using a cold plasma discharge (Figure 1). This plasma reactor has been developed because of its potential as an air cleaner system, degrading toxic VOCs whenever present. The chemical reactions occurring in the plasma result in the oxidation of VOC pollutants. We are able to follow the products formed and the extent of reaction in real time.

The advantage of the plasma discharge method is its efficiency for treatment of dilute pollutants in air. To follow the degradation of a given organic molecule, this molecule is vaporised in air and carried to the discharge with controlled concentration and air flow.

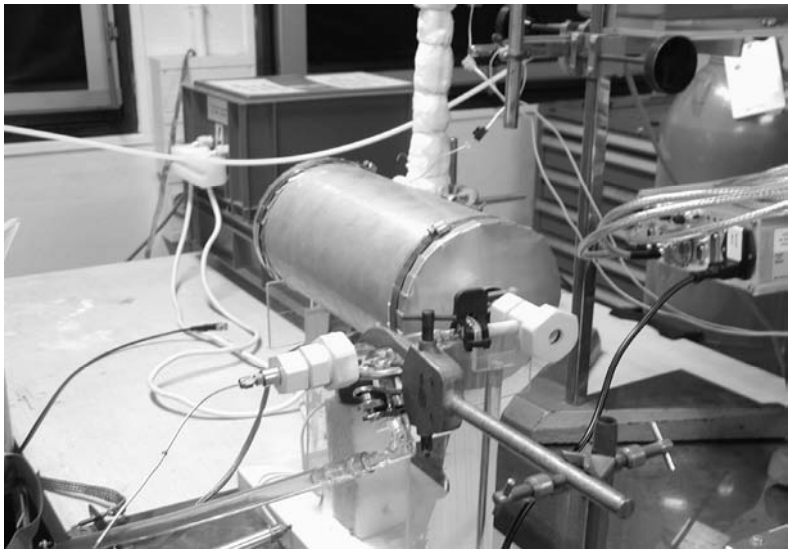

Figure 1: view of the plasma reactor.

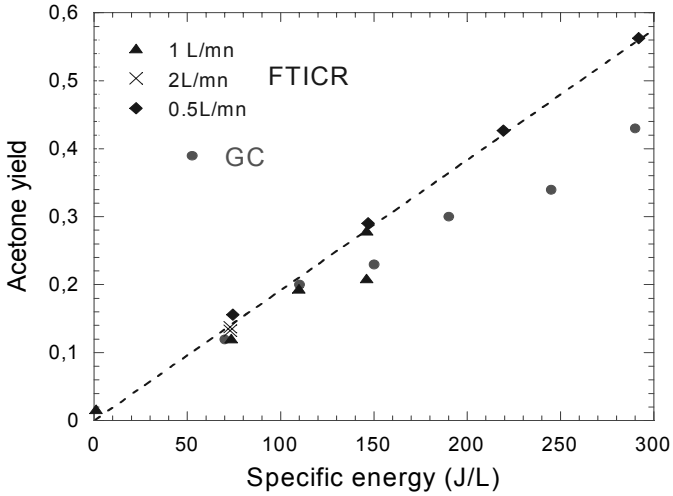

Figure 2: Acetone yield as a function of energy deposited in the discharge for different values of the gas flow. Comparison with GC measurements.

The effluent gases are transferred to the FTICR cell where they react with H_3O^+ ions. PTRMS analysis of the effluent gases allows to identify reaction products at concentrations of a few ppm and to follow the dependence of product amount and distribution with discharge power and gas flow. Owing to mass resolution, molecular formulae of the protonated species are determined without ambiguity. Results obtained with different organic compounds as a function of the plasma reactor parameters will be presented. Two representative molecules were chosen : 2-propanol and 2-heptanone.
The degradation scheme of 2-propanol is simple and leads to acetone as the main product. Mass spectrometric determination of the acetone yield shows a good agreement with GC measurements (Figure 2).
2-heptanone is representative of a class of odorous molecules contained in various foods. A more complex degradation scheme is observed, leading to carbonyl compounds with 1 to 4 carbon atoms. The vector gas composition has a determining influence on the nature of the products: in nitrogen, the detected ions are $C_3H_7O^+$, $C_4H_9^+$ and $C_2H_5O^+$. The reaction mechanisms in the discharge are under investigation.

Investigation of chemical ionization reactant ions for detection of sulfur compounds

A drawback of FTICR is its low dynamic range. Use of PTRMS in FTICR instruments is therefore difficult when the molecule of interest is present in very minor amount compared to other species undergoing proton transfer. For real-time monitoring of molecules in such cases, new specific chemical ionization reagents are being investigated.

Organic sulphides are present at trace levels in many mixtures of natural or industrial origin such as petroleum derivatives. Since they are toxic and poison catalysts, they are undesirable and their presence needs to be carefully monitored. Sulphides are basic and very nucleophilic compounds, these properties can be used for their selective detection by chemical ionization.

Electron ionization of dimethylether followed by ion-molecule reactions in the gas yields three major cations: methoxymethylene A, dimethyloxonium B and trimethyloxonium C.

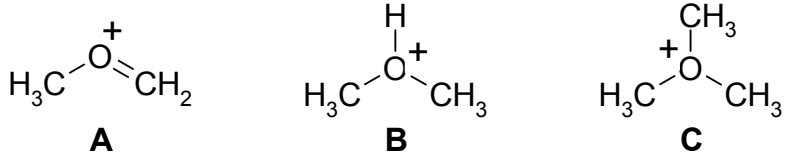

These cations are easily obtained and mass-selected in the FTICR cell. Each of them was tested for its ability to transfer a proton or a methyl group to representative organic sulphides such as dimethylsulphide, dimethyldisulphide, thiophene, and carbon disulphide.

Trimethyloxonium was unreactive towards sulphides, although it is an efficient methylating agent in solution. Dimethyloxonium effects fast proton transfer on all the sulphur derivatives tested, except carbon disulphide. As expected from its proton affinity it is more selective than H_3O^+. The reactivity of methoxymethylene consists mainly in methyl cation transfer. Although slightly slower than the preceding one, this reaction leading to (M+15) ion may be useful for sulphide

detection and identification. In the case of thiophene, methoxymethylene reacts through raw CH^+ transfer (Figure 3). This reaction likely involves electrophilic substitution followed by methanol elimination.

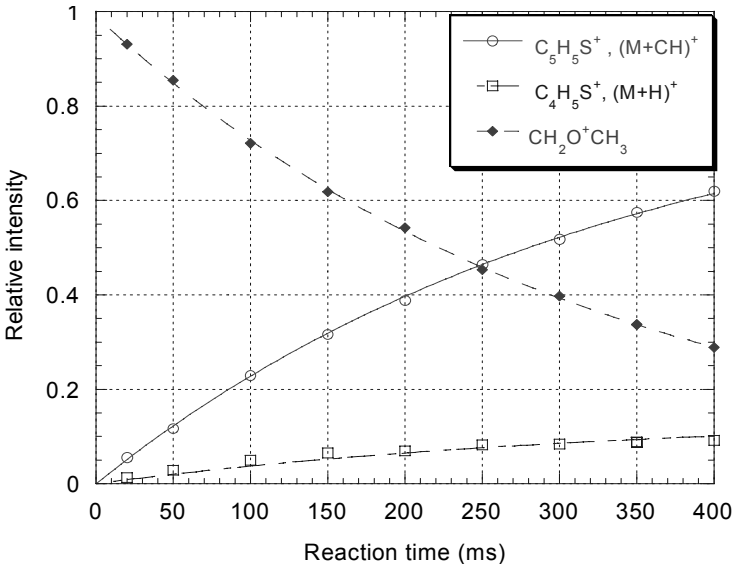

Figure 3: Kinetic study of the reaction of methoxymethylene cation with thiophene at a 9×10^{-7} torr pressure. The lines are fits according to pseudo-first order kinetics.

The different reactions follow a clean first-order kinetics, as seen on Figure 3. This is a necessary condition for using them as chemical ionization reactions for quantitative measurements. The analytical potentialities of mass-selected ions from dimethylether are further studied.

Conclusion

Compact FTICR instruments associated with proton transfer ionization are well suited for quantitative analysis of mixtures of differently volatile compounds, for instance plasma degradation products of 2-heptanone. As shown with 2-propanol, this method gives quantitative results consistent with GC analysis. In addition it allows continuous sampling.

Chemical ionization reactants complementing H_3O^+ are needed for detection of molecules which either are not protonated by H_3O^+ or are present in very minor amount against other protonable compounds. In this respect, mass-selected ions from dimethylether show interesting reactivity towards organic sulfides.

References

[1] G. Mauclaire, J. Lemaire, P. Boissel, G. Bellec, M. Heninger, MICRA: a compact permanent magnet Fourier transform ion cyclotron resonance mass spectrometer, European Journal of Mass Spectrometry, 10, 155-162, (2004).

[2] N. Blin-Simiand, P. Tardiveau, A. Risacher, F. Jorand, S. Pasquiers, Removal of 2-heptanone by dielectric barrier discharges - The effect of a catalyst support, Plasma Processes and Polymers, 2, 256-262 (2005).

[3] C. P. Burrows, Dimethyl ether chemical ionization, Mass Spectrometry Reviews, 14, 107-115 (1995)

Predicting Consumer Freshness Perceptions of Cakes by Using Descriptive Sensory Analysis and Headspace Volatile Composition

Samuel Heenan[1], Jean-Pierre Dufour[1], Conor Delahunty[1], Winna Harvey[2]

[1] *Sensory Science Research Centre, Department of Food Science, University of Otago, Dunedin, New Zealand, jean-pierre.dufour@stonebow.otago.ac.nz*

[2] *New Zealand Institute for Crop and Food Research Limited, Christchurch, New Zealand*

Abstract

Different cake (n=13) types were assessed by descriptive sensory analysis and analysed for headspace composition by Proton Transfer Reaction Mass Spectroscopy (PTR-MS). Regular consumers (n=102) of baked products rated perceived freshness of six of the 13 cake products by evaluating sample odour. Freshness ratings were quantified using a Labeled Magnitude Scale (LMS), labeled with "not at all fresh" and "greatest freshness imaginable". Partial Least Squares Regression (PLSR) was used to determine relationships between sensory attributes, volatile composition and consumer freshness perceptions. Five descriptive sensory attributes and six volatile compounds were positively correlated with the consumer freshness perceptions of cake odour. Using these PLSR models, consumer freshness judgments for the remaining seven cake samples assessed by descriptive sensory analysis and PTR-MS but not evaluated by the consumers, were predicted.

Introduction

The perceived freshness of baked products is one of the key determinants of acceptance. Consumers have a definite appreciation of what constitutes this freshness, based upon their individual experiences involving complex physiological and psychological processes. This perception is not easily described, particularly as it is likely to vary between different product types. Multivariate calibration can be applied to determine relationships between sensory characteristics defined and measured by a trained sensory panel and consumer perceptions, allowing the sensory characteristics associated with consumers' perceptions of products to be identified [1, 2]. Moreover, linking trained sensory panel data and data from a rapid sensitive instrumental technique such as PTR-MS by PLSR has enabled relationships between sensory attributes and volatile composition to be determined [3-5]. By correlating sensory attributes and volatile composition with consumer freshness assessments, an objective understanding could be used to explain the freshness as perceived by consumers. PLSR models that relate sensory character and volatile composition to consumer freshness assessments may be used to determine consumer freshness measurements of products not assessed by consumers but analysed by descriptive sensory and headspace PTR-MS analysis.

Experimental Methods

Cake products were selected from local bakeries (n=13). Six of the 13 cake products were presented in sealed brown glass bottles to regular cake consumers (n=102) balanced by age and

gender. Consumers removed the lid of these bottles, smelled the odour and rated freshness on a 150 mm labeled magnitude scale (LMS) labeled from “not at all fresh” to “greatest freshness imaginable”. This scale was used to maintain the uniformity of the freshness measurement [6]. Prior to rating freshness a text was read aloud to create a context for assessment, which intended to evoke a more affective response. A trained sensory panel carried out descriptive sensory analysis of all products (n=13) in duplicate using a defined vocabulary of 22 attributes. The headspace volatile composition of each product (n=13) was measured using PTR-MS. Cake products in triplicate were weighed (100 g) into 1 L Schott Duran bottles and allowed to equilibrate at room temperature for 1 h. Bottles were connected to the PTR-MS inlet flow via Teflon 1/16 ” tubing. The headspace was sampled at a flow rate of 50 ml/min. Data was collected over a mass range of m/z 20 to 180 using a dwell time of 0.2 s per mass. This cycle was repeated 5 times per sample. Mass ion intensities were recorded in concentration (ppb). Analysis of variance (ANOVA) was carried out on cake products’ (n=6) mean freshness ratings from consumer testing. With data from the six cakes evaluated by consumers, PLSR1 was applied to create three different models relating sensory attributes from descriptive analysis to consumer ratings of freshness [Model 1], volatile composition to consumer rating of freshness [Model 2] and simultaneously sensory attributes and volatile composition to consumer rating of freshness [Model 3]. Attributes and mass ions that contribute little information were removed from the models. Optimum models were selected based on root mean square error of prediction (RMSEP), which showed average uncertainty expected when predicting consumer freshness. These models were used to predict freshness of seven additional products.

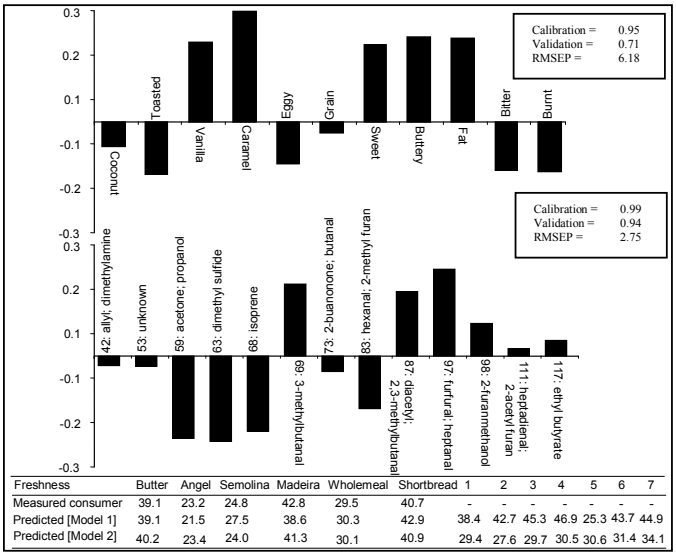

Freshness	Butter	Angel	Semolina	Madeira	Wholemeal	Shortbread	1	2	3	4	5	6	7
Measured consumer	39.1	23.2	24.8	42.8	29.5	40.7	-	-	-	-	-	-	-
Predicted [Model 1]	39.1	21.5	27.5	38.6	30.3	42.9	38.4	42.7	45.3	46.9	25.3	43.7	44.9
Predicted [Model 2]	40.2	23.4	24.0	41.3	30.1	40.9	29.4	27.6	29.7	30.5	30.6	31.4	34.1

Figure 1:PLS1 positive and negative loadings between sensory attributes (a) and volatile compounds (b) associated with consumer freshness ratings and PLS1 models (c) indicating measured consumer freshness ratings and predicted consumer freshness ratings

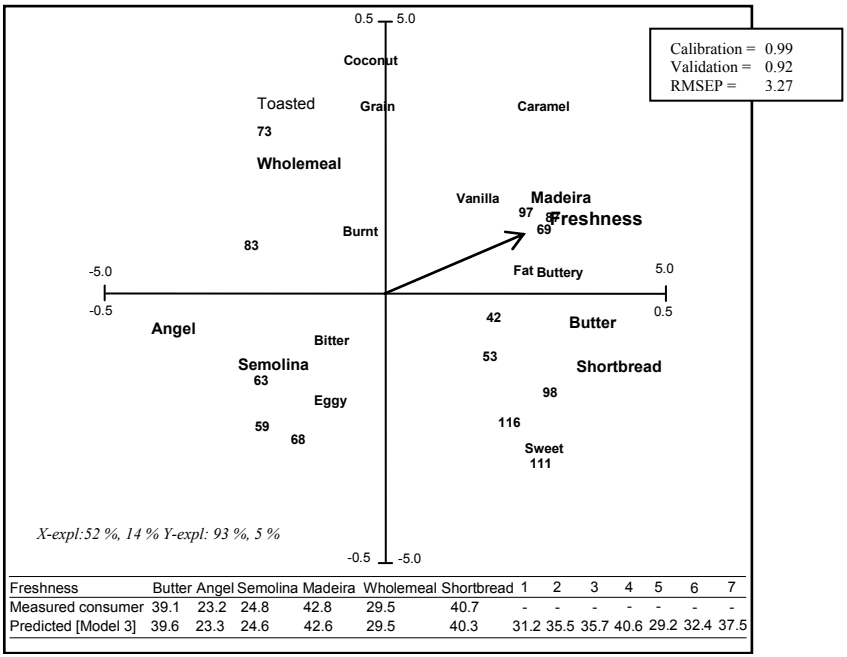

Freshness	Butter	Angel	Semolina	Madeira	Wholemeal	Shortbread	1	2	3	4	5	6	7
Measured consumer	39.1	23.2	24.8	42.8	29.5	40.7	-	-	-	-	-	-	-
Predicted [Model 3]	39.6	23.3	24.6	42.6	29.5	40.3	31.2	35.5	35.7	40.6	29.2	32.4	37.5

Figure 2: PLS1 analysis showing a biplot of the correlation between sensory data, compound mass concentration and consumer freshness ratings for 6 cakes. Shown are predicted versus measured freshness using PLS models with calibration, validation coefficients and RMSEP

Results & Discussion

Consumers significantly ($F_{(5,464)}$ = 16.661; $p<0.05$) discriminated freshness differences between cake (n=6) types by odour evaluation.

Eleven sensory attributes [Model 1] and thirteen mass compounds [Model 2] were correlated with consumer freshness ratings. Calibration coefficients (strength of the current models) were ≥ 0.95, while the validation coefficients (ability to predict new products) were ≥ 0.71 and RMSEP values range from 2.75 - 6.18 for both sensory and volatile composition data indicating models all had good predictive power (Figure 1). Fresh cake could be described as having a vanilla, caramel, sweet, buttery, fat odour, whilst least fresh cake was depicted as having coconut, toasted, grain, bitter, burnt odour (Figure 1a). PTR-MS analysis distinguished cake differences by their volatile composition and enabled correlations of specific mass ions associated with cake freshness. Fresh cake odour was associated with mass ions tentatively attributed to 3-methylbutanal, diacetyl, 2,3-methylbutanal, furfural, 2-furanmethanol, heptadienal, 2-acetylfuran, ethylbutyrate [7-9]. By simultaneously relating sample volatile composition and sensory character (X variables) to consumer freshness (Y variables) [Model 3] a biplot could be created to visually represent relative

differences between cake freshness. Freshest cakes were Madeira, butter and shortbread. Sensory attributes and volatile compounds associated with freshness is shown in Figure 2.

Predicted freshness appeared valid for 3 of the 7 additional baked cakes when comparing sensory [Model 1] and volatile composition [Model 2]. Additional cakes 2, 3, 4 and 6 displayed a high level of variation in predicted freshness when comparing [Model 1] and [Model 2], which may be the result of different sensory character or volatile composition unaccounted for in the original 6 cakes evaluated by the consumer. Less variation in predicted freshness was observed between [Model 2] and [Model 3].

Conclusion

Relating consumer freshness judgments to sensory descriptive analysis and volatile composition enabled an objective understanding of cake freshness. This approach clearly showed specific sensory characteristics and volatile compounds that were associated with the freshest cake's odour. PTR-MS headspace analysis displayed less variation in the predicted freshness when comparing with predictions made simultaneously with sensory attributes and volatile composition.

References

[1] J.M. Murray, C.M. Delahunty, and I.A. Baxter, Descriptive sensory analysis: Past present and future, Food Research International, 34(6), 461-471, (2001).

[2] F. Westad, M. Hersleth, P. Lea, and H. Martens, Variable selection in PCA in sensory descriptive and consumer data, Food Quality and Preference, 14(4-5), 463-472, (2003).

[3] F. Biasioli, F. Gasperi, E. Aprea, D. Mott, E. Boscaini, D. Mayr, and T.D. Mark, Coupling proton transfer reaction-mass spectrometry with linear discriminant analysis: a case study, Journal of Agricultural and Food Chemistry, 51(25), 7227-7233, (2003).

[4] F.J. Gallardo-Escamilla, A.L. Kelly, and C.M. Delahunty, Sensory characteristics and related volatile flavor compound profiles of different types of whey, Journal of Dairy Science, 88(8), 2689-2699, (2005).

[5] F. Biasioli, F. Gasperi, E. Aprea, I. Endrizzi, V. Framondino, F. Marini, D. Mott, and T.D. Mark, Correlation of PTR-MS spectral fingerprint with sensory characterisation of flavour and odour profile of Trentingrana cheese, Food Quality and Preference, 17(1-2), 63-75, (2006).

[6] L.M. Bartoshuk, V.B. Duffy, K. Fast, B.G. Green, J. Prutkin, and D.J. Snyder, Labeled scales (eg, category, Likert, VAS) and invalid across-group comparisons: what we have learned from genetic variation in taste, Food Quality and Preference, 14(2), 125-138, (2003).

[7] M.A. Pozo-Bayon, E. Guichard, and N. Cayot, Flavor control in baked cereal products, Food Reviews International, 22(4), 335-379, (2006).

[8] M.A. Pozo-Bayon, E. Guichard, and N. Cayot, Feasibility and application of solvent assisted flavour evaporation and standard addition method to quantify the aroma compounds in flavoured baked matrices, Food Chemistry, 99(2), 416-423, (2006).

[9] K. Buhr, S. van Ruth, and C.M. Delahunty, Analysis of volatile flavour compounds by Proton Transfer Reaction-Mass Spectrometry: fragmentation patterns and discrimination between isobaric and isomeric compounds, International Journal of Mass Spectrometry, 221(1), 1-7, (2002).

PTR-MS measurements of traffic-related emissions: Annual variations of the toluene/benzene ratio

Jürgen Dunkl, Ralf Schnitzhofer, Jonathan Beauchamp, Armin Wisthaler, and Armin Hansel

Institute of Ion Physics and Applied Physics / University of Innsbruck, Austria
juergen.dunkl@uibk.ac.at

Abstract

Continuous one-year-long PTR-MS measurements of benzene and toluene (and other volatile organic compounds; VOCs) were carried out alongside the alpine Inn valley A12 motorway in Tirol, Austria. Due to the measurement site's close proximity to the motorway, VOCs in the surrounding air are predominantly of anthropogenic origin, i.e from traffic-related emissions.

Data collected provided varied information about the VOC content of the local air at different times of the year, including details of annual variations in the toluene/benzene ratio. The toluene/benzene ratio here was observed to sink from 2:1 in the summer to 1:1 during wintertime. This changing ratio correlates well with the local ambient temperature and suggests that the summertime toluene source is stronger than that of benzene, which may be explained by temperature-dependent differences in evaporative losses of these two compounds. Such a result could have strong implications for atmospheric chemistry where the age of an air mass could be falsely determined if only a fixed fresh-emission toluene/benzene ratio of 2:1 is assumed.

Introduction

The ongoing discussions in Tirol about local air quality are especially fuelled by the abundant and ever increasing number of vehicles using the main motorway (the A12) through this region. Due to the mountainous landscape dilution of polluted air is restricted, resulting in especially high concentrations from traffic-related emissions on days with stable weather conditions (i.e. when there is restricted vertical dilution). In order to monitor and assess the air quality in Tirol a number of measurement sites have been established by the Tirolean government to routinely monitor certain compounds, including CO and NO_x ($NO+NO_2$), and meteorological parameters, e.g. ambient temperature. One of these sites is located directly alongside the A12 motorway in Vomp, where this study took place between February 2004 and May 2005.

The aim of this investigation was to study the annual variations of several VOCs and to determine the relationships between their source strengths (e.g. traffic numbers) and sinks (e.g. OH radicals, driven by meteorology). The results presented herein build on previous interpretations and discussions of seasonal VOC fluctuations studied at this location [1, 3, 10, 11].

Experimental Methods

This investigation took place within the Inn valley near the small town of Vomp (Tirol, Austria). The monitoring site is situated only a few metres from the A12 carriageway, making it ideal for immediate vehicle emission detection.

A PTR-MS instrument [5] was set up at this location for continuous detection of key organic compounds (including benzene and toluene) in the air near the motorway. The heated inlet, which was elevated approximately 4 m above ground level, was capped by a particulate filter and set up with a constant ambient air flow of 2 l min^{-1} to the PTR-MS. Measurements were carried out with continuous mass scans from m/z 20^+ to 200^+ amu, with each cycle lasting ca. 6 min. Routine measurements of CO were made using a Horiba APMA 360 Ambient CO Monitor (these measurements were discontinued at the end of 2004). NO_x was measured with a Horiba APNA 360 Ambient NO_x Monitor (using cross flow modulation type, reduced pressure chemiluminescence [CLD]).

Results & Discussion

A comparison between VOC levels on working days and on Sundays and public holidays showed that NO_x levels are lower on days when heavy duty vehicles (HDVs) are banned from the motorway. In contrast, concentrations of CO and aromatic compounds (e.g. benzene and toluene) remain constant throughout the week. Since most HDVs run on diesel fuel this suggests that NO_x is primarily emitted by diesel engines whereas the aromatics and CO come mainly from petrol engines associated with light duty vehicles (LDVs), which is in agreement with the results of an earlier study at this location [1]. Furthermore, comparison of benzene volume mixing ratios (VMRs) with those of CO reveal a linear relationship (see figure 1a), indicating that both compounds at this location must arise from the same source, again principally from LDV traffic.

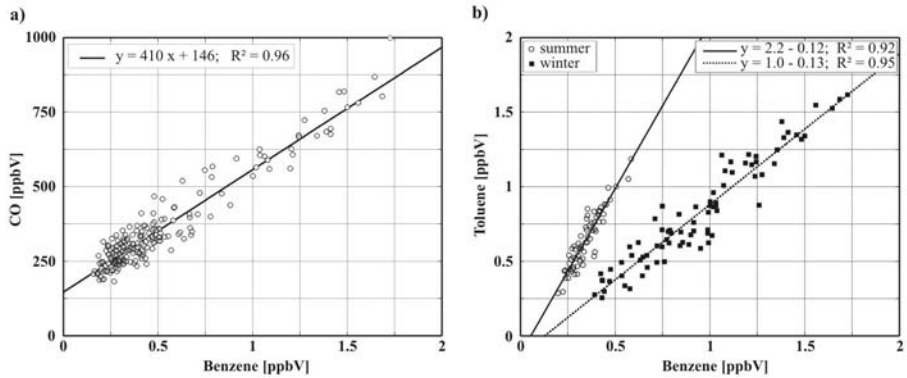

Figure 1: Correlation of a) CO vs. benzene and b) toluene vs. benzene (daily mean values, with linear data fits).

The aromatic compounds toluene and benzene are often observed to have a ratio of 2:1 (toluene/benzene) for fresh emissions [e.g. 6, 7]. This is clearly seen in these data (see figure 1b) but is only true during summertime, when the ratio is twice as high as that in winter (1:1) (as has also seen in other studies [7]). This varying ratio may arise for several reasons. Firstly, it is very *unlikely* to result from a change in petrol composition from summer to winter fuel, since the maximum amount of benzene and other aromatics in the fuel are both regulated and restricted [4] and generally have a liquid fuel toluene/benzene ratio of 5:1 [e.g. 6]. Increased benzene levels

arising from catalytic processes in the vehicle exhaust system are likely to be partly responsible for the ratio discrepancy between liquid fuel and gas-phase emissions of toluene and benzene: A new study on 3-way automobile catalysts [2] has shown that these devices induce benzene formation, i.e. by cracking higher aromatics, meaning that benzene is the predominant aromatic compound emitted from modern exhaust pipes. However, this fails to explain the summer-winter shift in the gas-phase toluene/benzene ratio and suggests that toluene must have another strong, temperature-dependent source in the summer. A previous study has shown that several components of fuel permeate through and evaporate out of the fuel-tank-to-engine lines differently with varying temperature [9]. Indeed, even though benzene is more volatile than toluene, the proportion of benzene coming from evaporative losses should remain fixed because the toluene/benzene ratio in the fuel itself remains approximately constant at 5:1 [6, 7].

A comparison of the toluene/benzene ratio with ambient temperature during nighttime (when the lifetime for toluene is increased due to reduced OH radical concentrations) (see figure 2a) reveals a relationship that is very similar to the vapour pessure curve of toluene (see figure 2b). This leads to the conclusion that toluene is most likely strongly emitted as temperature-dependent evaporative losses, resulting in higher levels with respect to benzene during summertime compared to winter.

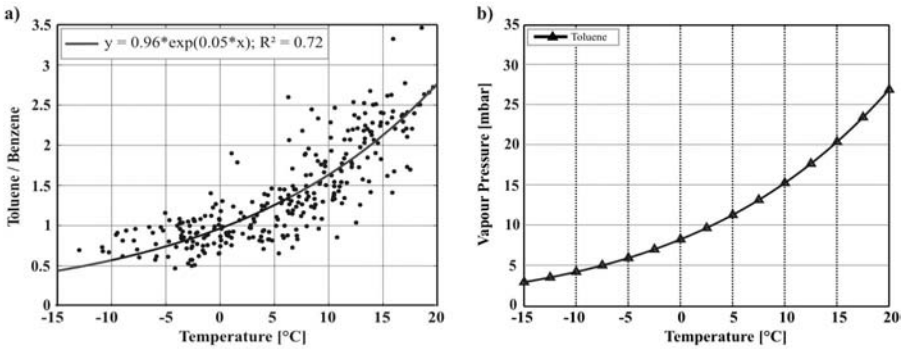

Figure 2: The toluene/benzene ratio (daily mean values from 23:00 to 05:00 CET for the whole year) vs. ambient temperature (2a) bears a strong resemblance to the calculated vapour pressure curve of toluene (2b).

Acknowledgements

The authors would like to thank the Amt der Tiroler Landesregierung, Landesforstdirektion Waldschutz/Luftgüte, in particular A. Weber, for the routinely measured NO, NO_2, CO, PM_{10}, and meteorological data.

References

[1] Beauchamp, J., A. Wisthaler, W. Grabmer, C. Neuner, A. Weber, and A. Hansel, 2004: Short-term measurements of CO, NO, NO_2, organic compounds and PM_{10} at a motorway location in an austrian valley. Atmospheric Environment, 38, 2511-2522.

[2] Bruehlmann, S., Novak, P., Lienemann, P., Trottmann, M., Gfeller, U., Zwicky, C. N., Bommer, B., Huber, H., Wolfensberger, M., and Heeb, N. V., 2006, Three-way-catalyst induces benzene formation: A precursor study. Applied Catalysis, in press.

[3] Dunkl, J., Schnitzhofer, R., Beauchamp, J., Wisthaler, A., and Hansel, A., Long-term Measurements of biogenic VOCs in an Austrian Valley – Discussion of seasonal Fluctuations of Isoprene and Monoterpene Concentrations, EGU06-A-06580; p. 489

[4] European Parliament and Council of the European Union, 1998. Directive 98/70/EC of the European Parliament and of the Council of 13 October 1998 relating to the quality of petrol and diesel fuels and amending Council Directive 93/12/EEC. Oficial Journal of the European Communities 350, 58-68.

[5] Hansel, A., Jordan, A., Holzinger, R., Prazeller, P., Vogel, W., Lindinger, W., 1995. Proton transfer reaction mass spectrometry: on-line trace gas analysis at the ppb level. International Journal of Mass Spectrometry and Ion Processes 149, 609-619.

[6] Harley, R. A., McKeen, S. A., Rodgers, M. O., Lonneman, W. A., 2001. Analysis of motor vehicle-related emissions during the Nashville/Middle Tennessee Ozone Study. Journal of Geophysical Research 106, 3359-3567.

[7] Heeb, N. V., Forss, A.-M., Bach, C., Reimann, S., Herzog, A., Jäckle, H. W., 1999. A comparison of benzene, toluene and C_2-benzenes mixing ratios in automotive exhausts and in the suburban atmosphere during the introduction of catalytic converter technology in the Swiss Car Fleet. Atmospheric Environment 34, 3103-3116.

[8] Prévôt, A.S.H., Dommen, J., Bäumle, M., Furger, M., 2000. Diurnal variations of volatile organic compounds and local circulation systems in an Alpine valley. Atmospheric Environment 34, 1413–1423.

[9] Rubin, J. I., Kean, A. J., Harley, R. A., Millet, D. B., Goldstein, A. H., 2006. Temperature dependence of volatile organic compound evaporative emissions from motor vehicles. Journal of Geophysical Research 111.

[10] Schnitzhofer, R., Dunkl, J., Beauchamp, J., Wisthaler, A., and Hansel, Influence of meteorological Variability on the Concentration of Traffic Air Pollutants in the River Inn Valley over the course of one year, EGU06-A-06568; p. 489

[11] Schnitzhofer, R., Beauchamp, J., Dunkl, J., Wisthaler, A., Weber, A., and Hansel, A., 2007. Long-Term Measurements of CO, NO, NO_2, Benzene, Toluene and PM10 at a Motorway Location in an Austrian Valley, Atmospheric Environment, submitted.

Interactions between BVOC emission and ozone uptake in forest species*

Silvano Fares[1], Francesco Loreto[1] and Jürgen Wildt[2]

[1]*CNR (National Research Council) – Istituto di Biologia Agroambientale e Forestale, Monterotondo Scalo, Rome*

[2]*Institute Phytosphere (ICG-III), Research Centre Jülich, 52425, Jülich, Germany*

Abstract

Plants are exposed to increasing levels of atmospheric ozone [1]. Trees, in particular in urban areas, are able to capture ozone from the air [2], and BVOC (Isoprene and monoterpenes) produced by plants should have a protecting role against oxidative stress [3]. We have investigated weather ozone uptake by plants emitting monoterpenes or isoprene enclosed in a tank reactor, and exposed to 45-210 ppb ozone, is associated to stomatal opening, and to ozone detoxification mechanisms, namely to the scavenging activity of BVOC. Isoprene-ozone reaction products (methacrolein and methyl-vinyl-ketone) were also measured. Light, temperature and CO_2 were controlled to modulate stomatal opening, ozone uptake, and emission of BVOC. In all plant species the stomatal flux of ozone was directly proportional to the stomatal conductance. However, ozone uptake was higher than expected on the basis of stomatal uptake in the monoterpene-emitting species (e.g. *Quercus ilex*), indicating that monoterpenes may effectively remove ozone in gas phase reactions in the leaf mesophyll.

References

[1] Altimir, N., Tuovinen, J-P., Vesala, T., Kulmala M., Hari, P. 2004. Measurements of ozone removal by Scots pine shoots: calibration of a stomatal uptake model including the non-stomatal component. *Atmospheric Envir.,* 38: 2387-2398.

[2] Fowler, D., Cape J.N., Coyle, M., Flechard, C., Kuylenstierna, J., Hicks, K., Johnson, C., Stevenson, D. 1999. The global exposure of forests to air pollutants. *Water, Air and Soil Pollution*, 116: 5-32.

[3] Velikova V., Tsonev T., Pinelli P., Alessio G.A., and Loreto F. 2005. Localized O3-fumigation for field studies of the impact of different ozone doses on photosynthesis, respiration, electron transport rate and isoprene emission in Mediterranean species. *Tree Physiology* 25:1523–1532.

Characterisation of organosulfates from the photooxidation of isoprene in ambient $PM_{2.5}$ aerosol by LC/ESI-linear ion trap MS

Yadian Gómez[1], Reinhilde Vermeylen[1], Willy Maenhaut[2], and Magda Claeys[2]

[1] *University of Antwerp (Campus Drie Eiken), Department of Pharmaceutical Sciences, Universiteitsplein 1, BE-2610 Antwerp, Belgium yadian.gomez@ua.ac.be*

[2] *Department of Analytical Chemistry, Institute for Nuclear Sciences, Ghent University, Proeftuinstraat 86, BE-9000 Gent, Belgium*

Abstract

Field observations of certain aerosol compounds, i.e., diastereoisomeric 2-methyltetrols and 2-methylglyceric acid, attributable to isoprene oxidation, and the experimental observation that isoprene under highly acidic conditions can lead to the formation of oligomeric, humic-like substances through heterogeneous reactions, re-opened the issue of secondary organic aerosol (SOA) formation from isoprene. In this context, a recent laboratory chamber study demonstrated that oligomeric, humic-like substances, i.e., organosulfates, are formed from the photooxidation of isoprene in the presence of sulfate seed aerosol [1]. In the present study, liquid chromatography/electrospray ionization-mass spectrometry (LC/ESI-MS) was used to examine the presence of organosulfates from the photooxidation of isoprene in $PM_{2.5}$ aerosol samples collected at K-puszta, Hungary, a mixed deciduous/coniferous forest site, during a 2003 summer field campaign. A motivation for examining these samples was that relatively high atmospheric concentrations of isoprene SOA compounds, i.e., 2-methyltetrols and 2-methylglyceric acid, were measured in a previous study [2].

For LC/ESI-MS analysis, an LXQ linear ion trap instrument (ThermoElectron) was used in the negative ion mode. Aerosol samples collected on quartz fiber filters were extracted with methanol. The extract residues were analysed without prior sample purification. LC separation was achieved with a Waters dC18 Atlantis column.

Organosulfates were identified on the basis of a *m/z* 97 ion [HSO_4^-] in their [M – H]$^-$ product ion spectra. Organosulfates from the following isoprene SOA products could be characterized: 2-methyltetrols, 2-methylglyceric acid, and 2-methyltetrol mono-nitrates. The 2-methyltetrols and 2-methyglyceric acid show one early eluting, tailing peak, while the 2-methyltetrol mono-nitrates, which are more hydrophobic, reveal five later-eluting resolved peaks. Experiments are in progress to improve the LC separation of the very hydrophilic organosulfate isoprene SOA compounds.

In addition to organosulfates from the photooxidation of isoprene, organosulfates of hydroxycarboxylic acids could also be identified, i.e., malic and tartaric acid sulfates, which have similar hydrophilic properties as the organosulfates of 2-methyltetrols and 2-methylglyceric acid. The atmospheric volatile organic compound precursor of malic and tartaric acid organosulfates in ambient $PM_{2.5}$ aerosol is at present unclear.

References

[1] J.D. Surratt, J.H. Kroll, T.E. Kleindienst, E.O. Edney, M. Claeys, A. Sorooshian, N.L. Ng, J.H. Offenberg, M. Lewandowski, M. Jaoui, R.C. Flagan, and J.H. Seinfeld, Evidence for organosulfates in secondary organic aerosol, Environmental Science and Technology, in press.

[2] A.C. Ion, R. Vermeylen, I. Kourtchev, J. Cafmeyer, X. Chi, A. Gelencser, W. Maenhaut, and M. Claeys, Polar organic compounds in rural $PM_{2.5}$ aerosols from K-puszta, Hungary, during a 2003 summer field campaign: Sources and diel variations, Atmospheric Chemistry and Physics 5, 1805-1814 (2005).

Customized solution for chemical plant monitoring

G. Hanel, A. Jordan, E. Hartungen, S. Haidacher, R. Schottkowsky, L. Märk, T. D. Märk

Ionicon Analytik Ges.m.b.H. Technikerstrasse 21a, 6020 Innsbruck, Austria

Abstract

The goal of this project was the development of a monitoring solution for dimethylsulfate in a chemical plant. This is the first approach to a new market for PTR-MS applications as a real-time continuous monitoring instrument. To achieve the customer's needs it was necessary to develop a customized solution that included hardware and software modifications.

The three key features of this solution were as follows:

1. Automatic set-up and optimization of the compact PTR-MS instrument

2. Calibration of the instrument for the VOC of interest (in this case dimethylsulfate)

3. Real-time sampling at twelve different points in the chemical plant

To meet these needs an extra rack was added to the compact PTR-MS instrument to house the additional valves and the calibration gas bottle. The long distance between the twelve sampling points (five to 50 meters) required the use of an additional membrane pump to keep the response time of the PTR-MS fast enough to meet the customer's requirements. To sample the different positions twelve 3-way valves are controlled by separate digital outputs that have been added to the RS232 server built-in to the PTR-MS. Additional three valves are used to allow for an automatic set-up and calibration procedure, which are also controlled by the extra digital outputs.

At the current development stage the system is only being used to monitor the dimethylsulfate level within certain ranges. A lower alarm level for the dimethylsulfate concentration is set to 5 ppbv, and an upper level is at 50 ppbv. Although the actual solution is tailored for this compound it would be easily possible to extend the solution to monitor up to 60 compounds continuously.

Currently the following procedures are foreseen:

Start-up of the instrument followed by an optimization and calibration check using the built-in calibration gas bottle. Previous calibrations are compared to the current for any significant changes in the performance that could lead to inaccurate monitoring results. After a successful performance check the instrument switches to sampling mode. In this mode all twelve different points are sampled for a preset sampling time, which is currently set to five seconds. The main monitoring screen shows a separate graph for each of the twelve sampling lines. The two alarm levels are also shown in the graph. A dimethylsulfate level higher than 5 ppbv gives a yellow colored alarm on the control screen. The 50 ppbv level displays a red colored alarm on the screen, which is coupled to an acoustic alarm via a digital output on the instrument.

The software package to monitor this system is specifically tailored to make the operation as simple as possible. Instrument-specific adjustments can only be done via a password protected service mode in the software. For experienced users and for error checking all other PTR-MS control and the Quadstar software features are still available.

Measurements of biogenic volatile organic compounds above a sub-arctic wetland in northern Sweden

Thomas Holst[1], Sean Hayward[1], Anna Ekberg[1], and Almut Arneth[1]

[1] *Department of Physical Geography and Ecosystems Analysis, Lund University, Lund, Sweden, thomas.holst@nateko.lu.se*

Abstract

We present first results of fluxes of biogenic VOC emitted from the vegetation at a sub-arctic wetland in northern Sweden, measured using the disjunct eddy covariance (DEC) technique with a Proton Transfer Reaction-Mass Spectrometer (PTR-MS) as scalar sensor.

Introduction

The quantity and environmental regulation of biosphere-atmosphere exchange of biogenic volatile organic compounds (BVOC) is still virtually unknown on ecosystem level, particularly in the high northern latitudes – systems that are likely to experience warming, permafrost melting and changes in vegetation distribution in the coming decades. We analyse the seasonal variation of BVOC (e.g., isoprene, acetone) fluxes from a sub-arctic wetland in northern Sweden (68°21' N, 18°49' E), using the disjunct eddy-covariance technique (DEC). DEC combines fast measurements of a range of BVOC by proton transfer reaction mass spectrometry and high-frequency data from a sonic anemometer. The flux derived from this method represents net emission of BVOC for a homogeneous footprint area of usually about 200 m². The initial analysis concentrates on the short but intense growing season; the ecosystem data can be compared with chamber measurements and modelling approaches for VOC emissions to investigate the processes underlying the observed emission flux.

Experimental Methods

Field site

The Stordalen field site is a typical sub-arctic mire located in northern Sweden, c. 10 km east of Abisko, and about 200 km north of the Arctic Circle. The annual mean temperature in Abisko (1913-2003) is –0.7°C, annual precipitation is about 300 mm. The warmest month is July with a mean temperature of +11°C. The vegetation period at Stordalen is very short and begins after snowmelt in June, senescence of the vegetation starts in September with first snow falls usually experienced by the end of this month.

The site at Stordalen is a homogeneous flat terrain with a sufficient fetch (>200 m) for flux measurements using Eddy Covariance (EC) methods. The mire is surrounded by birch forests and lakes. Close to the measurement tower the vegetation was dominated by *Eriophorum angustifolium* and *Carex rostrata* that reached a maximum height of 0.5 m.

Instruments

A sonic anemometer (Metek USA-1; Metek, Elmshorn, Germany) was mounted on a mast on the mire at a measuring height of 2.95 m above ground level. The tube inlet for the VOC concentration measurements was located directly under the scanning volume of the anemometer, air passed through a Teflon tube to a PTR-MS (Ionicon, Innsbruck, Austria) that was operated in a small trailer, located 12 m from the tower; air flow from the heated inlet was set to 20 l/min. A sub-sample of 0.3 l/min was taken from the inlet flow and analysed by the PTR-MS. A time lag of 4.6 s between anemometer and PTR-MS data was determined by cross correlation of vertical wind (w) and VOC concentrations, and has been considered during data analysis.

The drift tube pressure (p_{drift}) of the PTR-MS was kept at 2.2 mb and the drift tube was heated to T_{drift}=60°C, this led to a kinetic energy of E/N=130 Td inside the drift tube. During the vegetation period, the PTR-MS was operated with several different measurement sequences scanning for different sets of VOC components, among others Methanol (m33), Acetaldehyde (m45), Acetone (m59) and Isoprene (m69), with dwell times up to a maximum of 0.5 s each.

Flux calculations

To calculate fluxes of VOCs based on the quasi-continuous high frequency (20 Hz) vertical wind speed and the relatively slow, discontinuous measurements of VOC concentration, disjunct eddy covariance (DEC) techniques were used. For each VOC included in the measurement sequence, only at N discrete, short time intervals i of length τ (dwell time), measurements of the VOC concentration c are available. For this disjunct data set, a synchronized sub-sample of the continuous vertical wind data w was used and the resulting flux F_c was calculated according to

$$F_c = \frac{1}{N}\sum_{1}^{N} w'(i)\cdot c'(i),$$

where w' and c' are the instantaneous deviations from the mean values of w and c of the sub-sample [1].

Results

To characterize the footprint area of the VOC fluxes measured, the distance of the maximum contribution of the measured fluxes was calculated according to Schuepp et al. ([2], Fig. 1a) for stable and instable conditions. In Fig. 1b, the maximum distance that contributes to the measured flux is given [3]. At the Stordalen site, this distance lies within the homogeneous fetch even under stable conditions.

Fig. 2 shows a comparison of the sensible heat flux H, calculated from the full set of high-frequency data (20 Hz; H_{full}) and the disjunct sensible heat flux $H_{disjunct}$, derived from the sub-sample of disjunct data from measurements of Acetaldehyde (m45), Acetone (m59) and Isoprene (m69). The regression analysis gave high coefficients of determination (R^2 about 0.9), but $H_{disjunct}$ based on the limited data set was about 10% less than H_{full}. This was caused by neglecting smaller, high-frequency eddies due to the longer integration times of the PTR-MS measurements compared to the sonic anemometer.

A typical episode (20/8-27/8/2006) of measured fluxes of sensible heat H and Isoprene from the sub-arctic mire at Stordalen is presented in Fig. 3. During day time, the fluxes of sensible heat H and Isoprene were highest, but not well correlated, with isoprene reaching it's daily maximum about 3 h after H. During night time, as can be expected, isoprene fluxes were zero.

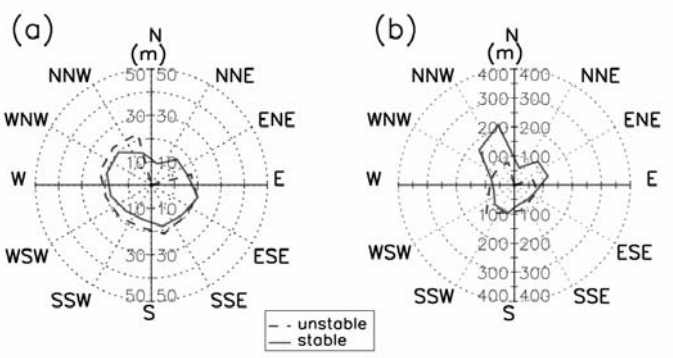

Figure 1: Footprint of the site at Stordalen according to (a) Schuepp et al. (distance of maximum contribution of measured flux) and (b) Wilson & Swaters (maximum distance that contributes to the flux) for stable and unstable conditions, calculated using data from 20/08 to 30/08/2006.

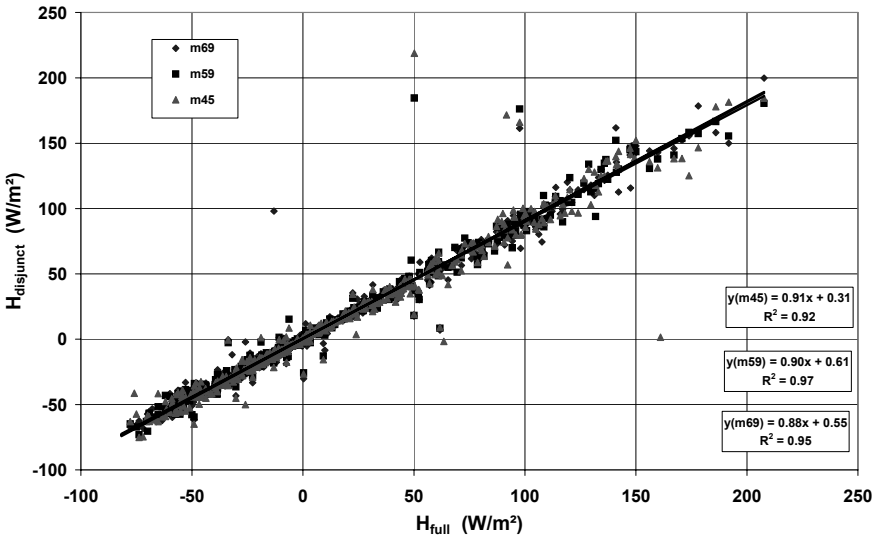

Figure 2: Comparison of the sensible heat flux H, calculated from the full data set and from the disjunct data sets of the measurement of Acetaldehyde (m45), Acetone (m59) and Isoprene (m69) in the period 20/08 to 31/08/2006 at the Stordalen site.

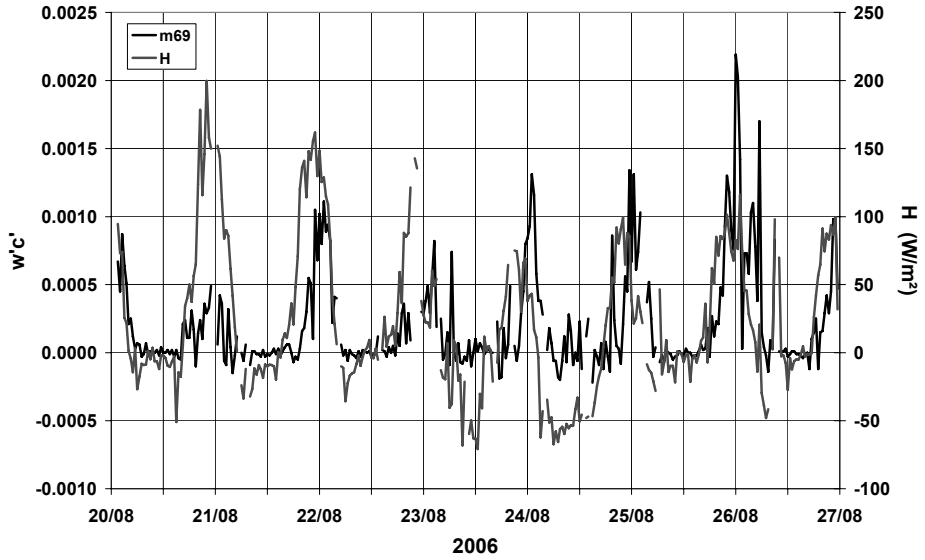

Figure 3: Measured fluxes of Isoprene (m69) and sensible heat H at a sub-arctic wetland site in northern Sweden during an episode in August 2006 (20/8, 12 utc to 27/8, 12 utc).

Discussion

First data of VOC fluxes measured at a sub-arctic wetland in northern Sweden using disjunct eddy covariance methods have been presented. The footprint area of the flux tower was found to be relatively small even under stable conditions and a comparison of high-frequency heat fluxes with disjunct heat fluxes showed only little underestimation of fluxes due to neglecting small eddies. The fluxes of BVOC measured at Stordalen will be compared to BVOC leaf-scale and chamber measurements, and they will provide an extensive data set for the development and validation of VOC emission models.

References

[1] H. J. I. Rinne, A. Guenther, C. Warnecke, J. A. de Gouw, and S. L. Luxembourg, Disjunct eddy covariance technique for trace gas flux measurements. Geophysical Research Letters 28, 3139, (2001).

[2] P.-H. Schuepp, M.-Y. Leclerc, J.-I. MacPherson, and R.-L. Desjardins, Footprint prediction of scalar fluxes from analytical solutions of the diffusion equation, Boundary-Layer Meteorology 50, 355-373, (1990).

[3] J. D. Wilson, and G. E. Swaters, The source area influencing a measurement in the planetary boundary layer: the 'footprint' and the 'distribution of contact distance', Boundary-Layer Meteorology 55, 25-46, (1991).

Qualitative and quantitative detection of Mycotoxin in cereals

E. Hartungen, A. Jordan, L. Märk, T. D. Märk

Ionicon Analytik Ges.m.b.H. Technikerstrasse 21a, 6020 Innsbruck, Austria

Abstract

The goal of the study is to develop a method to qualitatively and quantitatively detect Deoxynivalenol, Aflatoxin, Zearaleon, Ochratoxin A and Toxin T2 in cereals using a Proton Transfer Reaction Mass Spectrometer (PTR-MS) as a tool for fast quality control.

The first part of the study comprises the investigation of seven maize samples and one rye sample of different qualities (in terms of containing different amount of toxins). Six samples with Deoxynivalenol only, one with Deoxynivalenol, Zearaleon and Ochratoxin A and one containing all five toxins were used to check the ability to measure the Mycotoxin markers and to verify the correlation with HPLC measurements. For the measurements 6g of each sample were prepared in a 20 ml vial and heated up to a temperature of 80°C. After equilibration zero air was used to flush the vial with a flow of 60 ml/min. In between each sample zero air was used to monitor the background of the instrument.

First results show that it is possible to detect Deoxynivalenol in cereals at pptv levels. Other Mycotoxin markers could not be detected due to the extremely low concentrations and/or possible breakups. Results correlate with the previous HPLC measurements. Quantitative measurements and classification of the samples in “good” or “bad” needs a detailed study of all pure compounds and measurements of “good” and “bad” samples with known contamination of Mycotoxins.

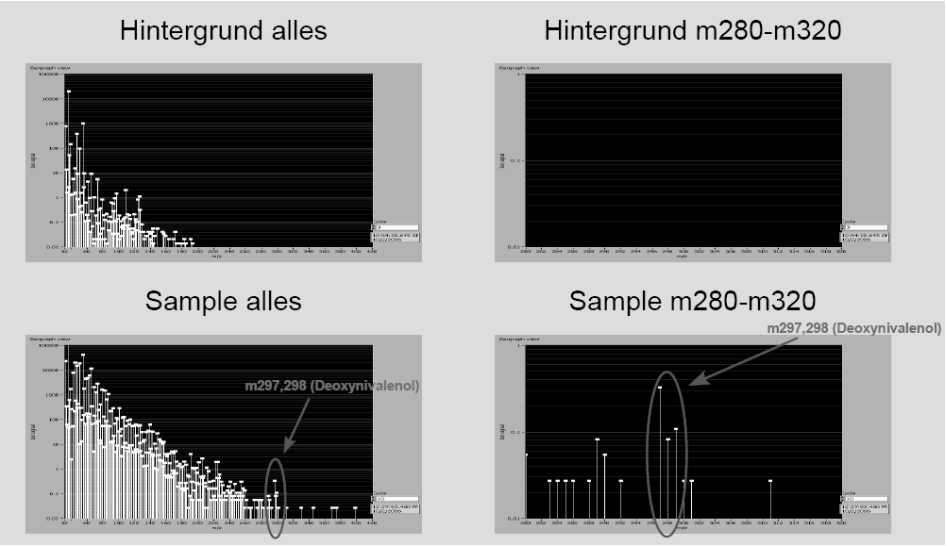

Future plans:

- Determination of breakup patterns and sensitivity of the PTR-MS for all relevant Mycotoxins.
- Determination of the best experimental setup conditions for the measurements of cereals.
- Exact correlation of the head space concentration with the contamination of the cereals determined by HPLC analysis.
- Verification of the ability to analyze the contamination of cereals directly at the transport containers.

Development of new PTR ion sources for soft and selective ionization

Satoshi Inomata[1], Hiroshi Tanimoto[2], and Nobuyuki Aoki[3]

[1] *Atmospheric Environment Division, National Institute for Environmental Studies, 16-2, Onogawa, Tsukuba, Ibaraki 305-8506, Japan, ino@nies.go.jp*

[2] *Asian Environment Research Group, National Institute for Environmental Studies, 16-2, Onogawa, Tsukuba, Ibaraki 305-8506, Japan*

[3] *National Metrology Institute of Japan, National Institute of Advanced Industrial Science and Technology, 1-1-1, Umezono, Tsukuba, Ibaraki 305-8563, Japan*

Abstract

Two types of ion sources based on hollow-cathode discharge were newly developed for soft and selective ionization of VOCs to couple with a proton transfer reaction time-of-flight mass spectrometer (PTR-TOFMS). By using an H_2O/[rare gas] discharge ion source, an ion drift tube can be operated at the field strength (E/N) of 33–46 Td at normal operating condition of reagent ions (H_3O^+) density. We found that the low E/N ratios in the drift tube greatly suppressed fragmentation for methyl nitrate. Possibility of a two-stage PTR ionization source to generate different reagent ions from H_3O^+ was examined using acetone, which was used as a reagent VOC_1 for the first-stage PTR. A single peak of protonated acetone, $(CH_3)_2CO{\bullet}H^+$, was observed at the intensity comparable to that of the protonated water clusters (i.e., $H_3O^+{\bullet}(H_2O)_{n=0,1,2}$). The second-stage PTR from $(CH_3)_2CO{\bullet}H^+$ took place in the presence of VOC_2, proton affinity of which was larger than that of acetone in sample air.

Introduction

Proton transfer reaction mass spectrometry (PTR-MS) is a technique that enables us to perform rapid analyses of volatile organic compounds (VOCs) with low detection limits [1,2]. PTR ionization is known as a soft ionization method that predominantly produces protonated molecules, however, fragment ions are sometimes observed. The PTR-MS technique provides only information on the mass-to-charge ratio, *m/z*, of ions produced by PTR ionization. This sometimes complicates the assignment of the ion signals, and requires a careful identification of the chemical species involved [3]. The fragmentation is caused mainly by the large kinetic energies for the protonation reactions, and in some cases by large excess energies of the protonation reactions. Commercial PTR-MS instruments are typically operated at field strength, E/N, of the ion drift tube of between 120 and 140 Td in order to minimize $H_3O^+{\bullet}(H_2O)_n$ clusters [1]. In particular, the primary ion, H_3O^+, is expected not to exist in the drift tube under the E/N condition with less than 80 Td [4].

In the present work, two types of ion sources based on hollow-cathode discharge were newly build and characterized for the soft and selective ionization of VOCs to couple with a proton transfer reaction time-of-flight mass spectrometry (PTR-TOFMS), recently developed in our laboratory [5,6]. One is an H_2O/[rare gas] discharge ion source that made it possible to operate at E/N of the drift tube in the range 33-46 Td and to keep amounts of H_3O^+ in the drift tube

predominant [7]. The other is a two-stage PTR ion source that selectively produces reagent ions, $VOC_1 \bullet H^+$, at the first stage by the proton transfer reaction of primary ions, H_3O^+ with VOC_1. If VOC_2 that has a larger proton affinity (PA) than that of VOC_1 is contained in a sample, the second PTR ionization occurs to produce $VOC_2 \bullet H^+$ ions with smaller excess energies of the protonation reaction than those of the protonation reaction of H_3O^+ with VOC_2 [8].

Experimental Methods

The instrument used in the present work has a hollow-cathode ion source coupled with a drift tube and an orthogonal time-of-flight mass spectrometer. The detailed instrumental setup has been described elsewhere [5,6]. Briefly, the combination of an ion source and drift tube consists of seven stainless-steel electrodes (ED1–ED7), an inlet lens (IL), and an orifice plate (OP) separated by static dissipative Teflon cylinders. Adjoining electrodes are connected by resistances, and high positive voltages are applied to the electrodes from ED1 to ED7 by a common direct current power supply. The voltages of the IL and the OP are controlled independently. The region from ED1 to ED3 acts as the ion source.

At normal operation, H_2O taken from the vapor pressure over distilled water was directed into the ion source as a reagent gas. Reagent ions (H_3O^+) and a small amount of $H_3O^+ \bullet (H_2O)_{n=1,2}$ clusters, generated in the ion source, were introduced into the drift tube and react with VOCs in sample gases that were introduced from a sampling port located beneath the ion-source region. The pressure of the drift tube was maintained at 5 Torr. The product ions from the proton transfer reaction, together with residual reagent ions, were ejected into an orthogonal time-of-flight mass spectrometer and then analyzed.

At the operation with an H_2O/[rare gas] discharge ion source, water vapor was introduced into the drift tube by bubbling with a carrier of rare gas. On the other hand, a new sampling port was attached between ED4 and ED5 at the operation with a two-stage PTR ion source. Sample was introduced from this second port and a reagent VOC was introduced from a port between ED3 and ED4. All mass spectra shown here were accumulated during 60 s at a repetition of 10 kHz (i.e. 6×10^5 scans).

Results and Discussion

H_2O/[rare gas] discharge ion source

Figure 1 shows the comparison of the results obtained at the operation using an H_2O/[rare gas] discharge ion source with those at the normal operation. Results using Argon as a carrier gas were shown. First of all, the intensity of H_3O^+ at E/N = 40 Td was comparable to that at E/N = 100 Td and the difference in the distributions of H_3O^+ and $H_3O^+ \bullet (H_2O)_{n=1,2}$ was not significant. Mass spectra of methyl nitrate obtained at each condition were shown in Figs. 1b and 1d. Signals of protonated methyl nitrate ($M \bullet H^+$, *m/z* 78) were quite small compared with those of fragment ions, NO_2^+ (*m/z* 46) at the normal operation [9]. Using this new ion source, the peak of protonated methyl nitrate become significantly intense compared with that of NO_2^+. Although total product ion counts become one eighth less than those at the normal operation, ion counts at protonated methyl nitrate become seven times larger than those at the normal operation. This will provide the selective detection of methyl nitrate. In addition, the detection sensitivity of acetone improved

approximately twice likely because the reaction time becomes longer. Similar results were also obtained using other carrier rare gases such as He, Ne, and Kr [7].

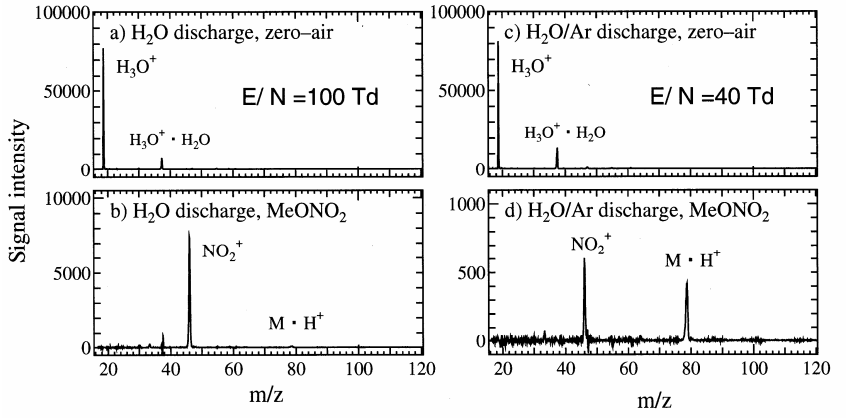

Figure 1: (a) Background and (b) sample mass spectra of methyl nitrate at normal operation with H_2O discharge ion source. (c) Background and (d) sample mass spectra of methyl nitrate at operation with H_2O/Ar discharge ion source.

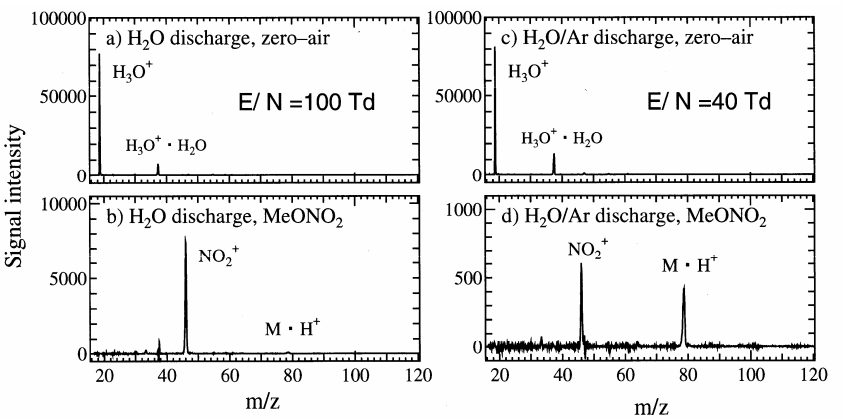

Figure 1: (a) Background and (b) sample mass spectra of methyl nitrate at normal operation with H_2O discharge ion source. (c) Background and (d) sample mass spectra of methyl nitrate at operation with H_2O/Ar discharge ion source.

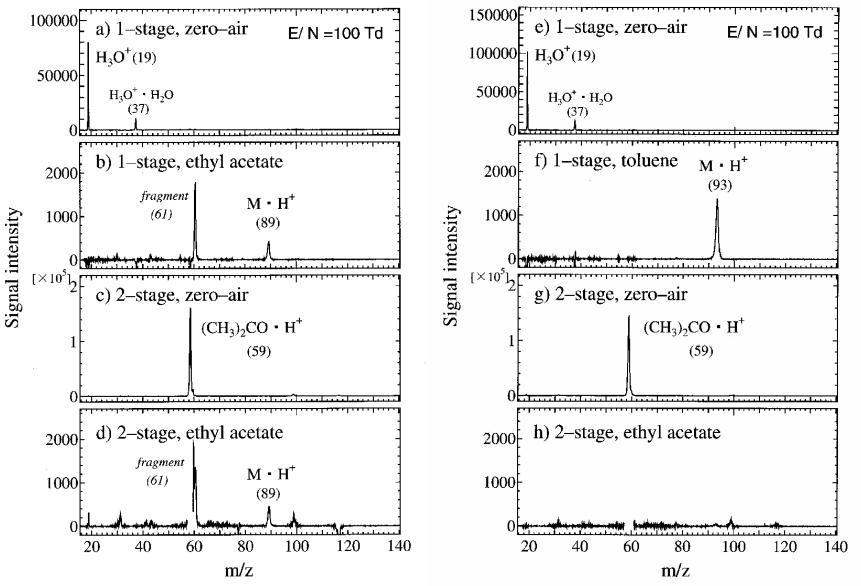

Figure 2: (a) Background and (b) sample mass spectra of ethyl acetate at normal operation. (c) Background and (d) sample mass spectra of ethyl acetate at operation with two-stage PTR ion source using acetone as a reagent VOC. (e) Background and (f) sample mass spectra of toluene at normal operation. (g) Background and (h) sample mass spectra of toluene at operation with two-stage PTR ion source using acetone as a reagent VOC.

Two-stage PTR ion source

The mass spectra obtained at the operation with a two-stage PTR ion source using acetone (PA = 812 kJ/mol [10]) as a reagent VOC_1 are shown in Figure 2. A single peak of $(CH_3)_2CO{\bullet}H^+$ was observed at *m/z* 59 by the first-stage PTR ionization as shown in Figs. 2c and 2g. The intensities of $(CH_3)_2CO{\bullet}H^+$ were as much as those of $H_3O^+{\bullet}(H_2O)_{n=0,1,2}$. Two VOCs, ethyl acetate and toluene, PAs of which are 836 and 784 kJ/mol, respectively [10], were introduced as a sample VOC_2. The second PTR ionization occurred for ethyl acetate to produce ptotonated molecules ($M{\bullet}H^+$, *m/z* 89) with fragment ions at *m/z* 61. Intensities of these ions were the same as those obtained at the normal operation (Fig. 2b vs. Fig. 2d), suggesting that the fragmentation is caused not by excess energies of the protonation reactions in this case. On the other hand, the second protonation did not occur in the case of toluene because the PA of toluene is less than that of acetone. Other reagent VOCs besides acetone were also examined [8]. By choosing an appropriate reagent VOC_1, this technique can distinguish VOCs having same molecular weight but different PA.

References

[1] W. Lindinger, A. Hansel, and A. Jordan, On-line monitoring of volatile organic compounds at pptv levels by means of Proton-Transfer-Reaction Mass Spectrometry (PTR-MS) Medical applications, food control and environmental research, International Journal Mass Spectrometry and Ion Processes 173, 191-241 (1998).

[2] W. Lindinger, A. Hansel, and A. Jordan, Proton-transfer-reaction mass spectrometry (PTR-MS): on-line monitoring of volatile organic compounds at pptv levels, Chemical Society Review 27, 347-354 (1998).

[3] C. Warneke, J. de Gouw, W. C. Kuster, P.D. Goldan, and R. Fall, Validation of atmospheric VOC measurements by Proton-Transfer-Reaction Mass Spectrometry using a Gas-Chromatographic preseparation method, Environmental Science & Technol. 37, 2494-2501 (2003).

[4] J.A. de Gouw, C. Warneke, T. Karl, G. Eerdekens, C. van der Veen, and R. Fall, Sensitivity and specificity of atmospheric trace gas detection by proton-transfer-reaction mass spectrometry, International Journal of Mass Spectrometry 223-224, 365-382 (2003).

[5] S. Inomata, H. Tanimoto, N. Aoki, J. Hirokawa, Y. Sadanaga, A novel discharge source of hydronium ions for transfer reaction ionization: design, characterization, and performance, Rapid Communications in Mass Spectrometry 20 1025-1029 (2006).

[6] H. Tanimoto, N. Aoki, S. Inomata, J. Hirokawa, and Y. Sadanaga, Development of a PTR-TOFMS instrument for real-time measurements of volatile organic compounds in air, submitted manuscript, (2006).

[7] S. Inomata, H. Tanimoto, and N. Aoki, manuscript in preparation.

[8] S. Inomata and H. Tanimoto, manuscript in preparation.

[9] N. Aoki, S. Inomata, and H. Tanimoto, Detection of C_1-C_5 alkyl nitrates by proton transfer reaction time-of-flight mass spectrometry, submitted in International Journal of Mass Spectrometry, (2006).

[10] W.G. Mallard (Ed.), NIST Chemistry WebBook, NIST Standard Reference Database Number 69, National Institute of Standards and Technology, Gaithersburg, MD, 2005 (http://webbook.nist.gov).

Aldehyde measurements and estimation of contribution from photochemical production in urban atmosphere

Shungo Kato[1], Masumi Ideguchi[1] , and Yoshizumi Kajii[1]

[1] Faculty of urban environmental sciences, Tokyo metropolitan university, Tokyo, Japan, shungo@atmchem.apchem.metro-u.ac.jp

Introduction

There are two main advantages of PTR-MS measurements for atmospheric species. (1) High frequency measurement. (2) Oxygenated VOC (OVOC) can be detected. OVOCs (alcohol, aldehyde, ketone etc.) have high polarity and are difficult to be measured by GC method. Aldehyde is an important species in both urban and rural atmospheric chemistry. It is emitted directly from sources (car exhaust etc.) to the atmosphere, especially in urban area. Also aldehyde is produced by photochemical reactions. Aldehyde is usually trapped by DNPH cartridge and analyzed by HPLC. It is hard work to analyze large amount of samples for short time resolution. Now PTR-MS can measure aldehyde automatically in high time resolution and large data set of aldehyde is available. It will be interesting to know the contribution of direct emission and photochemical production of aldehyde in urban atmosphere.

Experimental Methods

Urban atmospheric measurement were conducted during 2004 in the campus of Tokyo Metropolitan University, where is about 30km west of Tokyo city center. For each season, intensive measurements were conducted for about 5 days. VOC were measured by PTR-MS, and GC-FID method (sampled one hour interval during daytime). CO, O_3, SO_2, NOx/NO, and RO_2 radical were also measured. The results obtained by PTR-MS were calibrated by the results of GC-FID method for the species detectable by GC-FID [1]. Other species like OVOCs including acetaldehyde were calibrated using standard gas. Formaldehyde can be detected by PTR-MS, but the influence of water in the atmosphere will be large [2]. For rough estimation, the relative signal variation of formaldehyde (m/z=31) was trusted and the concentration was calibrated by the typical formaldehyde/acetaldehyde ratio in Tokyo area.

Results and Discussion

The typical anthropogenicaly emitted species like toluene showed higher concentration during nighttime and lower concentration during daytime because of the stability of the surface air. On the other hand, aldehyde showed higher concentration during daytime and lower concentration during nighttime. Also aldehyde concentration was higher during summertime and lower during wintertime.

The contribution from anthropogenic and photochemical production of acetaldehyde concentration was estimated. CO was used as the indicator of the anthropogenic emission and O_3 was used as the indicator of photochemical production. From the correlation plot of acetaldehyde and CO during nighttime, direct emission factor (α) was determined for each season. Then Δacetaldehyde ([observed acetaldehyde] – $\alpha \cdot$[CO]) and O_3 was plotted for daytime and the photochemical production factor (β) was determined for each season. In this way, estimated

acetaldehyde can be deduced by CO and O_3 concentration ($[Acetaldehyde]_{estimated} = \alpha \cdot [CO] + \beta \cdot [O_3]$). In figure 1, CO, O_3, observed acetaldehyde, and estimated acetaldehyde during summertime are shown. The observed and estimated acetaldehyde concentrations show good agreement.

Using the CO and O_3 data, the contribution of acetaldehyde anthropogenic emission and photochemical production were estimated for each season. The contributions of photochemical production during daytime are 32% (spring), 29% (summer), 26% (fall), 16% (winter). It is reasonable trend that higher photochemical production during spring and summer and lower in winter. In similar way, the contribution of photochemical production of formaldehyde was estimated.

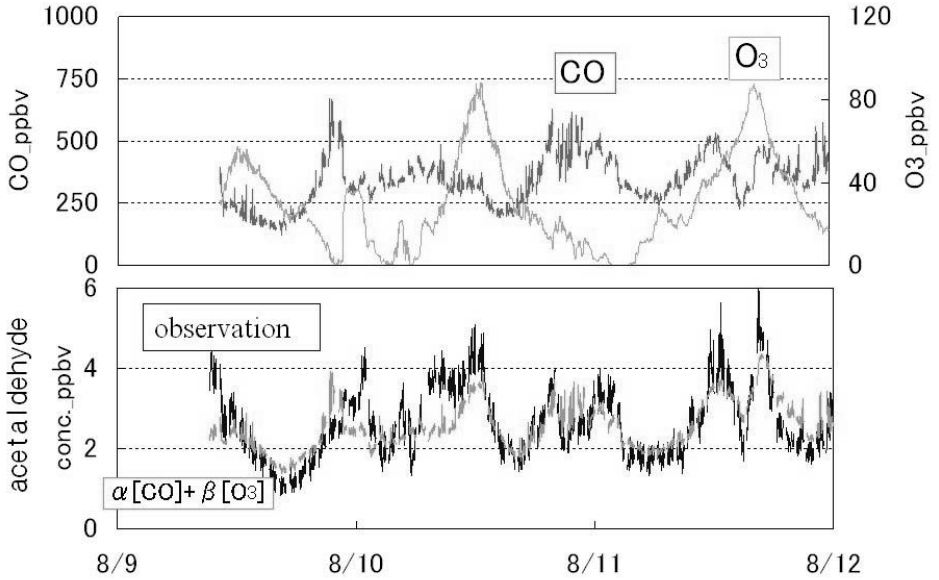

Figure 1: CO and O_3 concentrations in summer (Top). Observed acetoaldehyde concentration is compared with estimated acetaldehyde concentration from CO and O_3concentrations.

References

[1] S. Kato, Y. Miyakawa, T. Kaneko, Y. Kajii, Comparison with PTR-MS and GC-FID measurements and urban air measurement in Tokyo area, International Journal of Mass Spectrometry 235/2, 103-110, (2004).

[2] S. Kato, Y. Miyakawa, Y. Kajii, Calibration of PTR-MS for OVOCs, 2nd International Conference on Proton Transfer Reaction Mass Spectrometry and Its Applications, 45-46, (2005).

Correct equations for concentrations in the drift tube of a PTR-MS and potential implications for the calculated concentrations

Lothar Keck[1], Uwe Oeh[1] and Christoph Hoeschen[1]

[1] *Institute of Radiation Protection, GSF - National Research Centre for Environment and Health, 85758 Neuherberg, Germany, keck@gsf.de*

Abstract

The accepted relation for the concentrations of trace gases in the drift tube of a PTR-MS, [R], is not correct since it does not account for the different drift velocities of primary ions and protonated trace gases. The correct relation must include the ratio of the drift velocity of primary ions and the drift velocity of protonated trace gas, which can be significantly different from unity. The ratio of drift velocities disappears when expressing [R] in terms of the current densities. The noticed error might be just a formal one as long as the ratio of ion currents into the quadrupol mass spectrometer (QMS) of the PTR-MS equals the ratio of ion current densities near the end of the drift tube. If, however, the ratio of ion currents into the QMS is partly determined by the ratio of concentrations near the end of the drift tube, the error affects the established method for determining the transmission of the QMS and the calculation of concentrations from the measured count rates. Here we show the correct relation for the concentrations in the drift tube and discuss potential implications.

Introduction

Trace gas concentrations can be calculated from PTR-MS signals using measured count rates and the measured transmission of the QMS. These calculations are based on the well established formula for the concentrations in the drift tube [1], [2]

$$[R_i] = \frac{[R_iH^+]}{k_i \cdot t \cdot [H_3O^+]}, \tag{1}$$

where $[R_i]$ and $[R_iH^+]$ and are the concentrations of the non-protonated and protonated trace gases, $[H_3O^+]$ the concentration of the primary ions, k_i the reaction rate constant and t the reaction time. Unfortunately, the derivation of eq. (1) is apparently based on the equation

$$\frac{\partial[H_3O^+]}{\partial t} = -\sum_i \frac{\partial[R_iH^+]}{\partial t}, \tag{2}$$

where the concentrations refer to a gas parcel which is moving through the drift tube. Eq. (2) would be correct if H_3O^+ and R_iH^+ were at rest or if they were moving with the same drift velocity. However, the drift velocities of R_iH^+ are actually much lower than the drift velocity of H_3O^+. Hence, the increase of $\sum[R_iH^+]$ is higher than the decrease of $[H_3O^+]$. Thus, eq. (2) and (1) are not correct.

Correct relation for the concentrations in the drift tube

A one dimensional coordinate system fixed to the drift tube is used, x = 0 corresponds to the inlet and $x = L$ ($L \approx 10$ cm) to the outlet of the drift tube. The concentrations are generally determined by advection [3] and the sinks or sources due to the chemical reaction. We neglect the effect of diffusion for the ion concentrations due to their short residence time in the drift tube. For example, the correct equation for the concentrations of R_iH^+ is:

$$\frac{\partial[R_iH^+]}{\partial t} = -\frac{\partial\left(v_{R_iH}\cdot[R_iH^+]\right)}{\partial x} + k_i\cdot[R_i]\cdot[H_3O^+] \qquad (5)$$

with v_{R_iH} being the drift velocity of R_iH^+. Then, with further mathematical steps similar to the calculation shown in the PTR-MS manual we get

$$[R_i] = \frac{[R_iH^+]_L}{k_i\cdot t\cdot[H_3O^+]_L}\cdot\frac{v_{R_iH}}{v_{H_3O}} \qquad (6)$$

where the index "*L*" denotes the concentrations at the end of the drift tube. The additional factor of the ratio of drift velocities in eq. (6) as compared to eq. (1) will significantly decrease the values of $[R_i]$ and one may wonder why the error was not recognised from experimental evidence.

Potential implications for the calculation of concentrations

The ratio of drift velocities disappears when expressing $[R_i]$ in terms of current densities of R_iH^+ and H_3O^+. Thus, if the ratio of ion currents out of the drift tube into the QMS equals the ratio of current densities of the ions near the end of the drift tube, there's no need to consider the drift velocities. However, if the ratio of ion currents into the QMS would be equal to the ratio of concentrations of ions near the end of the drift tube, there would be practical consequences of the above discussion. In this case we may define the transmission T_{RiH} for the protonated component R_iH^+ as

$$I_{R_iH} = T_{R_iH}\cdot[RH^+]_L \qquad (7)$$

where I_{R_iH} is the count rate measured by the secondary electron multiplier (SEM) at the mass of RH^+. A similar expression holds for $[H_3O^+]$. With eq. (7), eq. (6) becomes

$$[R_i] = \frac{1}{k_i\cdot t}\cdot\frac{v_{R_iH}}{v_{H_3O}}\cdot\frac{I_{R_iH}}{I_{H_3O}}\cdot\frac{T_{H_3O}}{T_{R_iH}}. \qquad (8)$$

Hence there is, as usual, the need to determine the ratio of transmissions for H_3O^+ and R_iH^+, accomplished with samples containing a single trace gas R_k in high concentrations so that a decrease of the primary signal occurs. However, the additional factor in eq. (6) has the

consequence that a ratio of drift velocities must also be included in the relation between the transmissions and measured changes of the count rates:

$$\frac{T_{H_3O}}{T_{R_kH}} = -\frac{v_{H_3O}}{v_{R_kH}} \cdot \frac{\partial I_{H_3O}}{\partial I_{R_kH}} \quad . \tag{9}$$

The measured ratios of transmissions are then interpolated as a function of the mass, indicated by the index *int*.

Using eq. (9) with (8) yields the final result for the concentrations in the drift tube:

$$[R_i] = \frac{1}{k_i \cdot t} \cdot \frac{v_{R_iH}}{v_{H_3O}} \frac{I_{R_iH}}{I_{H_3O}} \cdot \left(-\frac{v_{H_3O}}{v_{R_KH}} \cdot \frac{\partial I_{H_3O}}{\partial I_{R_kH}} \right)_{\text{int}} \quad . \tag{10}$$

Thus, if the analyte R_i and the trace gases used to determine the ratio of transmission R_k at the mass of R_i have equal drift velocities, the two additional ratios of drift velocities in eq. (10) almost cancel out each other and eq. (10) can again be approximated by an established relation

$$[R_i] = \frac{1}{k_i \cdot t} \cdot \frac{I_{R_iH}}{I_{H_3O}} \cdot \left(-\cdot \frac{\partial I_{H_3O}}{\partial I_{R_kH}} \right)_{\text{int}} \quad . \tag{11}$$

However in general, v_{R_iH} and v_{R_kH} can be significantly different even when the two components have the nearly the same mass and the established relation (11) might be no good approximation for the correct relation (10).

Conclusions

A corrected formula for the concentrations in the drift tube of a PTR-MS was presented. The correction would affect the concentrations calculated from the count rates if the ratio of ion currents into the QMS would partly reflect the ratio of concentrations near the end of the drift tube rather than the ratio of current densities. The authors intend to design experiments to clarify this issue.

References

[1] A. Hansel, A. Jordan, R. Holzinger, P. Prazeller, W. Vogel and W. Lindinger, Proton transfer reaction mass spectrometry: on-line trace gas analysis at the ppb level, International Journal of Mass Spectrometry and Ion Processes 149/150, 609-619, (1995).

[2] W. Lindinger, A. Hansel and A. Hansel, On-line monitoring of volatile organic compounds at pptv levels by means of Proton-Tranfer-Reaction Mass Spectrometry (PTR-MS) Medical applications, food control and environmental research, International Journal of Mass Spectrometry and Ion Processes 173, 191-241, (1998).

[3] L. Landau and E. Lifschitz, Lehrbuch der theoretischen Physik, Band 6: Hydrodynamik, Akademie-Verlag, Berlin, (1978).

Coupling a FTICR mass spectrometer with a Proton Transfer Reaction ion source

Joël Lemaire[1], Laurent Clochard[2], Christophe Dehon[1], Hélène Mestdagh[1], Pierre Boissel[1] Gérard Mauclaire[2] and Michel Heninger[2]

[1] Laboratoire de Chimie Physique, UMR 8000 CNRS-Université Paris Sud, Bâtiment 350, 91405 Orsay France, joel.lemaire@lcp.u-psud.fr

[2] AlyXan, Bâtiment 207B, Centre Universitaire d'Orsay, 91405 Orsay, France.

Abstract

A small FTICR mass spectrometer featuring an cylindrical permanent magnet assembly producing in its center a magnetic field coaxial to the cylinder axis is developed in our laboratory. Its coupling with an external Proton Transfer Reaction ion source is described here. A sensitivity increase of several order of magnitude is expected compared to the previous version where ions are formed by ionization in the cell.

Introduction

Compact FTICR mass spectrometers show great promise as rugged gas analyzers well suited for the analysis of complex mixtures since good resolving powers can be reached and they provide for MS^n capability which can help in structure identification. In the simplest configuration primary ion formation and reaction with the gas to analyze and detection in mass is performed in the FTICR cell. This operating mode allows the use of a wide variety of reactant ions . However the sensitivity is limited to the ppm range. One way to go to a higher sensitivity is to do in line concentration through a permeable membrane. The other way, described in this contribution, is to separate the ion formation by chemical ionization from the mass analysis. A dedicated permanent magnet has been designed for this purpose and the first tests of ion injection in the magnetic field are underway.

Compact FTICR-MS

Our first apparatus, nicknamed MICRA, and based on a permanent magnet of cylindrical shape producing in its center a magnetic field perpendicular to the cylinder main axis has already shown many of the advantages of small FTICR-MS[1]. Its open cell configuration is well adapted for spectroscopy experiments and it has been widely used for ion structure determination by infrared multiple photons dissociation experiments at the free electron laser facility CLIO in Orsay[2-4]. It has been used with a wide variety of ionization modes: electron impact, chemical ionization from different precursors, laser ablation ionization, matrix assisted laser desorption ionization,.. Proton transfer reaction from H_3O^+ ions with air can be done in cell and after pumping out of the air gas pulse the resulting product ions can be detected . However this simple approach is limited to the detection of traces in the ppm range because of the maximum number of collisions that can be experienced by an ion without diffusing out of the cell.

This triggered the development of a new instrument where the protonating reaction is done externally to the FTICR cell. Differential pumping is implemented so that the background

pressure is always very low in the FTICR cell while the proton transfer reaction is done in a drift cell with air in the mbar range. This configuration is favorable for FTICR detection with a high mass resolving power and will also allow the use of several different ion sources such as electrospray ionization or laser ablation.

Permanent magnet configuration

The main challenge for doing FTICR-MS with a permanent magnet is to generate a high and homogeneous magnetic field while remaining compact enough for a transportable apparatus. Our first apparatus MICRA was based on the association of two Hallbach cylinders. With this design we obtained a radial field of 1.25 Tesla in the center of a 5 cm diameter bore with an homogeneity of 0.5 % in a $1cm^3$ volume.

In the new experiment presented here a permanent magnet assembly has been specially designed in order to produce a magnetic field coaxial with the magnet cylinder main axis. In this way ions can be moved in and out of the magnet assembly, by moving the ions along the magnetic field lines. The magnet is made of rare earth alloy segments whose shape and direction of magnetization are chosen so as to produce a homogeneous field inside the cylinder. The material is Neodyme Iron Boron, selected for its high coercivity and remanence.

The field produced in the middle of the 60 mm diameter bore has a magnitude of 1 Tesla, an homogeneity better than 0.2% over the whole ICR cell volume and its weight is 80 kg. The field has a circular symmetry which is favourable for FTICR detection.

Open Cylindrical cell

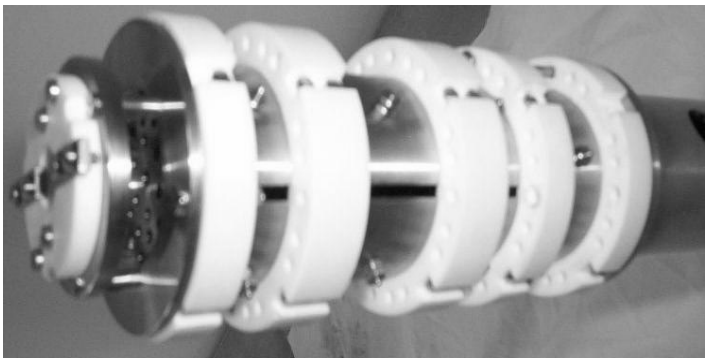

Figure 1: cylindrical ICR cell with the filament attached on the left side

The ICR cell is cylindrical, with a 20 mm inner diameter. The central section is divided in four segments corresponding to the excitation and detection plates. The lateral trapping sections are also divided in four so that the RF excitation signal can also be applied on two of the plates so that the ions see a more linear excitation. The cell is fitted on one side with a filament which can be used for in cell ionisation. The other side can be used to bring ions in the cell from an external ion source.

Real time analysis with an FTICR

In FCTICR-MS the whole mass spectrum is obtained for each mass detection event and there is no time advantage in detecting a smaller mass range. The detection duration depends only on the targeted resolution. High resolution detection is typically done with 1 second transients and 10 ms to 100ms transients can be used for lower resolution mass detection with a faster time response.

When ion production and reaction is done in cell the main time limitation comes from the pumping out time of the gas pulse. With the external ion production faster time resolution becomes accessible. However the main limitations will now come from the gas sampling and reaction chamber gas renewal. A fast FTICR detection sequence is nevertheless useful since signal from several sequences can be averaged to get a higher signal to noise ratio.

Results

First characterization of the new FTICR-MS has been done using in cell ionization either by electron impact or by in cell chemical ionization. Good performances have been obtained as shown on the spectra in Figure 2. The installation of the ion guides to drive the ions into the magnetic field is currently under way.

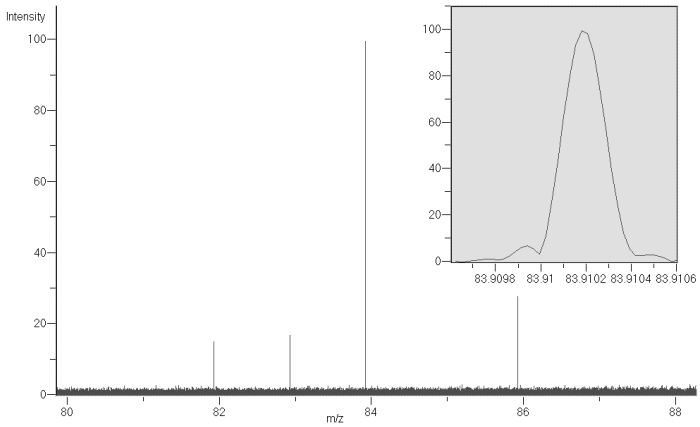

Figure 2 : mass spectrum obtained for the Krypton isotopes. The insert is a zoom on the more abundant istope $^{84}Kr+$ showing a mass resolv ing power of 380000.

Conclusion

We have already shown that small FTICR-MS based on permanent magnets have great potential as rugged mass detectors giving access to a high resolution for small masses. They are very versatile tools since various ionization modes can be used, and ions can be mass selected and reacted with neutrals inside the cell. However in cell PTRMS detection has a sensitivity limit of about 1ppm.

With the axial field magnet currently under development it will be possible to produce the primary ions and to react them with air before injecting them in the FTICR spectrometer for mass analysis. In this way the proton transfer reaction can be done in a drift tube and then analyzed in mass with high resolution. The instrument has already been tested using electron impact ionisation on neutral gases and the resolving power obtained in these conditions is very satisfactory.

References

[1] G. Mauclaire, J. Lemaire, P. Boissel, G. Bellec, M. Heninger, MICRA: a compact permanent magnet Fourier transform ion cyclotron resonance mass spectrometer, European Journal of Mass Spectrometry, 10, 155-162, (2004).

[2] J. Lemaire, P. Boissel, M. Heninger, G. Mauclaire, G. Bellec, H. Mestdagh, A. Simon, S. Le Caër, J.M. Ortega, F. Glotin, P. Maître, Gas phase infrared spectroscopy of selectively prepared ions, Phys. Rev. Lett., 89(27) 273002-1-4, (2002).

[3] O. Dopfer, J. Lemaire, P. Maitre, B. Chiavarino, M.E. Crestoni, S Fornarini, IR spectroscopy of protonated toluene: Probing ring hydrogen shifts in gaseous arenium ions, International Journal of Mass Spectroscopy, 249, 149-154, (2006).

[4] T.D. Fridgen, L.MacAleese, T.B. McMahon, J. Lemaire, P. Maitre, Gas phase infrared multiple-photon dissociation spectra of methanol, ethanol and propanol proton-bound dimers, protonated propanol and the propanol/water proton-bound dimmer, Physical Chemistry Chemical Physics, 8, 955-966, (2006).

Novel approach to study aroma release kinetics

Mateus M-L. [1], Lindinger C. [2], Liardon R. [1], Blank I. [1]

[1] *Nestlé Product Technology Center, CH-1350 Orbe, Switzerland, marie-louise.mateus@rdor.nestle.com*

[2] *Nestlé Research Center, CH-1000 Lausanne, Switzerland*

Abstract

Accurate modelling of aroma release kinetics is often difficult due to the lack of highly time-resolved measurements of process dynamics. PTR-MS overcomes this hurdle, but the identification of each species and its contribution to a given ion trace intensity may be necessary for accurate prediction of single compound kinetics within complex mixtures.

The feasibility of modelling the release kinetics of aroma compounds from dry roast and ground coffee using PTR-MS was investigated. First, the effect of superposition of isobaric species contributing to a specific m/z intensity on release kinetics was studied. Samples of coffee were purged with nitrogen and on-line release kinetics were compared with kinetics reconstituted from purge and trap samplings. Secondly, the release curves from both methods were fitted with the model of Weibull.

Concluding, the results showed that variations in the contribution of compounds to a specific m/z intensity can affect the modelling of the kinetics. However, these variations may remain lower compared to variations inherent in biological products. The accurate modelling of aroma release kinetics from coffee allowed discriminating fine variations in aroma release and determining the release mechanisms involved.

Background

Accurate modelling of aroma release kinetics is often difficult due to the lack of time-resolved measurements of process dynamics. PTR-MS permits on-line measurements. However, the identification of each species and its contribution to a given ion trace intensity may be necessary for accurate prediction of single compound kinetics. The objective of this project was to investigate the feasibility of modelling the release kinetics of aroma compounds in complex food systems using PTR-MS.

Methodology used

Experimental set-up

5g of roast and ground Colombia coffee were placed on a mesh inside a glass stripping cell (Figure 1). The sample was stripped for ~1 hour with 740 sccm of nitrogen at 90°C.

The effect of isobaric species on the determination of single compounds release kinetics was studied. Release kinetics obtained by PTR-MS were compared with reconstituted kinetics from Tenax trapping.

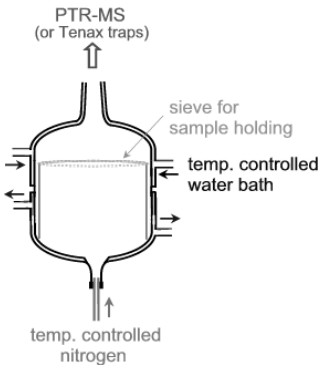

Figure 1: Stripping system for the study of aroma release kinetics from roast and ground coffee

Modelling of the release kinetics

Time intensity profiles were transformed into cumulated released amount (Figure 2), and fitted with the model of Weibull [2]:

Released amount [g]= $M_\infty * \left[1 - \exp\left(-(k*t)^n\right)\right]$

with: M∞: amount released at t=∞ [g]; k: scale parameter [s^{-1}]; n: shape parameter [-]

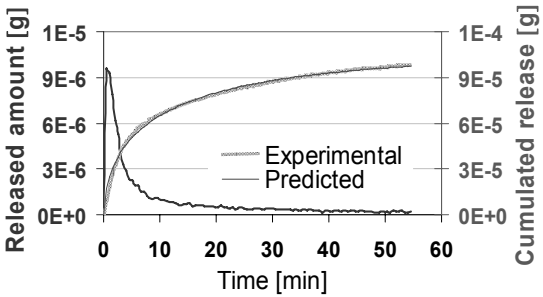

Figure 2: Intensity and cumulated amount curves of VOCs from roast and ground coffee

Validation of the Method

VOCs velocity profiles

Measuring the transfer function of the cell, compounds were spiked at the cell periphery or centre of the cell, as shown in Figure 3. In our study, the response time is much faster than the

expected and measured release kinetics (peak tail did not significantly alter the shape of the aroma release kinetics).

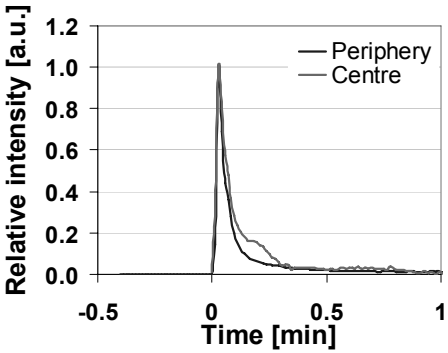

Figure 3: Response of the stripping system to an impulse of aroma compounds, at the centre and at the periphery of the cell

Identification of the isobaric compounds

The different compounds yielding to a specific m/z intensity were identified by collecting the coffee headspace on Tenax traps at several points of the release kinetics. The Tenax traps were analysed using a GC-PTR-MS coupling as presented in [1]. For each chromatogram, the intensity of the different contributing compounds was determined.

Significant variations of the Weibull's model parameters "k" and "n" were observed bet-ween PTR-MS and Tenax kinetics. An example is shown in Figure 4.

Small variations in contribution of different compounds to a specific m/z intensity (lower than 15%) were not taken into account to correct the parameters k and n (RSD < 5%).

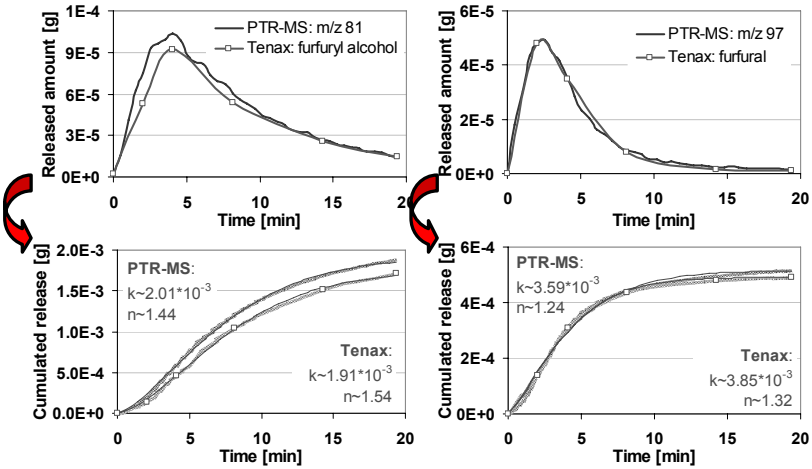

Figure 4: Effect of variation of the contribution to a specific m/z intensity on the shape of the compound kinetics. Examples for release kinetics of furfuryl alcohol and furfural.

Application: effect of coffee particles size on aroma release

An example for the release kinetics of pyridine from roast and ground coffee at defined particles size is presented in Figure 5.

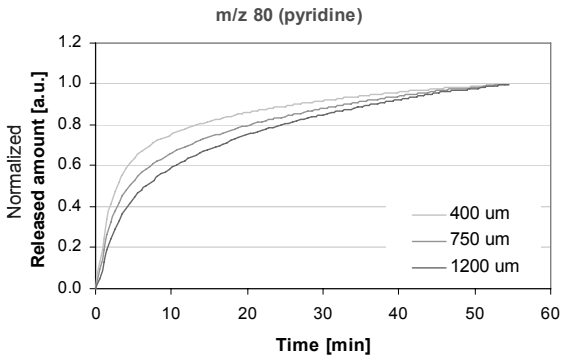

Figure 5: Effect of particles size on the cumulated released amount of VOCs from coffee

Results using the model of Weibull are presented in Figure 6. They indicate that:

1) Aroma release kinetics is faster at lower particles size (higher "k" value), which is not evident because of possible coffee bed packing effect

2) Diffusion may be the limiting mass transport mechanism: a value of the shape parameter "n"~0.6-0.7 has been assigned to diffusion mechanisms in various biological systems [2, 3]

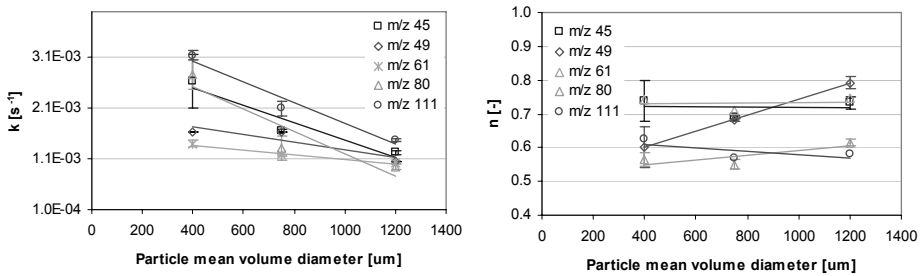

Figure 6: Effect of particles size on the rate constants "k" and "n" of the model of Weibull for acetaldehyde (m/z 45), methanethiol (m/z 49), acetic acid (m/z 61), pyridine (m/z 80) and methyl furfural (m/z 111).

General conclusions

The feasibility of modelling the release kinetics of aroma compounds from roast and ground coffee using PTR-MS was investigated. Variations in the contribution of different compounds to a specific m/z intensity can affect the modelling of the kinetics. However, these variations may remain lower compared to variations inherent in biological products. The accurate modelling of aroma release curves from coffee allowed discriminating fine variations in aroma release and determining the release mechanisms involved.

References

[1] Lindinger C., Pollien P., Ali S., Yeretzian C., Blank I., Märk T. Unambiguous identification of organic volatile compounds by Proton Transfer Reaction – Mass Spectrometry coupled with GC/MS. Analytical Chemistry (2005), 77, 4117-4124.

[2] Papadopoulou V., Kosmidis K., Vlachou M., Macheras P. On the use of the Weibull function for the discernment of drug release mechanisms. International Journal of Pharmaceutics (2006), 309(1-2), 44-50.

[3] Marabi, A., Livings, S., Jacobson, M., and Saguy, I. S. Normalized Weibull distribution for modeling rehydration of food particulates. European Food Research and Technology 217[4], 311-18. 2003.

Isoprene Photooxidation Product Study using Proton-Transfer-Reaction Mass Spectrometry (PTRMS) and a coupling of Gas Chromatography and PTRMS

Axel Metzger[1], A. Brunner[2], A. Gascho[1], J. Dommen[1], and Urs Baltensperger[1]

[1] *Laboratory of Atmospheric Chemistry, Paul Scherrer Institute, 5232 Villigen-PSI, Switzerland, axel.metzger@psi.ch*

[2] *Air pollution and Climate Research Group, Agroscope FAL Reckenholz, 8046 Zürich, Switzerland*

Abstract

Proton-transfer-reaction mass spectrometry (PTRMS) has emerged as a useful tool to study the atmospheric chemistry of volatile organic compounds (VOC). Although limitations occur as a certain compound is only characterized by its mass which is not unique. Therefore we performed smog chamber studies running a proton-transfer-reaction mass spectrometer (PTRMS) in parallel to a combination of gas chromatography and PTRMS (GC-PTRMS) which allows the different OVOCs detected at the same mass, to be separated based on their different retention times in the GC column. Studies of several precursors have been conducted including isoprene. Isobaric products of the isoprene photooxidation like methacrolein and methyl vinyl ketone have been tracked down and their concentrations were determined using the FID detection of the GC.

Introduction

Proton-transfer-reaction mass spectrometry (PTRMS) ability to measure many important oxygenated VOC (OVOC) and their oxidation products makes it a useful tool for smog chamber (SC) experiments. But in PTRMS, only the mass of the ionized trace gases is determined, which is not a unique indicator of the trace gas identity. Despite the ionization technique is rather soft fragmentation for certain compounds occurs. Therefore, it might be difficult to identify most of the individual oxidation products, because it is likely that many mass signals are produced from several substances being the parent peak or a fragment of it. A combination of gas chromatography and PTRMS (GC-PTRMS) in parallel to a second PTRMS was used in smog chamber experiments of several different VOC including isoprene. Isoprene is one of the most abundant non-methane hydrocarbons emitted into the troposphere with source strength of ~500 Tg/year [Guenther, Hewitt et al. 1995]. Recently special attention has been paid to isoprene as it could contribute largely to secondary organic aerosol formation due to its large source strength globally [Dommen, Metzger et al. 2006]. The main oxidation products of isoprene have been identified and their yields determined. Among them, the two most important isobaric products methacrolein (MACR) and methyl vinyl ketone (MVK). Concerning SOA formation the oxidation pathway via MACR seems to be more important [Kroll, Ng et al. 2005; Kroll Jesse H. 2006; Surratt, Murphy et al. 2006]. Therefore it is important to resolve their concentration in order to better understand the SOA formation from isoprene. We conducted smog chamber experiments applying the GC-PTRMS method to gain further insight into the isoprene photooxidation chemistry.

Experimental Methods

Photooxidation experiments were carried out in a 27-m^3 Teflon chamber. Experimental protocols are previously described [Paulsen, Dommen et al. 2005; Dommen, Metzger et al. 2006]. A suit of different experimental techniques is used to investigate gas phase chemistry and aerosol properties including proton-transfer-reaction mass spectrometry (PTR-MS) [Steinbacher, Dommen et al. 2003; Dommen, Metzger et al. 2006] and GC-PTRMS. The setup of the GC-PTRMS is described elsewhere [Brunner A. 2006]. GC-PTRMS allows the different VOC detected at the same mass, to be separated based on their different retention times in the GC column. A flame ionization detector (FID) was used in parallel to the PTRMS for an independent measurement of the OVOC.

Results and Discussion

In Figure 1 a counter plot of the PTRMS m/z vs. time is shown. The shading indicates the signal intensity. With time concentrations of the isoprene fragments (m/z: 69, 67, 41, 39) decrease and the build up of primary products MVK and MACR (m/z: 71, 45, 43) can be observed. Secondary and tertiary products arrive with a certain time delay (for example m/z 73, methylglyoxal). Products up to an m/z of 117 are observed.

In the upper panel of Figure 2 GC-PTRMS chromatograms are shown. Chromatograms are taken after 60 and 515 minutes of irradiation in the smog chamber. While after 60 min isoprene is still dominating and only the primary products start to appear, isoprene is almost completely reacted after 500 minutes and the primary products MACR and MVK as well as compounds at a m/z of 61, 75 87 and 113 dominate the gas phase.

In the lower panel of Figure 2 concentration time profiles of the PTRMS at m/z 69 (isoprene) and 71 (MVK+MACR) are shown as well as the concentrations of the primary products MVK and MACR. The two isobaric products are nicely separated in the GC and the sum of MVK+MACR (determined with GC-PTRMS) correlates excellent with the PTRMS m/z71 trace.

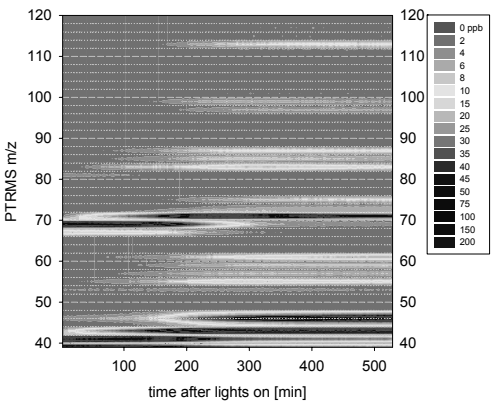

Figure 1: Illustration of the ion counts in all mass channels plotted vs. the course of the experiment. Colors indicate signal intensity of the respective compound/fragment.

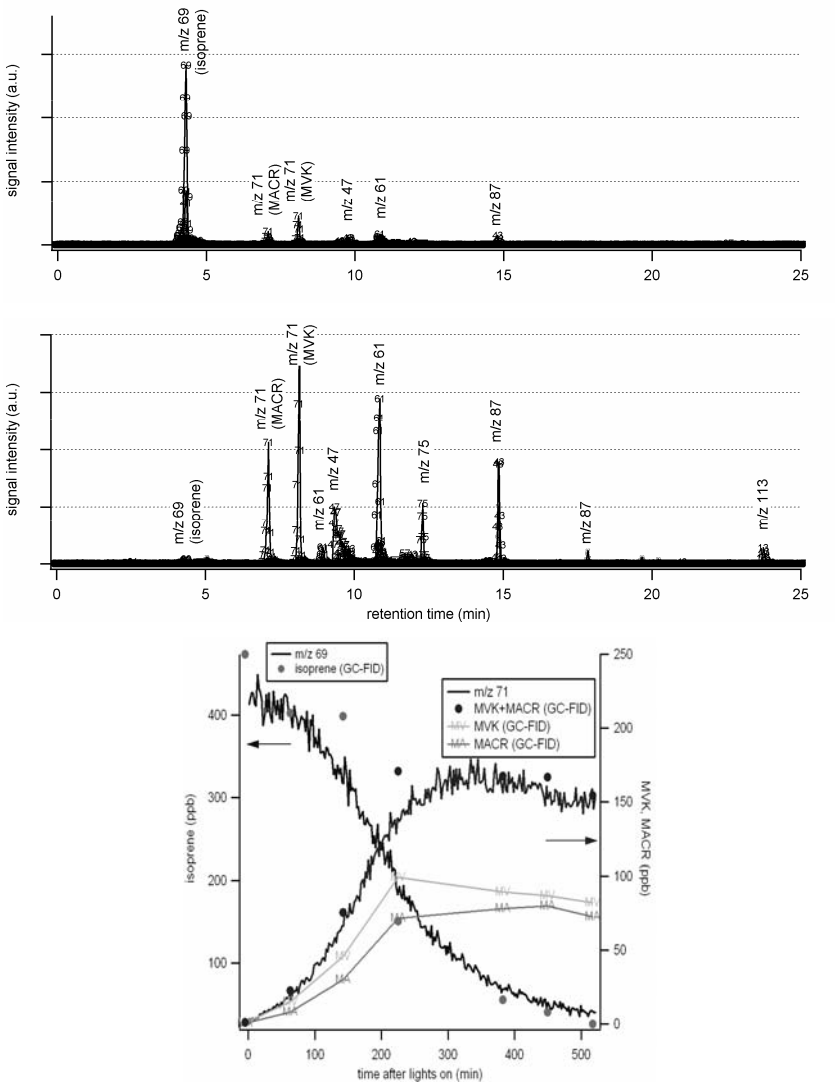

Figure 2: (upper panel) Chromatogram as measured with the PTRMS after 60 and 515 min of irradiation. (lower panel) The concentration time profile of isoprene, methyl vinyl ketone (MVK) and methacrolein (MACR) measured with GC-FID coupled to a PTRMS. In addition the concentration time profile of m/z 69, 71 which corresponds to the sum of both compounds measured with a second PTRMS is shown. Data were collected during a isoprene + NOx photo-oxidation experiment.

Conclusions

The performance of a GC-PTRMS was demonstrated by the means of isoprene smog chamber experiments. The ability to resolve isobaric compounds and the additional information about fragmentation pattern makes it an indispensable tool in smog chamber studies and for the analysis of PTRMS mass spectra.

References

Brunner A., S. C. (2006). In preparation.

Dommen, J., A. Metzger, et al. (2006). "Laboratory observation of oligomers in the aerosol from isoprene/NOx photooxidation." Geophysical Research Letters 33(13).

Guenther, A. B., C. N. Hewitt, et al. (1995). "A global model of natural volatile organic compound emissions." Journal of Geophysical Research 100(D5): 8873-8892.

Kroll Jesse H. , N. L. N., Shane M. Murphy, Richard C. Flagan, and John H. Seinfeld (2006). "Secondary Organic Aerosol Formation from Isoprene Photooxidation." Environ. Sci. Technol. 40(6): 1869 - 1877.

Kroll, J. H., N. L. Ng, et al. (2005). "Secondary organic aerosol formation from isoprene photooxidation under high-NOx conditions." Geophysical Research Letters 32(18).

Paulsen, D., J. Dommen, et al. (2005). "Secondary organic aerosol formation by irradiation of 1,3,5-trimethylbenzene-NOx-H2O in a new reaction chamber for atmospheric chemistry and physics." Environmental Science & Technology 39(8): 2668-2678.

Steinbacher, M., J. Dommen, et al. (2004). "Performance Characteristics of a Proton-Transfer-Reaction Mass Spectrometer (PTR-MS) derived from laboratory and field measurements." International Journal of Mass Spectrometry, 239, 117-128.

Surratt, J. D., S. M. Murphy, et al. (2006). "Chemical composition of secondary organic aerosol formed from the photooxidation of isoprene." Journal of Physical Chemistry A 110(31): 9665-9690.

Emission of volatile organic compounds from bacterial cultures

Tomas Mikoviny[1], Michael Bunge[2], Nooshin Araghipour[1], Rosa Margesin[2], Franz Schinner[2], Armin Wisthaler[1] and Tilmann D. Märk[1]

[1] *Institute of Ion Physics and Applied Physics, Innsbruck University, Austria*
tomas.mikoviny@uibk.ac.at

[2] *Institute of Microbiology, Innsbruck University, Austria*

Abstract

We have optimised the experimental set-up for PTR-MS measurements of volatile organic compounds (VOCs) emitted by bacterial cultures. Dynamic headspace measurements were carried out under controlled conditions for five types of medically relevant microorganisms (*Escherichia coli*, *Shigella flexneri*, *Salmonella flexneri*, *Helicobacter pylori*, *Candida tropicalis*). Quantitative and qualitative differences were found in the PTR-MS mass spectra obtained from the headspace of different bacterial cultures; strong temporal changes were observed in the headspace mass spectra when individual bacterial cultures were grown over 48 hours. The preliminary results indicate that PTR-MS can be used to discriminate between samples inoculated with different bacterial cultures and to monitor temporal changes in the inoculated medium.

Introduction

The identification of VOCs produced by medically relevant microorganisms using mass spectrometric methods is considered to be a relevant and important addition to conventional microbiological techniques [1, 2, 3]. Rapid detection of patterns associated with pathogenic organisms has the potential to decrease the amount of fatal cases of contracting certain diseases, such as the diagnosis of infectious diarrhoea [1]. The complexity of this problem means that currently only tentative identification of produced VOCs are possible. Metabolic profiles of cultivated bacteria, for example, differentiate the bacteria and may be used for bacterial fingerprinting [1,2]. However, only a limited amount of bacteria have been studied and reliability of this approach has so far not been proven.

In contrast to the methods used in [1,2] (solid phase microextraction, and agar plate culturing, respectively) liquid media have also been chosen for bacteria cultivation to obtain VOC patterns related to household biowaste [4]. Liquid media have the advantage of providing additional information of cell numbers and are easily homogenized with respect to standardized measurement procedures. As in many cases of PTR-MS measurements only tentative identification of VOCs are provided here.

To improve the measurements of VOCs emitted from bacterial cultures a condition-stabilized set-up has been built and tested on a variety of specific conditions that are generally used for selected bacteria stains. Here, the bacterial patterns obtained have been standardized for complex sample measurements.

Experimental Methods

VOC emissions from the following bacterial cultures were investigated: *Escherechia Coli*, *Shigella flexneri*, *Salmonella enterica*, *Candida tropicalis*, *Helicobacter pylori*.

The experimental set-up for the measurement of VOC emissions from bacterial cultures is schematically shown in Figure 1.

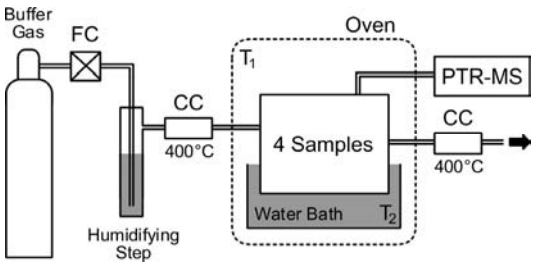

Figure 1: Schematic of the experimental set-up optimised for bacteria measurements (FC – flow controller, CC – Pt/Pd catalyst, T_1 – oven temperature, T_2 – water bath temperature, 25°C and 37°C, respectively)

40 ml of inoculated medium were placed in a 100 ml glass vial capped with a three-port Teflon® cap. One port was closed with a septum; this port was used for syringe sampling of the inoculated medium to determine bacterial numbers. The two other ports were used as inlet and outlet for a carrier gas flushed over the sample for dynamic headspace measurements. Synthetic air (80% N_2, 20% O_2) was usually used as a carrier gas; the *Helicobacter pylori* experiments were carried out using a special gas mixture (85% N_2, 5% O_2, 10% CO_2). Four vials (replicates) were prepared and placed in a water bath maintained at 37°C (25°C for *Candida tropicalis*). The carrier gas was first humidified and then passed over a Pt/Pd catalyst operated at 350°C to destroy any organic or microbiological contaminants. A total carrier gas flow of 800 ml/min was used with the total flow being equally divided between the four vials, i.e. the headspace of each vial was flushed at 200 ml/min. 50 ml/min from each vial were alternately fed to the PTR-MS instrument via a Teflon® solenoid valve. The overflow was discarded through a second Pt/Pd catalyst.

The PTR-MS operating parameters were as follows: drift tube voltage, 600V; drift tube pressure, 2.00±0.05 mbar; drift tube temperature, 60°C; O_2^+/H_3O^+ ratio ≤ 3%; inlet flow, 50-60 ml/min; inlet temperature, 60°C. Mass scans were recorded in the 20-300 amu range with a dwell time of 0.5s/amu. Mass signals were normalized to 1 x 10^6 cps primary ions ($H_3O^+ + H_3O^+ \bullet H_2O$) [ncps]. Only mass signals > 10 ncps (corresponding to ~ 0.2 ppb) were used for data analysis.

Results

The PTR-MS mass spectra of bacteria headspace showed ≤ 25 mass peaks above the 0.2 ppb cut-off level; levels ranged from < 1 ppb (m/e=132, 134) to ~ 3000 ppb (m/e=45).

A strong temporal variability was observed for most signals during the course of a typical 24 hour experiment. Different temporal patterns were observed: continuous increase, increase to reach a saturation level, increase to reach a peak level followed by a decrease ("peak").

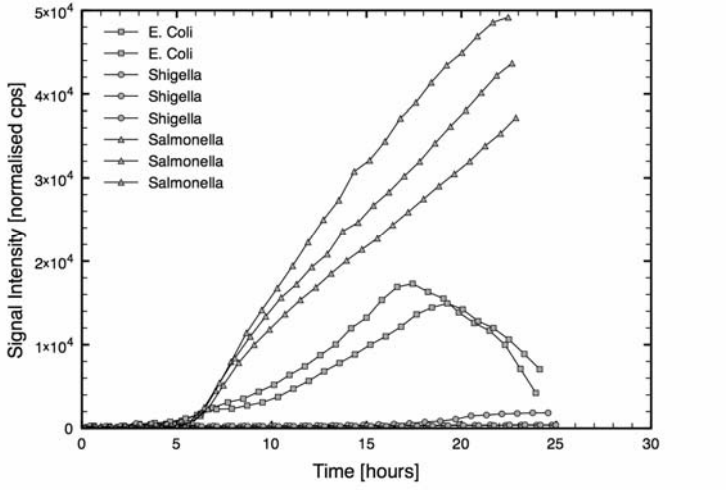

Figure 2: Time-dependent VOC production

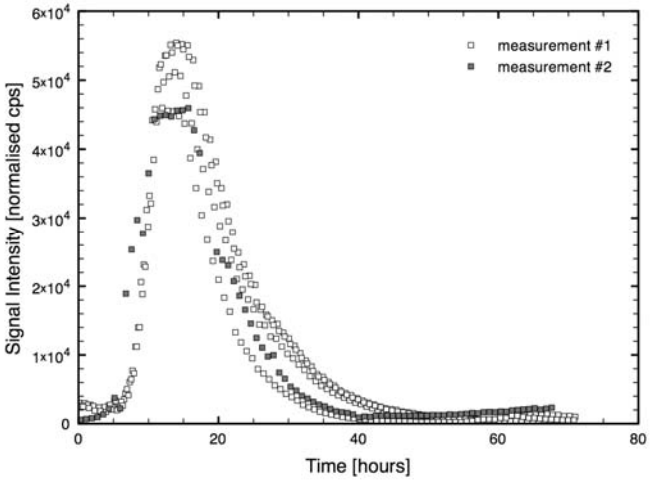

Figure 3: Reproducibility test of improved experimental set-up.

We classified discrimination conditions between different cultures:

- different temporal behaviour of a mass signal for different bacterial cultures
- quantitative differences in the mass spectra (different abundance)
- qualitative difference (presence or absence of specific mass signals)

The experimental setup was been tested for reproducibility. Figure 3 shows 2 distinct measurements of *Helicobacter pylori* where 4 inoculated samples were measured during measurement #1 and an additional single inoculated sample was measured during measurement #2. The qualitative and quantitative repeatability has been reached together with the temporal behaviour of the mass signal.

Conclusion

The preliminary results indicate that PTR-MS can be used to discriminate between samples inoculated with different bacterial cultures and to monitor temporal changes in the inoculated medium.

Systematic studies of complex samples are currently being carried out to gauge the possibility to identify bacteria using PTR-MS.

References

[1] C. J. S. Probert, P. R. H. Jones and N. M. Ratcliffe, A novel method for rapidly diagnosing the causes of diarrhoea, Gut 53, 58-61, (2004)

[2] M. Lechner, M. Fille, J. Hausdorfer, M. P. Dierich and J. Rieder, Diagnosis of bacteria *InVitro* by mass spectrometric fingerprinting: a pilot study, Curr. Microbiol. 51, 267-269, (2005)

[3] M. Lechner, H. Tigl and J. Rieder, Analysis of volatile compounds emitted by the *Helicobacter pylori* reference strai NCTC 11637 *In Vitro*, Helicobacter 11, 60, (2006)

[4] S. Mayrhofer, T. Mikoviny, S. Waldhuber, A. O. Wagner, G. Innerebner, I. H. Franke-Whittle, T. D. Märk, A. Hansel and H. Insam, Microbial community related to volatile organic compound (VOC) emission in household biowaste, Environmental Microbiology 8, 1960-1974, (2006)

Rapid Testing of Olive Oil Quality Using SIFT-MS

Daniel B. Milligan[1], Brett M. Davis[2], Senti T. Senthilmohan[1], Paul F. Wilson[1], and Murray J. McEwan [2]

[1] *Syft Technologies Limited, Christchurch, New Zealand, Daniel.Milligan@syft.com*

[2] *Department of Chemistry, University of Canterbury, Christchurch, New Zealand*

Abstract

Olive oil must be rigorously tested before it can be labeled as “extra virgin”, many of these tests are performed by analytical instruments but the final test still requires trained tasters. These tasters are used to detect defects such as rancidity. Ideally these tasters would also be replaced by instruments also.

Olive oil has been tested using SIFT-MS and propanal was found to be the predominant secondary oxidation product formed, while no significant increase was found in the concentrations of either hexanal or nonanal with increasing degree of rancidity. Propanal levels have been shown to correlate well with both the peroxide value and the sensory rancidity score.

Introduction

Olive oil must undergo many tests before being labelled 'extra virgin', all but one of which are performed instrumentally. The odd one out is a taste test performed by trained tasters. This test is used to search for defects such as rancidity. Rancidity is oil spoilage caused by oxidation, which occurs during prolonged or inappropriate storage. The challenge is to develop an objective, instrument-based test for olive oil rancidity.

Experimental Methods

Two olive oils were oxidised at 60ºC for several weeks and analysed for primary oxidation products by a peroxide assay. Organoleptic testing was used to detect sensory defects. SIFT-MS head-space analysis was used to detect volatile oxidation products. To evaluate the results, several brands of imported, bulk-produced olive oil were purchased from supermarkets and analysed.

SIFT-MS instrumentation

Selected Ion Flow Tube Mass Spectrometry (SIFT-MS) is a technique which allows real-time qualitative and quantitative analysis of whole-air samples[1]. It is well suited to real-time aroma analysis. Detection is achieved by selective reactions between gas phase ions and analyte molecules, which form distinctive product ions that are then analysed by mass spectrometry. Three different chemi-ionisation agents are available, H_3O^+, NO^+, and O_2^+.

Results: Detecting Rancidity in Real Time

A range of volatiles in headspace above the oxidised olive oils were measured each day during the oxidation process. No sample preparation was required. The dominant volatile species in the headspace of unoxidised olive oil is ethanol and methanol [2].

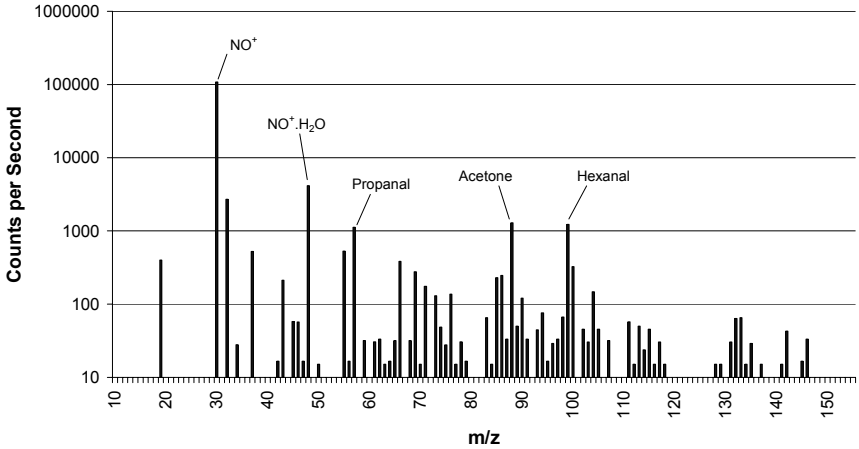

Figure 1: The NO^+ mass spectrum obtained from sampling the headspace above an oxidised olive oil. The compounds monitored as a measure of oxidation are labeled.

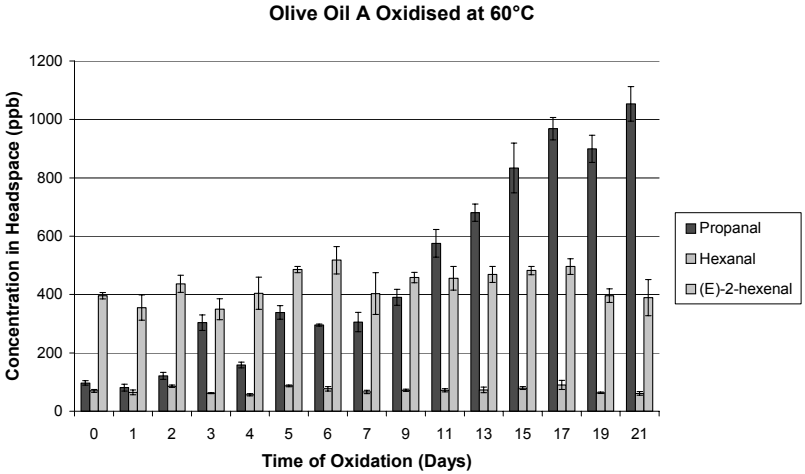

Figure 2: The time profile of volatiles in the headspace above a sample of olive oil oxidized at 60°C. Headspace measurements were taken each day.

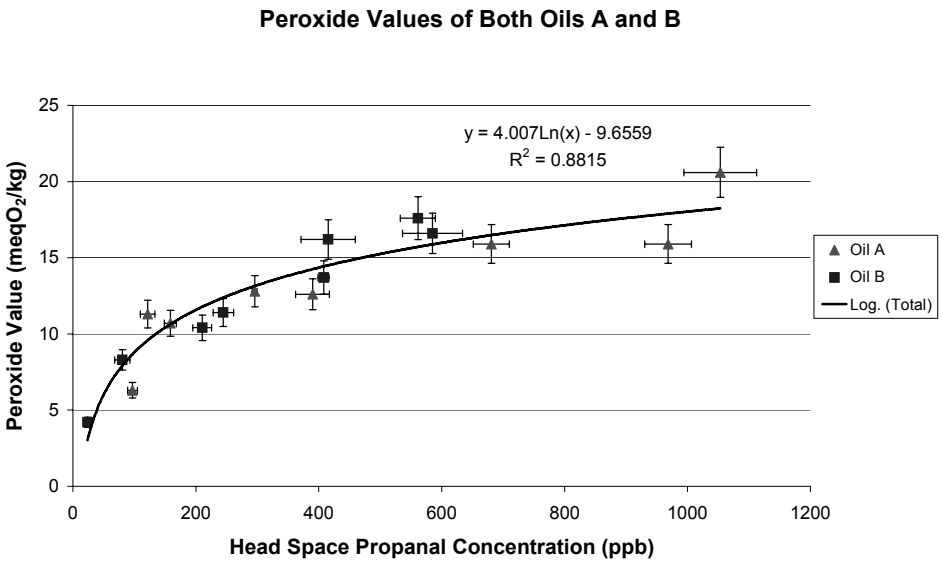

Figure 3: A comparison of the headspace propanal concentration for two olive oils undergoing oxidation with the peroxide value. The peroxide value is a measure of the amount of oxidation of the oil.

The headspace propanal concentration increases rapidly once the oil begins to oxidise. The concentration within the headspace correlates well with both the peroxide value (shown in Figure 3) and the rancidity results from the organoleptic panel.

Conclusions

Dominant volatiles in olive oil head-space are methanol and ethanol.

Propanal was found to be the predominant secondary oxidation product formed, while no significant increase was found in the concentrations of either hexanal or nonanal with increasing degree of rancidity.

SIFT-MS head-space propanal analysis showed good correlation with peroxide value.

The propanal levels showed good correlation with the sensory rancidity score.

Qualitative detection of the rancidity defect can be achieved, and more tasting data will allow quantitative detection as well.

High levels of propanal were found in supermarket olive oil 2, suggesting marked rancidity.

The results of this ongoing study show that SIFT-MS is a powerful, real-time technique for the detection of olive oil rancidity.

References

[1] P. Spanel and D. Smith, Selected ion flow tube mass spectrometry (SIFT-MS) for on-line trace gas analysis, Mass Spectrometry Reviews 24, 661-700, (2005).

[2] B. Davis, S. Senthilmohan, P. Wilson, and M. McEwan, Major Volatile compounds in head-space above olive oil analysed by selected ion flow tube mass spectrometry, Rapid Communications in Mass Spectrometry 19(16), 2272-2278, (2005).

Differentiation of monoterpenes by Collision Induced Dissociation with a Proton-transfer reaction Ion Trap Mass Spectrometer (PIT-MS)

Marco M.L. Steeghs[1], Elena Crespo[1], Cor Sikkens[1], Simona M. Cristescu[1], Frans J.M. Harren[1]

[1] *Life Science Trace Gas Facility, Molecular and Laser Physics, Institute for Molecules and Materials, Radboud University, Nijmegen, The Netherlands. e.crespo@science.ru.nl*

Abstract

The potential of Proton-Transfer Reaction Mass Spectrometry (PTR-MS) has been shown in many different fields, including atmospheric chemistry [1], medical science [2], and many biological and plant physiological fields [3]. Its high sensitivity, lack of sample preconcentration, its high time resolution, relatively low degree of fragmentation and the fact that it cannot measure the normal constituents of air, make it an excellent technique to monitor trace gas compounds in real-time. Those advantages, however, are accompanied by one disadvantage: compounds cannot be identified based on their mass only.

A novel way of approaching this problem is the development of a PTR mass spectrometer based on an ion trap mass spectrometer (Figure 1; [4]). The use of an ion trap has several advantages, among which the possibility to perform collision induced dissociation (CID) is the most interesting one. CID patterns of isolated ions can be obtained that are compound-specific, which helps to identify the underlying compound. The viability of such a system and the usefulness of CID have been proven before [5]. However, the compounds for which this is shown have still fairly simple structure. Monoterpenes are very interesting biological compounds, which are similar in structure and of which many different isomers exist. Here we study the fragmentation patterns of different monoterpene species, after dissociative proton-transfer and after collision induced dissociation (CID) in our newly developed Proton-transfer reaction Ion Trap Mass Spectrometer (PIT-MS).The CID patterns of all the monoterpenes studied are found to be distinguishable, making it possible to positively identify a monoterpene solely on the basis of its CID pattern [6].

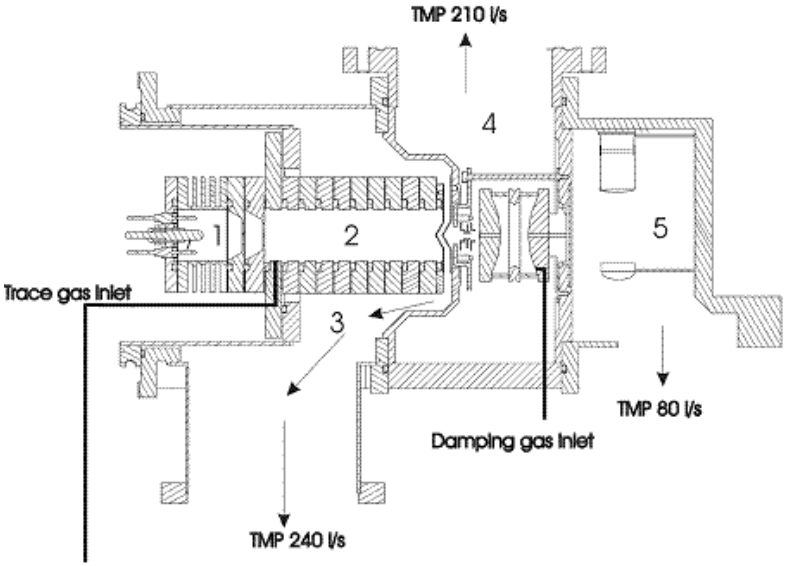

Figure 1: Nijmegen PIT-MS with 1) H3O+ ion source, 2) drift tube, 3) buffer chamber, 4) ion trap chamber and 5) detector chamber

References

[1] de Gouw, J. Warneke, C. Karl, T. Eerdekens, G. Van der Veen and R. Fall, Sensitivity and specificity of atmospheric trace gas detection by proton-transfer-reaction mass spectrometry, International Journal of Mass Spectrometry, 223-224 365-382, (2003).

[2] M. Steeghs, B. Moeskops, K.van Swam, S.M. Cristescu., P.T.J. Scheepers, F.J.M. Harren, On-line monitoring of UV-induced lipid peroxidation products from human skin in vivo using proton-transfer reaction mass spectrometry, International Journal of Mass Spectrometry, *in press* , 2006.

[3] M. Steeghs, H.P. Basis, J. de Gouw, P. Goldan, W. Kuster, M. Northway, R. Fall, J.M. Vivanco, Proton-Transfer-Reaction Mass Spectrometry as a new tool for real time analysis of Root-Secreted volatile organic compounds in Arabidopsis, Plant Physiology 135, 47-58, (2004).

[4] M.M.L. Steeghs, C. Sikkens, E. Crespo, S.M. Cristescu and F.J.M. Harren, Development of a Proton-transfer reaction Ion Trap Mass Spectrometer Online detection and analysis of volatile organic compounds, International Journal of Mass Spectrometry *in press* , 2006.

[5] C. Warneke, J.A. de Gouw, E.R. Lovejoy, P.C. Murphy, W.C. Kuster and R. Fall, Development of Proton-Transfer Ion Trap-Mass Spectrometry: On-line detection and identification of volatile organic compounds in air, American Society for Mass Spectrometry 16, 1316-1324, (2004).

[6] M.M.L. Steeghs, E. Crespo and F.J.M. Harren, Collision Induced dissociation study of 10 monoterpenes for identification in trace gas measurements using the newly developed Proton-transfer reaction Ion Trap Mass Spectrometer, submitted to International Journal of Mass Spectrometry.

Measurement of VOC fluxes above bare soil by PTR-MS

Martina Müsch, Jochen Tschiersch

GSF – National Research Center for Environment and Health, Institute of Radiation Protection, Ingolstaedter Landstr. 1, D-85764 Neuherberg, Germany, (muesch@gsf.de)

Abstract

First results of VOC flux measurements above bare soil are presented. The aim of the measurements is the characterization of the gas transfer of VOCs from the unsaturated soil layer to the atmosphere. For the parameterization the radon flux from the soil and the relevant meteorological and soil parameters are used. A Proton-Transfer-Reaction Mass Spectrometer (PTR-MS) was chosen for the VOC measurements because of its low detection limit and rapid response.

In pre-experiments soil probes were analyzed in a closed chamber. The chamber can be heated to simulate different soil temperatures. Several volatile compounds were found in these experiments and selected for the flux measurements. A dynamic chamber technique was used for flux determination. A chamber with a heated inlet line was installed above bare soil on a test field. The PTR-MS analyzed ambient and chamber air alternately. At the same site an accumulation chamber for the measurement of the radon exhalation rate from soil is in operation (radon exhalometer). Relevant meteorological and soil parameters are recorded simultaneously. Data for about 4 years are available for this site. The radon measurements showed that radon exhalation is dependent on various parameters like temperature, soil moisture, wind and barometric pressure.

The flux of different VOCs is nonuniform. While for methanol and acetone the upper soil layer seems to serve as a sink, other substances like dimethylsulfide and acetic acid show a positive flux. In these processes temperature was found to have a major impact. For more detailed investigation improvements in the measurement setup like the automation of the VOC chamber and the synchronization of the measurement cycles for the PTR-MS and the radon exhalometer are in process.

Coacervates for aroma modulation

Philippe Pollien, Fabien Robert, Christian Lindinger, Santo Ali, and Jean-Claude Spadone

Nestlé Research Center, Vers-chez-les-blanc, 1000 Lausanne 26 Switzerland
philippe.pollien@rdls.nestle.com

Abstract

Flavour modulation throughout eating or drinking experience is often required for numerous food and beverages. For that purpose, different entrapment systems able to modulate the kinetics of aroma release during the consumption event were evaluated on a model system. The release kinetics of aroma compounds loaded into coacervates or dispersed in maltodextrine (reference) were compared. A delayed release from coacervates was clearly observed for compounds having high lipophilicity.

Introduction

The aroma perception of food before and during consumption is a critical factor driving consumer preference. In order to obtain good sensory properties, the aroma compounds have to be delivered at appropriate rate and intensity over time (1). When tasting conventional products, the perception of aroma often decreases after a strong initial burst. Thus, flavour delivery systems become more and more crucial for food companies to modulate the aroma perception of their products.

An aroma model system built on the basis of volatility and lipophilicity of its constituents was used to assess the capability of delivery systems to modulate the concentration of volatiles in the headspace over time. On-line measurements were run by PTR-MS.

Experimental Methods

A model aroma system consisting of six volatile compounds of various known volatility and lipophilicity were encapsulated and the resulting capsules dispersed at 10% in maltodextrine. The following procedure was applied to build the release profiles: 20 mg of sample were put in a glass cell and 100 ml of hot water (70°C) were added. The headspace of the cell was continuously purged at 200 sccm with nitrogen. Prior introduced into the PTR-MS, the headspace was diluted with 5000 sccm nitrogen to avoid water saturation of the instrument. The release of aroma compounds was monitored on-line with a PTR-MS in MID mode. M/z 21 for the primary ion, m/z 37 for water (cluster) as well as specific ion traces for each volatile aroma compound were monitored with cycle time of 9s.

Inside an oven heated at 100°C a double-jacketed glass vessel, thermo-stabilized at 70°C by circulating water, was used to avoid cold points and to prevent water condensation.

Results

The on-line release curves were measured in triplicates with an average variability of about 10%. In the case of linalool dispersed on maltodextrine, a maximum intensity was observed 0.1 min after complete dissolution, which corresponds to the time needed to purge the dead volume of the cell. Immediately after the aroma burst, the signal decreased rapidly to the baseline intensity,

which is the typical behavior for fast-solubilized material. In the case of entrapment system containing linalool, the aroma was delivered more slowly in the headspace to reach a maximum intensity after more than 1min, and decreased progressively afterwards. The average size of the entrapping capsules did not seem to affect linalool delivery.

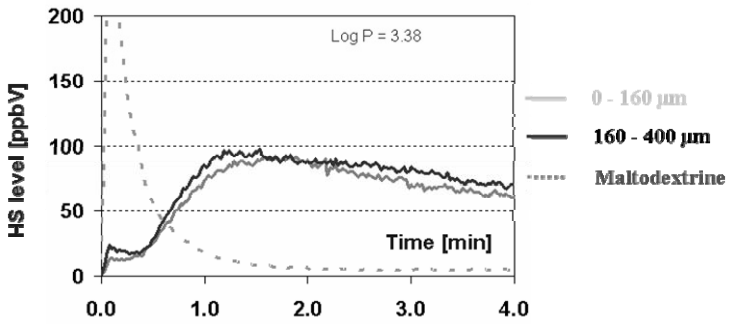

Figure 1: Headspace delivery of linalool dispersed in maltodextrine, or entrapped.

Discussion

As compared to a dispersion in maltodextrine, the entrapment of linalool allowed a modulation of its delivery in the headspace, which was clearly evidenced by on-line PTR-MS measurements. Further sensory evaluations should help to define the best combination of flavour delivery systems able to match consumer expectations.

References

[1] I. Baek, R.S.T. Linforth, A.Blake, A.J. Taylor, Sensory perception is related to the rate of change of volatile concentration in-nose during eating of model gels, Chemical Senses, 24, 155-160, (1999).

Disjunct eddy covariance measurements of biogenic volatile organic compound fluxes from a boreal Scots pine forest

Risto Taipale[1], Janne Rinne[1], Taina M. Ruuskanen[1], Maija Kajos[1], Hannele Hakola[2], Heidi Hellén[2], and Markku Kulmala[1]

[1] *Department of Physical Sciences, University of Helsinki, Helsinki, Finland, risto.taipale@helsinki.fi*

[2] *Air Chemistry Laboratory, Finnish Meteorological Institute, Helsinki, Finland*

Abstract

Large quantities of terpenoid compounds are emitted into the atmosphere from boreal coniferous forests. In addition, boreal forests are estimated to emit significant amounts of non-terpenoid volatile organic compounds (VOCs). In order to quantify these emissions in the canopy scale and to assess their relative importance in comparison with terpenoid emissions, we carried out micrometeorological flux measurements above a boreal Scots pine forest. The flux measurements were conducted using the disjunct eddy covariance method and the associated VOC analysis was done online using proton transfer reaction mass spectrometry. The measured emissions of non-terpenoid VOCs consisted of acetaldehyde, acetone, and methanol. They were on the same order of magnitude as the monoterpene emissions. In order to include non-terpenoid VOCs in emission inventories, further studies aiming at emission algorithm development are required. In future studies, we will estimate the effects of chemical reactions on measured fluxes by a stochastic Lagrangian transport model with simplified chemistry.

Introduction

There are several methods for measuring VOC emissions from vegetation (for a review, see [1]). Chamber methods are used at the leaf and branch scale, whereas micrometeorological surface layer flux methods give emissions at the canopy scale. Fluxes at the regional scale can be obtained using atmospheric boundary layer mass balance and gradient methods. The eddy covariance method is the most direct micrometeorological method. Because its basic idea is simple and it does not require any empirical parameterizations, it is a very useful tool in flux measurements. However, its application has been limited to relatively few VOCs due to the requirement of fast response sensors. Another approach to eddy covariance flux measurements is the disjunct eddy sampling method (see, for example, [2–4]). It relaxes the requirement for fast concentration measurement and thus expands the range of VOCs that can be investigated using the eddy covariance method.

During the summer 2005, we conducted the first disjunct eddy covariance (DEC) measurements of biogenic VOC fluxes in a European boreal forest ecosystem. The VOC analysis was done using proton transfer reaction mass spectrometry (PTR–MS, [5]), which allows online measurement of numerous VOCs, along with some of their atmospheric oxidation products. In this paper, we present the DEC measurement setup and some preliminary results. The theoretical basis of the DEC method is explained by Rinne et al. [4] in an accompanying paper in this same issue. We have also carried out ambient concentration measurements and chamber experiments in

a boreal forest using PTR–MS. The results from these experiments are presented by Rinne et al. [6] and by Ruuskanen et al. [7].

Experimental methods

The measurements were conducted in a boreal forest ecosystem at the SMEAR II measurement station (Station for Measuring Forest Ecosystem–Atmosphere Relations II) of the University of Helsinki in Hyytiälä, southern Finland (61° N, 24° E, 180 m a.s.l.) .The forest around the station is dominated by Scots pine (*Pinus sylvestris*) with some Norway spruce (*Picea abies*), European aspen (*Populus tremula*), and birch (*Betula pendula* and *pubescens*). A detailed description of the measurement station is given by Vesala et al. [8] and by Hari and Kulmala [9].

During June–August 2005, we carried out concentration profile measurements and micrometeorological flux measurements using the DEC method. The vertical profiles were measured using a profiling system with five sampling heights. Four of the sampling heights (4, 7, 10, and 14 m) were located below the top of the canopy (16 m) and the fifth above the canopy (22 m). In this profiling system, air was brought down from all the sampling heights continuously and a valve system was used to select one height at a time. The highest sampling height was used in the flux measurements.

In the DEC measurements, the wind velocity was measured with a three-dimensional sonic anemometer (Solent HS1199, Gill Instruments Ltd.) using a sampling frequency of 10 Hz. The VOC concentrations were measured online with a PTR–MS instrument (Ionicon Analytik GmbH, [5]). The PTR–MS was calibrated using a VOC standard (Apel–Riemer Environmental Inc.) approximately once a week. To identify which VOCs contribute to a particular mass and to validate the concentrations measured by PTR–MS, air samples were collected into adsorbent tubes filled with Tenax–TA and Carbopack–B. These samples were analyzed with a gas chromatograph mass spectrometer (see [10]).

The PTR–MS measurement cycle contained 14 masses which were measured within six seconds. Seven of the measured masses are related to VOCs: M33 (methanol, protonated mass), M45 (acetaldehyde), M59 (acetone), M81 (monoterpene fragment), M99 (hexenal), M101 (hexanal), and M137 (monoterpenes). A sampling time of 0.5 seconds was used for these masses. M37 is attributed to water clusters ($H_2OH_3O^+$) that are formed in the reaction chamber of the PTR–MS. Since the signal of M37 is dependent on ambient water vapour concentration, it could be utilized, especially during the daytime, to determine the lag time between the wind and concentration measurement. The other six masses that were measured were needed either in concentration calculations or in instrumental inspections.

The flux averaging time was 45 minutes. After three-dimensional coordinate rotation to force the vertical mean wind to zero [11] and linear detrending of the wind and concentration time series, the VOC flux was determined by calculating the covariance between the vertical wind velocity and the VOC concentration. An arithmetic average was calculated for every averaging period to determine the fluctuating components from the time series. However, neither frequency response corrections nor data quality tests [11] have been made to the results presented below.

Results and discussion

The measurements carried out during the summer 2005 proved that our measurement setup utilizing PTR–MS is capable of performing disjunct eddy covariance measurements of biogenic VOC fluxes above a forest. The results of the DEC measurements conducted between 14th and 17th July 2005, along with air temperature and photosynthetic photon flux density data, are shown in Figure 1. Significant upward fluxes of methanol, acetaldehyde, acetone, and monoterpenes were observed. The diurnal pattern of fluxes is clear for all these compounds. The average fluxes during the measurement period were 182 μg m^{-2} h^{-1} for methanol, 52 μg m^{-2} h^{-1} for acetaldehyde, 146 μg m^{-2} h^{-1} for acetone, and 556 μg m^{-2} h^{-1} for monoterpenes.

The measurements showed that emissions of non-terpenoid VOCs from the Scots pine forest were on the same order of magnitude as monoterpene emissions. In order to include non-terpenoid VOCs in emission inventories, further studies aiming at emission algorithm development are required. In future studies, we will estimate the effects of chemical reactions on measured fluxes by a stochastic Lagrangian transport model with simplified chemistry (see, for example, [12]).

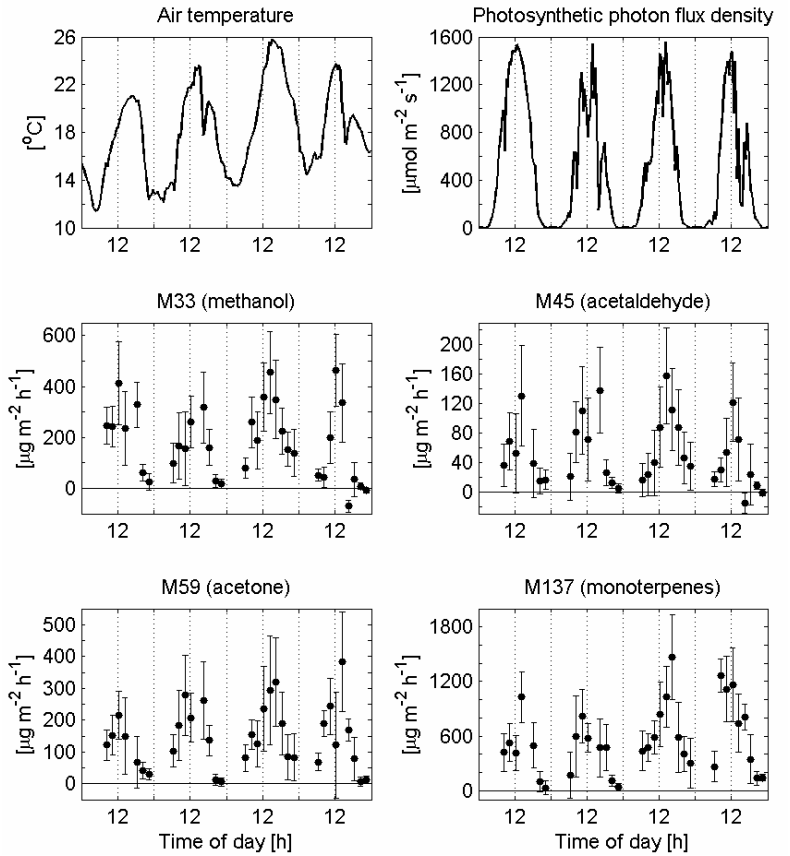

Figure 1: Biogenic volatile organic compound fluxes, air temperature (at 4 m), and photosynthetic photon flux density (at 18 m) measured at the SMEAR II measurement station during 14th–17th July, 2005.

References

[1] W. F. Dabberdt, D. H. Lenschow, T. W Horst, P. R. Zimmerman, S. P. Oncley, and A. C. Delany. Atmosphere–surface exchange measurements. Science 260, 1472–1481, (1993).

[2] D. H. Lenschow, J. Mann, and L. Kristensen. How long is long enough when measuring fluxes and other turbulence statistics? Journal of Atmospheric and Oceanic Technology 11, 661–673, (1994).

[3] H. J. I. Rinne, A. B. Guenther, C. Warneke, J. A. de Gouw, and S. L. Luxembourg. Disjunct eddy covariance technique for trace gas flux measurements. Geophysical Research Letters 28, 3139–3142, (2001).

[4] J. Rinne, R. Taipale, C. Spirig, T. M. Ruuskanen, T. Markkanen, T. Vesala, A. Brunner, C. Ammann, A. Neftel, T. Douffet, Y. Prigent, P. Durand, and M. Kulmala. Measuring ecosystem scale VOC emissions by PTR–MS. This issue, (2007).

[5] W. Lindinger, A. Hansel, and A. Jordan. On-line monitoring of volatile organic compounds at pptv levels by means of Proton-Transfer-Reaction Mass Spectrometry (PTR–MS). Medical applications, food control and environmental research. International Journal of Mass Spectrometry and Ion Processes 173, 191–241, (1998).

[6] J. Rinne, T. M. Ruuskanen, A. Reissell, R. Taipale, H. Hakola, and M. Kulmala. On-line PTR–MS measurements of atmospheric concentrations of volatile organic compounds in a European boreal forest ecosystem. Boreal Environment Research 10, 425–436, (2005).

[7] T. M. Ruuskanen, P. Kolari, J. Bäck, M. Kulmala, J. Rinne, H. Hakola, R. Taipale, M. Raivonen, N. Altimir, and P. Hari. On-line field measurements of monoterpene emissions from Scots pine by proton-transfer-reaction mass spectrometry. Boreal Environment Research 10, 553–567, (2005).

[8] T. Vesala, J. Haataja, P. Aalto, N. Altimir, G. Buzorius, E. Garam, K. Hämeri, H. Ilvesniemi, V. Jokinen, P. Keronen, T. Lahti, T. Markkanen, J. M. Mäkelä, E. Nikinmaa, S. Palmroth, L. Palva, T. Pohja, J. Pumpanen, Ü. Rannik, E. Siivola, H. Ylitalo, P. Hari, and M. Kulmala. Long-term field measurements of atmosphere–surface interactions in boreal forest combining forest ecology, micrometeorology, aerosol physics and atmospheric chemistry. Trends in Heat, Mass and Momentum Transfer 4, 17–35, (1998).

[9] P. Hari and M. Kulmala. Station for Measuring Ecosystem–Atmosphere Relations (SMEAR II). Boreal Environment Research 10, 315–322, (2005).

[10] H. Hakola, V. Tarvainen, T. Laurila, V. Hiltunen, H. Hellén, and P. Keronen. Seasonal variation of VOC concentrations above a boreal coniferous forest. Atmospheric Environment 37, 1623–1634, (2003).

[11] M. Aubinet, A. Grelle, A. Ibrom, Ü. Rannik, J. Moncrieff, T. Foken, A. S. Kowalski, P. H. Martin, P. Berbigier, Ch. Bernhofer, R. Clement, J. Elbers, A. Granier, T. Grünwald, K. Morgenstern, K. Pilegaard, C. Rebmann, W. Snijders, R. Valentini, and T. Vesala. Estimates of the annual net carbon and water exchange of forests: The EUROFLUX methodology. Advances in Ecological Research 30, 113–175, (2000).

[12] C. Strong, J. D. Fuentes, and D. Baldocchi. Reactive hydrocarbon flux footprints during canopy senescence. Agricultural and Forest Meteorology 127, 159–173, (2004).

Monitoring herbivore induced VOC emissions from plants

A. Schaub[1], J. Beauchamp[1], R. Mumm[2], M. Dicke[2], and A. Hansel[1,3]

[1] *Ionicon Analytik GmbH, Innsbruck, Austria, andrea.schaub@uibk.ac.at*

[2] *Laboratory of Entomology, University of Wageningen, Wageningen, The Netherlands*

[3] *Institute of Ion Physics and Applied Physics, Leopold-Franzens University, Innsbruck, Austria*

Abstract

Plants emit increased amount of volatile organic compounds (VOCs) in response to herbivore stress. Some of these volatiles are known to have a signalling effect on predators. We carried out experiments to study the volatile emissions from lima beans which were infested with spider mites. The infested leaves emitted green leaf volatiles (GLV), methylsalicylate, monoterpenes and DMNT (E-4,8-dimethyl-1,3,7-nonatriene). On-line PTR-MS data showed that these compounds are mainly emitted in presence of light.

Introduction

Plants emit increased amounts of volatile organic compounds (VOCs) in response to herbivore attack [1,2]. Such release of herbivore-induced VOCs is known to have a signalling effect that helps the natural enemy of the herbivore to locate its prey [3]. The temporal evolution of these herbivore-induced emissions is of great interest in terms of their ecological function in plant-insect-predator interaction and biological pest control.

Until now most VOC measurements of herbivore-induced emissions used trapping techniques which involve rather long sampling time before GC-MS analysis. While GC-MS is known to have excellent compound identification capabilities, it is not an on-line method. The advantage of PTR-MS is its ability to measure plant VOC emissions virtually in real time, thus retaining important information on emission dynamics. Simultaneous GC-MS and PTR-MS measurements are capable to provide information about quantitative and qualitative changes in plant emissions with high time resolution. Within the European Marie-Curie Training Network ISONET we carried out experiments focussing on herbivore-induced emissions from plants.

Experimental Methods

We carried out climate chamber experiments using leaf cuvettes supplied with scrubbed (free of ozone and VOCs) and humidified air. We used lima beans (*Phaseolus lunatus*) infested with spider mites (*Tetranychus urticae*) and measured VOC emissions of infested lima bean leaves compared to non-infested leaves over a period of ~40 hours. While PTR-MS was monitoring continuously, TENAX samples for GC-MS analysis were taken several times.

PTR-MS fragmentation patterns of specific VOCs which were identified by GC-MS analysis was determined using pure chemical compounds. The compound list includes green leaf volatiles (z-3-Hexenol, z-2-Hexenal, z-3- Hexenyl acetate, Hexyl acetate), monoterpenes (ocimene and

limonene), oxygenated monoterpenes (linalool, 1,8-cineol), methylsalicylate (MeSa), DMNT ((E)-4,8-dimethyl-1,3,7-nonatriene), and TMTT ((E,E)-4,8,12-trimethyl-1,3,7,11-tridecatetraene).

Results

In response to spider mite infestation we observed higher emission of GLV and MeSa (Figure 1), as well as of 2-Butanone ($m73^+$ tentatively identified as 2-Butanone), DMNT, TMTT and sum of monoterpenes (data not shown) from the infested leaf compared to a non-infested leaf.

PTR-MS on-line measurements showed immediately at the start of the measurements emission of GLV and MeSa from the infested and control leave. Such an emission relates to plants response to mechanical stress due to mounting of the enclosures. In darkness no emission of sum of GLV, MeSa, and several other VOC were observed from both leaves. In presence of light the spider mite infested leaf emitted higher amounts of sum of GLV whereas the control had very low emission. On day 1 emission of MeSa was higher from the infested leaf compared to the control leaf and emission was highest between 13-15h. On day 2 immediately after switch on of light the infested leaf emitted GLV and MeSa. In contrast to day 1 the control leaf emitted neither of both compounds on day 2.

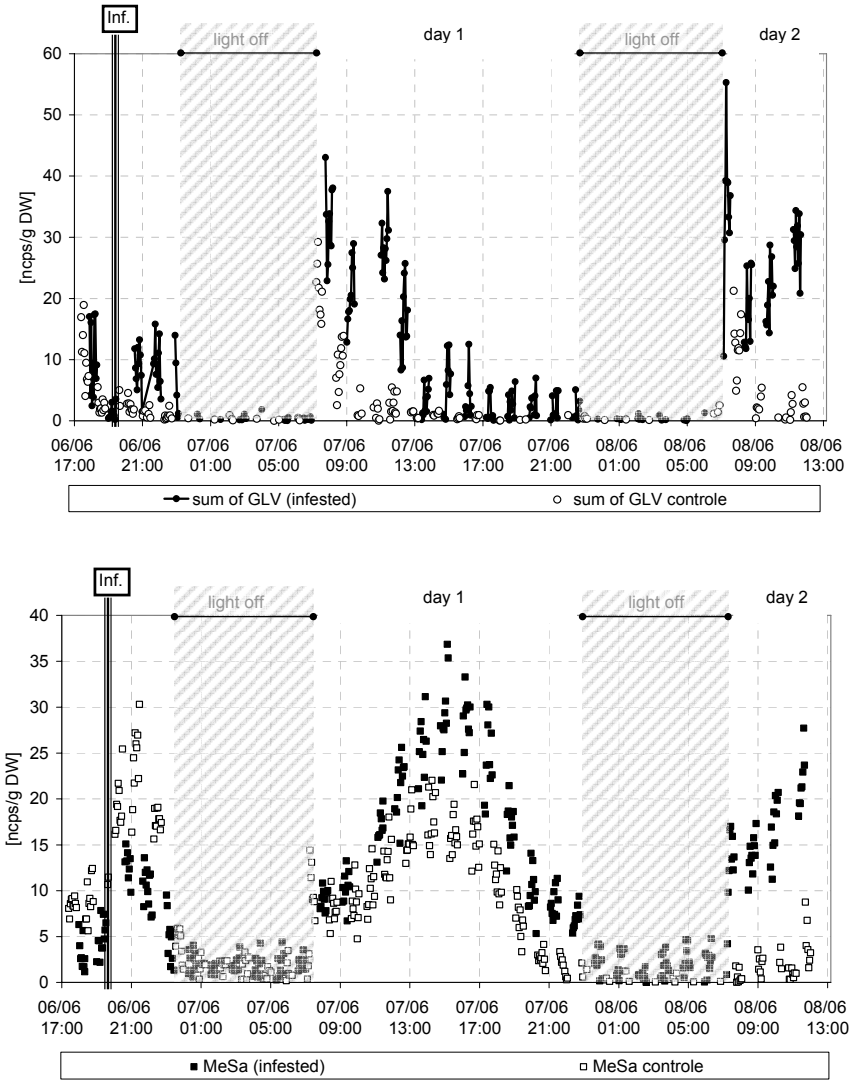

Figure 1: Example for induced emissions of sum of GLVs(top graph) and MeSa (bottom graph) from a spider mite infested lima bean leaf compared to a non-infested leaf (07:00-23:00 light on; 23:00-07:00 light off). Spider mite infestation started at 19:40 on 06/06 (day 1).

Discussion

Both leaves emitted GLV and MeSa which are known to be induced in response to biotic or abiotic stress, thus we observed at the beginning of the experiment unspecific emission of these compounds also from the non-infested leaf. The effect of spider mite attack is shown in emission of GLV and MeSa which was higher during the first and second day. Most striking feature is the absence of herbivore induced VOC emission in absence of light. In addition the diurnal cycle of MeSa indicate a light dependency on emission. Such a light dependency was also observed for 2-Butanone, DMNT, TMTT and sum of monoterpenes. Interestingly the emission of monoterpenes showed a second increase in the evening, which reason is not yet known.

Acknowledgements

We thank Dr. Armin Wisthaler and Dr. Martin Graus for advice in PTR-MS data evaluation. This work was carried out within the European Marie-Curie-Training Network ISONET, contract number MRTN-CT2003-504720.

References

[1] P.W. Paré, and J.H. Tumlinson, De novo biosynthesis of volatiles induced by insect herbivory in cotton plants. Plant Physiology 114, 325-331, (1997).

[2] R.M.P. Van Poecke, and M. Dicke, Indirect Defence of Plants against Herbivores: Using Arabidopsis thaliana as a Model Plant. Plant Biology 6, 387-401, (2004).

[3] M. Dicke, A.A. Agrawal, and J. Bruin, Plants talk, but are they deaf? Trends in Plant Science 8 (9), 403-405, (2003).

[4] J.G. De Boer, M.A. Posthumus, and M. Dicke, Identification of volatiles that are used in discrimination between plants infested with prey or non-prey herbivores by a predatory mite. Journal of Chemical Ecology 30, 2215-2231, (2004).

Vertical Distribution of Air Pollutants in the Inn Valley Atmosphere in Winter 2006

Ralf Schnitzhofer[1], Michael Norman[1], Jürgen Dunkl[1], Armin Wisthaler[1], Alexander Gohm[2], Friedrich Obleitner[2], and Armin Hansel[1]

[1] Institut für Ionenphysik und Angewandte Physik, University of Innsbruck, Innsbruck, Austria, armin.hansel@uibk.ac.at

[2] Institut für Meteorologie und Geophysik, University of Innsbruck, Innsbruck, Austria

Abstract

In order to obtain a three dimensional picture of the spatial distribution of air pollutants in the Inn valley in wintertime, the field campaign INNOX (NO_x-structure in the Inn Valley during High Air Pollution) was carried out in January/February 2006. For this purpose continuous ground based measurements were performed. Additionally, vertical profiles of various air pollutants and meteorological parameters were measured throughout the whole valley atmosphere on six selected days. A tethered balloon was used for carrying meteorological devices and the inlet line of ground level on-line instruments in order to cover the lowest atmospheric layers up to 150 m AGL (above ground level). At higher altitudes a research aircraft from MetAir (http://www.metair.ch) was operated. Preliminary results show not only strong vertical but also horizontal gradients in air pollutant concentrations.

Introduction

Currently there is much debate on public and political levels how to deal with air quality problems in Tirol. There is clear evidence that traffic contributes significantly to air pollution (e.g., [1]). Being one of the main traffic routes between southern and northern Europe, the Brenner route (eastern Inn- and Wipp valley) faces high HDV (heavy duty vehicles) traffic density. The traffic volume in the eastern Inn valley has doubled from 1980 to 2000 [2] and it is predicted to further increase by ca. 40% until 2012 [3]. Although technical progress in car industry reduces vehicles emissions it can not equalize the effect of gradual traffic increase. Therefore additional strategies to improve air quality are necessary. Currently the government implemented a HDV ban during nights and a speed limit (100 km/h) during the winter season (November – April) for the Inn valley motorway (A12). The speed limit imposed in 2006 is supposed to reduce the LDV (light duty vehicles) emissions of NO_x and Particulate Matter by approximately 30% [4]. However, meteorological conditions that control dispersion and dilution of pollutants, decide whether high emissions lead to high immissions of pollutants or not. These effects are considered through the timing of the traffic restrictions. The formation of a stable boundary layer during nighttime keeps pollutants, which are emitted from the surface, trapped at low levels. This processes leads to high concentrations of pollutants in the lowest air layers. Typically the associated low-level temperature inversion breaks up shortly after sunrise, however, in winter it can persist throughout the day [3]. That is why emissions should be minimized during the nights and especially in wintertime. The diurnal and seasonal variations are particularly well pronounced in valleys where topography not only favours the build up of stable cold pools, but also channels the flow and limits its speed [5]. Additionally, a thermal wind system, that in the Inn valley occurs on 30% of all days [6] leads to a recirculation of polluted air [7]. These strong

influences of topography and meteorology cause morning concentrations of NO_x in the Inn valley in winter to be up to nine times higher than over flat terrain with the same emission source strength [8]. The goal of the INNOX-campaign is to obtain a detailed three dimensional picture of air pollutant distribution and to study the key transport and dilution processes of pollutants in winter in this specific topographic area.

Experimental Methods

The INNOX-campaign took place in January/February 2006 near the town Schwaz in the Inn valley, Tirol, Austria. During this period ground based measurements of certain VOCs (Volatile Organic Compounds) were performed using a PTR-MS (Proton-Transfer-Reaction Mass-Spectrometer). In addition, the vertical distribution of various air pollutants was determined on six chosen days. For this purpose miscellaneous analytical systems were carried on the two platforms: a research aircraft from the MetAir AG (Switzerland) and a tethered balloon (Fig. 1).

Figure 1: The two measurement platforms of the INNOX-project can be seen on this picture: The research aircraft (type: Dimona) which measured from about 150 to about 2200 m AGL (crest height) and the Balloon (filled with Helium) that rose to about 150 m AGL.

The balloon carried a teflon tube up to an altitude of 150 m AGL. Through this tube the air was sucked to a PTR-MS and a CO-analyser. Additionally a radiosonde was fixed next to the teflon tube inlet which transmitted meteorological data (air temperature, wind, humidity and pressure) to the ground station. With this setup it was possible to obtain detailed vertical profiles in the lowest atmospheric layers, where the air quality is usually worst and the strongest gradients in pollutants concentrations occur. Additionally the diurnal variations of the thermal stratification and pollutant concentrations were observed with up to 10 soundings per day.

The research aircraft collected vertical profiles from 150 to 2200 m AGL (crestline). It carried more than 100 kg of measurement equipment including instruments for measuring aerosols, CO, NO_x, VOC, and meteorological parameters. The temporal resolution of up to 10 Hz allowed to obtain a three dimensional picture of the distribution of pollutants in the Inn valley atmosphere.

Results and Discussion

Figure 2 shows two profiles of benzene and potential temperature on 1st February 2006. In the morning the very variable volume mixing ratio (VMR) of benzene is around 2 ppbv near ground. Above 20 m AGL the VMR decreases quite fast to a value below 0.5 ppbv at 100 m AGL. The profile of the potential temperature shows a strong near-surface temperature inversion. In the afternoon the VMR of Benzene is homogenous at a level of about 0.7 ppbv up to 120 m AGL. At that height an inversion separates this mixed layer from the air aloft where the VMR is about 0.4 ppbv.

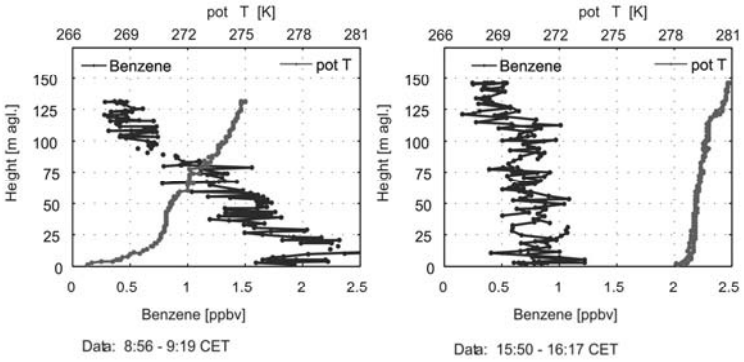

Figure 2: Vertical profiles of Benzene and the potential temperature in the morning (left) and in the afternoon (right) on 1st of February 2006.

How thin the highly polluted layer really is becomes obvious when looking at the profiles of the entire atmosphere (Fig. 3). Here data from measurements in the morning of 1st February 2006 are plotted. At the elevation up to 500 m AGL the VMR of benzene decreases by a factor of ten. At about 1000 m AGL background levels of air pollutant compounds are reached. The potential temperature shows stable stratification until 1500 m AGL, with the strongest temperature increase near the ground. CO shows a higher background level than benzene because of its longer atmospheric lifetime. Interestingly isoprene, which is typically emitted from trees during the growing season, occurs at relatively high concentrations. It shows the same spatial distribution as benzene and CO, which suggests that isoprene is emitted at the bottom of the valley. At the moment it is not clear where this isoprene comes from.

Another interesting result of our investigation is the strong horizontal gradient of air pollutants in the valley. At the sunny side of the valley a thin slope wind layer develops during the day in which polluted air can be transported up to 1500 m AGL (not shown here).

There is clear evidence that the thermal stratification in the valley atmosphere is the important factor for pollution levels in the lowest Inn valley winter atmosphere. Especially in the morning the vertical mixing is poor and emitted pollutants are captured in a very shallow air volume in which pollutant levels are often beyond guideline limits. During the day some mixing occurs and vertical transport along the sunny slopes takes place. However, during these fair weather conditions in winter there is no effective process to exchange air masses in the valley atmosphere.

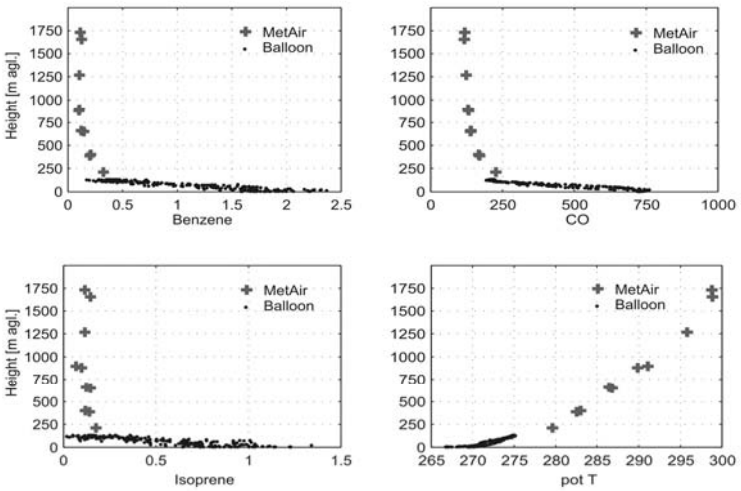

Figure 3: Vertical profiles of Benzene, CO, Isoprene and the potential temperature in the morning (9:00 – 11:15 CET) on 1st of February 2006.

References

[1] Beauchamp, J., Wisthaler, A., Grabmer, W., Neuner, C., Weber, A., Hansel, A., 2004. Short-term measurements of CO, NO, NO_2, organic compounds and PM_{10} at a motorway location in an Austrian valley. Atmospheric Environment 38, 2511-2522.

[2] Verkehrsclub Österreich, 2004. Verkehr ist wachsendes Gesundheitsproblem. Available at: [http://www.vcoe.at/publikationen/factsheets/VCOeFactsheetGesundheitundVerkehr.pdf.]

[3] Thudium, J., 2003: Szenarien der Entwicklung des Schweren Güterverkehrs 2002 - 2012, Auswirkungen des Nachtfahrverbots auf der A12 Oktober 2002 - Jänner 2003. Ökoscience, im Auftrag der Tiroler Landesregierung.

[4] Thudium, J., 2004: Luftschadstoffemissionen im Unterinntal 2003. Ökoscience, im Auftrag der Tiroler Landesregierung.

[5] Dreiseitl, E., and D. Stöhr, 1991: Emission - Meteorologie - Immission. Studie im Auftrag der Tiroler Landesregierung.

[6] Vergeiner, I., Dreiseitl, E., 1987. Valley winds and slope winds - observation and elementary thoughts. Meteorol. Atmos. Phys. 36, 264-286.

[7] Griesser, E., 2003. Quantitative Simulation des NO_x-Konzentrationsverlaufes während der Belastungsepisode im November/Dezember 1999. Master's thesis, Universität Innsbruck.

[8] Wotawa, G., Seibert, P., Kromp-Kolb, H., Hirschberg, M.-M., 2000. Verkehrsbedingte Stickoxid-Belastung im Inntal: Einfluss meteorologischer und topographischer Faktoren. Endbericht zum Projekt Nr. 6983 Analyse der Schadstoffbelastung im Inntal des Jubiläumsfonds der Österreichischen Nationalbank.

Dynamic Gas Dilution System for Accurate Calibration of Analytical Instruments such as PTR-MS

Wolfgang Singer[1], Jonathan Beauchamp[1], Jens Herbig[1], Jürgen Dunkl[1], Ingrid Kohl[1], and Armin Hansel[1,2]

[1] *Ionimed Analytik GmbH, Innsbruck, Austria, office@ionimed.com*

[2] *Institute of Ion Physics and Applied Physics, Leopold-Franzens University, Innsbruck, Austria*

Abstract

The accuracy of quantitative volatile organic compound (VOC) detection is substantially enhanced if the analytical measurement instrument is calibrated for the compounds of interest. We have developed a dynamic gas dilution system that provides variable but known quantities of different standard compounds in a carrier gas stream, enabling accurate calibrations to be made. This gas calibration unit (GCU) has been designed as a standalone device for use with all analytical VOC instruments, but can particularly be used to automatically calibrate an Ionimed/Ionicon PTR-MS. The GCU is currently available in two versions: The 'basic' version enables routine calibrations to be made at ambient/cylinder air humidity; the 'standard' version allows the relative humidity (rH) of the carrier gas to be varied between rH ~25 % and rH ~95 % (at a maximum temperature of ambient conditions). A further 'high-end' version, which should be available by the end of 2007, will include calibration possibilities at higher humidities (at 40 °C) and with varying CO_2 content (intended particularly for breath gas or biological process monitoring applications).

General description of operation

The GCU provides a constant stream of dry/humid VOC-free air in which a steady (but variable) flow of standard gas (at known quantities) is mixed; this results in a carrier gas stream containing known volume mixing ratios (VMRs) of the compounds required for calibration. An overview of operation of the standard GCU is as follows:

Ambient air (drawn in via an internal pump) or cylinder gas (e.g. synthetic air or nitrogen) may be used as the GCU carrier gas. A set of valves allow this gas flow to either by-pass or be directed through a water bubbler (for dry and humid conditions, respectively). This flow subsequently enters a dew point mirror (DPM), which is used to set the desired humidity of the carrier gas from rH ~25% to rH ~95 % (at ambient temperature conditions). The gas exiting the DPM is regulated by a mass flow controller (MFC) to maintain a constant, known flow. A VOC-scrubber at the exit of the MFC destroys most organic compounds present in the carrier gas flow, thus a dry/humid VOC-free air flow at a known flow rate is generated. (This scrubber also allows the GCU to be used as a zero-air generator to provide clean air for other applications, such as headspace measurements.) A calibration gas enters this carrier gas stream via a second MFC, enabling different VMRs of target (standard gas) compounds to be established within the carrier gas. This calibration gas may be taken either from the internal, refillable gas canister provided with the GCU (and filled with one of three currently available gas mixtures; see details below) or from an externally connected cylinder of standard gas.

GCU in combination with PTR-MS

Regular PTR-MS calibrations are necessary to monitor the instrument's performance and to provide accurate quantification of the compounds being measured. The GCU allows a calibration to be performed at different compound VMRs (see below; figure 2), enabling a (linear) calibration curve to be produced that provides a value for the instrument's sensitivity for each respective compound (see below; figure 3). The GCU also enables the PTR-MS instrument's limit of detection (LOD) for a particular compound to be assessed.

PTR-MS measurements are linear at VMRs ranging from the instrument's detection limit to 10 ppmv. The calibration gas standards currently available contain compounds at VMRs of approximately 1 ppmv. A PTR-MS calibration, however, should be performed in the detection range of interest. The standard configuration of the GCU comes with a 3000 ml min^{-1} (at standard temperature and pressure; STP) MFC for the zero-air flow (operating range of 60-3000 ml min^{-1}; optimum zero-air flow range between 250-1500 ml min^{-1}, outside which the VOC-scrubbing efficiency is reduced), and a 20 ml min^{-1} (at STP) MFC for adding the standard gas (0.4-20.0 ml min^{-1}). In this configuration and with the presently available calibration gas containing VOCs at ~1 ppmv per compound, a calibration range from approximately 0.3 ppbv (300 pptv) to 75 ppbv (0.75 ppmv) may be covered.

The maximum and minimum dilution ratios accessible and their respective VMRs for a 1 ppmv gas are:

Maximum dilution:	0.4 / (1500+0.4) [ml min^{-1}]	= 0.27×10^{-4}	→ 0.3 ppbv
Minimum dilution:	20.0 / (250+20) [ml min^{-1}]	= 0.75	→ 75 ppbv

A graphical representation of the high sensitivity (hs) PTR-MS detection range and the calibration range offered by the GCU is given in figure 1.

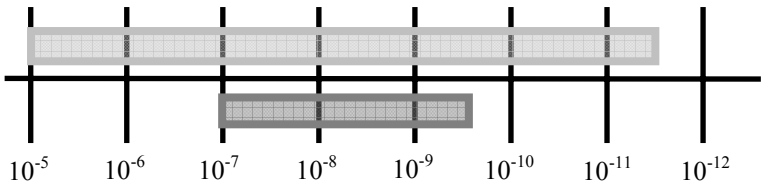

Figure 1: Upper box: VMR linearity range of hs-PTR-MS; Lower box: gas VMRs accessible by the GCU.

By selecting a required range of VMRs for calibration a 'calibration sequence' can be configured to measure the desired compounds. The raw data cycles from an example calibration of four compounds is shown in figure 2 (top). For this calibration an initial set of zero-air measurements (20 cycles) was followed by a gradual stepwise increase (with 20 measurement cycles per step) of

the calibration gas mixed into the carrier gas stream. A final zero-air measurement was made to test the stability and reproducibility of the instrument background signal on these masses. The second part of figure 2 (bottom) shows a humidity-dependent calibration of acetone. Again, this was a step-function calibration with zero-air measurements made at the beginning and end of the measurement sequence. The change in humidity in this case had only a minimal effect on the acetone signal: Dry and humid sensitivities of acetone were 25.4 and 25.2 ncps $ppbv^{-1}$, respectively (ncps refers to absolute count-rates normalised to a primary ion signal – including water clusters – of 10^6 cps; calibration curves not shown). Following a calibration the individual data can be normalised to the hydronium (plus water cluster) primary ion signal and the background (zero-air) signal for each mass can be subtracted, resulting in a net ncps signal per compound, per VMR. The resulting plot of these net ncps data versus VMR for the individual compounds gives a linear relationship, with the gradient providing the instrument's sensitivity per compound (figure 3). A LOD (e.g. at S/N=2) may also be estimated using the zero-air data.

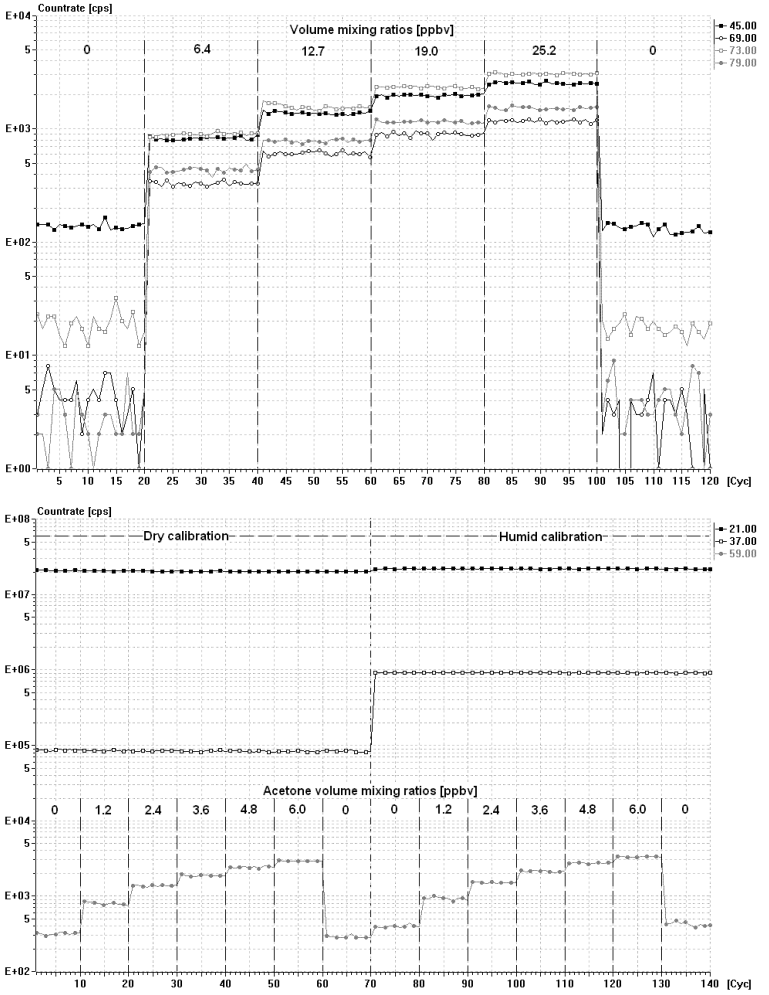

Figure 2: Top: PTR-MS calibration routine of four standard gas compounds (acetaldehyde, 45^+; isoprene, 69^+; 2-butanone, 73^+; benzene, 79^+). VMRs shown are mean values of all four compounds together. Bottom: Calibration of acetone (59^+) for dry and humid conditions. The increased humidity in the second half of the calibration is clearly seen in the increased hydronium cluster ion (37^+) signal. The 0 ppbv count-rates at the beginning and end of both calibrations represent zero-air from the GCU.

Hardware-Software Interface

Although the GCU can be configured manually (i.e. selection of carrier gas via pump or cylinder, MFC flows, etc.), it may also be connected to and operated by an external computer (e.g. that of the PTR-MS) via a USB port. This allows for full automation of dilution flows, enabling a PTR-MS calibration to run via a standard sequence, thereby cutting back laboratory personnel time for such a procedure and reducing a calibration to a simple task.

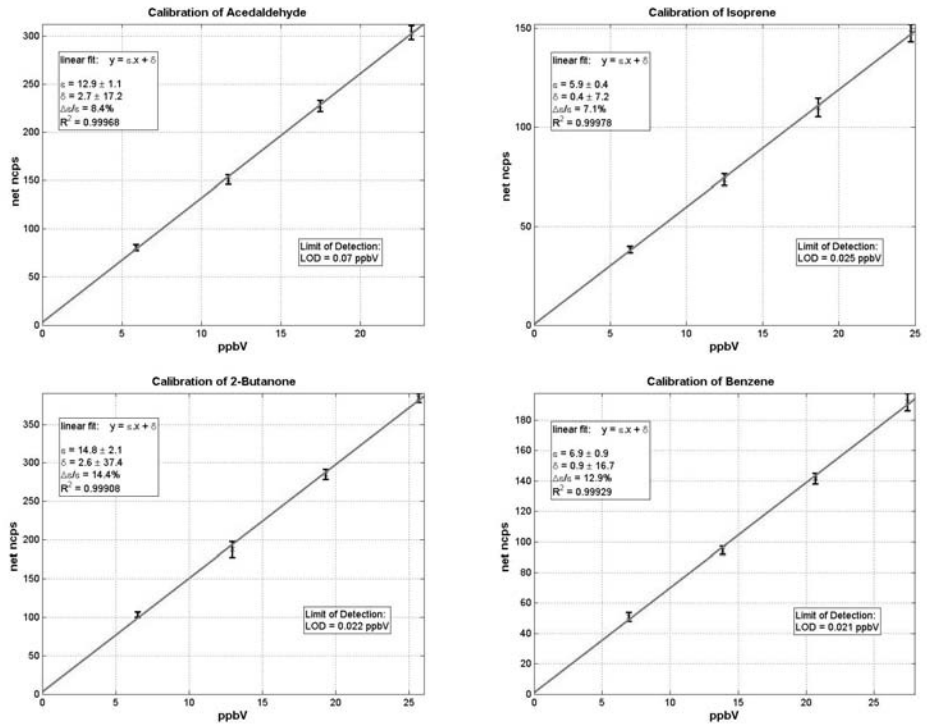

Figure 3: Calculating and plotting the normalised count-rates (ncps) versus the VMRs for each particular compound yields the measured sensitivity, ε, of the individual substance. (Sensitivities here, in ncps ppbv^{-1}, are: acetaldehyde, 12.9; isoprene, 5.9; 2-butanone, 14.8; benzene, 6.9.) The limit of detection (LOD; at S/N = 2) for each compound, based on the background signal of the respective mass, may also be calculated using the calibration data.

Future perspectives

Currently the GCU valves (e.g. to select dry/humid conditions) must be operated manually. Ionimed plans to upgrade these with electronic valves to provide a fully-automated, computer-controlled feature (e.g. for use in a measurement sequence). In addition, in the current 'standard' version a change in humidity from dry to humid, or vice versa, requires an equilibration time of at

least one hour. A planned future upgrade of the GCU will enable faster switching between different humidity levels at much reduced time scales. A 'high-end' version of the GCU is also planned to cater to PTR-MS uses requiring calibrations at higher humidity levels, which is primarily intended for those working in the fields of breath gas research or biotechnology. This planned concept, featuring an internal heating system, will allow rH 100 % at 40 °C to be achieved. Furthermore, for this high-end version, a CO_2 gas inlet and MFC will be integrated to allow calibration for high CO_2 applications (e.g. desirable for breath gas measurements, fermentations, etc.).

Gas Standards Currently Available

At present we can provide three different mixtures of calibration gas with the GCU, as listed in the following table:

Compound	Volume Mixing Ratio in each Gas Standard [ppmv]		
	Gas Mixture #1	Gas Mixture #2	Gas Mixture #3
Formaldehyde	-	0.92	1.00
Methanol	1.40	1.17	-
Acetonitrile	1.04	0.99	-
Acetaldehyde	1.18	1.05	1.10
Ethanol	1.30	1.03	-
Acrolein	-	-	0.98
Acetone	1.20	1.05	-
Propanal	-	-	1.06
Isoprene	1.26	1.05	-
Crotonaldehyde	-	-	0.98
2-Butanone	1.31	1.05	-
Benzene	1.40	0.99	-
Valeraldehyde	-	-	0.96
Toluene	1.17	0.98	-
Hexanal	-	-	0.99
O-Xylene	1.23	1.02	-
M-Xylene	1.24	1.03	-
Heptanal	-	-	0.91
a-Pinene	1.14	0.95	-
Octanal	-	-	0.81
Nonanal	-	-	0.74
Decanal	-	-	0.57

Detection of processed animal proteins in feedstuffs: evaluation of PTR-MS

Saskia van Ruth[1], Leo van Raamsdonk[1], Nooshin Araghipour[2], and Jennifer Colineau[1]

[1] *RIKILT – Institute of Food Safety, Wageningen UR, P.O. Box 230, NL-6700 AE Wageningen, the Netherlands, saskia.vanruth@wur.nl*

[2] *Institut für Ionenphysik, University of Innsbruck, Technikerstr. 25, A-6020 Innsbruck, Austria*

Abstract

Proton Transfer Reaction Mass Spectrometry (PTR-MS) was evaluated for detection of various processed animal proteins in compound feeds. The headspace of the samples was mass analysed (mass range *m/z* 20-150) and the headspace concentrations calculated. The concentrations were subjected to Principal Component Analysis in order to examine if PTR-MS could discriminate between meat-and-bone meals (MBMs), fish meals, and feeds fortified with these processed animal proteins (PAP). The averages of the groups were discriminated satisfactory and in a logical order. However, the groups showed overlap. The present study showed the potential of PTR-MS for screening compound feedstuffs, but further research would be required to examine improvements.

Introduction

The most likely route of infection of cattle with bovine spongiform ecephalophaty (BSE) is by consumption of feeds containing processed animal proteins. This route of infection resulted in feed bans. The bans were initially aimed at ruminant feeds (regulation 2001/1999/EC). Later the ban was extended to all feeds for farmed animals (regulation 2003/1234/EC). This extended ban overrules temporarily the 'species-to-species ban' (regulation 2002/1774, EC). This ban prohibits the feeding of animal-specific proteins to the same species. However, this regulation is effectively inactive as it requires support of species-specific identification methods, which are not available presently [1].

Microscopy has been acknowledged as the standard method and allows the detection at the present limit of 0.1% PAPs in feeds [2]. Microscopy requires extensive training of personnel and does not reliably differentiate between species specific MBMs, e.g. those originating from ruminants and non-ruminants. Method development in this area has received substantial attention over the last few years. It remains a challenge, however, to distinguish species specific MBMs especially at the detection levels required (0.1%).

The aim of the present study was to evaluate Proton Transfer Reaction-Mass Spectrometry for the detection of various PAPs in compound feedstuffs.

Experimental Methods

Materials

Various types of MBMs (11 samples, 4 types), fish meals (4 samples), compound feeds for bovine (3 samples, vegetable origin) and feeds fortified with PAPs (15 samples) were examined. Pure MBMs included mammalian, ruminant, poultry, and feather MBMs. Fortified feeds consisted of vegetable material with and without addition of 0.1% or 0.5% MBM and with and without 5% fish meal. In total, 29 samples of PAP material, feedstuffs, or combinations of feedstuffs and PAP were examined. The origin of the samples have been specified previously [3,4] and their identity was confirmed by microscopy.

Methods

Sample material (1.5 g) was placed in a 250 ml glass flask at 30°C. The sample was equilibrated for at least 30 min prior to analysis. During the analysis the headspace of the sample was drawn at a rate of 3 ml/min by a vacuum pump, and was led through a heated Teflon transfer line (50°C) into the PTR-MS. The headspace was mass analysed according to the method described by Lindinger et al. [5]. A constant drift voltage of 600 V and a pressure of 2.1 ± 0.1 mbar in the reaction chamber was applied. Data were collected for mass range *m/z* 20-150 at a rate of 0.2 s/mass. Each sample was measured for at least 5 cycles. The average headspace concentrations measured during cycles 2, 3 and 4 were calculated as described previously [6] after background and transmission corrections. Average headspace concentrations were subjected to Principal Component Analysis (PCA).

Results and Discussion

The headspace of the 100% PAP samples and the compound feeds for bovine fortified with PAP were examined by PTR-MS analysis. Concentrations were calculated and were subsequently subjected to PCA. A plot of the first two dimensions of the PCA carried out on all the data is presented in Figure 1. The average factor scores for the MBMs, fish meals, and feeds are displayed in a PCA plot of the first two dimensions in Figure 2. A high negative score on the first dimension is observed for the MBM. The scores on the first dimension increase in the following order for the other samples: MBM<Feed+MBM<Feed<Feed+Fish meal+MBM< Feed+fish. These results show that nearly all samples were separated on the first dimension. The 100% fish meals showed a high negative loading on the second dimension. The discrimination of the means of the samples in a logical order reveals the potential of this type of methodology for feed sample screening. However, the sample groups showed overlap (Fig. 1), which means that further optimisation would be required to distinguish samples unambiguously. With the present sample set it was not possible to distinguish consistently between the various MBMs.

Campagnoli and co-workers [7] evaluated electronic nose technology for detection of various MBMs with a 10 (non-specific) sensor instrument. Their study revealed that ENose could identify samples with either MBM or fish meal, but samples fortified with both components were not discriminated from samples containing fish meal solely.

For control of EU regulations, unambiguous assignment of unknown samples to the feed or feed+MBM groups is of paramount importance. The present study showed that PTR-MS is an

interesting approach for screening compound feedingstuffs. It is a fast, non-destructive, cost-effective alternative. However, further studies for further evaluation, optimisation of the methodology and statistics is required.

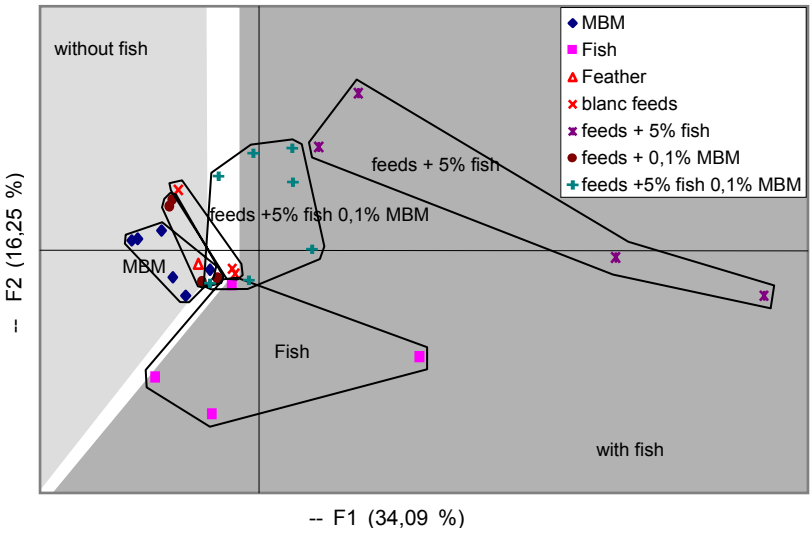

Figure 1: First two dimensions of PCA on concentrations measured by PTR-MS for a variety of feeds, PAPs and feeds fortified with PAPs (F+number=Feed, e.g. F1; 100% PAPs in capitals): factor scores of samples .

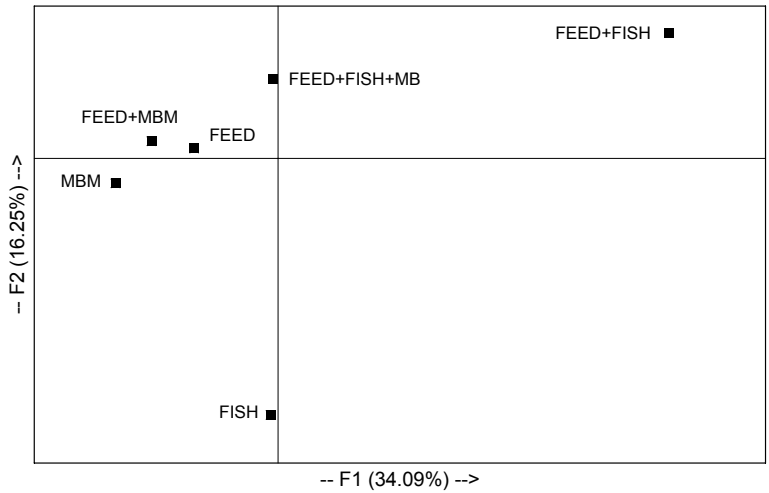

Figure 2: First two dimensions of PCA on concentrations measured by PTR-MS for a variety of feeds, PAPs and feeds fortified with PAPs (F+number=Feed, e.g. F1; 100% PAPs in capitals): average factor scores of sample groups.

Acknowledgement

Authors wish to acknowledge Ms Wilma Hekman (RIKILT, the Netherlands) for the microscopic verification of the identity of the sample material.

References

[1] L.W.D. van Raamsdonk, C. von Holst, V. Baeten, G. Berben, A. Boix, and J. de Jong, New developments in the detection and identification of processed animal proteins in feeds, Animal Science and Technology, (2006) in press.

[2] L.W.D. van Raamsdonk, J. van Cutsem, J. Zegers, G. Frick, J.-S. Jorgenson, V. Pinckaers, J. Bosch, and I. Paradies-Severin, The microscopic detection of animal proteins in feeds, Biotechnologie, Agronomie, Société et Environment. 8, 241-247, (2004).

[3] G. Gizzi, C. von Holst, V. Baeten, G. Berben, L.W.D. Van Raamsdonk. Determination of Processed Animal Proteins, including meat and bone meal, in animal feed, JAOAC 87, 1334-1341 (2003).

[4] L.W.D. van Raamsdonk and H. van der Voet, A ring trial for the detection of animal ttissues in feeds in the presence of fish meal, RIKILT report 2003.012, RIKILT, Wageningen (2003).

[5] W. Lindinger, A. Hansel, A. Jordan, On-line monitoring of volatile organic compounds at pptv levels by means of proton-transfer-reaction mass spectrometry (PTR-MS): medical applications, food control and environmental research, International Journal of Mass Spectrometry and Ion Processes 73, 191-241 (1998).

[6] A. Hansel, A. Jordan, R. Holzinger, P. Prazeller, W. Vogel, and W. Lindinger, Proton transfer reaction mass spectrometry: on-line trace gas analysis at the ppb level. International Journal of Mass Spectrometry and Ion Processes 149/150, 609-619 (1995).

[7] A. Campagnoli, L. Pinotti, G. Tognon, F. Cheli, A. Baldi, and V. Dell'Órto, Potential application of electronic nose in processed animal proteins (PAP) detection in feedstuffs, Biotechnologie, Agronomie, Société et Environment 8, 253-255 (2004).

Can PTR-MS Measure Propylene Quantitatively in the Atmosphere?

Carsten Warneke[1,2], Joost de Gouw[1,2], Dan Welsh-Bon[1,2], William C. Kuster[1],

[1] NOAA Earth System Research Laboratory, Boulder, Colorado, USA, carsten.warneke@noaa.gov

[2] Cooperative Institute for Research in Environmental Sciences, University of Colorado, Boulder, Colorado, USA

Abstract

Propylene is detected by PTR-MS on mass 43. Many other volatile organic compounds (VOCs) such as, acetone, acetic acid, acetaldehyde, peroxy acetyl nitrate (PAN), and many alkanes and alkenes also produce ions on mass 43. We have used a combination of a gas chromatographic (GC) pre-separation and detection by PIT-MS (proton-transfer ion trap-mass spectrometry) to determine the interferences for the propylene measurements. The corrected propylene measurements using PTR-MS and PIT-MS are inter-compared with GC measurements during measurement campaigns in Houston, Texas, and Mexico City.

Introduction

In the summer of 2006 we deployed a proton-transfer ion trap mass-spectrometry (PIT-MS) instrument onboard the NOAA research vessel *Ronald H. Brown* and a PTR-MS onboard the NOAA WP-3D research aircraft to study the ozone chemistry in Houston, Texas, as part of the Texas Air Quality Study (TEXAQS2006). In spring of 2006 the PIT-MS was deployed at a ground site in Mexico City as part of the MILAGRO campaign. During both studies GC-PIT-MS analysis were done in parallel to the ambient air measurements using PTR-MS, PIT-MS and also GC-FID.

Propylene is an important trace gas for the production of ozone. It is emitted in large quantities by anthropogenic sources such as vehicle exhaust and industrial processes. Especially in Houston, Texas, where a large number of oil refineries and other crude oil related industries are located, propylene and also ethylene are emitted by a large number of point sources, regularly causing high ozone in the summer months.

Propylene, detected at mass 43 with PTR-MS, suffers from various interferences on this mass. In this work we investigate, if PTR-MS is capable of quantitative measurements of propylene.

Experimental Methods

The VOC measurements in this work were mostly made by PTR-MS and PIT-MS, which is a PTR-MS type instrument that features an ion trap mass spectrometer instead of a quadrupole mass filter [1]. Additional VOC measurements were obtained by gas chromatographic techniques, both on-line and from canister sampling, and detailed inter-comparisons with PTR-MS and PIT-MS measurements of many different compounds, propylene not included, have been made with generally favorable results [2,3,4].

GC-PIT-MS analysis were done using a home-built GC system that acquires a sample in five minutes and uses a DB-5 column for gas chromatographic separation, where one chromatogram takes about 20 minutes. The column effluent is directly injected into the PIT-MS, where a full mass spectrum is acquired every two seconds during the chromatogram [5].

Results and Discussion

The results of four GC-PIT-MS chromatograms of mass 43 acquired on the *Ronald H. Brown* in and around the Houston industrial region during the TEXQAS2006 air quality study are shown in Figure 1. The first panel shows a chromatogram measured out in the Gulf of Mexico in an area of relatively clean air. The two peaks are identified as fragments from acetaldehyde and acetone, respectively. The second chromatogram was taken in the ship channel Turning Basin downwind of Houston downtown. The main peak is identified as propylene, but acetaldehyde and acetone are also prominent. The chromatogram taken in Jacinto port was just downwind of the Shell refinery. The main peak is identified as propylene, but a large number of other compounds also contribute to the signal on mass 43. The last chromatogram was taken in an area called Barbour's Cut in the Houston ship channel. The main peak was identified as vinyl acetate, which is used as a solvent in a nearby industrial facility. Here it should be mentioned that PAN and acetic acid, both also contributing to the signal on mass 43, cannot be detected with GC-PIT-MS.

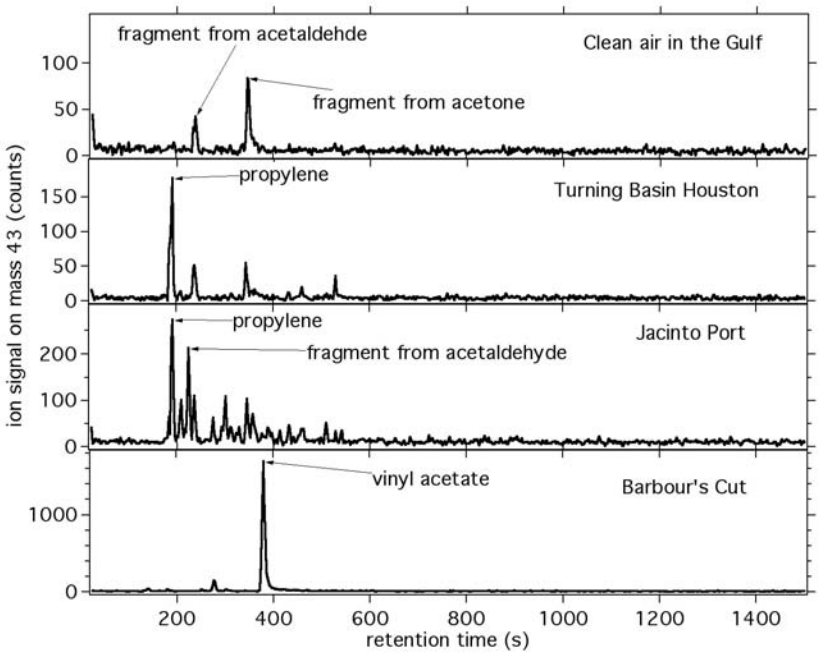

Figure 1: GC-PIT-MS chromatograms of mass 43 acquired in and around the Houston industrial area.

Figure 2 shows the results from the PTR-MS measurements during a flight with the NOAA WP-3 aircraft over Texas on September 19, 2006. This flight was designed to measure the Houston emissions and subsequently follow the urban and industrial plume further downwind as it gets more processed. Also intercepted were some plumes of industrial facilities that are known propylene emitters.

Shown in the first panel are the raw data for mass 43 (propylene + other VOCs) and mass 59 (acetone) measured by the PTR-MS. In the second panel the contribution from acetone, which seems to be the largest contributor to mass 43 during this flight, is subtracted from the mass 43 signal. Also shown in this graph is the propylene GC measurement from canister samples collected during the flight. It can be seen that the corrected PTR-MS "propylene" measurement agrees fairly well with the GC.

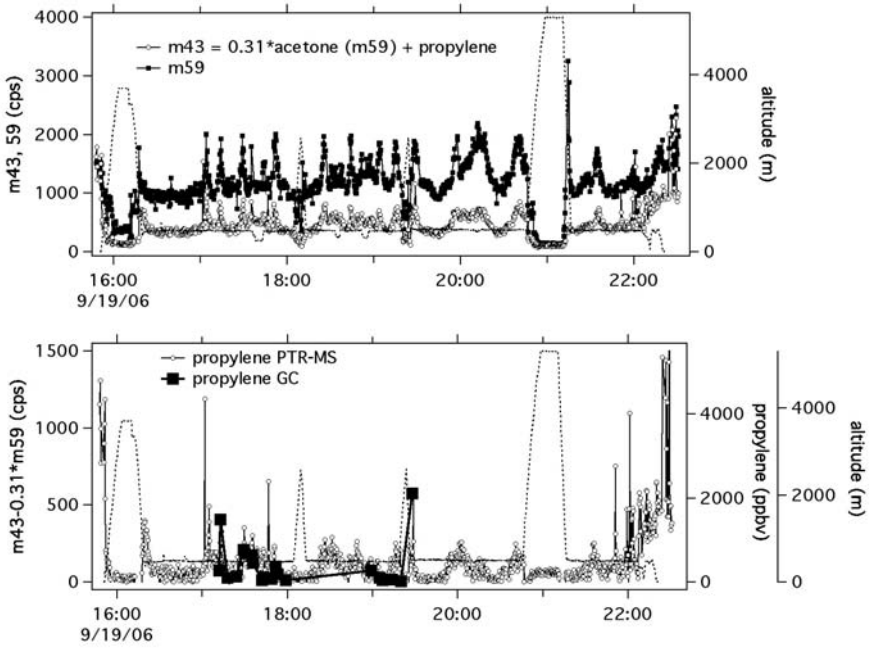

Figure 2: PTR-MS raw data for mass 43 and mass 59 (upper panel). Corrected PTR-MS propylene measurements and comparison with GC data (lower panel). (Propylene data are courtesy of Elliot Atlas, University of Miami).

During the TEXAQS2006 flights, the *Ronald H. Brown* cruise and the Mexico City experiment, measurements for most of the interfering VOCs are available to correct the mass 43 measurements. The resulting PTR-MS and PIT-MS propylene data, corrected for the known interferences, will be compared with the available GC measurements.

References

[1] C. Warneke, J.A. de Gouw, E.R. Lovejoy, P.C. Murphy, W.C. Kuster, R. Fall, Development of proton-transfer ion trap-mass spectrometry: on-line detection and identification of volatile organic compounds in air, Journal of the American Society of Mass Spectrometry 16, 1316-1324 (2005).

[2] J.A. de Gouw, P.D. Goldan, C. Warneke, W.C. Kuster, J.M. Roberts, M. Marchewka, S.B. Bertman, A.A.P. Pszenny, W.C. Keene, Validation of proton transfer reaction-mass spectrometry (PTR-MS) measurements of gas-phase organic compounds in the atmosphere during the New England Air Quality Study in 2002, Journal of Geophysical Research 108, 4682, doi:10.1029/2003JD003863 (2003).

[3] J.A. de Gouw, et al., Volatile organic compounds composition of merged and aged forest fire plumes from Alaska and western Canada, Journal of Geophysical Research 111, D10303, doi:10.1029/2005JD006175 (2006).

[4] Warneke, C., S. Kato, J. A. de Gouw, P. D. Goldan, W. C. Kuster, M. Shao, E. R. Lovejoy, R. Fall, and F. C. Fehsenfeld (2005), On-line VOC measurements using a newly developed PIT-MS instrument during NEAQS-ITCT 2004: Inter-comparison and identification, Environ. Sci. Technol., 39, 5390-5397, (2005).

[5] C. Warneke, J.A. de Gouw, W.C. Kuster, P.D. Goldan, Validation of atmospheric measurements by proton-transfer-reaction mass spectrometry using a gas-chromatographic pre-separation method, *Environ. Sci. Technol.* 37,2494-2501, (2003).

In-Situ Evidence for Free-Troposheric Longrange Transport of a Siberian Forest Fire Plume to the North Pole Region

Armin Wisthaler[1], Erik Swietlicki[2], Michael Tjernström[3], Armin Hansel[1] and Caroline Leck[3]

[1] *Institute of Ion Physics and Applied Physics, Innsbruck University, A-6020 Innsbruck, Austria*

[2] *Div. of Nuclear Physics, Lund University, P.O. Box 118, S-22100 Lund, Sweden*

[3] *Department of Meteorology, Stockholm University S-10691 Stockholm, Sweden*

Introduction

Recent modeling studies by Stohl and co-workers [1-3] suggest the occurrence of summertime long-range transport to the Central Arctic of continental pollution in general, and of boreal forest fire plumes in particular. The simulations indicate that polluted continental air masses are lifted and transported towards the pole, leaving the Arctic boundary layer (ABL) largely unaffected by these long-range transport phenomena. This is in agreement with ground-based observations at high northern latitudes (> 85°N), where very clean atmospheric conditions are generally found during the summer months [4,5]. This postulated summertime long-range transport of continental pollution to the Arctic free troposphere is however poorly constrained by observations at high northern latitudes. Here we present the first in-situ evidence for the presence of a Siberian forest fire plume at ~ 3 km altitude close to the North Pole in summer 2001.

Experimental Methods

The summer 2001 Arctic Ocean Expedition (AOE-2001) led the Swedish icebreaker Oden to the central Arctic, mostly north of latitude 85°N in July-August 2001. The Oden was equipped with a helicopter to obtain vertical profiles of aerosol particle number concentrations in various size ranges (36 flights), as well as organic trace gases such as acetone, acetonitrile and dimethyl sulfide (in 14 out of the 36 flights). The aerosol particle size concentrations were measured at 1 Hz in several size ranges using two Condensation Particle Counters (TSI UCPC 3025, TSI CPC 3010) and an Optical Particle Counter (OPC, Climet CI-500, >300 nm). Organic trace gases were measured by PTR-MS (Proton Transfer Reaction-Mass Spectrometry). This technique has previously been successfully used for measurements of acetonitrile in biomass burning related studies [6-8].

Here we mainly focus on results obtained during a research flight (Flight #23) that reached the helicopter ceiling height of 3.6 km at 88.3°N, 2°W on August 8, 2001, 18:09-19:11 UTC.

Results

Figure 1 shows the vertical profiles of acetonitrile and aerosol particle number concentrations for particles >300 nm.

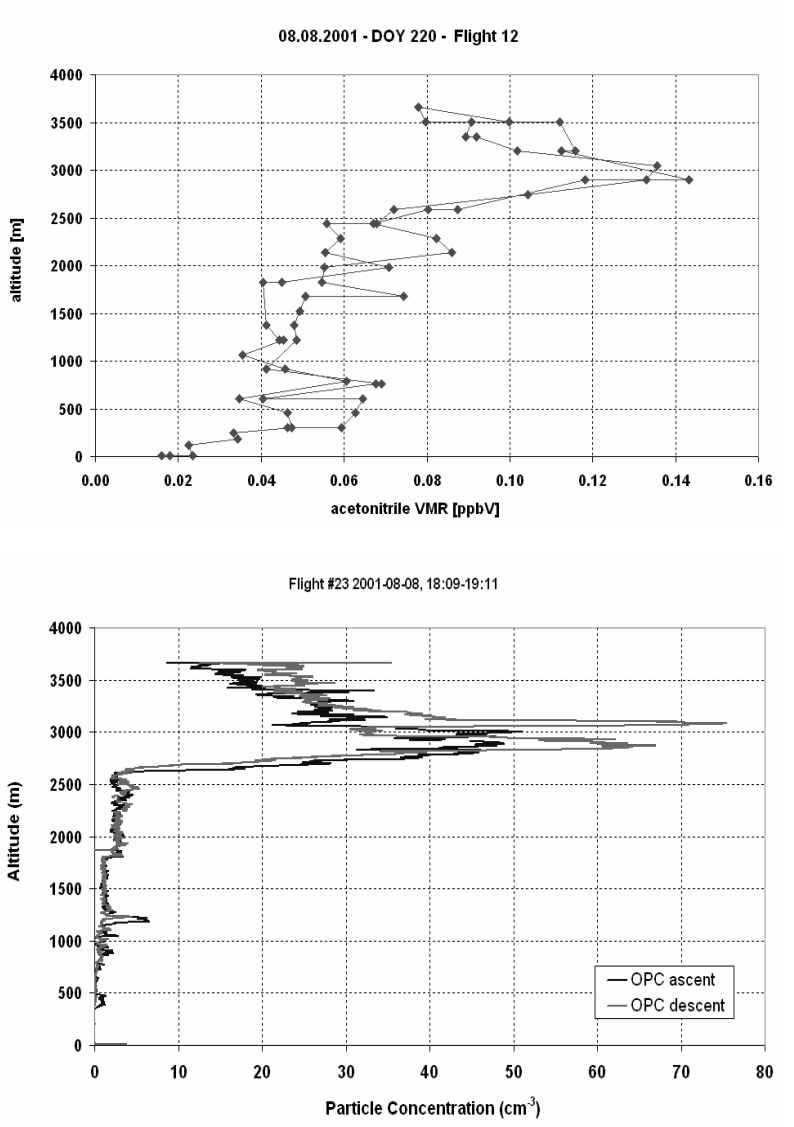

Figure 1. Vertical profiles of acetonitrile (PTR-MS) and aerosol particle number concentrations >300 nm (OPC) and during Flight #23 up to the helicopter ceiling height of 3.6 km at 88.3°N, 2°W on August 8, 2001. The plume from forest fires in NE Siberia was observed at altitudes >2600 m.

Acetonitrile (CH_3CN) is a specific tracer for biomass burning [9]. Considering the long atmospheric lifetime of acetonitrile (on the order of months) and the low levels observed in the ABL, the Arctic Ocean must act as a sink for acetonitrile. The positive acetonitrile gradient above the ABL can be explained by long-range transport from lower latitudes (Figure 1). The enhancement of acetonitrile in the layer at ~ 3 km may be explained by long-range transport of a forest fire plume. The number concentrations of particles detected in the OPC (>300 nm) also increase drastically when entering the plume (Figure 1).

There is supporting evidence from fire maps and dispersion modelling that the plume intercepted during Flight #23 on 8 Aug 2001 above 2600 m altitude originated from NE Siberian forest fires. Various fire map products consistently show no or little large-scale biomass burning in Canada and Alaska, during August 2001, while there were large forest fires seen in NE Siberia. During the time period of interest (3-8 Aug 2001), TOMS and SeaWIFS images show large smoke plumes moving north-eastwards from Siberia, over the Bering Strait. The polar coverage of these remote sensing data is however poor. Dispersion modelling using the NAAPS (Naval Research Laboratory Aerosol Analysis and Prediction System) model [10] predicts that during August 2001, boreal forest fire plumes reached the central Arctic and the North Pole on two occasions. The first event started around August 1-2 with the plume moving northwards from Siberia over the Arctic Ocean and influencing the Pole between August 4-8. The NAAPS model indicates that the transport of Siberian smoke is transported mostly in coherent synoptic “filaments” or plumes, and is typically seen ahead of fronts over Siberia [11]. Occasionally the plumes also move towards very high latitudes, as seen in August 2001.

Discussion

We present the first in-situ evidence of free-tropospheric long-range transport of plumes originating from forest fires at lower latitudes (NE Siberia) to the summertime central Arctic (88.3°N). The elevated concentrations of acetonitrile clearly point to a biomass burning source. Acetonitrile was also strongly correlated with aerosol particle number concentrations for sizes >300 nm in the same plume.

The Arctic boundary layer (ABL) was otherwise observed to be largely unaffected by these long-range transport phenomena. The radiation balance of the summertime central Arctic is largely governed by the presence and properties of the low-level clouds at the top of the ABL at <200 m altitude. Since the ABL is typically capped by a strong inversion, there is little vertical mixing from aloft into this cloud layer. The in-situ observations presented here and supporting dispersion modeling indicate that long-range transport from ground sources at lower latitudes into the central Arctic free troposphere may be frequent in summertime, when melting of pack ice is very sensitive to even minor changes in the radiation balance. However, due to the strong inversion, the polluted air masses aloft are not efficiently mixed downwards and are therefore less likely to affect the cloud microphysics of the lowest clouds. Cloud reflectivity, and hence the climate sensitivity, should therefore be more influenced by the aerosol particles present in the surface air than in the free-tropospheric air originating from distant sources. Wet deposition of light-absorbing aerosol material from the plume aloft and onto the snow and pack ice is nevertheless a possible mechanism by which pollution from lower latitudes might affect the Artic summertime radiation balance.

Acknowledgements

We wish to acknowledge the Swedish Polar Research Secretariat, the Swedish Natural Science Research Council, the Nordic Council of Ministers, the K&A Wallenberg Foundation, Bundesministerium für Bildung, Wissenschaft und Kultur, and Verein zur Förderung der wissenschaftlichen Ausbildung und Tätigkeit von Südtirolern an der Landesuniversität Innsbruck.

References

[1] Stohl, A., E. Andrews, J. F. Burkhart, C. Forster, A. Herber, S. W. Hoch, D. Kowal, C. Lunder, T. Mefford, J. A. Ogren, S. Sharma, N. Spichtinger, K. Stebel, R. Stone, J. Ström, K. Tørseth, C. Wehrli, and K. E. Yttri (2006): Pan-Arctic enhancements of light absorbing aerosol concentrations due to North American boreal forest fires during summer 2004. J. Geophys. Res. In press.

[2] Stohl, A. (2006): Characteristics of atmospheric transport into the Arctic troposphere. J. Geophys. Res. 111, D11306, doi:10.1029/2005JD006888.

[3] Stohl, A., S. Eckhardt, C. Forster, P. James, N. Spichtinger (2002): On the pathways and timescales of intercontinental air pollution transport. J. Geophys. Res. 107, 4684, doi:10.1029/2001JD001396.

[4] Leck, C., M. Tjernström, P. Matrai, E. Swietlicki, and K. Bigg. Can Marine Micro-organisms Influence Melting of the Arctic Pack Ice? EOS, Vol. 85, No. 3, 20 January 2004, pp. 25, 30, 32.

[5] Leck, C., E.D. Nilsson, K. Bigg, and L.Bäcklin,The atmospheric program on the Arctic Ocean Expedition in the summer of 1996 (AOE-96) - A technical overview - Outline of experimental approach, instruments, scientific objectives, J.Geophys. Res. 106, 32,051-32,067, 2001.

[6] Sprung, D., C. Jost, T. Reiner, A. Hansel, and A. Wisthaler (2001) Airborne measurements of acetone and acetonitrile in the tropical Indian Ocean boundary layer and free troposphere: Aircraft-based intercomparison of AP-CIMS and PTR-MS measurements, J. Geophys. Res. 106, 22, 28511-28528.

[7] Wisthaler, A., A. Hansel, R. R. Dickerson, and P. J. Crutzen (2002) Organic trace gas measurements by PTR-MS during INDOEX 1999, J. Geophys. Res. 107(D19), 8024, doi:10.1029/2001JD000576.

[8] De Gouw, J. A., C. Warneke, A. Stohl , A. G. Wollny, C. A. Brock, O. R. Cooper, J. S. Holloway, M.Trainer, F. C. Fehsenfeld, E. L. Atlas, S. G. Donnelly, V. Stroud, and A. Lueb (2006) Volatile organic compound composition of merged and aged forest fire plumes from Alaska and western Canada. J. Geophys. Res. 111, D10303, doi:10.1029/2005JD006175.

[9] Lobert, J. M., D. H. Scharffe, W. M. Hao, and P. J. Crutzen, Importance of biomass burning in the atmospheric budgets of nitrogen containing gases, Nature, 346, 552- 554, 1990.

[10] NAAPS (2006) http://www.nrlmry.navy.mil/flambe/index.html and http://www.nrlmry.navy.mil/aerosol), both accessed 29 Sept. 2006.

[11] Reid, J. S., D. L. Westphal., A. Walker, S. A. Christopher, E. M. Prins, C. O. Justice, K. A. Richardson, E. A. Reid, T.F. Eck (2003) Modeling and mechanisms of intercontinental transport of biomass-burning plumes, AGU Fall Meeting, San Francisco, Eos Trans. AGU, 84(46), Fall Meet. Suppl., Abstract A11I-06.

Quantitative Determination of Isobaric Volatile Organic Compounds Using Proton Transfer Reaction − Linear Ion Trap (PTR-LIT) Mass Spectrometry

Levi H. Mielke[1] (lhmielke@purdue.edu), David E. Erickson[1], Scott A. McLuckey[1], Armin Wisthaler[3], Armin Hansel[3], Christopher H. Doerge[3] and Paul B. Shepson[1,2]

[1]*Departments of Chemistry*

[2]*Earth and Atmospheric Sciences, Purdue University*

[3]*Institut für Ionenphysik, Universität Innsbruck, Austria*

[4]*Jonathan Amy Facility for Advance Instrumentation, Purdue University*

Abstract

Several low molecular weight isobaric volatile organic compounds (VOCs) occur in the atmosphere in the low ppb to ppt range. Proton transfer reaction mass spectrometry (PTR-MS) allows for quantitative determination of VOCs in real time at ppt concentrations, but cannot discern isobaric species. Although 3-D quadrupole ion traps are capable of MS/MS, they suffer from limited ion storage capacity and ion trapping efficiency. Here we pursue the application of a linear quadrupole ion trap in combination with proton transfer reaction chemical ionization to provide the advantages of specificity associated with MS/MS with improved performance characteristics relative to 3-D ion traps. In our application the LIT is operated at a drive frequency of 2.0 Mhz. Ions are sequentially ejected by ramping the rf voltage and then bent orthogonally to a secondary electron multiplier. The rf drive has been adapted to enable isolation of specific ions, collision induced dissociation (CID), and dipolar excitation. Two atmospherically important isomers, methyl vinyl ketone (MVK) and methacrolein, yield (M+H)+ parent ions at m/z 71. These isomers can be differentiated given that both species have a common CID fragment at m/z 43, while only methacrolein yields a CID fragment at m/z 41. Initial CID experiments of methacrolein in the PTR-LIT have focused on maximizing the m/z 41 to m/z 43 ratio to lower the limit of detection for discerning methacrolein from MVK. This presentation will describe the instrument, its modifications, and performance characteristics as a tandem mass spectrometer for the measurement of atmospheric isomers.

Performance Assessment of a Recently Developed High Resolution PTR-TOFMS Instrument

M. Müller, M. Graus, A. Wisthaler and A. Hansel

Institute of Ion Physics and Applied Physics, University of Innsbruck, Innsbruck, Austria, M.Mueller@uibk.ac.at

Abstract

The High Resolution Proton Transfer Reaction Time-of-Flight Mass Spectrometer (PTR-TOFMS) recently developed at the University of Innsbruck is a powerful new analytical tool for on-line analysis of volatile organic compounds. The conventional PTR-MS instrument uses a quadrupole mass spectrometer (QMS) for ion separation and ion detection. The QMS keeps peak widths almost constant to 1 mass unit. Isobaric ions, i.e. ions that have the same nominal mass but a different exact mass, cannot be separated. The Innsbruck High Resolution PTR-TOFMS has a mass resolving power of ~ 4000 (FWHM) and is thus capable of distinguishing between a variety of isobaric ions. For example, the mass peak of protonated ethanol, $C_2H_6O.H^+$(m/z=47.049) can be clearly separated from protonated formic acid, $CH_2O_2.H^+$ (m/z=47.013) (see Figure 1). This is not only a great advantage for the identification of trace gases in complex sample matrices but can also significantly improve the detection limit in cases where the background signal is isobaric and thus separated in the PTR-TOFMS. Detection limits as low as 20pptv were obtained for a one minute integration period. The performance characteristics of the newly developed High Resolution PTR-TOFMS instrument will be discussed in detail and compared to the characteristics of a standard PTR-MS instrument.

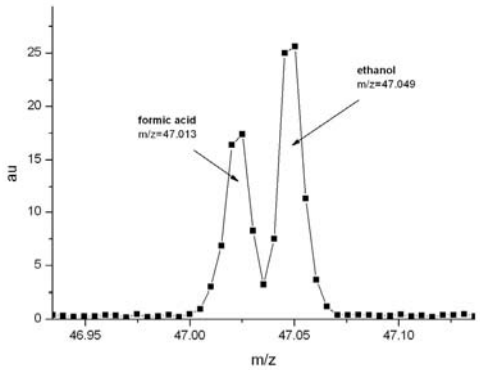

Figure 1: The protonated ethanol peak at m/z=47.049 can be distinguished from the protonated formic acid peak at m/z=47.013.

Acknowledgement

The development of this High Resolution PTR-TOFMS prototype is a cooperation of the Leopold Franzens University of Innsbruck and Ionicon Analytik Ges.m.b.H. as our industrial partner in the consortium. We thank Ionicon, and in particular Alfons Jordan, Gernot Hanel and Stefan Haidacher for their support. The TOF-MS system was funded by the University of Innsbruck („Uni Infrastruktur 2004“ Programms, GZ.10.220/2-VII/2004). The project is financially supported by the Austrian Research Funding Association (FFG; Basisprogramm – Brückenschlag 1, P.-Nr. 810074)

9. Index of Authors

A

Alfarra M.R. 27
Ali S. 116, 124, 216
Amelynck C. 127
Ammann C. 76, 80, 141,
Andres-Momtaner D. 86
Antille N. 124
Anttila T. 10
Aoki N. 92, 180
Aprea E. 132
Araghipour N. 136, 204, 238
Arneth A. 174

B

Baltensperger U. 27, 200
Bandur R. 15
Barta C. 140
Beauchamp J. 166, 223, 232
Behnke K. 86
Biasioli F. 110
Blake R.S. 41
Blank I. 195
Boissel P. 156, 191
Bouvier-Brown N. 70
Brilli F. 140
Brunner A. 27, 76, 80, 141, 200
Brunner C. 146
Buettner A. 118, 149
Buhr K. 149
Bultinck P. 127
Bunge M. 204

C

Carlin S. 132
Case A. 38
Claeys M. 25, 171
Clochard L. 191
Cody R. 47
Colineau J. 238
Crespo E. 102, 154, 212
Cristescu S.M. 102, 154, 212

D

Dalla Via J. 136
Davidson B. 80
Davis B.M. 208
de Gouw J. 54, 243
Debie E. 127
Dehon C. 156, 191
Delahunty C. 161
Dicke M. 223
Dinar E. 10
Doerge C. H. 252
Dommen J. 27, 80, 200
Douffet T. 76
Dufour J.-P. 161
Dunkl J. 166, 227, 232
Durand P. 76

E

Eisele F.L. 4, 31
Ekberg A. 174
Ellis A.M. 41

Erickson D.E. 252

F

Fares S. 170
Fortunati A. 140
Friedli H. 4

G

Gaeggeler K. 27
Gascho A. 27, 200
Gasperi F. 132
Gohm A. 227
Goldstein A.H. 70
Gómez Y. 171
Graber E.R. 10
Graus M. 97, 253
Gross D. 27

H

Hanson D.R. 4
Harren F.J.M. 102, 154, 212
Hartungen E. 173, 178
Harvey W. 161
Hayward S. 174
Haidacher S. 173
Hakola H. 218
Hanel G. 173
Hansel A. 97, 104, 166, 223, 227, 232, 247, 252, 253
Heenan S. 161
Hellén H. 218
Heninger M. 156, 191
Herbig J. 232
Hikida T. 63
Hirokawa J. 92
Hoeschen C. 146, 187
Hoffmann T. 15
Hoffmann S. 15
Holst T. 174
Holzinger R. 70
Hudry J. 124
Huey L.G. 38

I

Ideguchi M. 185
Inomata S. 92, 180

J

Jocher M. 80, 141
Jorand F. 156
Jordan A. 173, 178

K

Kajii Y. 185
Kajos M. 218
Kalberer M. 27
Karl T. 75
Kato S. 185
Keck L. 146, 187
Kim S. 38
Knighton B. 59
Kohl I. 232
Kulmala M. 76, 218
Kuster W.C. 243

L
le Coutre J. 124
Leck C. 247
Lee A. 70
Lemaire J. 156, 191
Liardon R. 195
Lindinger C. 116, 195, 216
Loivamäki M. 86
Loreto F. 85, 140, 170
Lovejoy E.R. 20

M
Maenhaut W. 171
Margesin R. 204
Märk T.D. 132, 136, 173, 178, 204
Märk L. 173, 178
Markkanen T. 76
Mateus M-L. 195
Mauclaire G. 191
Mauldin R.L. 4
McEwan M.J. 208
McLuckey S.A. 252
McMurry P.H. 31
Mentel T. 10
Mestdagh H. 156, 191
Mestres M. 118
Metzger A. 27, 200
Mielke L.H. 252
Mikoviny T. 136, 204
Milligan D.B. 208
Monks P.S. 41
Müller M. 97, 253
Mumm R. 223

N
Naganuma M. 63
Norman M. 104, 227
Nowak J.B. 38

O
Obleitner F. 227
Oeh U. 146, 187

P
Pasquiers S. 156
Pollien P. 116, 216
Popp P.J. 48
Prevot A.S.H. 27

R
Rathbone G. J. 31
Reinnig C. 15
Reynaud B. 124
Rinne J. 76, 80, 218
Riziq A.A. 10
Robert F. 116, 216
Rudich Y. 10
Ruuskanen T.M. 76, 218

S
Sadanaga Y. 92
Schaub A. 223
Schieberle P. 149
Schinner F. 204
Schnitzhofer R. 166, 227
Schnitzler J-P. 86
Schoon N. 127

Schottkowsky R. 173
Senthilmohan S.T. 208
Shepson P.B. 252
Shimono A. 63
Sikkens C. 154, 212
Simiand N. 156
Singer W. 232
Sjostedt S. 38
Smith J.N. 31
Spadone J-C. 116, 216
Spirig C. 76, 80, 141
Spitaler R. 136
Steeghs M.M.L. 102, 154, 212
Stickel R. 38
Swietlicki E. 247

T

Taipale R. 76, 218
Tanimoto H. 92, 180
Tanner D.J. 4, 38
Taraniuk I. 10
Tardiveau P. 156
Teuber M. 86
Thekedar B. 146
Thomson D.S. 20
Thornberry T. 20
Tjernström M. 247
Tschiersch J. 215
Turnipseed A. 38

V

van Raamsdonk L. 238
van Ruth S. 238
Vargas O. 38
Vermeylen R. 171
Versini G. 132
Vesala T. 76

W

Warneke C. 54, 243
Warnke J. 15
Warscheid B. 15
Welsh-Bon D. 243
Whyte C. 41
Wildt J. 170
Wilson P.F. 208
Wisthaler A. 97, 104, 136, 166, 204, 227, 247, 252, 253
Wyche K.P. 41

Z

Zanen P. 102

innsbruck university press in Conference Series:
Series Editors: K. Habitzel, T. D. Märk, S. Prock, B. Stehno

Also available by *i*up in this series:

Contributions – 2nd International Conference on Proton Transfer Reaction Mass Spectrometry and Its Applications – ISBN: 3-901249-78-8
Editors: A. Hansel, T. D. Märk

41st Symposium on Theoretical Chemistry – Innsbruck, Austria September 5–7, 2005
ISBN: 3-901249-80-X – Editors: Bernd M. Rode, Bernhard R. Randolf

Contributions – 15th Symposium on Atomic and Surface Physics and Related Topics
ISBN: 3-901249-82-6 – Editors: V. Grill, T. D. Märk

Microlearning: Emerging Concepts, Practices and Technologies
Proceedings of Microlearning 2005: Learning & Working in New Media Environments
ISBN: 3-901249-83-4 – Editors: Theo Hug, Martin Lindner, Peter A. Bruck

Zukunftsplattform Obergurgl 2006:
Forschungsplattformen innerhalb der Leopold-Franzens-Universität Innsbruck
ISBN: 3-901249-86-9 – Editors: M. Grumiller, T. D. Märk

Bildung schafft Zukunft
1. Innsbrucker Bildungstage, 17. – 18. November 2005
ISBN: 3-901249-87-7 – Editor: Heidi Möller

Die Wiederentdeckung der Langsamkeit
Tagungsband zum gleichnamigen Symposion anlässlich
des Tages der psychischen Gesundheit 2005 – ISBN: 3-901249-88-5
Editors: Matthias A. Brüstle, Wolfgang Weber

Pangeo Austria 2006
ISBN: 3-901249-93-1 – Editor: Monika Tessadri-Wackerle

Proceedings of the 7th International Workshop on Adjoint Applications in Dynamic Meteorology
ISBN: 3-901249-98-2 – Editors: M. Ehrendorfer, R. M. Errico

Micromedia & e-Learning 2.0: Gaining the Big Picture
Proceedings of Microlearning Conference 2006
ISBN: 3-901249-99-0 – Editors: Theo Hug, Martin Lindner, Peter A. Bruck

PROTON TRANSFER REACTION – MASS SPECTROMETRY

IONIMED
ANALYTIK

Providing trace gas solutions for:

- > breath gas analysis
- > headspace monitoring in biotech & medicine
- > online supervision of fermentation processes

For more information visit our website:
www.ionimed.com

Technikerstrasse 21a A-6020 Innsbruck Austria Tel.: +43 512 507 4810 Fax.: +43 512 507 9818 Email: office@ionimed.com

Acknowledgement of Conference Sponsors:

The conference organizers would like to thank our corporate and institutional sponsors for supporting this conference:

PFEIFFER VACUUM Austria

IONICON ANALYTIK GmbH

WINN – West Austrian Initiative for Nano Networking

IONIMED ANALYTIK GmbH

ISBN-10: 3-902571-03-9
ISBN-13: 978-3-902571-03-8